UNIVERSITY *of the*
WESTERN CAPE

OPTIMISATION OF SELECTIVE EXTRACTION TECHNIQUES AS A TOOL FOR GEOCHEMICAL MAPPING IN THE SOUTHERN AFRICA REGION

By

AKINYEMI, SEGUN AJAYI

B.Sc (Hons.) Geology, University of Ado Ekiti, Nigeria.

A thesis submitted in fulfilment of the requirements for the degree of Magister Scientae (M.Sc) in the Faculty of Science, Earth Sciences Department, University of the Western Cape, Bellville, South Africa.

Supervisor: Professor Charles D. Okujeni
Earth Sciences Department,
University of the Western Cape.
South Africa.

May 2008

DECLARATION

I, Akinyemi Segun Ajayi declare that the Optimisation of Selective Extraction Techniques as a tool for Geochemical Mapping in the Southern African Region is my own work, that it has not been submitted for degree or examination in any other university, and that all the resources I have used or quoted have been indicated and acknowledged by means of complete references.

……..
May 2008.

ACKNOWLEDGEMENTS

With open heart filled with joy and gratitude, I gratefully acknowledge the contribution of my supervisor, Prof. Charles Okujeni whose suggestion and critical appraisal during the write up made a successful completion of the work. Thank you Sir and God bless.

I am highly indebted of thankful appreciation to my wonderful parents, brothers, cousin, nephews and my fiancée for their unflinching support and love during my course of this work. I know my parents love me that they brought me to the world. My sacred message is I love you all.

I sincerely thank the following special people; Kole Amigun, Richard Akinyeye, Oluwaseun Fadipe, Solomon Adekola, Segun Adelana, Ademola Rabiu, Victor Ojumu, Kayode Ajayi, Billy Oborien, Tunde Silas Olowomeye and Niyi Isafiade for their moral support and contribution which directly or indirectly assisted me towards the successful completion of this work .

With esteem sense of appreciation I would like to thank the Head of Department and the entire staff member of the Earth Sciences Department, University of the Western Cape for the warmth, candid support and encouragement throughout the period of my stay in the Department. I am proud to belong to such a dynamic, multicultural and multiracial society with a lot of opportunities to grow.

Without implying a second fiddle position. I am short of words to express my rare special thanks to Mrs Bronwen Honigwachs, Mr Reginald Domoney, Mr Peter Meyer, Mr Shaheen Jamaloodien and Mrs Caroline Barnard for their warmth, unflinching support and encouragement throughout the course of this study in the Department of Earth Sciences, University of Western Cape. My message is such people like you make a difference in the World full of hatred, strife and conflict.

I would also like to thank my project mates; Unati Umshumi, Ntatyi Langa, Jingjing Xu and Jade Yang for their assistance and moral support during the course of this work. My special appreciation also goes to Patrick Ackon for his assistance and moral support during the course of this noble work. I would also thank him immensely for the analytical data and samples he made available for this work.

Without mincing words my appreciation goes to the entire postgraduate students of the Department of Earth Sciences, University of Western Cape for the warmth, love and support during the course of this study. The comradeship and oneness will linger on and endures for a long time. I wish all of you success in your future endeavours.

I must also thank Dr Andreas Spath and his laboratory assistant for the multielement analysis with the use of Induced Coupled Plasma Mass Spectrometry (ICPMS) in the Department of Geological Sciences, University of Cape Town.

I would also use this medium to thank the entire management and staff of the University of Ado Ekiti, Nigeria for their unwavering and unflinching support enjoyed throughout the course of this work. My message is thank you and God bless you all.

The financial support of the German Academic Exchange Service (German DAAD Scholarship) is specifically acknowledged. Without this singular gesture the successful completion of the work would not have been achieved within a reasonable time limit.

Without half measures, my special thanks go to the Almighty God for his love, mercy, kindness and grace that endures forever and ever in my life.

ABBREVIATIONS

AAS: Atomic absorption spectrometry

ICPMS: Induced coupled plasma mass spectrometry

ARL: Aqua regia leach

TAL: Triple acid leach

CH: Cold hydroxylamine hydrochloride leach

HH: Hot hydroxylamine hydrochloride leach

PCA: Principal component analysis

HCl: Hydrochloric acid

HNO3: Nitric acid

PPM: Part per million

PPB: Part per billion

Au:	Gold	**Cr:**	Chromium		
Pt:	Platinum	**Re:**	Rhenium		
Ni:	Nickel	**Os:**	Osmium	**As:**	Arsenic
Co:	Cobalt	**Rb:**	Rubidium	**Rh:**	Rhodium
Cu:	Copper	**Pd:**	Palladium	**Ru:**	Ruthenium
Zn:	Zinc	**Ag:**	Silver	**Pb:**	Lead
Mn:	Manganese	**Ba:**	Barium	**Se:**	Selenium
Cd:	Cadmium	**U:**	Uranium	**Sr:**	Strontium

ABSTRACT

The complex nature and composition of regolith cover in Southern Africa is a major challenge to geochemical mapping for concealed mineralization. Some of the setbacks to successful geochemical exploration may be ascribed to the use of various partial extraction techniques, without a profound understanding of the regolith components and their composition.

This investigation therefore focuses on the use of hydroxylamine partial extraction geochemistry for geochemical mapping in regolith over two contrasting environments viz; aeolian sand-calcrete regolith over Au mineralization at Amalia Blue Dot Mine in South Africa and lateritic regolith covering the Ni-Cu deposit at Kabanga Main and Luhuma in Tanzania.

Regolith samples from the above areas were sieved and extracted with hydroxylamine hydrochloride solution and analyzed for multi-element by AAS and ICP-MS techniques. A stepwise optimization of the hydroxylamine extraction technique of samples from both areas was carried out and incorporated into the analytical programme (in a pilot study).

Results of hydroxylamine partial extraction generally gave better anomaly contrast and reflection of bedrock mineralization than the conventional aqua regia techniques that were previously used in the region. The results however show that lateritic regolith may be best extracted using 0.25M hydroxylamine while 0.1M concentration appears most suitable for extraction of aeolian-calcrete regolith.

The above results are corroborated by principal component analysis of the analytical data that show various element associations, e.g. with Fe-Mn oxides while others possibly belong to the loosely adsorbed or exchangeable group.

The geochemical maps in the pilot study areas at Amalia, Kabanga and Luhuma show elevated element contents or clusters of anomalies of diverse elements associated with Fe-Mn oxides. Geochemical mapping at Kabanga with deeply concealed mineralization however shows variability of subdued element patterns over mineralized areas.

Geochemical signatures associated with hydroxylamine hydrochloride partial leach are therefore characterized by a lower geochemical background than that using conventional aqua regia leach. This study leads recommending for further investigations into partial extraction of the exchangeable group of elements, possibly using ammonium acetate.

TABLE OF CONTENTS

LIST OF FIGURES

LIST OF TABLES

CHAPTER ONE

1. INTRODUCTION

Regolith is a collective term used to describe earthy material like weathered rock or accumulated residual, e.g. laterite, calcrete, silcrete, and transported soils or sedimentary cover, e.g. colluviums, alluvium, and salt lake deposits etc. (Smith, 1996). These can host precious and valuable trace metals that are bonded in various mineral phases in the weathering products.

The complex and varied nature of the regolith environment has proved to be a major challenge to successful geochemical exploration (Anand & Smith, 1993; Lintern et al., 1999). In most cases the morphological, petrological and compositional characteristics of the insitu or residual regolith are different from those of the rocks and occasionally from the ore deposits from which they are derived. These may in turn affect the geological, geochemical and geophysical exploration procedures and considerably limit their use.

These challenges to exploration posed by regolith cover can be worsened by the presence of transported overburden and basin sediments especially for geochemical procedures based on surface or near surface sampling (Anand and Butt, 1998). However, a clear understanding of the landform types, in terms of preservation, erosional activities and accumulation remain a *sinequanon* to the understanding of the regolith cover, sampling strategy and realization of the differences in geochemical behaviours (Anand and Butt, 1998; Butt et al., 2000; Okujeni et al., 2005).

Aeolian sand and calcrete dominated regolith widely occurs in the semi-arid to arid regions of Southern Africa. These regolith types occur in various landform regions under the variable intensity of aeolian activity (Okujeni et al., 2005). For example, in semi arid region of the north western parts of South Africa, aeolian activity still prevails in a terrain covered by aeolian sand and an underlying calcrete and sedimentary rock horizons. Similar regolith profiles also occur for example in the western parts of Zimbabwe, where aeolian activities have ceased, possibly due to change in climatic conditions (Okujeni, 1999). A great proportion of the Kalahari Formation in the north-western part of South Africa is integral part of wind blown regolith materials that are preserved in various depositional basins. The aeolian sands are widely concealed by calcrete or lateritic profiles, the latter often occur as lateritic duricrust.

Lateritic profiles and lateritization processes are prevalent in subtropical and tropical humid climates of Africa, which encloses vast areas of southern Africa. Climatic change for over 100Ma in Southern Africa has resulted in a subdued intensity of the lateritization process and a modification of the pre-existing lateritic profiles, mainly formation of duricrusts and its truncation. The lateritic duricrust is indurated material composed of various structural forms of secondary segregations such as nodules and pisoliths, cemented by a matrix of clay and Al and /or Fe oxides. The lateritic duricrust can occur in some places over basement rocks while in other places it underlies the aeolian sand and calcrete regolith. The nodular and pisolithic horizon has evolved by partial collapse, involving local vertical and lateral movement after chemical wasting of Fe oxides and clays which is known as lateritic residuum (Anand & Smith, 1993; Anand et al., 1993).

The complex nature of the regolith composition in the Southern African regions coupled with the resultant cumulative chemical overprint due to climatic change over a long period has often mitigated against proper recognition of geochemical signatures and therefore poses a major challenge during geochemical exploration. Correct identification of regolith component and the use of suitable partial extraction technique is therefore of critical importance in exploration work difficult in Southern African region (Anand & Butt, 1998).

The use of suitable partial extraction technique hinges on understanding the processes underlying the emplacement of ore-related geochemical signatures on regolith components. There are widely accepted processes of element dispersion such as infiltration and evapo-transpiration, electrochemical dispersion processes, cyclical dilantancy pumping, supercedency, and dispersion facilitated by biological processes (Kelley et al., 2004). Moreover, there is an opinion in geochemistry that the previously unbounded metals are transported toward the surface following the above described mechanism of dispersion from mineralization at depth (McBride, 1994). There abound some prevalent controversies as to the dominant mechanisms of transport of the element from oxidizing mineralization at depth, as to whether it is by diffusion or fast-ion migration through faulting, waterborne or gaseous. However, there is a general consensus that the principal resident sites in the secondary environment for the migrating elements comprising hydrous Fe-oxides, Mn-oxides, humic and fulvic components of humus material and clay minerals (Nolan et al., 2003). Strikingly enough, the aeolian sand and lateritic regolith considered in this study have the Fe-Mn oxides in common. Early research also indicated that organic matter and hydrous

coatings of iron and manganese are the most common surface-active phases in the environments ranging from soils to water (Hall et. al., 1995).

Numerous chemical extraction techniques have been used to investigate metal distribution in soils and sediments, e.g. total leach (aqua regia and triple acid leach), partial extractions, and selective extractions. Total leach, otherwise known as aqua regia leach, is a conventional digestion method available in all the commercial laboratories. The aqua regia leach aggressively attacks oxides, carbonates, sulphides, chlorides, most sulphates and partially attacks clays. Contrastingly, there are some new methods of controlled dissolution/extraction techniques, such as Enzyme leach and the Mobile Metal Ion (MMI) method; both are partial extractions rather than selective dissolution of bonded metals in sediments/soils (i.e. loosely attached ions, leached by weak acids). They extract part of a geochemical phase or phases, rather than a selected mineral in soils or sediments. The Mobile Metal Ion (MMI) technique measures mobile metal ions in surface soils that are occasionally released from ore bodies and travel upward to the surface and bond by soil forming processes. The Mobile Metal Ion (MMI) is a high-resolution technique which increases the magnitude of the signal to noise ratio which can be of benefit in terrain types where the conventional method (aqua regia) has resolution problems. It gives superior resolution for most metals including Gold (Au), where the degree of weathering is great and surficial cover/materials is a critical factor. Its superior spatial resolution can also be of potential great benefit (Mann et al., 1998).

The enzyme leach extraction technique was developed and successfully applied in the discovery of a Missippi Valley-Type zinc ore deposit in USA (Yeager et al., 1998). This technique selectively leaches metals that are loosely bound ions to various mineral sites where the enzyme acts as a catalyst during the reaction processes. It was adjudged to have capability of detecting mineralized bedrock buried to 300m by transported overburden. In most cases the anomaly-to-background ratio normally exceeds 100times (Clark, 1993).

The Mobile Metal Ion (MMI) technique was developed in Australia by Wamtech Pty Ltd. This technique has been widely used by the X-ray Assay laboratory (XRAL) in North America (Mann et al, 1995b) and has the capability of producing a high anomaly contrast in a vertical position above the mineralization buried in up to 450m of overburden. This technique has been mostly applied in non-glaciated, and to tropical environments under geomorphic conditions of relict, erosional and depositional landscapes. However, its practical application in an environment where

anomalies are at sub-ppb level is quite doubtful especially in depositional settings located in glaciated regions of North America (Wamtech Proprietary Limited, 1997). MMI techniques have been successfully used worldwide in passive (not constantly eroding aeolian environment) aeolian environments (Mann et. al., 1998). Application of this method in active aeolian regolith environments appears to be less successful, which may partly explain conflicting views in several case studies on application of these techniques in exploration for Pb/Zn deposits in the Transvaal sequence and Au deposits in the Kraaipan Greenstone Belt (MMI workshop 1999., Viljoen and Kiefer, 1999).

Trace metals can be partitioned into various geochemical phases in soil and sediments. Tessier et al (1979) listed some of these as: 1.) Exchangeable geochemical phase where metals that are held in exchangeable form on the major components of sediment like clay, hydrated oxides of Fe, Mn, humic acids. 2) Bound to carbonate with significant trace metal concentration associated with the sediment/soil carbonates. 3.) Bound to Fe and Mn oxides, which represents the content of each metal bound to iron and manganese oxides that would be released under reducing condition (Panda et al., 1995); also includes absorption site for trace metals by particulate organics and clays. (Drever, 1988). 4.) Bound to organic matter/sulphides and 5.) Metals in residual form.

Of the five different geochemical phases in regolith highlighted by the Tessier et al., 1979 in his work, the hydrous oxides of manganese and iron are the most common geochemical phase in regolith materials that play host to precious and base metals. The oxides of manganese and iron are present as coatings on minerals or as fine discrete particles in aeolian sand. The scavenging capacity per unit mass of manganese (Mn) oxides for heavy is greater than that of iron (Fe) oxides which is caused in part by the complex mineralogical structure of these oxides. Both iron (Fe) and manganese (Mn) form mixed oxides, due to their similar chemical properties. Amorphous iron oxyhydroxide is chemically more reactive than the crystalline oxides, and this property makes it suitable for selective dissolution. The reagent that can be used to selectively leach adsorbed metals from manganese and /or some of the iron oxides in regolith materials is known as hydroxylamine hydrochloride ($NH_2OH.HCl$) (Chao, 1984). $NH_2OH.HCl$ extraction designed to dissolve iron and manganese oxyhydroxide oxides, is quite similar to enzyme leach, but required more extreme conditions. Hydroxylamine hydrochloride also has a very low neutralization potential, and is sensitive to changes in pedogenic calcrete ($CaCO_3$). Similar to other reagents (ammonium acetate, oxalate/ascorbic acid solutions) that are chosen or formulated to selectively leach elements from the five different geochemical phases in regolith materials, hydroxylamine hydrochloride

selectivity is governed by the following factors, temperature, sample weight, and shaking time/residence time. $NH_2OH.HCl$ leach has been widely employed as a geochemical exploration tool (Kelley et al., 2003; Gray et al., 1999; Dalrymple et al., 2005). This method was proved to be effective and economic as it is an inexpensive and easy exploration method in areas of transported overburden (Kelley et al., 2003).

This work is focussed on evaluating the geochemical expression of varieties of regolith overburden overlying mineralization from two contrasting environments. These are lateritic regolith overlying the Ni-Cu mineralisation at Kabanga in Tanzania and aeolian-calcrete regolith over Au mineralisation at Amalia in South Africa.

The objective is to assess the use of hydroxylamine as a partial extraction technique for geochemical mapping of concealed bedrock, mineralization in terms of the following aims;

- A re-evaluation of existing analytical data of soil samples from Amalia and Kabanga to create a baseline for this study
- Optimizations of the hydroxylamine hydrochloride leach technique and comparison of these results with those of existing analytical data (baseline study).
- Geochemical mapping using hydroxylamine hydrochloride leach and appraisal of its ability to reflect bedrock and concealed mineralisation.

1.4. Site and location of study areas

1.4.1 Location and accessibility of Blue Dot Mine, Amalia

The Blue Dot Gold mine is situated on the following farms; Goudplaats 96 HO, Abelskop 75 HO and Bothmasrust 76 HO in the Amalia Greenstone Belt. It lies within Schweizer-Reneke district in the Northern Province and approximately 10km southeast of Amalia and 20km south-west of Schweizer-Reneke Township. (Fig 1.1). The study area is situated within the southern limb of the Kraaipan Greenstone belt, which lies between Christiana and Amalia town (Ackon, 2001). The study site occupies an area of 22Sq.Km and lies within the Longitude $E27^0$15'00" and Longitude $E27^0$19'00" and Latitude $S25^0$0'35" and Latitude $S25^0$0'78". The area is gently undulating to flat-lying; the most dominant topographic expression of the terrain is the erratic exposure of north-south trending ridge. Most part of the area is dotted with isolated exposures of Greenstones and Banded Iron Formation (BIF) (Kiefer, 2004).The study site is covered by relatively thick

overburden of Aeolian regolith (predominantly sands and calcrete). The thickness of the regolith overburden in the study site/project area varies from outcrop to up to 5m. The exploration and mining activities have been carried out in the small proportion of the Amalia Greenstone Belt. The entire area is poorly exposed and the underlying rocks were completely covered by the aeolian regolith sands.

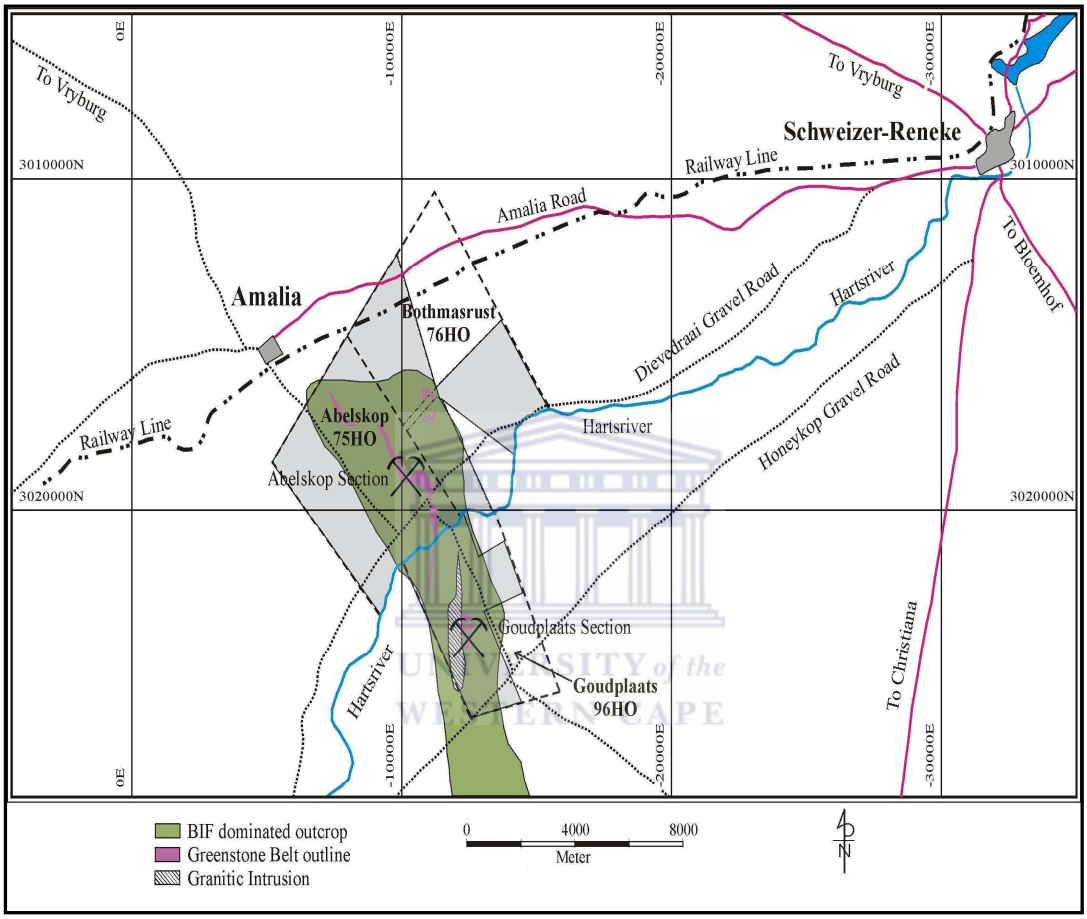

Fig 1.1 Locality plan of the Blue Dot Mine(blue = Harts river, red = Main road, dotted black line = Gravel road, dash-dot line = railway, dashed line = farm boundary, grey Mineral rights Holding Blue Dot Mine Greenstone Belt position adopted from the geological sheet Christiana (2724)(After Kiefer 2004).

1.4.2 Location and accessibility of Kabanga main nickel project

The Kabanga nickel project from where samples were taken is situated in the north-western part of Tanzania. It is approximately 200 km from Lake Victoria in the south-western part of the studied area, which is adjacent to the Burundi border (Fig. 2.4). It is approximately 385km west of Bulvanhuhu gold mine, and 100km northwest of the Tulawaka gold project that is currently under construction (Simon, 2003). The area is dotted with undulating steep to very steep hills with a sub-

plateau on top. The Luhuma nickel project is located just under 10km south of the Tanzania-Burundi-Rwanda main road and about 55km Northeast of Kabanga nickel project.

1.5 Background to present study

1.5.1 The Blue Dot Mine/Amalia gold prospect

The Blue Dot mine area comprises Abelskop, Bothmasrust and Goudplaats mineralized sections. The study site was first mapped in 1906 by A.L Du Toit and later by Anhaeusser et al., (1991) during the period of gold boom in the area. However, the detailed geology has remained unclear due to poor exposure of outcrops in the area due to thick cover of Kalahari sands. There were reported occurrences of ore zones at Amalia/Blue Dot, in the Abelskop, Bothmasrust and Goudplaats areas. Generally, the ores are found to occur as traces of sulphides either in the form of pyrrhotite and/or pyrite replacement parallel to foliation in magnetite-rich layers. The style of mineralisation is a vein stock work type mineralization with sulphidation of hematite-magnetite layers and partly carbonate altered chert layers, which is associated with quartz carbonate veining. The recent geochemical studies in the study site recommend the sampling of the laminated to hardpan carbonate horizon and the basal zone of the aeolian sand horizon for any future exploration work (Okujeni et al., 2005).

Exploration for mineral resources in transported regolith in Southern Africa has reached an advanced stage, particularly in regions where there is a good exposure of the underlying rocks. The previous work in the region using conventional (aqua regia leach) exploration methods has delineated most of the reported mineral deposits. Exploration work has also progressed within the aeolian sand/calcrete components cover in the north western part of South Africa.

1.5.2 Kabanga and Luhuma nickel-copper deposits

The Kabanga nickel sulphides mineralization is associated with ultramafic bodies intruded into metasediments in a geological setting, it is comparable to the Thompson nickel belt in Manitoba, Canada. The mineralization was first discovered in 1976 during a regional reconnaissance exploration of northwest Tanzania by a multinational team under the United Nations Development Program (UNDP) (van Straaten, 1984). The concession was acquired by a Canadian mining company in 1990s, the exploration work in the area actually started in 1990 to 1993; during that period about 34 drilled boreholes were put in place by Sutton

Resources. A new deposit, called Kabanga North, was discovered in 1992 through a joint venture between the Sutton resources and BHP Inc. of Australia. This deposit is relative more economic than the Kabanga main deposit. This property was relinquished in 1994 as a result of securities problems caused by the large influx of refugees from the neighboring Burundi and Rwanda. The description of the mineralization is based on extensive geological mapping, drill core logging and geophysical survey in the Kagera Region of northwestern Tanzania by BHP Minerals International Exploration Inc. and Sutton Resources Ltd. Between 1991 and 1995. The Kabanga Nickel Project was acquired by a Canadian exploration and mining company, Barrick, in the Sutton Resources transaction of 1999. Since the acquisition of the property Barrick has significantly enhanced the value of the project by increasing the known resource estimate at Kabanga Main and discovering an adjacent new deposit.

The preliminary geochemical analysis of the soil samples from the Kabanga and Luhuma was carried out with a view to establish the best grain size for geochemical exploration (Simon, 2003). The <212μm soil fraction was recommended as the most suitable for future geochemical exploration work.

Exploration success has also been achieved in the lateritic regolith terrain of the north western part of Tanzania (Kabanga main). Exploration work has progressed to a new adjacent prospect called Kabanga north, which is reported to be relatively more economic than Kabanga main, and recently Luhuma nickel-copper prospect which is about 55km north-east of the Kabanga nickel project. The previous conventional exploration work conducted in the area using derived litho geochemical vectors has classified some elements into clusters reflecting their host minerals, for instance oxides and sulphides (Simon, 2003). Successful delineation of mineralized / intrusive from the barren zone was achieved, and based on this Luhuma study site was chosen as a potential area for exploration work.

1.6 Climate, Topography and drainage

1.6.1 Topography of the North West Province

The North West Province has the most uniform terrain of all the South African provinces, with an altitude ranging from 920-1782 metres above sea level. The central and western regions are characterised by flat or gently undulating plains. The windblown sands associated with the arid environment of the Kalahari group cover the entire study area. This Southern portion is

predominantly covered with windblown sands with an average thickness of 112m (Zimmerman, 1994) and the north eastern portion with a much lower thickness. It is covered with a mixture of calcrete and sands. This underlying calcrete is commonly believed to be formed as a result of evaporation of the upward moving underground water in the study area. Hence, the north eastern portion is dotted with isolated exposures of calcrete boulders and rubbles with a low-lying topography. The topography and regolith materials in Amalia Blue Dot Mine are believed to be products of weathering history and hence, of the past and present processes of weathering and geochemical dispersion.

1.6.2 Climate and vegetation of the North West Province

The climatic conditions within the North West Province vary significantly. The extreme western region has an arid climate receiving less than 300mm of rainfall per annum. There is a variation in the rainfall pattern, the western region receives less than 300mm per annum, the central region receives around 550mm per annum and the eastern and south-eastern region receives over 600mm per annum. The western part receives rain in the late summer (peaking in February). The central part receives rain in the mid summer (peaking in January) while the eastern part receives rain in early summer (peaking in December). The low rainfall in the region is supplemented by dew and frost occurs in the night. The northwest is characterized by a great variation of seasonal and daily temperature, being very hot in summer with a daily average high temperature of 32^0 C in the month of January and is mild to cold in the winter with an average daily minimum in July at 0.9^0 C according to the weather statistics report (Kiefer, 2004). Given the arid to semi-arid conditions of the study area, the vegetation comprises plants that adapt to such climatic conditions (Xerophytes). Therefore, the Amalia Blue Dot Mine area in the North West Province is vegetated with Kalahari thornveld and shrub bushveld. The land use in the area is predominantly livestock farming. (Cattle farming). The predominant vegetation in the Blue Dot mine, Amalia area is grass. However, the surroundings of the Abelskop and Bothmasrust hills, where the soil cover is very thin, is covered with an abundance of shrubs which comprise mainly the acacia family specifically camel-thorn (i.e. acacia giraffe) and the less abundant shepherd trees (Boschia albitrunca). The alluvium-filled valleys of Abelskop and Goudplaats are mostly covered by grass, while where the soil cover is very thick, around Goudplaats 96 HO and northern part of Abelskop hill, covered with vast stretches of grass with isolated patches of bushes and shrubs (Ackon, 2001).

1.6.3 Topography, Climate and Vegetation of Northwest Tanzania

The landscape of mainland Tanzania is generally flat and low along the coast but, a plateau at an average altitude of about 1,200m constitutes the greater part of the country. Isolated mountains groups rise in the northeast and northwest. The topographic features of Tanzania include the highest and lowest parts of Africa (Mt. Kilimanjaro at 5,895 m and Lake Tanganyika at 358 m below sea level). The Great Rift Valley, which is often marked by long, narrow and deep depressions, often filled with lakes, is another main topographic feature of the country(Agrawal et al., 2003) (Fig 2.4).The Kagera area is generally hilly and partly mountainous. The average annual rainfall is about 1137mm (Simon, 2003).The Kagera and Ruvuvu rivers drain this area particularly near and around Kabanga Ni-project.

The climate ranges from tropical to temperate in the highlands and is characterized by the long dry spell from May to October and a period of low rainfall from November through April and a few days/weeks of heavy downpours (Agrawal et al., 2003.). The beginning of the rainy season varies from region to region. For example, along the coast, the rainy season is between March and May as well as October and December. These areas receive about 1,500 mm of rain per annum and the temperature is between 20 - 30°C. The highlands in the central part of the country are generally dry and receive 500 to 850 mm of rain and have a temperature of 10 - 35°C. The hottest period falls between November and February (25°C - 31°C) while the coldest period occurs between May and August (15° - 20°C). The short rains are received from October to December while the long ones from March to May each year. Almost 2/3 of Tanzania would have an equatorial climate, were it not for the high altitude of much of the country.

The diverse topography of Tanzania is accompanied by an enormous variation in its soil patterns and vegetation; the most fertile soils in the country are volcanic soils. The vegetation varies from tropical rainforest, woodland and bush land savannah to semi-arid and short-grass savannah. It is usually dry and hot in the central plateau, hot and humid in the coastal areas, and cool and moist in the highlands.

CHAPTER TWO

2.1 GEOLOGY

The study areas are located in two regions with very contrasting geology, in terms of age and rock types. The first area is located in the North western part of Tanzania, which is mainly Proterozoic in age (Pina, 1999) (Fig 2.1). The study area being investigated is as follows; Kabanga main, Kabanga north and Luhuma prospect which fall within an Ankolean tectonic setting underlain by metasedimentary and mafic-ultramafic intrusive rocks. They are partly covered by the lateritic regolith materials. The second area is located in the North western part of South Africa, Amalia in the Kraaipan Greenstone Belt (Fig 1.1). The Amalia Blue Dot Mine study area comprises of Abelskop, Bothmasrust and Goudplaats mineralized sections that are underlain by succession of Archean ultramafic-mafic assemblages, banded iron formation (BIF) and metasedimentary rocks(Kiefer, 2004)(Fig 2.6). These poorly exposed successions of rocks are enveloped by the granitoids. The Amalia Blue Dot Mine area is partly covered by the aeolian regolith materials.

2.2 Regional geology

The north western part of Tanzania falls within metasedimentary rocks of the Karagwe – Ankolean tectonic setting. This Karagwe-Ankolean tectonic setting is part of the large Meso-proterozoic Kibaran Orogenic belt, which stretches NE-SW across the Eastern part of the Democratic Republic of Congo, comprising Kivu and Shaba areas, to the western part of Uganda through Burundi, Rwanda, NW Tanzania (Rumuvegeri, 1991). Towards the eastern part of the Ankolean – tectonic domain lies the unmetamorphosed molasses type of Bukoban sediments (Fig 2.1). This domain is characterized by metasedimentary rocks of the Neo-proterozoic age i.e. post-Ubendian (1800-1700Ma), with a minimum age of about 1330Ma., the oldest date for intrusive granites in Burundi (Cahen et al., 1984).This Karagwe-Ankolean system is also known as Burundian Supergroup in Burundi and Rwanda. The metasedimentary rocks (probably derived from the Tanzania and Congo Cratons) were metamorphosed during the major intracratonic meso-Proterozoic Kibaran Orogeny at about 1300Ma (Pina, 1999). The typical rock types in the area comprise quartzites, phyllites, quartz schist and andalusite bearing mica schist adjacent to synkinematic granite batholiths, metavolcanic rocks are found to be generally rare. (Ikingura et al., 1992, Grey, 1967).

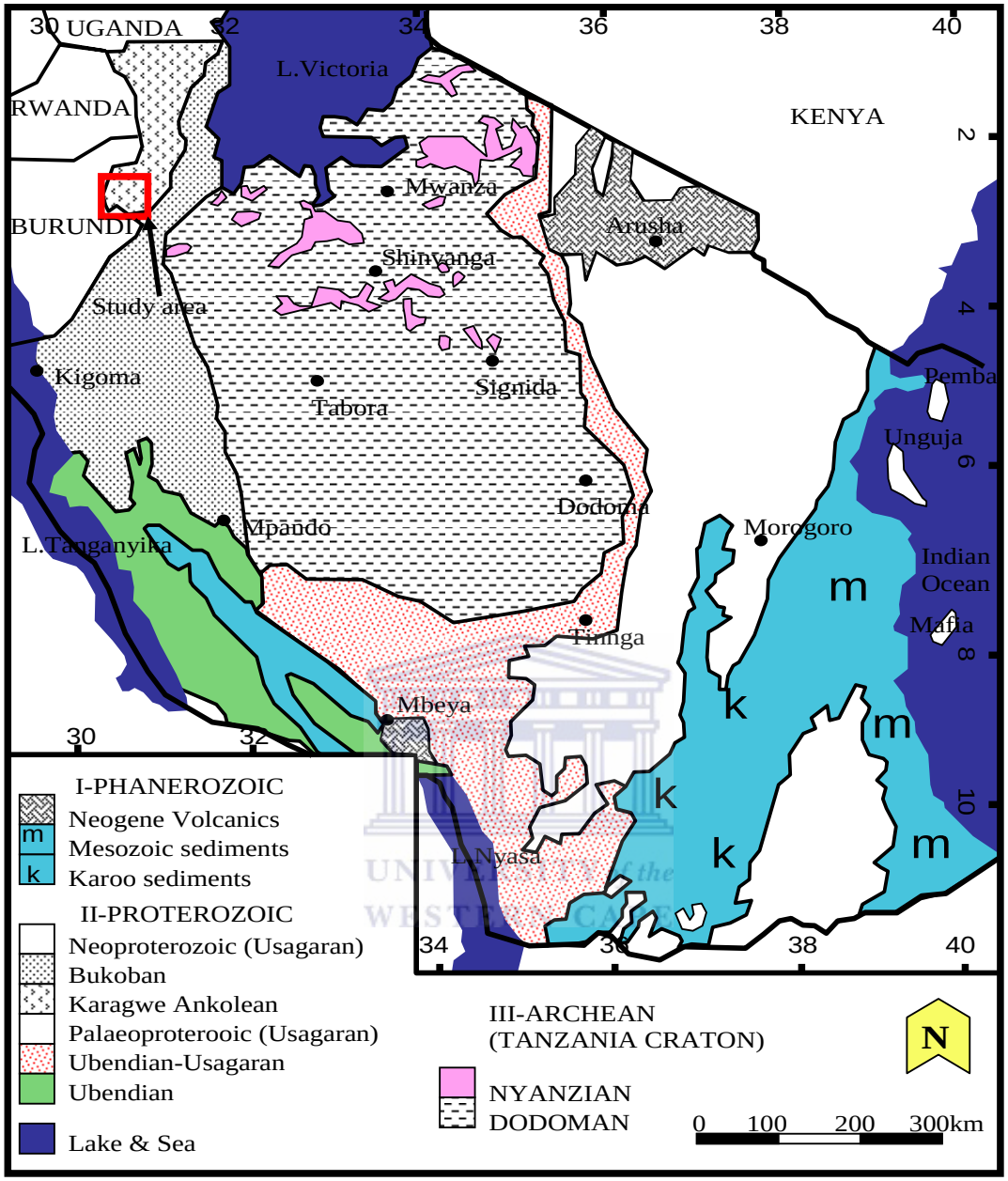

Fig 2.1 Geological map of Tanzania and location of study area (After Muhongo 1994) modified from Simon (2003).

2.2.1 Lithostratigraphy

The lithologies of the Karagwe-Ankolean tectonic setting, this Kabanga area, can be subdivided into three units as follows; the upper, middle and lower units (Table 1). The upper unit comprises of the purple phyllites and quartzite; the middle unit consists of the orthoquartzite and graphitic schist and the lower unit comprises of the massive bedded orthoquartzite, sheared basal schist and

phyllonites (Harris, 1961). These rocks have been folded along N to NNE trending axes with local cross-folding.

2.2.2 Geology of Kabanga and Luhuma area

Both Kabanga and Luhuma prospects are within the Karagwe-Ankolean tectonic domain of the Mesoproterozoic age (Fig 2.3). The rocks of the Karagwe-Ankolean tectonic domain are in the NW of Tanzania and occupy the western part of the three districts of Bukoba, Biharamulo and Ngara. In the eastern parts of Kungwe Bay on Lake Tanganyika, far to the south of the named districts, lies the Itiaso series that may be correlated with the Karagwe Ankolean (Fig 2.1). Other series thought to be part of the domain are Buanji and Ukinga. Two major lithological units underlie the Kabanga area, the metasedimentary rocks and mafic-ultramafic igneous intrusive bodies (Fig 2.3). The metasedimentary rocks are fine-grained metamorphosed banded metapelites, schist and the coarse grained quartzite. The metasedimentary rocks are intruded in the eastern part of the studies area by ultramafic bodies as shown by the geophysical map of the area (Simon, 2003). To the west of the Kabanga area lies relatively large, usually foliated syntectonic granite popularly referred to as Bushubi batholiths which appear to extend from the north of Rulenge through Muyenzi, Bukiriro and Kabanga extending to Burundi (Table 1). The Kabanga deposits in north western Tanzania are situated where the host rocks have undergone low-to medium-grade metamorphism, and subsequently developed a north-easterly to northerly structural trend. (Tack et al., 1994).

Table 2.1 A simplified stratigraphy of the Karagwean-Ankolean tectonic domain. (Modified from Harris 1961; Gray, 1967, Rumgeveri 1991, Ikingura et al., 1992 & Muhongo, 1994).

Age(Ma)	TECTONIC UNIT	STRATIGRAPHY&EXPLANATION	
900-1050	Post-tectonic granites (e.g. Nyamakombe, Mukerere, and Maleba plutons.		
1275±11	Musongati mafic-ultramafic intrusion in Burundi	Purple phyllites, quartzite	Upper Unit
1300	KARANGWE-ANKOLEAN TECTONIC-DOMAIN	Orthoquartzite and graphitic schist	Middle Unit
	Late syntectonic granites(e.g. Bushubi batholith around Kabanga, Bukiriro, Muyenzi and Rulenge	Massive bedded orthoquartzite sheared basal schist and phyllonites.	Lower Unit
		Ukingan (Southern Tanzania); comprise argillites, arenites, which unconformably overlie Ubendian system.	

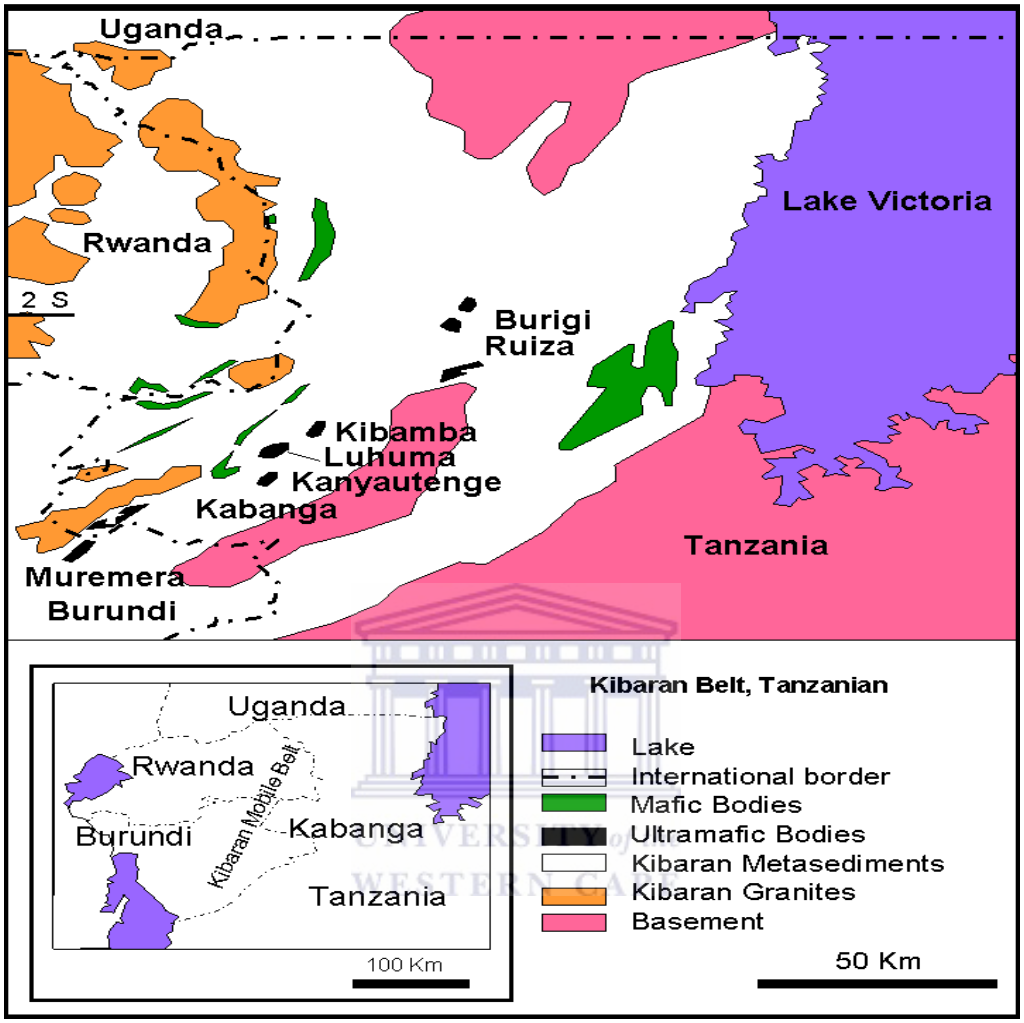

Fig 2.2 Map showing geological setting of both Kabanga and Luhuma areas (After Evan et al., 2000).

Luhuma has a similar geological setting to the well studied Kabanga. The geology of the area is characterized by metasedimentary rocks comprising of metapelites (MPEL) and mafic-ultramafic rocks. The metapelites are found occurring as a small unit at the centre of the studied area very close to the mafic-ultramafic bodies (Fig 2.2). The large part of Luhuma area is covered with the undifferentiated spotted schist while graphitic schist occupies the eastern parts of Luhuma area. There is also a reported occurrence of recrystallised quartzite outcrops in the area. Little is known about the stratigraphic of the Luhuma area. However, based on outcrop relationships, there is close structurally similarities between the outcrops of both Kabanga and Luhuma with respect to strike and dip appearing at almost same direction. The information gathered from the drill holes affirmed

the similarities between the Kabanga and Luhuma. The mafic-ultramafic intrusive rocks have been mapped out by geophysical methods both on regional and local scale. The intrusive bodies were obviously structurally controlled. The field mapping exercise carried out in the area (Simon, 2003) on the scale of 1:20000 revealed that these bodies are poorly exposed but few exposures were mapped, in some places just over geophysical signature. There was no reported evidence of overturning in the metasedimentary rocks in Luhuma area as in the well studied Kabanga area.

2.2.3 Nickel-copper ore deposit at Kabanga

The Ni-Cu sulphide ore deposits in Kabanga seems to occur as groups of several small volume bodies of complex shape loosely associated with a parent mafic-ultramafic intrusion (Evan et al., 1999). The ore bodies were found to be geometrically inclined to the southern part (Kabanga Main) of the studied site. The ore bodies were divided into different blocks as follows; in the southern part Kabanga Main and adjacent MNB (Main North Body) deposit which were discovered in 2001. Also, in the northern part Kabanga North, Kabanga North extension and Kabanga/MNB (Main North Body) extension were discovered in 2002. The sulphide mineralization at both Kabanga Main and Kabanga North occur in three different zones viz; (i) peripheral vein zone (synonymously called detached ore in this study) is in the form of massive sulphide vein or disseminated sulphide within metasediments (MPEL) or mafic sills in the original footwall (Fig 2.3), (ii) contact mineralization which occurs at the basal contact(west-east) of both Kabanga North and Kabanga Main intrusive and (iii) the central zone type which is commonly associated with magmatic layering of silicate cumulate(olivine) minerals, olivine and pyroxene(Evans et al., 2000). It is characterised by the net-textured sulphides within these layers which occur commonly in discrete forms. The mineralization was reported to have hosted approximately 21 million metric tonnes grading 1.66% Ni, 0.23% Cu, and 0.14% Co calculated at a cut-off grade of 0.7% Ni, and contains a higher-grade resource of 12.7 million metric tonnes grading 2.1% Ni and 0.16% Co using a 1.2% Ni cut-off (Danielson, 1997).

The description of the nickel sulphide mineralization is based on extensive geological mapping, drill core logging and geophysical surveys in the Kagera region of north western Tanzania by BHP Minerals International Exploration Inc. and Sutton Resources Ltd between the period of 1991 and 1995, Anglo American Company also in 2001, Barrick limited and Anglo American between 2001 and 2004. In recent Falconbridge are operating in the Kabanga Ni-Cu prospect.

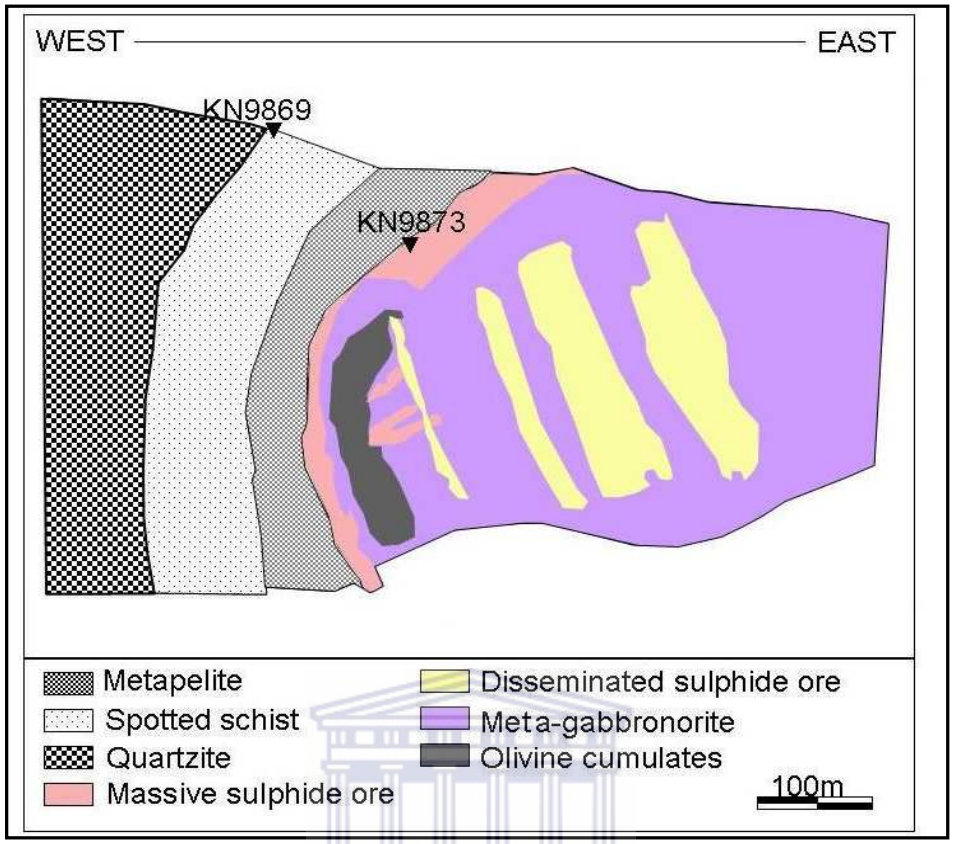

Figure 2.3 The sketch of Kabanga Main Ni -Cu sulphide deposit in cross section and the approximate locations of drill holes KN9869 and K9873, over which soil profiles were established (modified from Simon (2003)).

The Kabanga mafic-ultramafic intrusions are made up of largely olivine-pyroxene sulphide orthocumulate rocks, these have a discordant side walls, but largely conformable basal and upper margins (Duchesne et al., 2004). The Kabanga deposit has intrusions that were reported to act as conduits or feeders to some more voluminous gabbro and gabbro norite sills that are commonly found in the upper part of the stratigraphic position of the Karagwe-Ankolean sequence (Table 1).

2.2.4 Regolith distribution in Kabanga and Luhuma

The Kabanga Main, Kabanga North and the Luhuma prospect are covered by a thick blanket of lateritic regolith. The lateritic cover tends to occur as large blanket in the southern portion of the magmatic intrusion in Kabanga prospect (Kabanga Main). The lateritic regolith associated with the both ultramafic bedrocks and primary Ni sulphide mineralisation is reported to be enriched in the nickel (Ni). The pronounced lateritization in this domain has been proposed as a reason for the enhancement of nickel (Ni) values observed in the regolith materials from this terrain. The

previous work by Sutton Resources in the areas shown that the blanket of lateritic regolith in this terrain is a major challenge to successful exploration work. This was made worse by little knowledge of the regolith geochemistry in the domain. The diamond drill holes at different stages of exploration missed the ore target causing high cost risks to the drilling programme.

2.2.5 Regional geology and stratigraphy of the Kraaipan Greenstone belt.

The Kalahari Goldridge and Amalia Blue Dot mine are underlain by the Kraaipan Greenstone belts, north western parts of South Africa. The age of the Kraaipan greenstone is uncertain. Based on the available age data 3010 to 2920Ma could represent the possible of the Witwatersrand sediments (Poujol et al., 2002). The Kraaipan Group is composed of metamorphosed volcano-sedimentary and associated granitoid rocks occurring as isolated exposures extending from the southern Botswana in the north, and almost to the Vaal River near Christiana in the south. Extensive Ventersdorp Super group volcanic rocks covered the granite-greenstone in the region between Amalia and Schweizer- Reneke in the south, and Delareyville and Geysdorp in the north (Fig 2.4).

The Kraaipan granite-greenstone were geographically divided into two; northern domain and southern domain for the purpose of description (Anhaeusser and Walvaren, 1999). The Kraaipan rocks in the northern domain occur in three narrow NNW-trending belts, which are separated by different types of granitic, gneissic and migmatitic rocks while in the southern domain there is an occurrence of a greenstone belt (Kiefer, 2004)(Fig 2.4).

These volcano-sedimentary rocks (Anhaeusser and Walvaren, 1999) otherwise known as Kraaipan greenstones belts were intruded in the eastern part by granitic rocks of Schweizer-Reneke dome. The volcanic rocks of the Kraaipan Group are made up of metamorphosed and hydro thermally altered commonly massive and pillowed tholeiitic, andesitic basalt and volcanic tuffs. These rocks have undergone various stages of deformation, metamorphism and hydrothermal alteration to formed amphibole-chlorite-epidote schists commonly associated with the Banded Iron Formation (BIF) but the former is rarely exposed however, from all the rocks they are best exposed. The Kraaipan formation is subdivided into three sub-formations: the Gold ridge, Ferndale, and Khunwana Formations which comprise amphibole of tholeitic composition, calcareous schist, clastic sedimentary rocks and banded iron formation (BIF) (Fig 2.4). The Kraaipan granite-greenstone belts are blanketed by Tertiary-Recent Kalahari Group sediments, which is composed

of wind-blown loose sands, consolidated sand and calcrete. Despite this cover variety of granitic rocks are found to outcrop sporadically in the region. At least three granitoids varieties are recognised in the region (Zimmerman, 1994). The recorded varieties are discussed as follows:

(i) Foliated leucogneisses and migmatites (tonalitic and trondhjemitic gneisses), these are found to contain xenolithic bodies of Kraaipan amphibolites and banded iron formations (BIF), the typical outcrops are found widely dispersed, from the Botswana border in the north, to Amalia in the south

(ii) Fine-to medium-grained grey or pink, homogenous and in some places, weakly foliated, massive granitoids with cross cutting-dykes and veins. They are quite similar to the nearby Scheweizer Reneke Dome (Zimmerman, 1994).

(iii) Coarse-grained to pegmatite, homogenous, pink granite usually referred to as Mosita adamellite. All the three varieties of the granitoids contain xenoliths of Kraaipan rocks hence they appear to be younger than the greenstone developed in the area.

2.2.6 Local geology of the Amalia Greenstone Belt

The Amalia greenstone belt has a NNW-SSE that is approximately 4km wide and 55km long and is flanked on the eastern part by the granitic rocks of the Schweizer Reneke Dome. The Amalia belt underwent metamorphism of green schist facies during several periods of deformation which caused upright cleavage, small scale and large scale folding (best preserved in BIF) (Kiefer, 2004). The tonalitic and trondhjemitic gneisses are found to contain fragments of the amphibolite that occur to the west of the Amalia greenstone belt. The exposed rocks of the Amalia greenstone belt occur as steeply dipping green schist facies metamorphic assemblages comprising units of oxide facies banded iron formation (BIF), quartz-chlorite schist, amphibole-chlorite schists and quartz-carbonate rocks. (Jones and Anhaeusser, 1991; Kiefer, 2004) (Fig 2.5). The banded iron formation (BIF) is made up of fine layers (in most cases 1-10mm thick) of alternating hematite/magnetite and microcrystalline chert (Jones and Anhaeusser, 1993). The eastern and western contacts of the Amalia greenstone are unexposed (covered by wind-blown Kalahari sand) and in this case only inferred contact can be shown (Jones and Anhaeusser, 1991). The northern part of the greenstone belt also disappears under the blanket of the Ventersdorp lava in the proximity of Amalia Blue Dot Mine (Fig 2.4).

The Amalia Blue Dot Mine consists of 4 exposed areas dominated by outcropping Banded Iron Formation (BIF). Bothmasrust North, Bothmasrust South, Abelskop and Goudplaats (Fig 2.4 & 2.5). The lithologies comprise metamorphosed, strongly deformed, altered mafic-ultramafic rocks and minor sedimentary rocks represented by amphibolite, quartz-sericite schist, quartz-carbonate-chlorite schist, and plagioclase-carbonate- chlorite schist and carbonate talc schist (Kiefer, 2004). Three stages of deformation are recorded to have affected the Amalia greenstone belt (Anhauesser et al., 1991) are discussed as follows; (i) The early compressional phase of deformation (d_1) which occurred along the northeast-southwest axis which is believed to be responsible for the formation of early small scale tight folds observed in the Banded Iron Formation (BIF). The same compressional tectonic event is credited to be responsible for the development of the cleavage observed throughout the greenstone belt. (ii) The principal deformation event (d_2) which is possibly caused by the intrusion of the granitic rocks. This event leads to the formation of large-scale folding and warping of the Banded Iron Formation (BIF) and greenstone lithologies. The deformation caused a kinking of d_2 cleavage and lineations observed in the Banded iron Formation (BIF) and green schist as well as leading to the formation of bedding parallel slip and brecciation of the host rock which was influenced by the repeated replacement by quartz and calcite veins and (iii) The third stage of deformation (d_3) is reputed to produce minor structures, such as late stage, small-scale, disharmonic F_3 folds and faults. This late stage deformation is known to have caused right-lateral movement along a major NE-SW shear zone(exposed at Goudplaats Gold mine) which caused extensive rotational slip and deformation of the Banded Iron Formation(BIF), the greenschists and the granitic rocks. Mineralization of the Banded Iron Formation is closely associated with the degree of deformation imposed by the d_2 event and the amount of mineralizing fluid that was able to pass through the Banded Iron Formation (BIF) following faulting and brecciation caused by the d_3 deformation (Anhauesser et al., 1991).

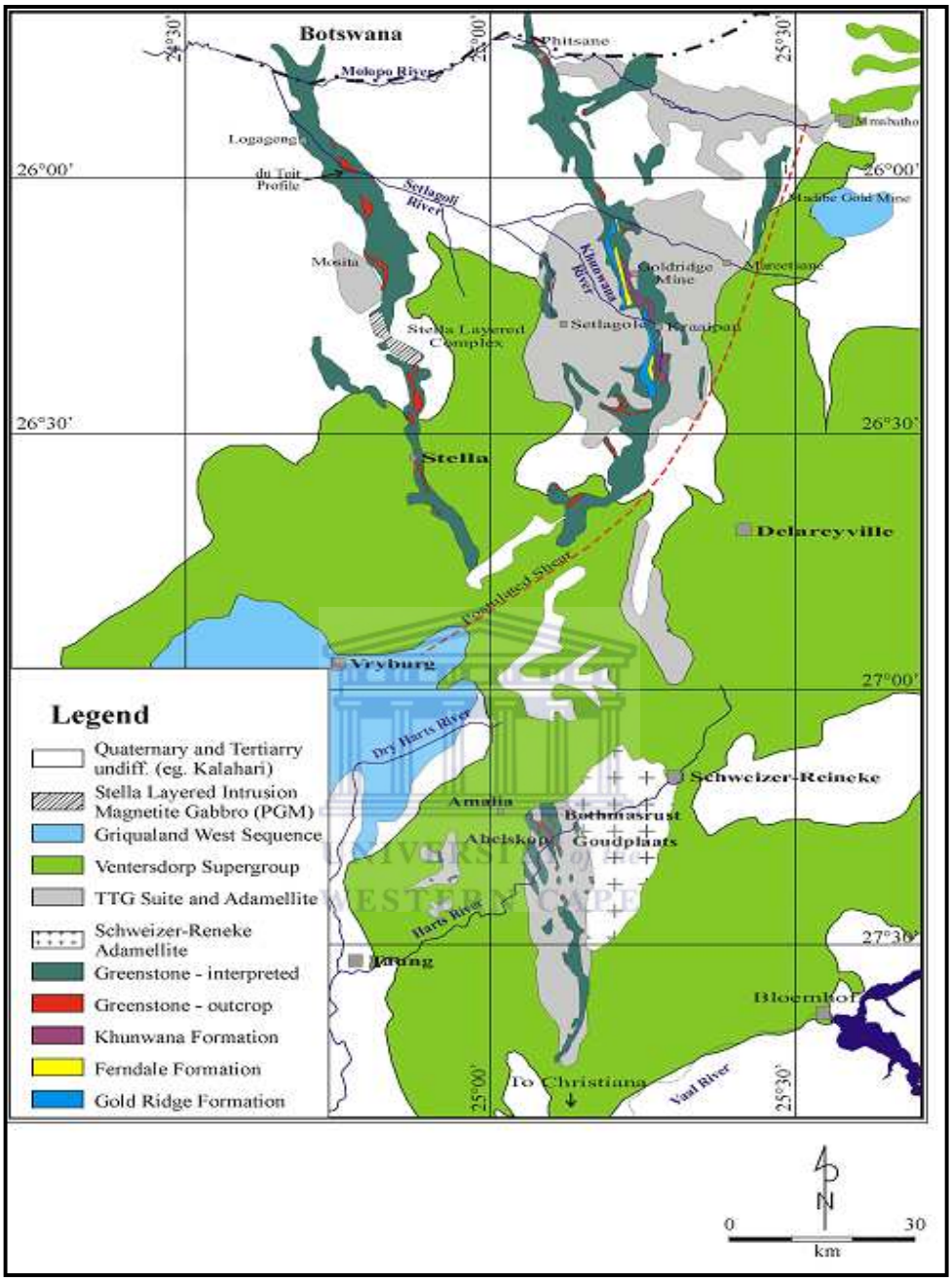

Figure 2.4 Geology of the Amalia and Kraaipan Terranes modified from Anhaeusser and Walvaren (1999) and Mowatt (1998). (After Kiefer (2004)).

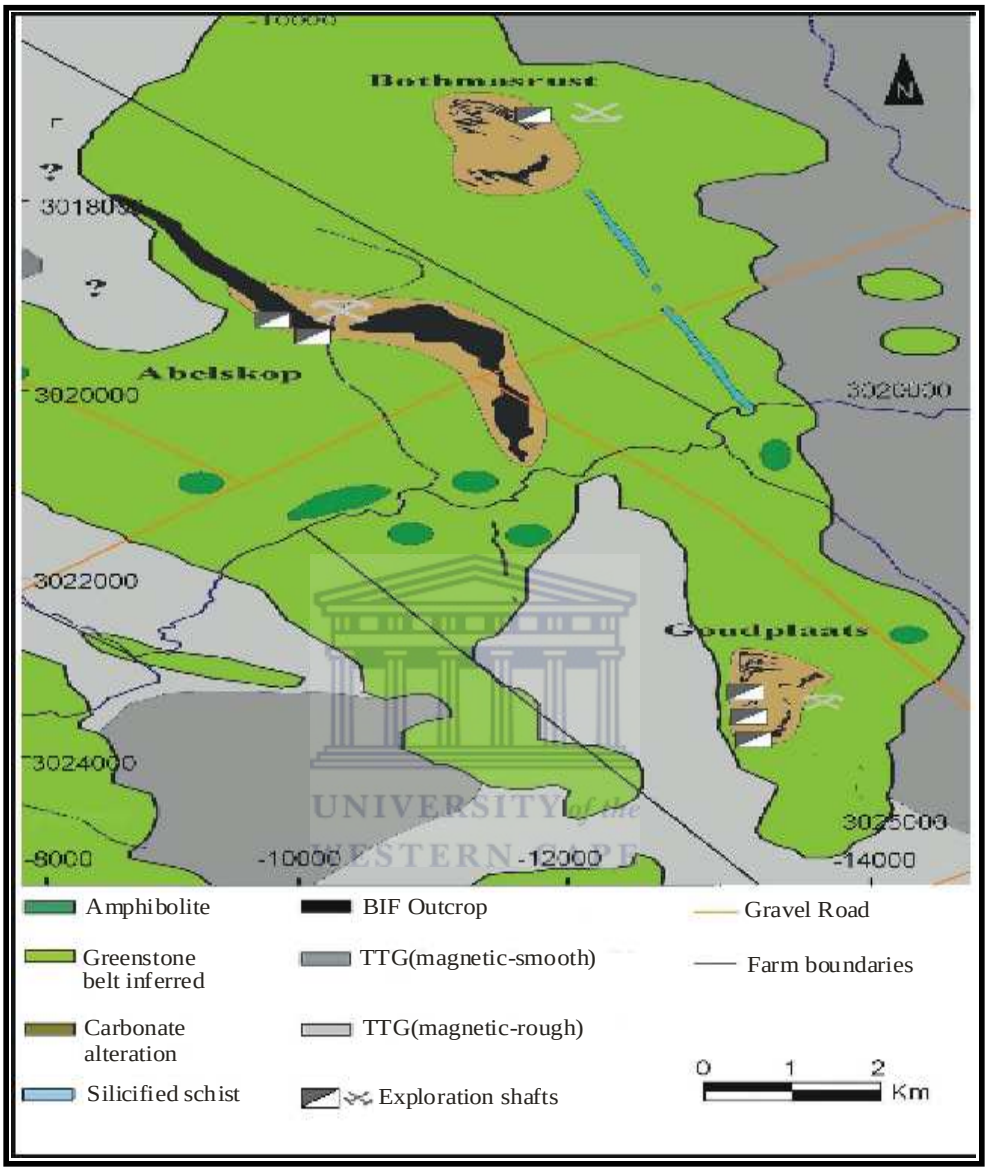

Fig 2.5 Local geology of the Amalia Blue Dot Mine areas (After Kiefer (2004)).

2.2.7 Gold mineralization at Amalia Blue Dot Mine

The style of mineralization at Amalia is of a vein/stock type mineralization, with sulphidation of hematite-magnetite layers and a partly carbonate-altered chert layer which is associated with quartz-carbonate veining (Kiefer, 2004). This causes massive to finely disseminated sulphide

mineralization along the contact zones of quartz vein and banded iron formation (BIF). The more iron rich banded iron formation (BIF) behaves more ductile, less fracturing, veining and less mineralized. The chert rich banded iron formation (BIF) is more mineralized. The sulphide mineralization is simple and dominated by traces of pyrrhotite, chalcopyrite, and gold. Therefore suggesting sub-green schist to upper green schist facies conditions during mineralization. Most of the pyrite occurs as clusters of cubic crystals, where the size is in direct relation to the distance from the quartz veins. The mineralization of the banded iron formation has a close association with the degree of deformation (Anhaeusser et al., 1991). In the Bothmasrust and Goudplaats the gold mineralization are found to be concentrated in faulted and brecciated banded iron formation (BIF). The fault itself is not mineralised. The non stratiform vein-type gold deposit hosted by the Abelskop Main BIF unit is characterised by a close association between gold, iron sulphide minerals and veins. Changes in fluid composition with progressive mineralization are evident from Goudplaats and Abelskop. At a later stage, the fluids change to a copper rich fluid phase forming chalcopyrite (Kiefer, 2004). Pyrite is the main sulphide mineral with traces of chalcopyrite and pyrrhotite. Gold is hosted by one iron formation. (Abelskop main BIF unit) and restricted to late crosscutting quartz veins and iron sulphide rich zones adjacent to the veins (Kiefer, 2004).

2.2.8 The Regolith in the Amalia Blue Dot Mine

In most part of Australia and Africa the regolith is formed continuously for over 100million years in a variety of climate, and hence is an expression of cumulative effects of this long weathering history (Anand and Butt, 1998). The negative effect of weathering with respect to its impact on the geological, geophysical, geochemical mapping and exploration techniques, often limits their use. The effects of weathering can be used in exploration, for example, by exploiting secondary geochemical dispersion haloes, some of which give targets many times larger than the source deposit. The weathering processes often lead to the formation of profiles that reflect the interplay of weathering, erosion activities and transportation/relocation of weathered materials over a long period of history. In the most incomplete weathering profile there is a general upward sequence of parent rock, saprock, saprolite clay zone mottled zone, lateritic duricrust, lateritic gravel and soil (Anand and Butt, 1998).

The regolith in the Amalia Blue Dot Mine consists of *in-situ* weathered basement rocks, overlain by a colluvium and a valley-filled sedimentary sequence comprising carbonate-impregnated pebbly to coarse/medium-grained sands at the base, followed by an upper reworked friable/laminated calcrete (Okujeni et al., 2005). These discrete regolith units are unconformably overlain by fine- to

medium-grained ferruginized aeolian sand. The thickest and most laterally extensive regolith sequence occurs along major drainages. Broad valleys and deep channels permitted widespread development and preservation of thick colluvial and alluvial sediments, which were subsequently overlain by aeolian sand.The high relief portion of the study site is reportedly covered by rubbles, screes, scattered outcrops of greenstone and Banded Iron Formation (BIF). The relatively low lying areas are beneath the Abelskop and Bothmasrust ridges and their surroundings are partly covered by aeolian sand and scree (Ackon, 2001). The high relief areas (ridges) are covered by soil with a brownish to brick-red coloration, friable sand with abundant concretions of iron oxide. Transported aeolian sand covered a vast region of the flat lying topography with a varying thickness from less than 1metre to 5m in the study site. Regolith materials of less than 1m in thickness are found to cover the northern, southern and eastern part of the study site and typical example can be found around the east of Bothmasrust, the northern section of Goudplaats and around Abelskop hill. The regolith components in this region are medium to fine grained and contain higher mottled quartz and iron oxide content at the base. The intensity of the iron coatings of the quartz grains in the regolith materials in the study site varies from high-medium-low mottleness. The intensity of the mottling is highest in the high relief portion of the study site; this observation suggests subtle interaction between the bedrock and the overlying regolith materials which is typical of the erosional and regolith regime environment. (Anand and Smith, 1993). The iron coated regolith materials otherwise called Ferruginous regolith materials are abundant and widespread in both Australia and Africa. It has been successfully used as a sample media in Gold (Au) exploration in Yilgarn Craton of Western Australia. (Anand, 2001).

CHAPTER THREE

3. MATERIAL AND METHODS

3.1 Field work

The materials for this study were collected from two contrasting regolith environments as follows; insitu lateritic regolith materials collected from Kabanga and Luhuma in the north western part of Tanzania (Simon, 2003) and aeolian transported regolith materials from Amalia Blue Dot Mine, north western part of South Africa (Ackon, 2001). A follow-up field visit was made to the Amalia Blue Dot Mine study site between November and December 2004 during which the sampling sites were studied.

3.1.1 Kabanga and Luhuma

The field work at Kabanga and Luhuma area was undertaken between December 1999 and February 2000 (Simon, 2003). The regolith mapping and soil sampling was undertaken within this period. The soil sampling was carried out with the use of GPS based on the UTM zone 36 datum as shown in Fig 3.2.

- Samples were taken at intervals of 50meters in the Kabanga along the traverses L9893N, L9850N, L11528 and L11670N that cut across the Kabanga North and Kabanga Main mineralization (Fig 3.1).
- Sampling at Luhuma was undertaken along a 100x100 sampling grid, part of which is shown in Fig 3.2. The soil samples were taken at the depth of approximately 20cm using a hand shovel. About 500grammes of the regolith samples were reportedly taken and subsequently preserved in plastic bags.

In all 42 samples collected from Kabanga and Luhuma were made available for the purpose of this study.

3.1.2 Amalia Blue Dot Mine

The field study and soil sampling (Fig 3.3) was carried out in September 1999 for the approximate period of two weeks (Ackon, 2003). A soil Auger was used in the collection of the regolith samples at an interval of 250m. Approximately 500 grammes of the samples were taken at the topmost and basal layers of aeolian sand and subsequently preserved in the plastic bags. A total of 278 samples were collected from both the upper and lower soil horizons in Amalia Blue Dot Mine. Sixty-nine of these samples was taken from lower soil horizon along traverses.

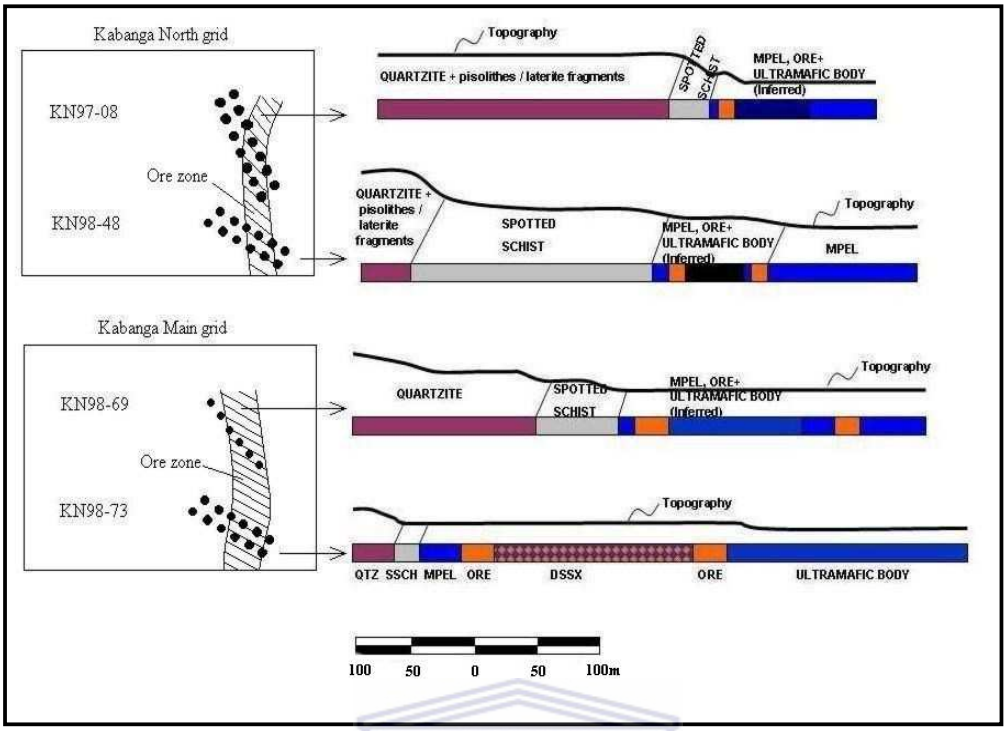

Figure 3.1 Kabanga Main & and North geology & sampling plan modified from Simon (2003).

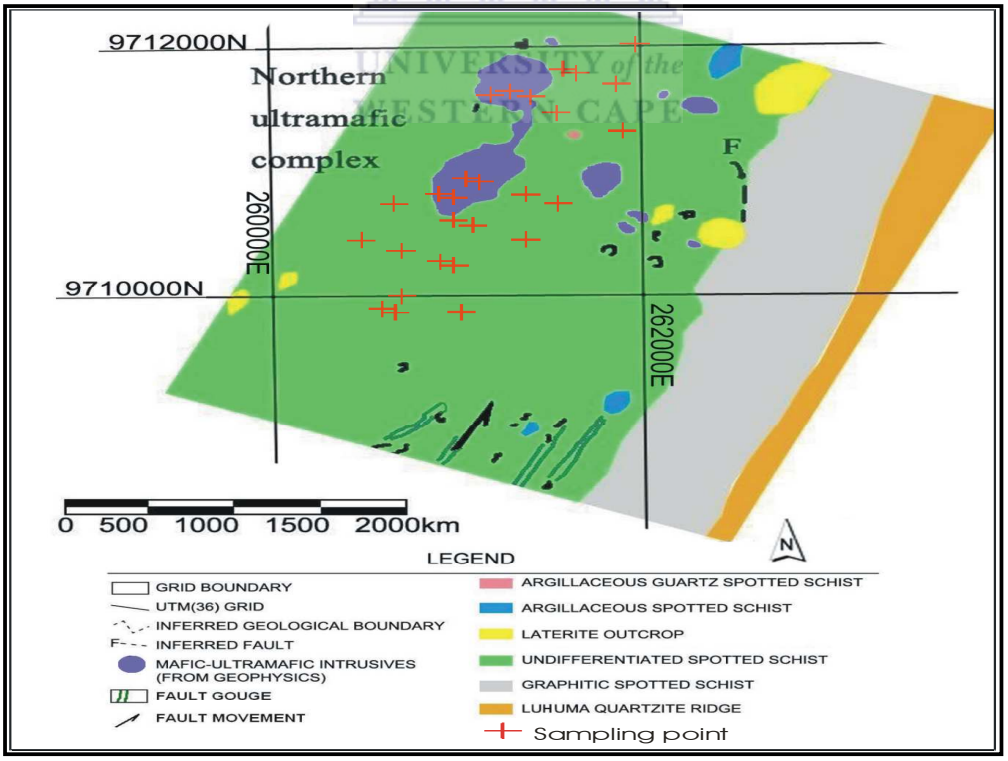

Figure 3.2 Luhuma prospect geology and sampling plan modified from Simon (2003).

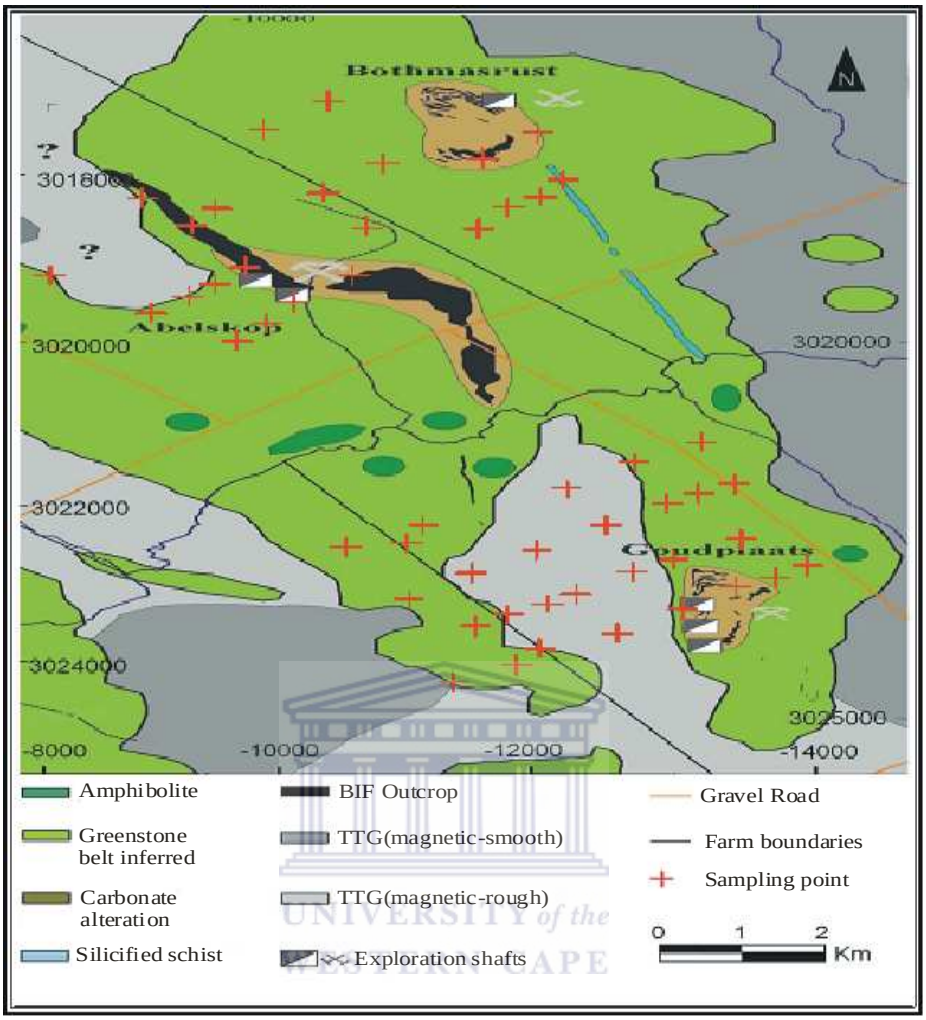

Figure 3.3 Amalia Blue Dot Mine prospect geology from Kiefer (2004) and sampling plan.

3.2 Sample preparation

The soil samples taken from Kabanga Main and Luhuma were sieved into the following mesh sizes as follows: >122 µm, <122 µm and <75 µm soil fractions (Simon, 2003). Previous exploratory work in the area has figured out which fraction gave the best geochemical response. Less than 75 µm soil fractions gave the best response (Simon, 2003). The <75 µm soil fractions is not available for this work. Less than 122 µm soil fractions are associated with low background geochemical noise (Simon, 2003). Therefore <122 µm soil fraction were therefore used in this study. The samples taken from Amalia Blue Dot Mine were sieved into the following; mesh sizes; <75 µm, <125 µm, and >125 µm fractions. The sieved fractions were kept in the plastic bags. Previous works in this study site have recommended the use of finer fractions of regolith material

for future exploration geochemical work (Ackon, 2001). The amorphous Fe and Mn oxides are mostly concentrated in the finer fractions thereby given higher geochemical response (Yang, 2006).

3.3 Partial/selective extraction techniques

Partial and selective leach dissolved the weakly bound ions absorbed into the sample matrix e.g. soil and weathered soil fragments. Selective extractions are designed to only attack specific component within a sample. Some reagents dissolve precipitated carbonates or other salts, while other attacks Mn-oxides or amorphous Fe-oxides, or extract ions held in organic complexes.
The partial extractions which often have a low pH (acid) might attack all of these components within a sample to some extent. The degree of dissolution depends to a large extent on the intensity of weathering that a sample has undergone and resultant secondary mineral species in the sample.
The aeolian sand may have in abundance loosely absorbed Fe and Mn oxides components (Ackon, 2001). Hydroxylamine hydrochloride is capable of attacking the Mn-oxides or amorphous Fe-oxides component in soil and sediments (Tessier et al., 1979). Some of the disadvantages of hydroxylamine leaches are however as follows; i) The hydroxylamine leaches often have limited use in deeply buried mineralised terrains ii) Selectivity can vary from sample to sample depending on the varying mineralogy of the sample suite and overall changes in the leach solution during the leach process (McAlister and Smith, 1999).

The selective ability of hydroxylamine depends on the parameters such as concentration of reagent, the time and nature of contact, ratio of solid-to-solution, temperature and the composition of the sample (Fonseca and da Silva, 1998; Hall et al., 1996). Previous investigation of the parameters like effective sample weight, effective sample size, and temperature were carried out (Yang, 2006 and Xu, 2006). The results obtained showed that the use of one gram of the aeolian sand, <75 μm size fraction and water bath temperature of 50ºC are effective parameters for the hydroxylamine hydrochloride leach.
These parameters were determined using transported regolith samples taken from the north-eastern sector of Morokweng impact structure, northwest, South Africa. The detail of these established parameters has been reported in the work of Yang (2006) and Xu (2006).

This study focussed on a comparative appraisal of hydroxylamine hydrochloride and aqua regia partial leaches of samples from two contrasting terrains. The data from aqua regia (AR) and triple

acid leach (TAL) are used in this work to establish a geochemical baseline. The hydroxylamine hydrochloride (HH) leaches that were used to accomplish this work are as follows; i) cold hydroxylamine hydrochloride leach. ii) hot hydroxylamine hydrochloride leach. The details of the condition of reaction of the partial leaches are as follows;

3.3.1 Partial extraction using aqua regia

The aqua regia solution was prepared by the combination of nitric acid and hydrochloric acid in the ratio of 1:3 (Chao, 1984). One gram of the samples was extracted with 30ml of the aqua regia solution in an Erlenmeyer conical flask covered with a lid. The aliquots were heated at 180ºC for one hour on a sand bath. The aliquots were allowed to cool down for 1 hour and filtered into another Erlenmeyer conical flask. Aliquots were later put into a sample bottle for the analysis of the following suite of elements Ni, Co, Cu, Pb and Zn in all the samples by Atomic Absorption Spectroscopy (AAS) (Simon, 2003).

< 122 μm sieved fractions from 42 regolith samples taken from Kabanga Main and Luhuma nickel-copper prospect were extracted using aqua regia solution. The aqua regia leach is designed/formulated to extract element from the oxides, carbonates, sulphides, chlorides, most sulphates and partially clays. Similarly <75μm sieved fractions of the 17 regolith samples taken along a profile from Amalia Gold prospect were extracted with TAL. The triple acid leach is a combination of hydrofluoric acid, nitric acid and hydrochloric acid in the ratio of 2:1:1 (Chao, 1984; Fonseca and da Silva, 1998).

3.3.2 Hydroxylamine hydrochloride partial extraction

Cold hydroxylamine hydrochloride leach at room temperature (22-25ºC) can selectively leach manganese oxides which are known to be powerful scavenger of heavy metals (Kelley, 2003). Manganese exists in several oxidation states and variety of amorphous and crystalline forms. As a result manganese oxides have extraordinarily high cation exchange capacity (CEC) and therefore absorb different trace elements on its surfaces. Cold hydroxylamine leach doesn't dissolve crystalline iron oxides but dissolve small amount of amorphous hydrous iron oxide (Kelley et al., 2003).

Hot hydroxylamine at higher concentration with elevated temperature (50ºC) under acidic condition is capable of effectively dissolving amorphous iron oxides while leaving crystalline iron oxide intact. Amorphous iron oxide is a much more effective scavenger than crystalline forms of

iron oxide in neutral to slightly alkaline condition. The hot hydroxylamine leach is quite therefore informative about metal ion mobility (Kelley et al., 2003).

Hydroxylamine hydrochloride solutions were prepared using a reagent with 98% purity as follows;
0.1M hydroxylamine hydrochloride = 6.95g $NH_2OH.HCl$ add 10ml of 10% HNO_3 and then made up to one litre with distilled water.
0.15M hydroxylamine hydrochloride = 10.43g $NH_2OH.HCl$ add 15ml of 10% HNO_3 and then add distilled water till 1000ml and stir up to dissolve.
0.2M hydroxylamine hydrochloride = 13.90g $NH_2OH.HCl$ add 20ml of 10% HNO_3 and then add distilled water till 1000ml and stir up to dissolve.
0.25M hydroxylamine hydrochloride = 17.37g $NH_2OH.HCl$ add 25ml of 10% HNO_3 and then add distilled water till 1000ml and stir up to dissolve.

Preparation of hydroxylamine hydrochloride solution in dilute HCl for extraction of amorphous Fe-hydroxides phase was advocated by Hall et al., (1995). In this work dilute nitric acid (HNO_3) was used as it provides a more stable background during ICP-MS analysis.

Cold hydroxylamine hydrochloride ($NH_2OH.HCl$) concentration was varied between 0.1M and 0.25M in nitric acid (HNO_3). One gram of the samples was extracted with 90ml of the hydroxylamine hydrochloride in plastic bottles and cover with a lid. The solutions were shaken for 1 hour at room temperature and allowed to settle down. The extract was filtered into an Erlenmeyer conical flask and subsequently preserved in sample bottles for measurement of the following suite of elements; Ni, Co, Cu, Mn, and Fe with Atomic Absorption Spectrometry (AAS). The effective temperature parameter for hydroxylamine hydrochloride leaching technique was determined using the selected lateritic regolith samples taken from Kabanga and Luhuma. This involved the use of both cold and hot hydroxylamine hydrochloride partial extraction.

In hot hydroxylamine hydrochloride leach, one gram of samples was extracted with 90ml of hydroxylamine hydrochloride in plastic bottles and covered with a lid. The solutions were heated in the water bath at 50°C for 1 hour. The samples were removed from the water bath after 1 hour and allowed to cool down. The extractants were filtered into an Erlenmeyer conical flask and preserved in sample bottles (Fig 3.4). The following suites of element; V, As, Rb, Ag, Cd, Os, Au, Zn, Pd, Pb, U, Se, Ru, Cr, Cu, Rh, Pt, Ir, Re, Ba, Fe, Mn, Co, and Ni were analysed using Induced Plasma

Couple Mass Spectrometry (ICPMS). Ten selected regolith samples each from Amalia Blue Dot and Kabanga Main was used for this orientation work.

Similar hot hydroxylamine leach reaction condition was used for the main study conducted on the samples taken from both lateritic and aeolian regolith environments. The analysis of ; V, As, Rb, Ag, Cd, Os, Au, Zn, Pd, Pb, U, Se, Ru, Cr, Cu, Rh, Pt, Ir, Re, Ba, Fe, Mn, Co, and Ni were done with the Induced Plasma Couple Mass Spectrometry (ICPMS) in the Department of Geological Sciences, University of Cape Town.

The main study involved the use of established optimum extraction condition in the orientation studies to extract metals using hydroxylamine hydrochloride (HH). In all 42 lateritic regolith samples taken from both Kabanga (Main & North) and Luhuma Ni-Cu prospect were extracted under established optimum reaction condition of 0.25M hot hydroxylamine hydrochloride solution. Sixty-nine aeolian transported regolith samples taken at both lower and upper horizon along a profile were extracted using 0.1M hot hydroxylamine hydrochloride solution.

3.4 Geochemical analysis

A Varian model spectral AA-10 Atomic Absorption Spectrometer was used for the measurement of the following suites of element; Ni, Co, Cu, Mn and Fe during the first orientation studies using the lateritic regolith samples from Kabanga and Luhuma.

Table 3.1 Instrument parameters for AA-10 Atomic Absorption Spectrometer

Instrument Parameter	Nickel(Ni)	Cobalt(Co)	Copper(Cu)	Manganese(Mn)	Iron(Fe)
Wavelength	232.0nm	240.7nm	324.8nm	279.5nm	248.3nm
Band pass	0.2nm	0.2nm	0.2nm	0.2nm	0.2nm
Lamp current	7mA	7mA	4mA	6mA	7mA

The following procedures were used to prepare reagents for calibration of the Atomic Absorption Spectrometry (AAS). Standard solution for the analysis was prepared by making 50ppm of the

Stock solutions. The serial dilutions of the stock solution were made using de-ionised water to prepared standards with the following concentrations ranges: 5ppm, 10ppm, 15ppm, and 20ppm. The standard solutions were subsequently used to calibrate the Atomic Absorption Spectrometry (AAS).

The instrument parameters for Induced Couple Plasma Mass Spectrometry (ICPMS) are not available to the author since the leached samples were sent to the Department of Geological Sciences, University of Cape Town for analysis.

3.5 Quality control

The analytical accuracy and precision of the analytical method were carried out to ensure good data quality. The quality control were carried out as follows; comparative evaluation of the certified concentrations of NIST-1643d standard and measurement on the ICPMS. Duplicate samples and blanks were also introduced into the analytical programme.

3.5.1 Semi quantitative analysis (ICP-MS)

The comparative evaluation of the certified concentrations for the NIST-1643d standard with the results obtained on the ICP-MS in this run allowed assessment of the analytical error on the run. The results are presented in the Table 3.2. Although a semi-quantitative run is expected to be within 20% error, this particular run shows a much greater analytical accuracy, most samples fall within 5% of their known concentrations. The standards do not include all analyte elements, so there are some elements for which the accuracy is not known. Duplicate analyses were not carried out for semi quantitative analysis due to time constraint. This is required in order to determine the precision of the semi quantitative analytical method.

Fig 3.4 Picture showing the extract in the sample bottles.

3.5.2 Duplicate analyses

Comparison of data obtained from sample and duplicates were carried out to allow assessment of the level of the precision of the analytical method used. Samples from both Kabanga (Ni-Cu prospect) and Amalia Blue Dot Mine were used for this purpose. Both laboratory and duplicate samples were made for the selected regolith samples. The results of duplicate analyses for both nickel and gold are presented in the Appendix E_1 and E_2. The result shows that the error associated with most of the measurements fall below 10% of the relative percent difference (RPD).

The precision control scatter plot for nickel, copper and gold are shown in the Figures 3.5 and 3.6. The scatter plot shows variability in the result obtained from both laboratory and duplicate analyses. In the overall assessment the analysis shows good precision of <10%.

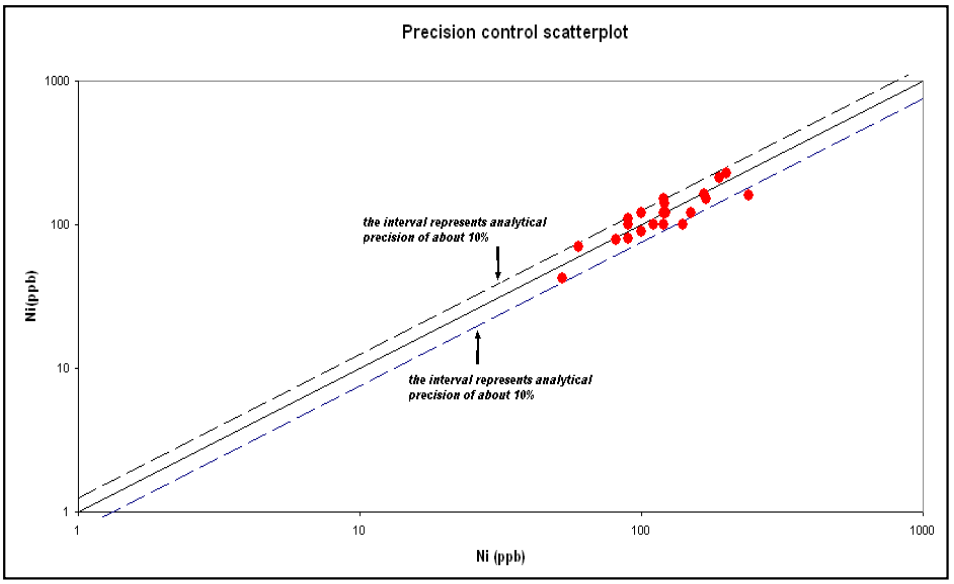

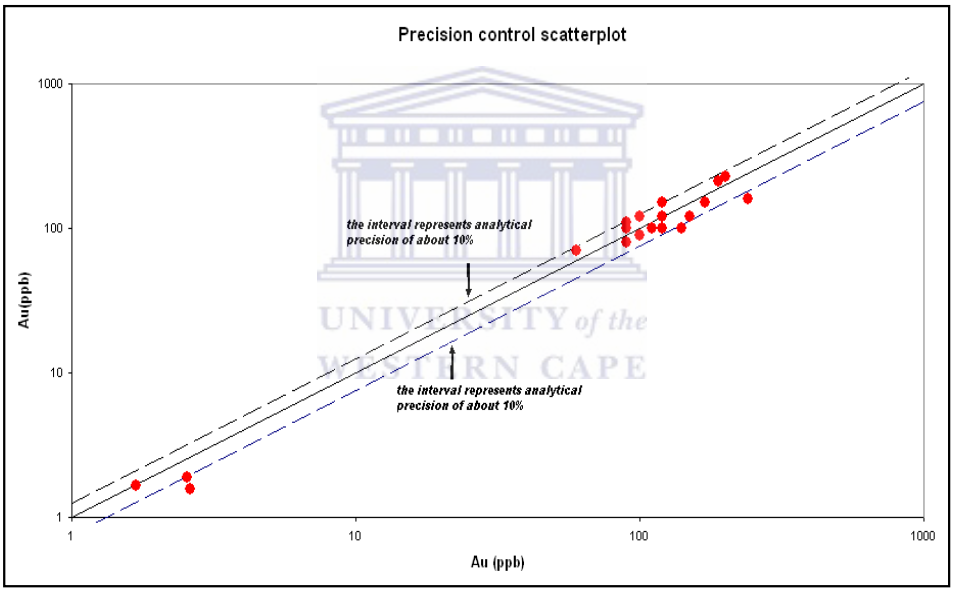

Figure 3.5 Precision control scatter plot for nickel and gold at 0.1M hydroxylamine leach (Lower horizon in Amalia Blue Dot Mine samples).

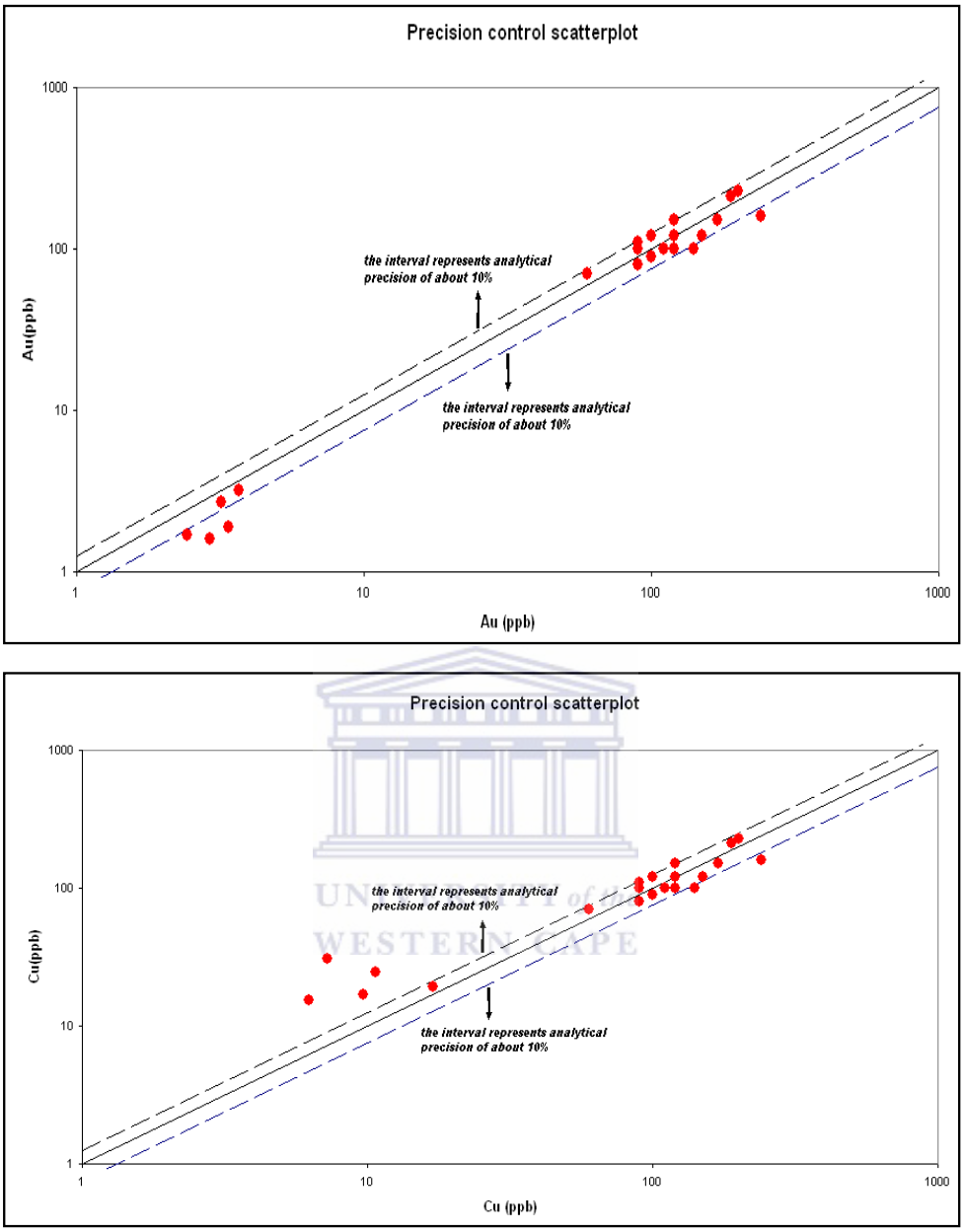

Figure 3.6 Precision control scatter plot for gold and copper at 0.25M hydroxylamine leach (Kabanga Main samples).

Table 3.2 ICP-MS results for standard NIST-1643d

Elements	NIST-1643d (Expected)	Read	% Error
Cr	18.5	16.7	-5.3
Mn	37.7	37.4	-0.3
Fe	91.2	58.2	-22.1
Co	25.0	25.1	0.2
Ni	58.1	57.4	-0.6
Cu	20.5	21.2	1.6
Zn	72.5	75.5	2.0
As	56.0	56.3	0.2
Se	11.4	12.6	5.0
Rb	13.0	12.1	-3.5
Pb	13.0	12.1	-3.5
Ba	506.5	518.3	1.2
Sr	294.8	303.1	1.4
Cd	6.5	6.5	0.5

3.6 Data evaluation

The data obtained from the analyses was evaluated by the principal component analysis (PCA) with the use of the statistical package XLSTAT 753 while the statistical parameters of background (median), threshold and anomalous values were estimated/calculated using X-PLOT software programme. Principal component analysis is a technique used to established different associations among variables or elements in the study sites in order to minimise bias in geochemical data from these sites. The geochemical maps were plotted using Surfer 8® software.

CHAPTER FOUR

RESULTS

4. Preamble

This chapter comprises the analytical results of samples taken from:

- The lateritic regolith overlying the Kabanga Main & Kabanga North (Ni-Cu ore deposits) and Luhuma prospects in Tanzania.
- The aeolian sand regolith covering the gold mineralisation at Amalia Blue Dot Mine in South Africa.

The results will be presented in two parts; first the orientation studies that will followed by the presentation of the results of the main study.

The orientation studies comprise of the following data sets;

The first data set that was taken from previous work undertaken by Simon (2003) and Ackon (2001) for the purpose of re-evaluating them. These two previous investigations mainly focussed on the use of aqua regia partial extraction and triple acid leach (HNO_3: $HClO_3$: HCl) of aeolian sand and lateritic soils from Amalia and Kabanga respectively. The aim of the revaluation of the data sets is to provide a baseline for appraisal and optimization of the hydroxylamine hydrochloride (HH) partial extraction that is the main focus of this investigation.

The analytical data, the summary statistics and related plots are presented in the Appendix A_1-A_2 and Figures 4.1 & 4.4 respectively. Plots of element concentrations along geotraverses that transects the Amalia gold mineralization and the Ni mineralization at Kabanga are shown in Fig 4.2 & 4.3 and Figs. 4.5 - 4.8.

The second data set are results from cold and hot hydroxylamine partial extraction of regolith samples taken from the Kabanga mineralisation. These data sets were used to study the effect of variable temperature conditions on the nature of geochemical signatures derived from hydroxylamine hydrochloride partial extraction of samples. These data sets are presented in Appendix B_1-B_2; the data summary and the related plots are documented in Table 4.2 & Figs 4.9 - 4.10.

The last data set of the orientation work comprise of a multi-element analysis of regolith samples from Amalia and Kabanga. Prior to the ICP-MS analysis, the samples were leached using hot hydroxylamine hydrochloride of variable concentration.

The multi-element data are presented in Appendix C_1 & C_2. Various graphical presentations of these data as well as the statistical summary are shown in Table 4.2 & 4.4, Figs 4.12 - 4.17 for Amalia, and Figures 4.20 - 4.25 for Kabanga respectively.

The results of the main study comprise of:

Multi-element analytical results of over 150 regolith samples, that were taken from mineralised areas at Amalia and Kabanga. These samples were leached by hydroxylamine hydrochloride partial extraction under conditions established from the orientation studies and analysed by ICP-MS. The analytical data are presented in Appendix C_1 & C_2.

A statistical summary of analytical data and the related plots are shown in Table 4.6 & 4.7, Figures 4.21 - 4.28 for Amalia, Figures 4.31 - 4.34 for Kabanga and Figures 4.36 - 4.41 for Luhuma respectively.

4.1 Orientation studies

Box and whiskers plots (generated with S-PLOT) were used to describe the distribution pattern elements concentration ranges contained in the regolith samples. For the purpose of presenting the element data in geochemical maps, box and whiskers diagrams have been used to estimate background and anomalous values for each variable (element) under investigation (Figure 4.1 & Table 4.1). Element contents above the 75th percentile and outliers in each of the box plots are regarded as anomalous values as this represent a recognizable break or flexing point in the element distribution patterns (O' Connor and Riemann, 1993). These estimates have been used to appraise the predictive strength of geochemical signature associated with the geochemical data derived from ARL and TAL leaches.

The ARL and TAL partial leach data were therefore plotted along respective sample traverses and the resulting geochemical trends compared to estimated values from the box and whiskers plots. This enabled the predictive strength of element patterns and geochemical anomalies to be determined, such as: the contrast of the anomaly to background concentration, the width of the anomaly and the ability of the element pattern to reflect underlying bedrock. The predictive strength of the ARL and TAL leaches were then compared with those of hydroxylamine hydrochloride partial leach in section 4.1.2.3 & 4.1.2.4.

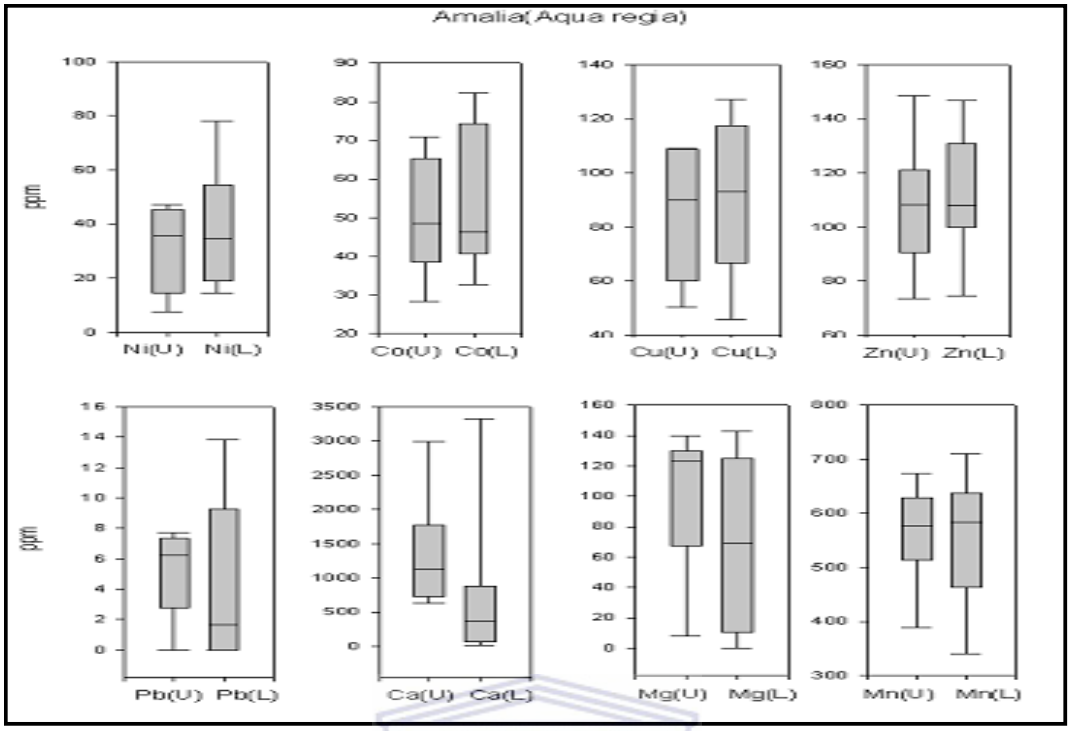

Fig 4.1 Box and whisker plots showing element contents in the upper (U) and lower (L) horizon in Amalia Blue Dot Mine. The middle line corresponds to the background value (median); lower and upper bounds of the box indicate 25th and 75th percentiles respectively. Values above the 75th percentile are considered. Element contents between the 50th and 75th percentiles are regarded as the threshold. (Turkey, 1977).

Table 4.1 Estimated background-anomalous values of the various elements (in ppm) in samples taken from Amalia Blue Dot.

Triple acid leach						
Amalia samples						
Upper horizon				**Lower horizon**		
Element	Background	Threshold	Anomaly	Background	Threshold	Anomaly
Ni	32.5	45.1	50.3	34.64	53.6	77.14
Co	47.5	65.2	70.1	46.27	74.5	83.07
Cu	90.06	107.2	107.2	93.23	118.1	128.6
Pb	6.22	7.01	7.6	1.64	9.12	13.85
Zn	107.2	120	150	107.93	132.4	148.5
Mn	576.11	625.2	675.2	582.69	645.3	720.4
Ca	1133.02	1750	3000	365.58	807.5	3400
Mg	123.14	128	140	69.48	125.6	148.5

4.1.1 Amalia Blue Dot Mine

Figures 4.2 and 4.3 show Ni, Co, Cu, Zn and Mn contents in a soil traverse across the Au mineralization at Goudplaats section at Amalia. The mineralization is hosted by the BIF unit that is located in the central parts of the traverse. The BIF unit is flanked by granite to the east and greenstone to the west. The general topography gently slopes towards the east.

In Figs. 4.2 and 4.3, elevated contents of Cu, Ni, Co and Zn concentration, up to 2 times higher than the estimated background values occur in the upper soils overlying the mineralization. The widths of the anomalies are up to 150 metres wide and are most pronounced in the Cu, Ni, and Co distribution pattern.

Anomalous contents of the above elements occur beyond the mineralised area to the east, thus following the general slope of the topography. The resulting asymmetrical dispersion train of the above elements to the east are about 500 meters wide. Generally, the contents of Ni, Co and copper are higher in soils overlying the greenstones but these shows a weak contrast to estimated background concentration.

The concentration levels of Cu, Ni, Co and Zn in the lower soil are generally higher than those measured in the upper soil. Lead and manganese contents and other element included in the investigation do not show reflection of bedrock or meaningful trends over the mineralization areas.

Gold contents (not presented in the figure) in soils show elevated contents over areas underlain by greenstone and mineralization. Au anomalous values are up to 2 times the background concentration (Ackon, 2001).

The element distribution pattern in the triple acid leach appears associated with elevated background values and therefore a weak anomaly/background contrast.

Generally, the distribution patterns of all the elements only show a weak contrast in soils over unmineralised and mineralised greenstone or BIF.

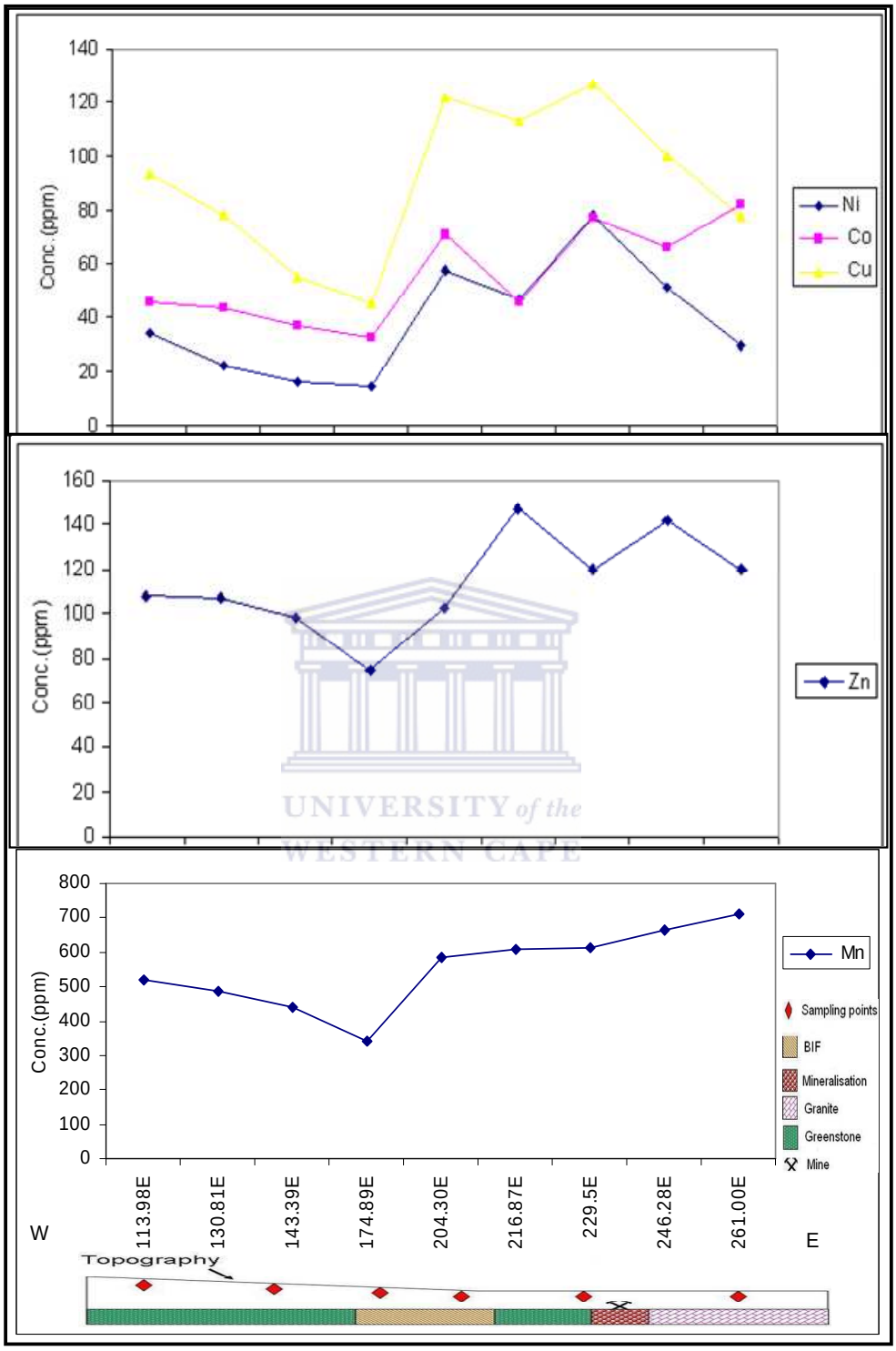

Figure 4.2 Distribution of Ni, Co, Cu, Mn and Zn in the samples taken at the basal horizon along a profile (Amalia Blue Dot Mine); Triple acid leach by Ackon (2001).

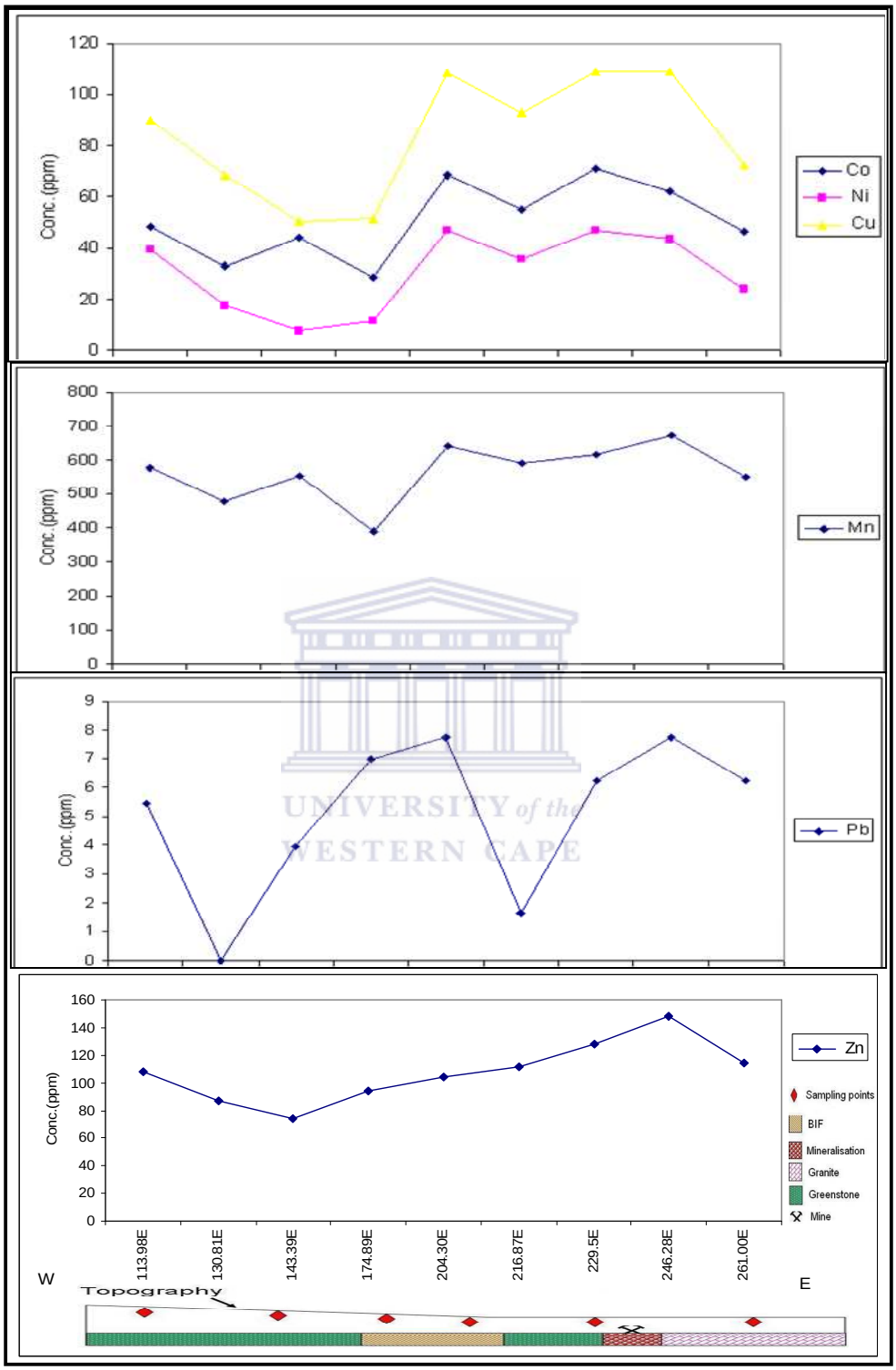

Figure 4.3 Distribution of Ni, Co, Cu, Mn, Zn and Pb in the samples taken at the upper horizon along a profile (Amalia Blue Dot Mine); Triple acid leach by Ackon (2001).

4.1.2 Kabanga (Main and North)

Box and whiskers plots were also used to estimate the background, threshold and anomalous concentration ranges for various elements analysed in samples from regolith overlying the Kabanga Ni-Cu deposit (Table 4.2). Element content in samples was also plotted along respective sample traverses and the resulting geochemical trends compared to estimated values from the box and whiskers plots (Table 4.2).

Figure 4.5. shows Cu, Ni, Co, Zn and Pb distribution patterns in traverse L9893N, which cuts across the Kabanga Main mineralization with a footwall host rocks comprising of quartzite and spotted schist and two ore zones, which are enclosed within the ultramafic rocks at a depth of over 150m. Elevated contents of Cu, Co, Ni, Pb and Zn, up to 3 times higher than the background values occur in soils overlying the ultramafic body and accompanying mineralization. The contents of the above elements are generally high over the ultramafic body and associated mineralization.

Distribution pattern of Ni, Co, Cu, Zn and Pb along traverse L11528N is presented in Fig. 4.6. The mineralization is hosted in meta-pelites while its hanging wall comprises of quartzite and spotted schists. The mineralisation is concealed at a depth of 390m. Slightly elevated contents of Cu and Zn occur in soil overlying the mineralised zone. The remaining elements do not show a meaningful trend that relates to mineralization or bedrock. Elevated contents of the above elements show a weak contrast to estimated background concentration.

Figure 4.7 and 4.8 show contents of Cu, Ni, Co, Zn and Pb distribution patterns in traverse L9850N and L11670N which cuts across the Kabanga main and Kabanga north mineralization. Both traverses have similar subsurface geology. In traverse L9850N, element contents are subdued in soils overlying the main orezones followed by pronounced enrichment, up to 10 times higher than the background values, in soils overlying the ultramafic body. Elevated contents of the above element occur over laterites in traverse L11670N and decrease towards the location of mineralization in the east. The elevated contents of Cu, Ni, Co, Zn and Pb in traverse L11670N show a weak contrast to estimated background concentration.

The reflection of bedrock and concealed mineralisation by element contents in soils overlying the Kabanga main and Kabanga north mineralisation is therefore variable to inconsistent. The controlling factors appear to be the concealment of mineralised zone at depths of over 400m and the wide of lateritic pisolites over unmineralised areas; the latter could be associated with false anomalies of Ni and Co (Simon, 2003).

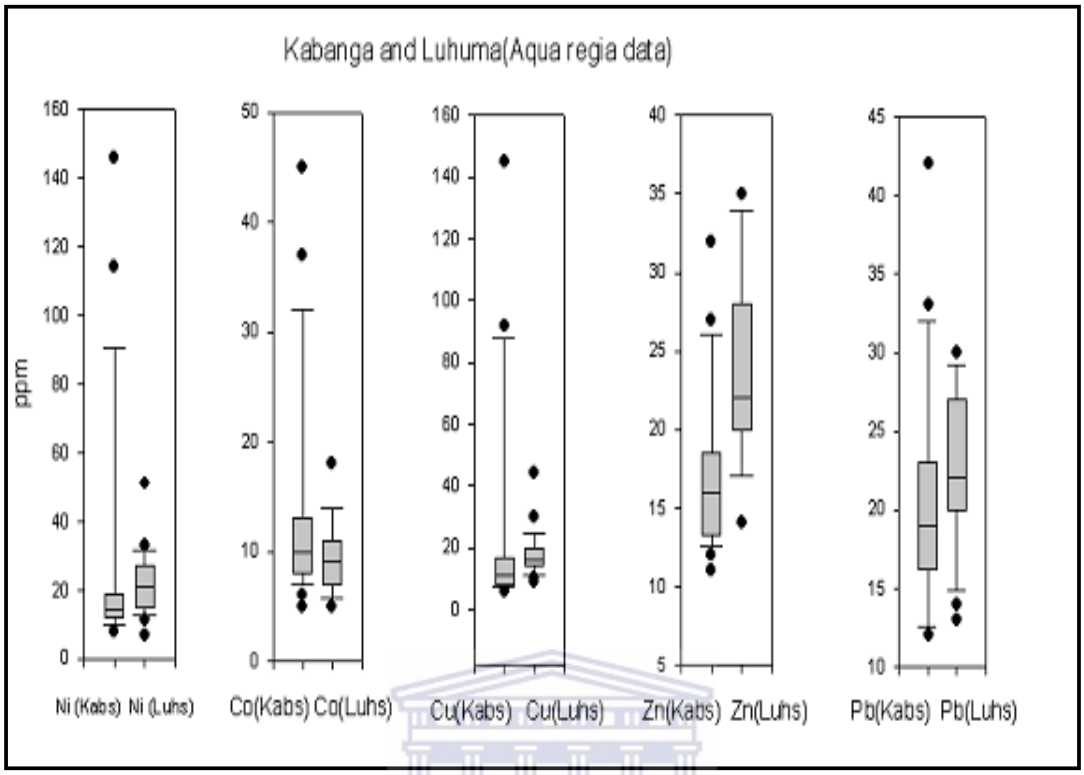

Fig 4.4 Box and whisker plots showing element contents in the Kabanga (Kabs) and Luhuma (Luhs) study sites. The middle line corresponds to the background value (median); lower and upper bounds of the box indicate 25th and 75th percentiles respectively. Values above the 75th percentile are considered. Elements contents between the 50th and 75th percentiles are regarded as the threshold (Turkey, 1977).

Table 4.2 Estimated background-anomalous values of the various elements (in ppm) in samples taken from Kabanga and Luhuma.

AQUA REGIA DIGESTION						
Kabanga samples				**Luhuma samples**		
Element	Background	Threshold	Anomaly	Background	Threshold	Anomaly
Ni	16.5	19.5	115	21.3	39.2	38.3
Co	10.5	12.5	35.4	8.56	13.8	18.5
Cu	14.2	18.5	92.54	16	31.92	30.12
Pb	18.5	23.5	33.5	21.5	27.6	31.4
Zn	16.2	18.3	26.6	22.5	27.5	35.01
Mn	NA	NA	NA	NA	NA	NA
Ca	NA	NA	NA	NA	NA	NA
Mg	NA	NA	NA	NA	NA	NA

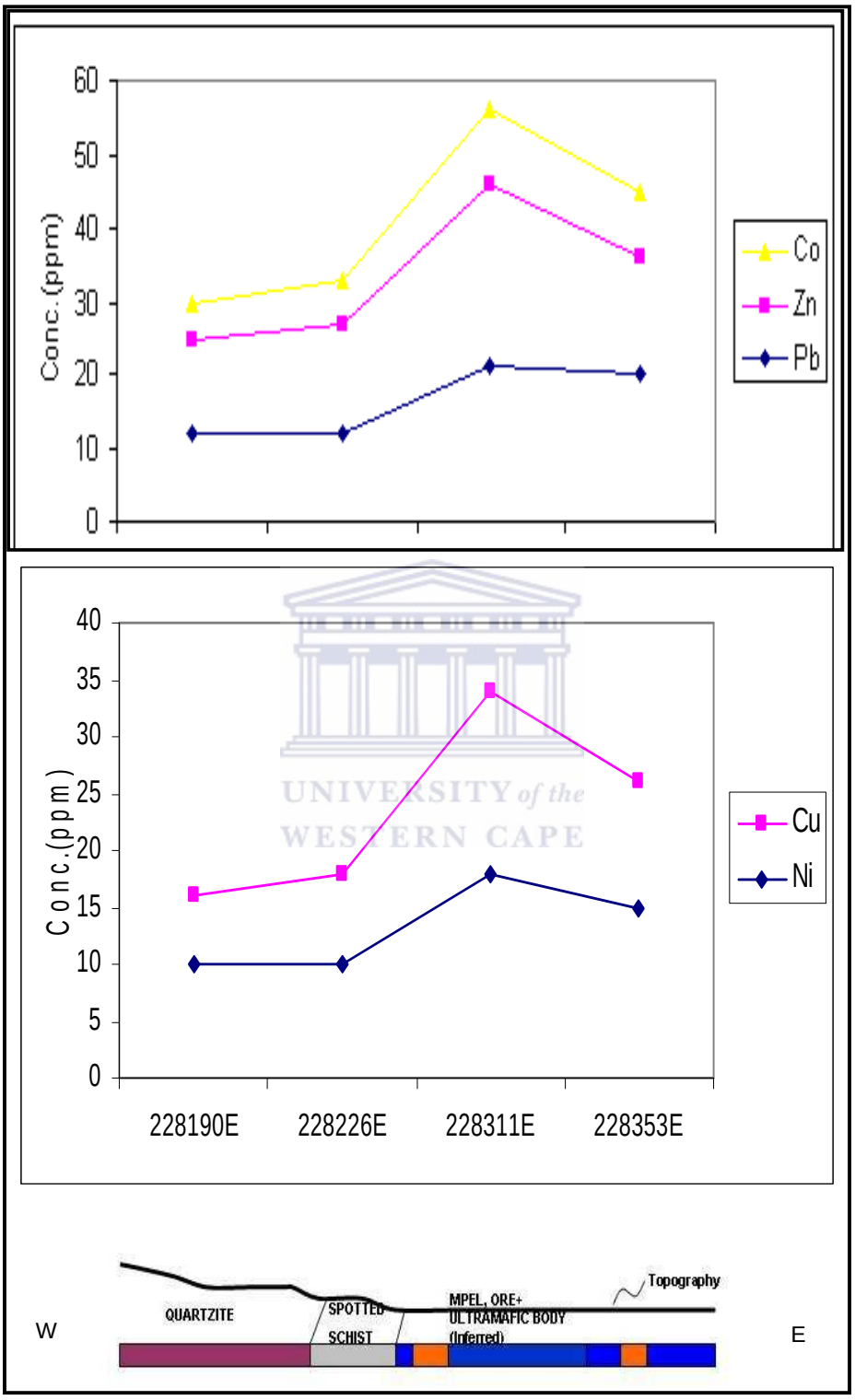

Figure 4.5 Distribution of Ni, Co, Cu, Zn, and Pb in the samples taken along a profile L9893N (Kabanga Main); Aqua regia leach by Simon (2003).

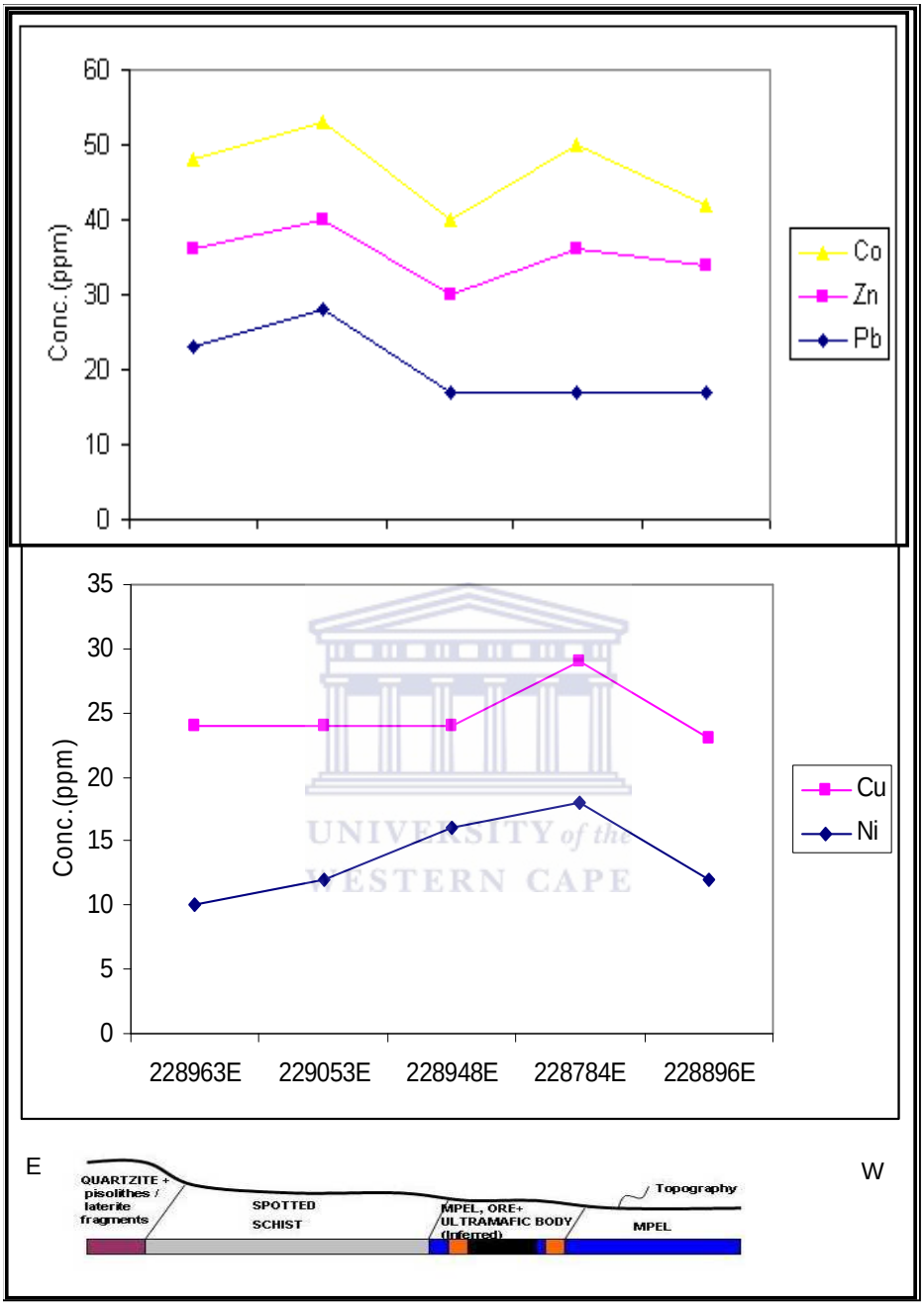

Figure 4.6 Distribution of Ni, Co, Cu, Zn, and Pb in the samples taken along a profile L11528N (Kabanga North); Aqua regia leach by Simon (2003).

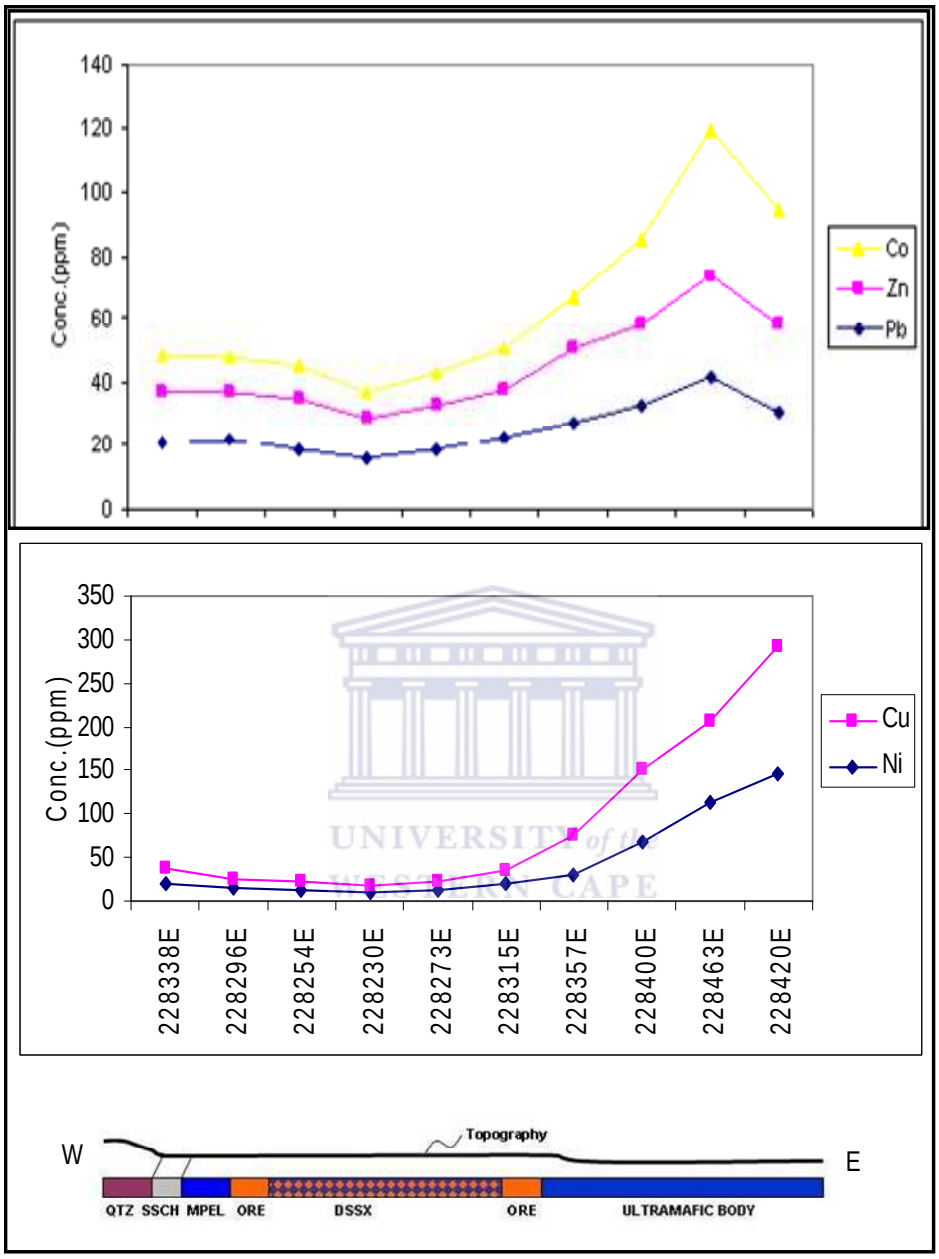

Figure 4.7 Distribution of Ni, Co, Cu, Zn, and Pb in the samples taken along a profile L9850N (Kabanga Main); Aqua regia leach by Simon (2003).

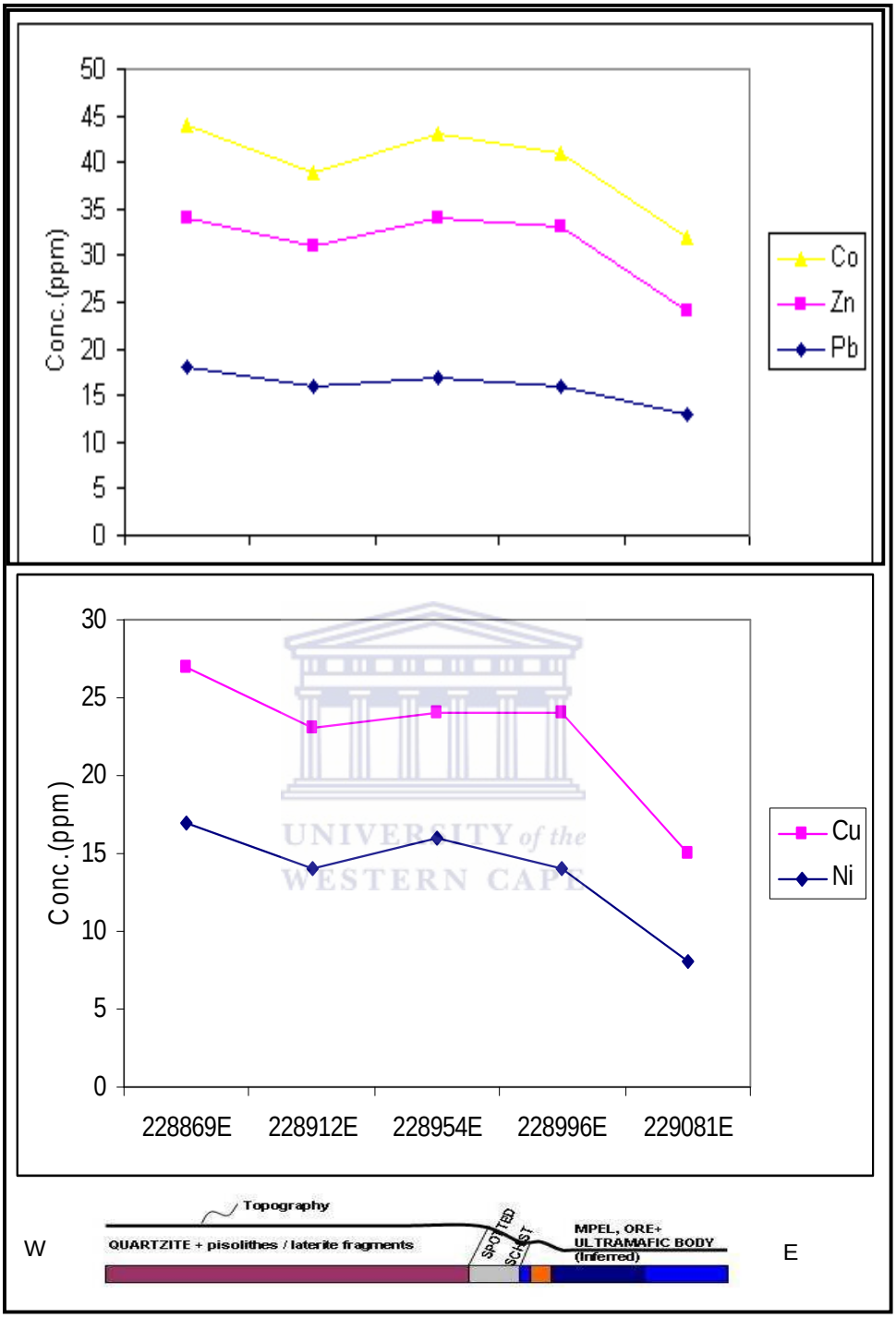

Figure 4.8 Distribution of Ni, Co, Cu, Zn, and Pb in the samples taken along a profile L11670N (Kabanga North); Aqua regia leach by Simon (2003).

4.1.3 Hydroxylamine partial leach

The results of the partial extraction of soils by aqua regia leach (ARL) and triple acid (TAL) leach are associated with occurrence of weak or an absence of pronounced geochemical anomalies over mineralization at Kabanga and Amalia. A major objective of this investigation is to improve the geochemical signatures associated with mineralization in both areas by hydroxylamine leach. Hydroxylamine partial leach is very appropriate for regolith composed of ferruginous components that commonly occur in both areas of study (McAlister et al., 1999). Optimum application of hydroxylamine partial leach is however subject to numerous conditions that require strict controls, which include dependency of leach on pH, hydroxylamine concentration, temperature and weight of sample. This section presents the results of studies aimed at;

- Selecting a temperature for the partial extraction and
- Studying the relationships between element extractability pattern in various hydroxylamine hydrochloride concentrations and the chemistry of concealed bedrock/mineralization.

4.1.3.1 Optimum temperature for hydroxylamine partial extraction

Five regolith samples each close to mineralization selected from Kabanga and Luhuma were used to optimise the use of cold and hot hydroxylamine hydrochloride for partial selective extraction. The ensuing data are presented in Appendix B_1-B_2; the data summary in Table 4.3 and graphical presentations in Fig 4.9.

The trends in Table 4.3 and Fig 4.9 can be summarized as follows:

- The overall degree of element extractability is up to 6 times higher in hot than cold hydroxylamine partial extraction. Exceptions to the above trend occur in soils from the Luhuma prospect (Table 4.3).
- Hydroxylamine concentration (strength) does influence the degree of element extractability and the latter appears to be poorer towards higher concentration of hydroxylamine (0.25M), especially for hot extraction.
- Copper and to extent cobalt generally show poor extractability in hot extractions especially at low hydroxylamine concentration (Fig 4.9).

The important features of the section 4.1.3.1 are as follows;

- The variable pattern of element extractability is dependent on multiple factors that amongst others include the dependency of concentration of solute/solvent interaction versus temperature.

- The result justifiably supports the further use of hot extraction. This would allow temperature as a fixed parameter, thus enabling a closer monitoring of the influence of hydroxylamine concentration on element extractability.

Table 4.3 Summary data for both cold and hot hydroxylamine hydrochloride digestion for Kabanga main and Luhuma samples.

Kabanga samples									**Luhuma samples**							
Cold hydroxylamine					**Hot hydroxylamine**				**Cold hydroxylamine**				**Hot hydroxylamine**			
0.1M																
Element	Min.	Max.	Mean	Std.Dev	Min.	Max.	Mean	Std.Dev	Min.	Max.	Mean	Std.Dev	Min.	Max.	Mean	Std.Dev.
Ni	5.4	15.3	9.9	4.36	36.9	43.2	40.14	2.59	4.5	9.9	7.74	1.97	36.9	39.6	37.8	1.27
Co	6.3	9.9	8.28	1.33	9	67.5	36.54	25.16	53.1	57.6	55.98	1.84	6.3	122	48.6	44.31
Cu	33.3	34.2	33.84	0.49	10.8	11.7	11.52	0.4	0.9	2.7	1.8	0.64	10.8	12.6	11.88	0.75
Mn	0.9	72.9	19.26	30.28	10.8	72	29.88	24.74	56.7	109	52.2	18.9	38.7	125	71.28	34.01
Fe	25.2	130.5	70.02	44.29	48.6	508.5	243.7	169.54	57.6	85.5	70.2	12.29	104.4	350	260.1	93.26
0.15M																
Element	Min.	Max.	Mean	Std.Dev	Min.	Max.	Mean	Std.Dev	Min.	Max.	Mean	Std.Dev	Min.	Max.	Mean	Std.Dev.
Ni	12.6	18.9	15.84	2.43	38.7	45	41.76	2.26	7.2	11.7	9.72	1.73	39.6	41.4	40.68	0.99
Co	7.2	16.2	13.68	3.68	36.9	126	69.84	39.68	63	76.5	69.84	5.04	54.9	82.4	67.14	12.08
Cu	33.3	35.1	33.84	0.81	10.8	11.7	11.16	0.49	7.2	11.7	9.72	1.73	10.8	11.7	11.52	0.4
Mn	1.8	14.4	7.2	5.25	9.9	13.5	10.62	1.61	35.1	71.1	54.72	15.17	10.8	19.8	13.68	3.57
Fe	20.7	94.5	40.32	30.83	20.7	525.6	148.3	215.03	95.4	129	105.3	13.84	104	504	275	144.4
0.20M																
Element	Min.	Max.	Mean	Std.Dev	Min.	Max.	Mean	Std.Dev	Min.	Max.	Mean	Std.Dev	Min.	Max.	Mean	Std.Dev.
Ni	17.1	22.5	19.8	20.7	45	46.8	45.9	0.64	11.7	16.2	14.04	1.87	43.2	57.6	47.52	5.74
Co	16.2	21.6	18.18	18	63.9	190.8	118.8	52.54	82.8	92.7	87.48	3.99	76.5	137	98.82	23.31
Cu	33.3	34.2	33.84	0.49	9.9	12.6	11.16	1.03	0	2.7	1.26	1.03	11.7	13.5	12.24	0.81
Mn	2.7	9	4.86	18.9	9	9.9	9.54	0.49	32.4	62.1	48.6	11.99	9	11.7	10.26	1.03
Fe	6.3	41.4	23.04	4.5	47.7	441	117.8	151.12	91.8	140	112.1	18.53	221	369	300.8	70.12
0.25M																
Element	Min.	Max.	Mean	Std.Dev	Min.	Max.	Mean	Std.Dev	Min.	Max.	Mean	Std.Dev	Min.	Max.	Mean	Std.Dev.
Ni	21.6	28.8	26.64	3.03	47.7	55.8	50.22	3.21	18	18	18	0	47.7	51.3	48.6	1.56
Co	20.7	24.3	22.68	1.84	83.7	115.2	102.2	15.01	1.12	1.39	1.25	0.1	80.1	134	106.7	24.67
Cu	34.2	36	34.56	0.81	9	11.7	10.26	1.03	0.9	1.8	1.62	0.4	9.9	10.8	10.26	0.49
Mn	3.6	8.1	5.58	1.73	9.9	12.6	11.34	1.03	47.7	139	75.42	36.18	9	14.4	11.34	2.51
Fe	7.2	69.3	25.56	25.41	60.3	117	95.58	22.5	145	229	195.8	31.81	49.5	201	127.4	61.45

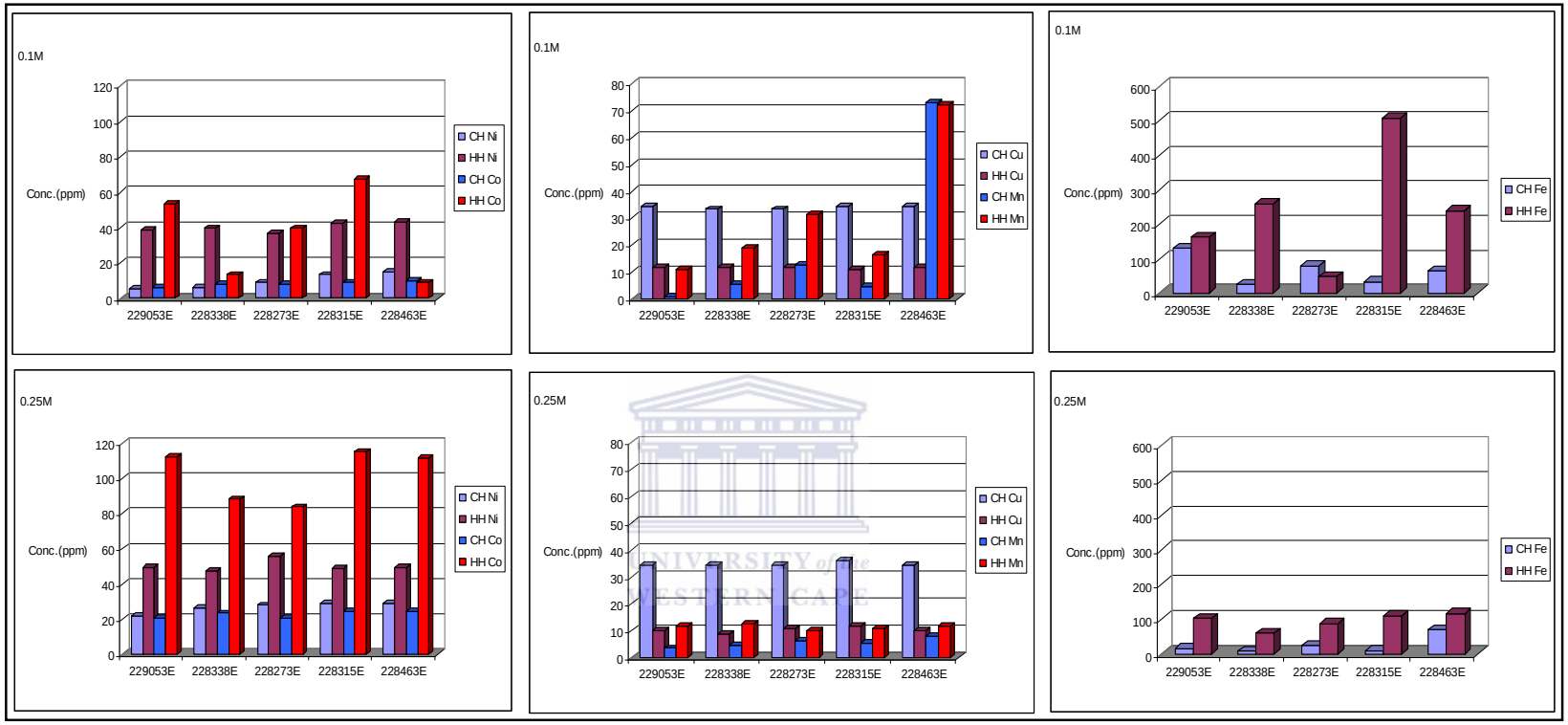

Figure 4.9 0.1M and 0.25 M cold and hot hydroxylamine hydrochloride digestion diagram (Kabanga samples).

*** CH - Cold hydroxylamine hydrochloride
*** HH - Hot hydroxylamine hydrochloride

4.1.4 The influence of hydroxylamine concentration on element extractability.

Element extractability into hydroxylamine solution is dependent on many factors that amongst others include the concentration of solvent and temperature. This section seeks to look into the influence of hydroxylamine concentration on element extractability after having established the hot partial leach as most suitable for this work. A total of 20 regolith samples along sample traverses that cut across mineralisation were selected from Amalia (aeolian sand) and Kabanga Main areas and used for these investigations.

With temperature set at 50^0C, the concentration of hydroxylamine used for extraction was varied in order to determine;

- the degree and changing patterns of extractability of various elements into leach liquor.
- how the variable degree and changing patterns of element extractability from regolith samples relates to geochemical signatures from bedrock and the chemistry of the underlying bedrock and concealed mineralization.
- the optimum analytical conditions for the use of hydroxylamine partial extraction in geochemical mapping and mineral prospecting purpose.

Analytical data for this study are presented in Appendix C_1 and statistically summarized into Tables 4.4 and 4.5 for Amalia and Kabanga samples respectively. The geometric mean concentration of each element was plotted against hydroxylamine of variable concentration; the mean concentration of each element is taken to represents the degree of element extractability from investigated samples (Figures. 4.10 & 4.11). These plots portray different extractability response in variable hydroxylamine hydrochloride concentration as illustrated by the different shapes of curves. The overall curve shapes can be used to classify the pattern of extractability of elements in soils over the Amalia Blue Dot Mine and Kabanga Ni-Cu Mine into four groups as follows;

- Group I comprises of majority of the elements, whose degree of extractability decreases with increasing strength of hydroxylamine concentration and these include Ni, Co, Ba, Mn, Ru, Sr, Pd, Rb and Ag.

Table 4.4. Summary statistics of the hot hydroxylamine hydrochloride digestion of the samples taken along a profile in Amalia (Lower horizon).

Amalia samples(Lower horizon)					**(All data in ppb)**				**n = 10**							
0.1M					**0.15M**				**0.2M**				**0.25M**			
Element	Min.	Max.	Mean	Std Dev.	Min.	Max.	Mean	Std Dev.	Min.	Max.	Mean	Std Dev.	Min.	Max.	Mean	Std Dev.
Ni	24.72	165.3	84.95	63.72	2.46	57.81	26.87	22.29	1.27	22.39	8.73	7.83	1.22	14.04	6.054	4.78
Co	48.94	209.75	126.2	56.16	1.39	38.47	20.08	13.97	0.81	8.43	3.39	2.96	0.34	1.95	1.025	0.63
Cu	38.55	64.53	53.56	11.58	22.61	43.28	31.62	6.796	12.28	47.89	31.37	12.02	18.93	100.1	36.39	31.6
Zn	9.56	51.95	27.9	14.76	5.63	10.22	7.86	2.031	3.53	5.84	4.71	0.93	13.13	37.56	20.64	9.24
As	14.52	29.08	19.26	5.12	24.63	28.96	26.45	2.01	35.71	45.72	39.35	3.72	44.43	58.89	51.22	5.43
Se	10.16	37.46	19.97	10.89	19.35	38.19	25.97	7.45	5.09	25.6	15.98	8.58	4.24	38.51	15.28	13.51
Rb	8.53	19.52	12.6	4.12	4.23	8.56	5.99	1.47	2.68	5.93	4.38	1.08	1.36	3.88	2.88	0.86
Sr	68.19	171.93	113.4	47.2	4.06	27.6	19.44	8.49	1.32	8.5	4.66	2.79	1.4	4.18	2.27	1.03
Pd	0.48	1.78	1.12	0.46	0.57	1.25	0.92	0.24	0.14	1.03	0.72	0.34	0.12	0.43	0.27	0.16
Ag	0.07	1.69	0.64	0.66	0.02	0.89	0.4	0.32	0.01	0.28	0.142	0.13	0.29	0.69	0.49	0.28
Mn	2994	15334	7160	4222	125.1	2016.4	1167.5	710.1	29.66	401.27	173.7	131.1	16.66	97.73	58.53	31.65
V	32.95	80.74	51.32	17.52	26.86	59.9	40.71	13.31	29.66	401.27	173.7	131.1	36.03	83.66	62.32	15.43
Cd	0.189	0.65	0.32	0.22	0	N/A	N/A	N/A	0	N/A	N/A	N/A	0.07	0.07	0.07	N/A
Ba	361.5	2874.1	1099	911.95	0	N/A	N/A	N/A	12.05	168.63	92.28	72.77	10.15	76.85	34.99	24.72
Re	0.3	0.3	N/A	N/A	0	N/A	N/A	N/A	0	N/A	N/A	N/A	0	N/A	N/A	N/A
Os	9.33	141.03	54.03	59.06	37.94	540.31	385.5	183.3	5.116	60.49	27.39	29.23	2.08	45.07	19.62	22.59
Ir	0.76	0.03	0.25	0.197	0.8	97.31	31.47	44.83	0.13	0.13	0.13	N/A	0.12	0.12	0.12	N/A
Cr	0	N/A	N/A	N/A	0	N/A	N/A	N/A	0	N/A	N/A	N/A	0	N/A	N/A	N/A
Au	0.47	14.15	5.88	7.27	0.78	2.19	1.49	1	0.25	0.25	0.249	N/A	1.23	1.23	1.23	N/A
Pb	16.14	75.11	31	22.04	8.28	42.35	14.41	5.78	4.46	10.61	8.29	2.69	3.11	6.19	5.13	1.11
U	0.26	0.79	0.42	0.21	0.28	0.41	0.326	0.05	0.25	0.49	0.38	0.08	0.23	0.44	0.33	0.07
Ru	0.17	0.17	0.17	N/A	0	N/A	N/A	N/A	0	N/A	N/A	N/A	0	N/A	N/A	N/A
Rh	0.31	0.31	0.31	N/A	0	N/A	N/A	N/A	0	N/A	N/A	N/A	0	N/A	N/A	N/A
Pt	1.27	1.27	N/A	N/A	0.04	0.22	0.13	0.13	0.02	0.02	0.02	N/A	0	N/A	N/A	N/A

Table 4.5 Summary statistics of the hot hydroxylamine hydrochloride digestion of the samples taken along a profile in Kabanga Main.

Kabanga main samples					**(All data in ppb)**			**n = 10**								
0.1M					**0.15M**				**0.2M**				**0.25M**			
Element	Min.	Max.	Mean	Std Dev.	Min.	Max.	Mean	Std Dev.	Min.	Max.	Mean	Std Dev.	Min.	Max.	Mean	Std Dev.
Ni	2.19	51.32	16.81	21.75	1.52	13.47	5.73	4.94	1.43	7.78	3.45	2.67	14.91	5.52	2.98	1.85
Co	3.8	34.74	12.79	13.63	0.41	6.49	2.42	2.53	0.29	1.19	0.7	0.32	0.35	0.67	0.52	0.14
Cu	8.31	68.12	22.59	25.54	3.14	14.27	9.13	4.2	2.67	15.33	10.02	5.35	6.22	17.02	10.17	4.23
Zn	0.88	23.15	8.51	10.23	4.42	12.12	8.92	4.011	0.65	21.96	11.31	15.07	16.08	43.4	24.46	11.24
As	20.97	27.69	24.57	2.7	31.98	36.82	34.26	1.72	42.64	49.83	45.97	3.55	59.22	64.32	60.75	2.07
Se	1.99	9.89	6.97	3.479	0.12	17.76	6.94	7.08	0.61	19.38	8.04	9.14	3.09	14.47	8.89	4.38
Rb	13.68	38.87	19.91	10.67	3.19	9.85	5.57	2.57	1.91	6.88	3.2	2.09	1.24	4.33	2.16	1.24
Sr	40.52	889.5	384	459.5	3.62	162.7	47.73	68.91	1.38	13.91	4.71	5.36	1.74	3.19	2.28	0.64
Pd	0.33	2.44	1.472	0.84	0.24	1.01	0.77	0.36	0.19	1.03	0.71	0.36	0.2	0.61	0.37	0.16
Ag	0.27	1.27	0.77	0.71	0.03	0.08	0.05	0.04	0	N/A	N/A	N/A	0.06	0.08	0.07	0.02
Mn	110.2	4994	1989	2461.8	31.07	1032	325.6	435.58	20.43	130.1	52.46	47.02	20.03	64.41	33.12	18.67
V	9.76	72.22	36.38	23.34	26.29	42.38	36.84	6.53	41.38	63.51	54.65	8.48	74.06	84.29	79.68	4.07
Cd	0.1	0.39	0.22	0.12	0.03	0.08	0.05	0.04	0.06	0.19	0.14	0.06	0.07	0.19	0.16	0.05
Ba	203.6	1490	665.7	594.64	0.03	0.08	0.05	0.03	8.78	86.57	29.93	32.67	7.26	23.49	14.58	7.78
Re	0.03	0.09	0.07	0.02	0.08	0.04	0.03	0.01	0.06	0.14	0.09	0.03	0.03	0.11	0.06	0.03
Os	5.86	146.6	51.51	64.67	0.17	137.5	25.31	53.75	2.31	63.23	24.86	27.45	1.26	49.15	19.29	21.37
Ir	0.05	0.36	0.141	0.15	1.49	102.7	35.31	45.81	0.03	0.15	0.07	0.05	0.02	0.13	0.07	0.04
Cr	7.2	15.95	11.57	6.19	4.16	4.16	4.16	N/A	2.64	7.69	5.17	3.57	3.78	11.98	9.48	3.84
Au	0.53	4.84	2.46	1.56	0.66	3.96	1.75	1.29	0.97	3.89	2.56	1.14	2.42	3.67	3.11	0.48
Pb	6.33	43.89	26.12	14.19	9.04	17.05	13.9	3.26	7.95	15.85	7.89	3.19	5.77	19.49	11.79	5.27
U	0.19	0.83	0.58	0.26	0.11	0.66	0.38	0.23	0.15	0.98	0.47	0.34	0.13	0.83	0.46	0.29
Ru	0.06	0.18	0.11	0.05	0.01	0.18	0.11	0.06	0.09	0.19	0.14	0.04	0.74	0.21	0.15	0.05
Rh	0.03	0.11	0.06	0.04	0.04	0.06	0.05	0.01	0.02	0.08	0.05	0.03	0.03	0.13	0.09	0.04
Pt	0	N/A	N/A	N/A	0.03	0.29	0.13	0.14	0.17	0.17	0.17	N/A	0.02	0.09	0.05	0.04

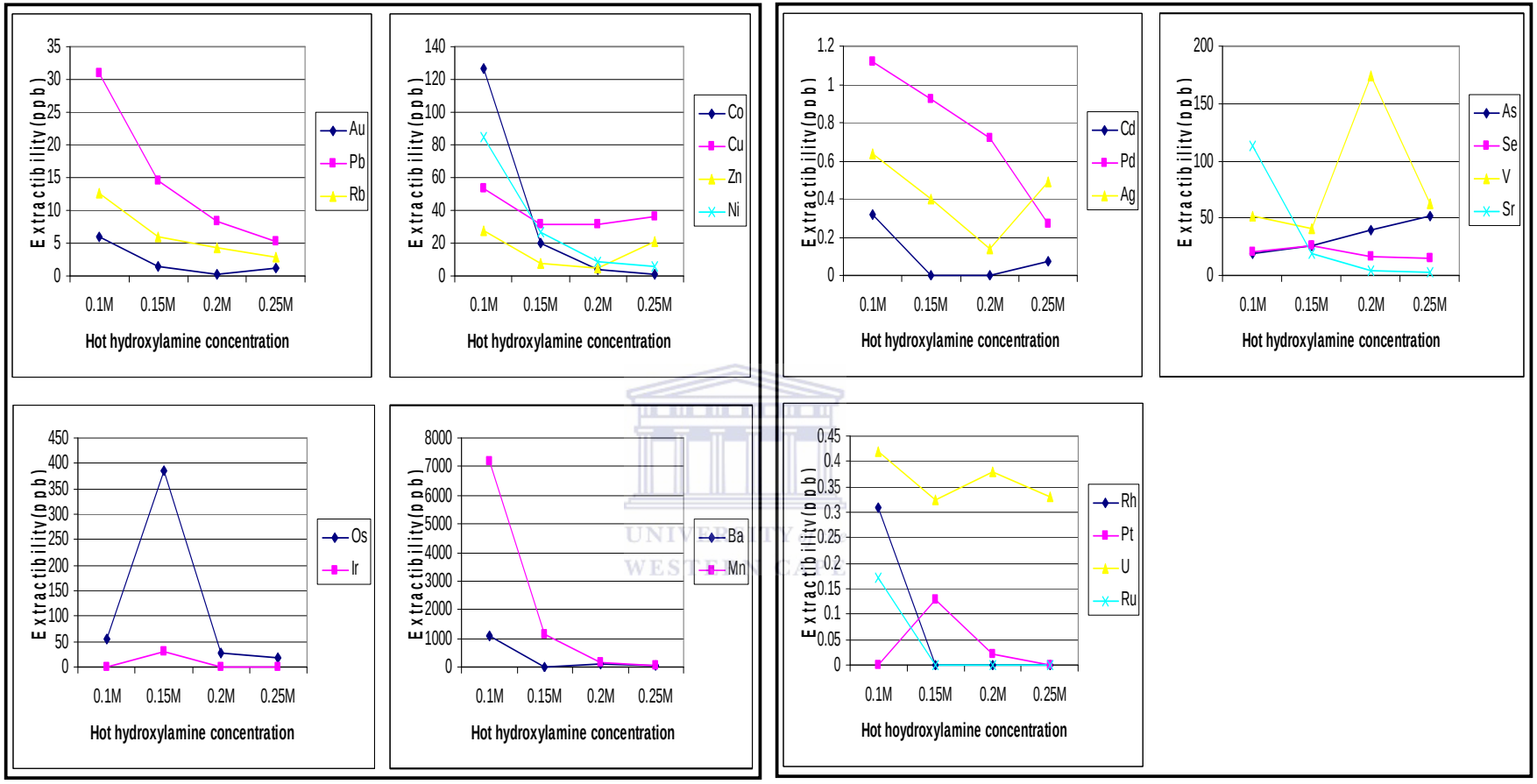

n =10 samples

Fig 4.10 Plot for both hot hydroxylamine hydrochloride leach (HNO3 base) showing amount of element in solution with increments in the concentration of hydroxylamine (Amalia Blue Dot Mine samples).

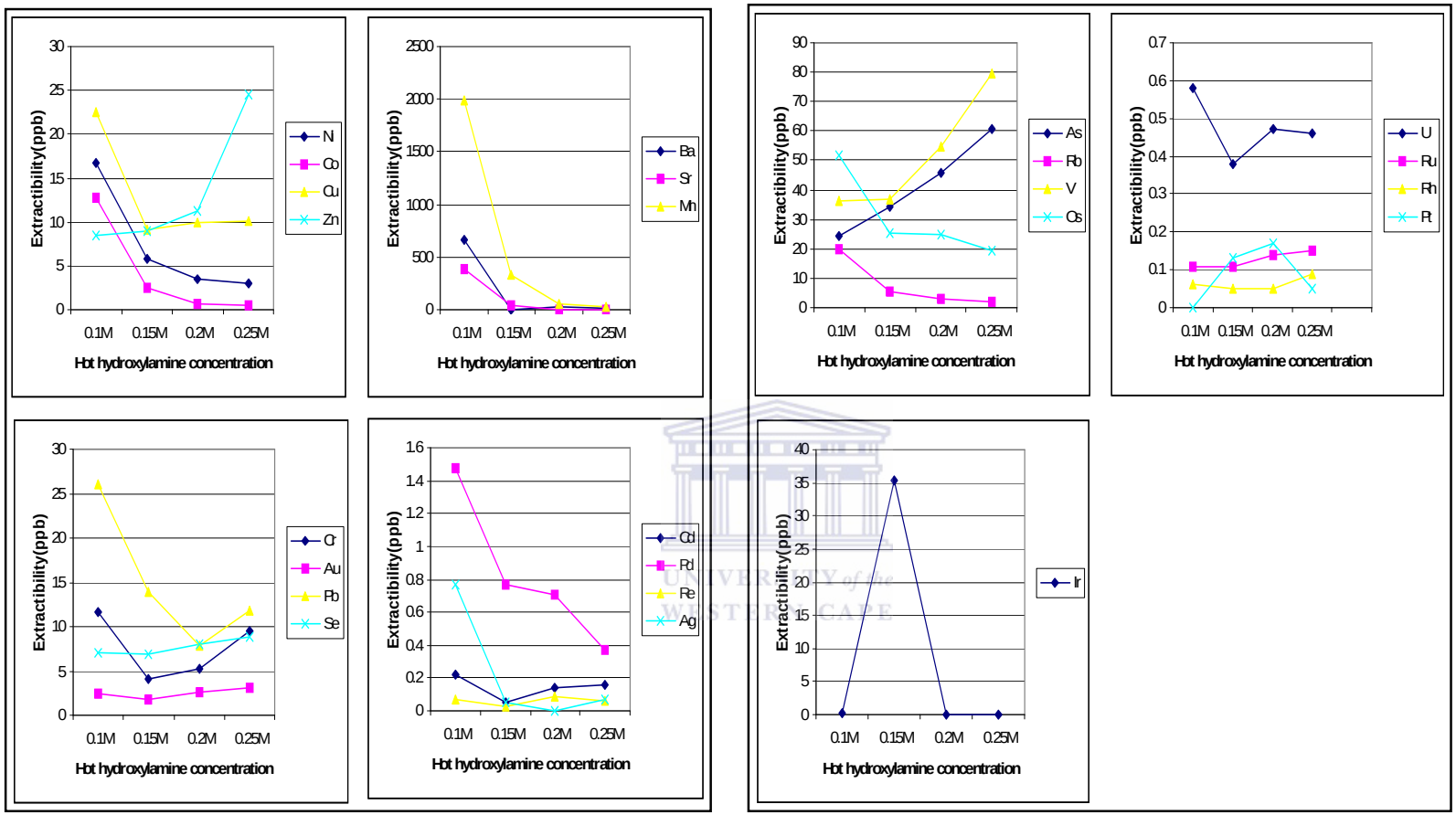

n =10 samples

Fig 4.11 Plot for hot hydroxylamine hydrochloride leach (HNO3 base) showing amount of element in solution with increments in the concentration of hydroxylamine (Kabanga samples).

- Group II are element (s) whose extractability curves increase with increasing hydroxylamine concentration such as As, V and Zn.
- Group III featuring Cu, Ag, Cr, Au, U, Cd, Re, Se, Ru, Rh and Pb with extractability curves show a minimum peak at intermediate hydroxylamine concentration.
- Group IV consist of elements with extractability curves generally show a maximum peak at intermediate hydroxylamine concentration such as Os, Ir and Pt.

Analytical data for each hydroxylamine partial leach (0.1-0.25M) were treated with principal component analysis (PCA) to corroborate the above trends and identify groups of elements that behave similarly. Another objective is determining changing patterns of element association in variable concentration of hydroxylamine leach. This may significantly contribute to understanding the relationship between the patterns of element extractability and the mineral phases being leached.

PCA was carried out using XLSTAT. Principal component I vs. II plots were used along with various tables of Eigen values. Details on techniques and applications of PCA analysis are well documented elsewhere, for example Wilkinson et al. (1999).

Principal component plots was generated with XLSTAT to show pattern of element association in both Amalia and Kabanga are presented in Figures 4.11a&b and 4.12a&b and the Eigen values, percentage variance and cumulative percentage are in the Tables 4.6a&b. The plot of principal component I & II for element data for partial extraction (Figures 4.12a &b and Figures 4.13a&b) show changing patterns of element clustering with variable strength of hydroxylamine hydrochloride concentration. The total data variability for principal component I & II in each plot is above 65percent (Tables 4.6a&b).

Two major clusters of elements can be observed in Figures 4.12a&b at 0.1M and 0.25M leaches for Amalia soil. This may suggest leaching or extraction of element more from single mineral phase (Fe-Mn-oxides and hydroxides). The overall element association patterns are similar but this appears to change into three clusters at 0.15M and 0.2M hydroxylamine partial leach respectively. These changing patterns may be indicative of extraction of various mineral phases within the Mn-Fe oxide and hydroxide spectrum.

Table 4.6a Eigen values for the principal component analysis (PCA) for the analytical data from different concentration of hydroxylamine hydrochloride leach.

Amalia (Lower horizon)						
0.1M				**0.15M**		
Value	Eigen value	%Variance	Cumulative%	Eigen value	%Variance	Cumulative%
F1	11.09	48.23	48.23	7.54	41.89	41.89
F2	6.9	30.02	78.25	4.69	26.03	67.93
F3	2.64	11.46	89.71	3.23	17.95	85.89
F4	1.55	6.73	96.44	1.91	10.95	96.48
F5	0.82	3.56	100	0.63	3.52	100
0.2M				**0.25M**		
Value	Eigen value	%Variance	Cumulative%	Eigen value	%Variance	Cumulative%
F1	10.61	46.14	46.14	71.5	37.64	37.64
F2	6.49	28.26	74.39	5.81	30.57	68.21
F3	3.39	14.77	89.16	3.09	16.29	84.5
F4	2.49	10.84	100	1.61	8.47	92.98
F5	NA	NA	NA	1.34	7.03	100

Table 4.6b Eigen values for the principal component analysis (PCA) for the analytical data from different concentration of hydroxylamine hydrochloride leach.

Kabanga Main						
0.1M				**0.15M**		
Value	Eigen value	%Variance	Cumulative%	Eigen value	%Variance	Cumulative%
F1	12.55	54.56	54.56	10.21	42.56	42.56
F2	5.99	26.09	80.65	6.57	27.36	69.92
F3	3.7	16.09	96.73	5.13	21.36	91.27
F4	0.37	3.27	100	2.09	8.73	100
0.2M				**0.25M**		
Value	Eigen value	%Variance	Cumulative%	Eigen value	%Variance	Cumulative%
F1	10.61	46.14	46.14	12.17	50.71	50.71
F2	6.49	28.26	74.39	5.15	21.45	72.15
F3	3.39	14.77	89.16	3.47	14.46	86.61
F4	2.49	10.84	100	3.21	13.39	100

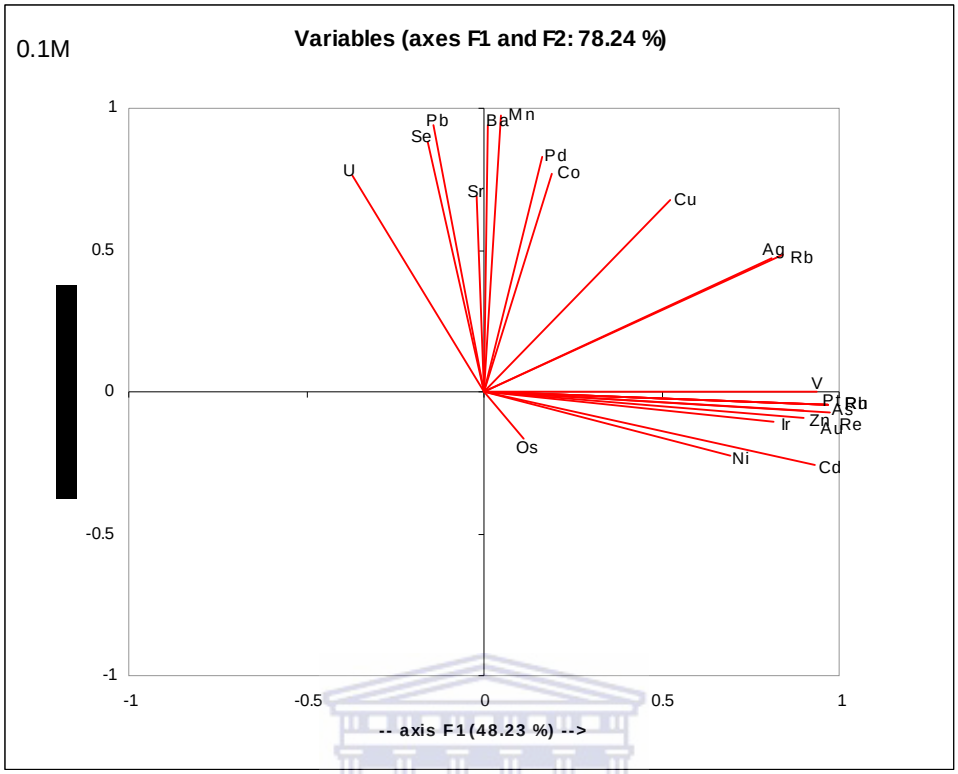

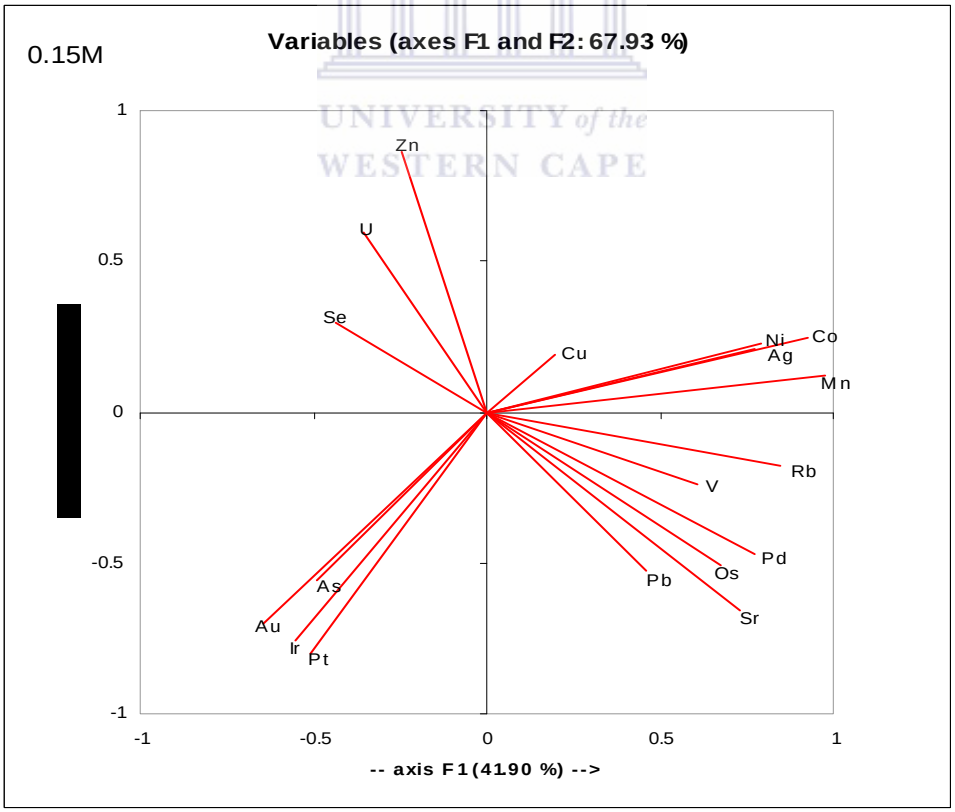

Figure 4.12a Principal component analysis plots for different concentration of hydroxylamine hydrochloride leach (Amalia samples).

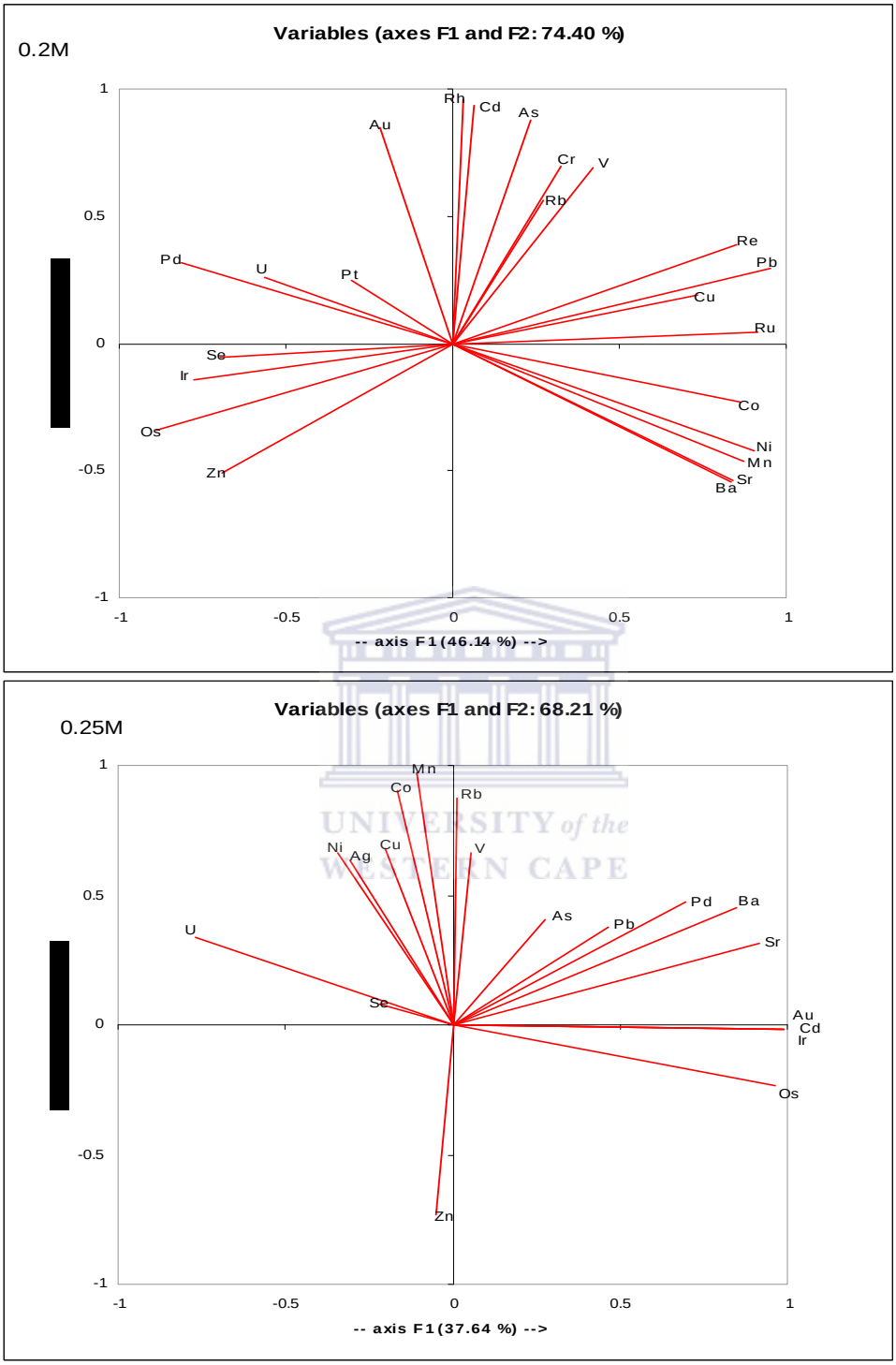

Figure 4.12b Principal component analysis plots for different concentration of hydroxylamine hydrochloride leach (Amalia samples).

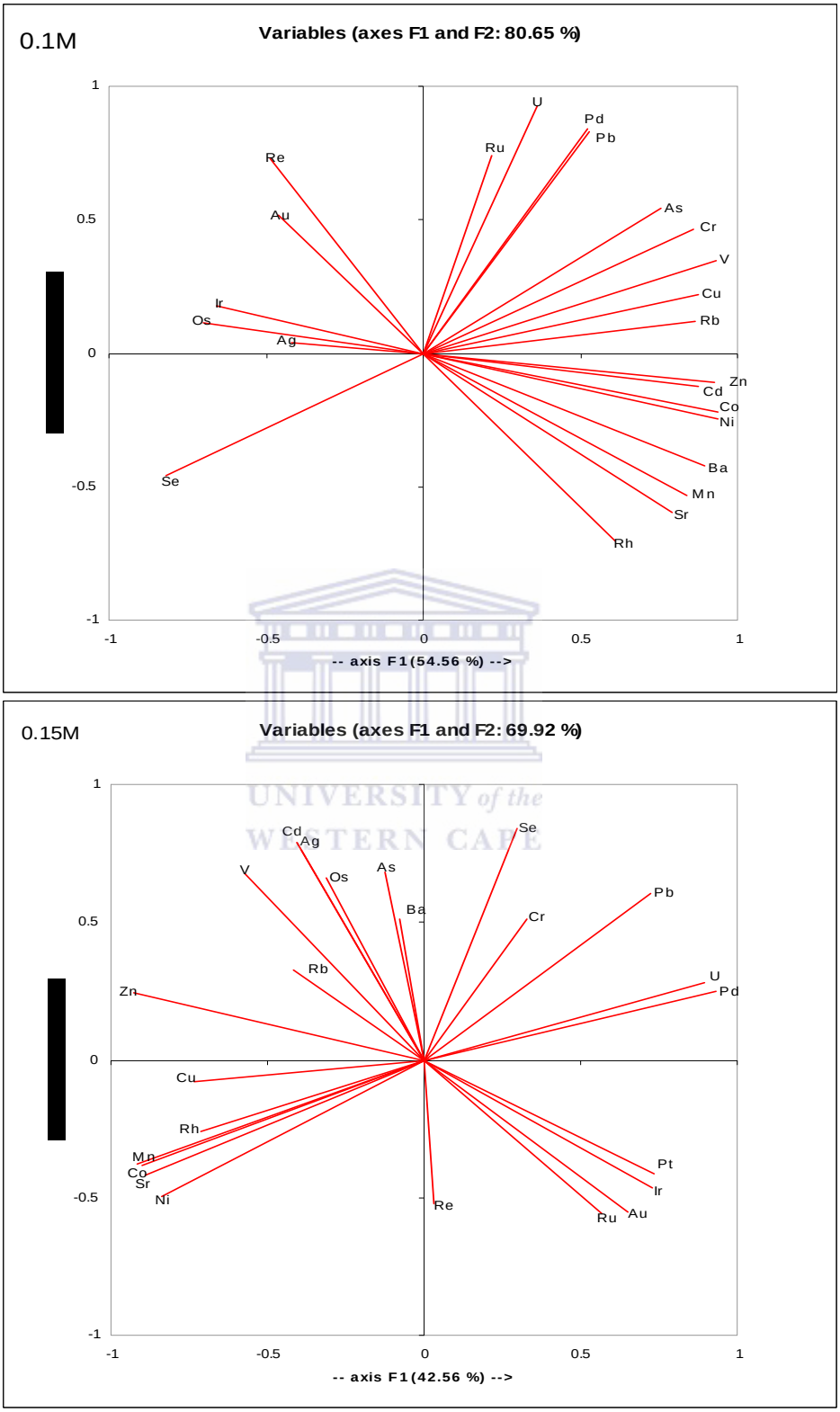

Figure 4.13a Principal component analysis plots for different concentration of hydroxylamine hydrochloride leaches (Kabanga samples).

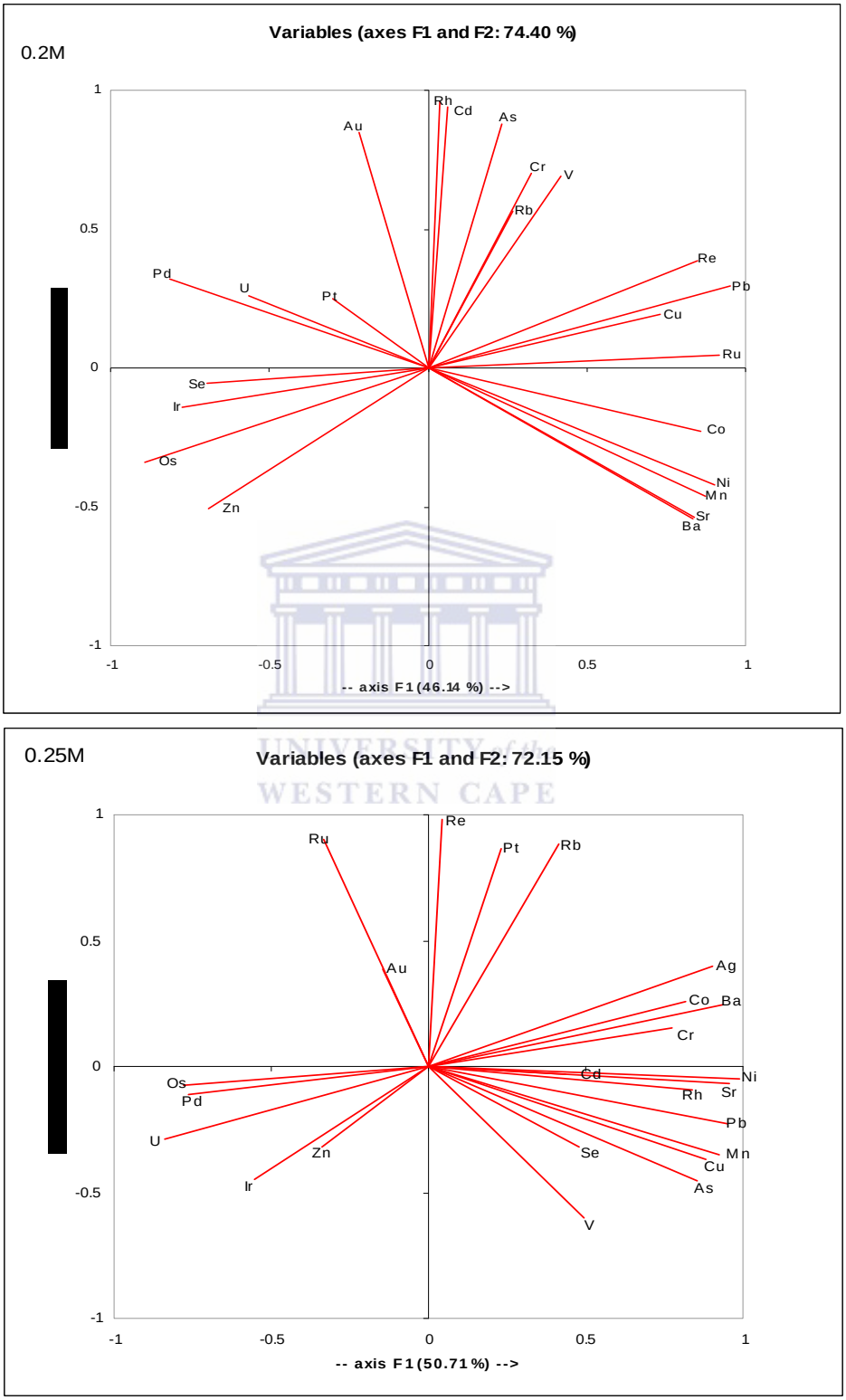

Figure 4.13b Principal component analysis plots for different concentration of hydroxylamine hydrochloride leaches (Kabanga samples).

Three major clusters of elements association can be observed in Figures. 4.13 a & b at 0.1M - 0.25M partial leaches for soil overlying Kabanga Ni-cu ore deposit. This may suggest leaching or extraction of elements from more than single mineral phase i.e. Fe/Mn-oxides/hydroxides and perhaps crystalline Fe oxides (McAlister et al., 1999). These obvious changing patterns may be indicative of difference in the mineralogical composition in the soils. Thus aeolian regolith materials may contain more loosely adsorbed amorphous Mn and Fe component than the lateritic regolith.

Analytical data from each hydroxylamine leach were plotted against each geological traverse to understudy how the changing patterns of element extractability from regolith samples relates to geochemical signatures from underlying bedrock.

4.1. 4. 1 Amalia

Element distribution in soil traverses are plotted against the geology and sites of mineralization in Figures. 4.14 - 4.16 and other are shown in the Appendix A_1-A_3. These plots comprise of results from hydroxylamine partial leaches (0.1-0.25M) and aqua regia leach and allow a comparative appraisal of both techniques.

Pronounced apical anomalous values about x7ppb higher than the background concentrations of Au, Pt and Ba, in 0.1M hydroxylamine partial leach occur in soils over the Au deposit at Goudplaats (Figures 4.14 & 4.15); these also show maximum extractability at 0.1M hydroxylamine.

Anomalous contents of Cu, Zn, Ni, Mn and Pb with contrast up to 4 times the background contents occur in soils over the Au mineralization at Goudplaats and are flanked by slightly elevated contents in soils over the greenstone rocks (Figures 4.14 - 4.16).

The geochemical signatures by 0.1M hydroxylamine hydrochloride are therefore characterised by wider anomalous zones and more contrasting background to anomaly ratio than those obtained by TAL and AR leach. Recognisable patterns are as follows.

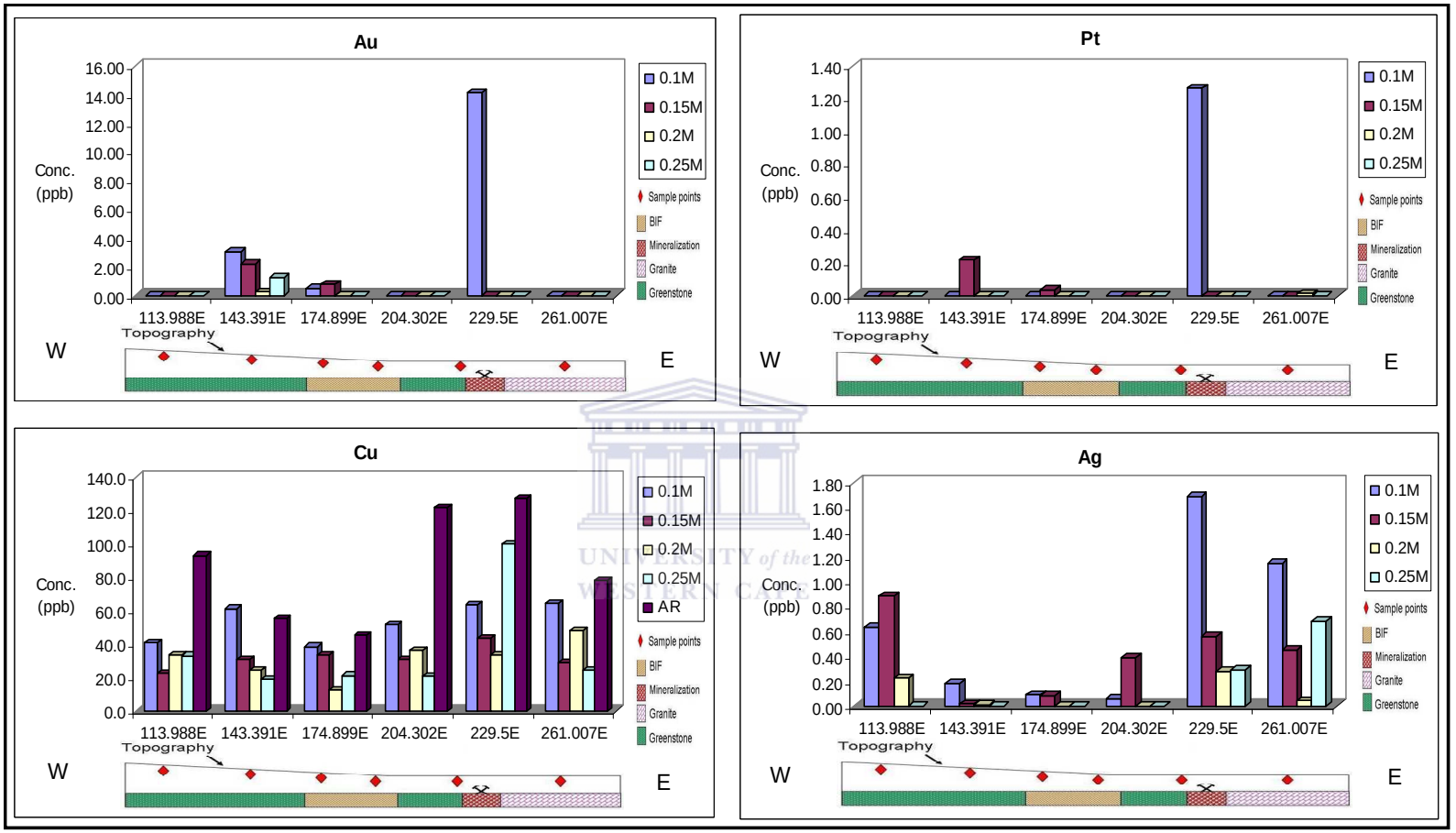

Figure 4.14 The plots of Au, Pt, Cu and Rb distribution in regolith samples from Amalia Blue Dot Mine at different concentration of hot hydroxylamine hydrochloride leach.

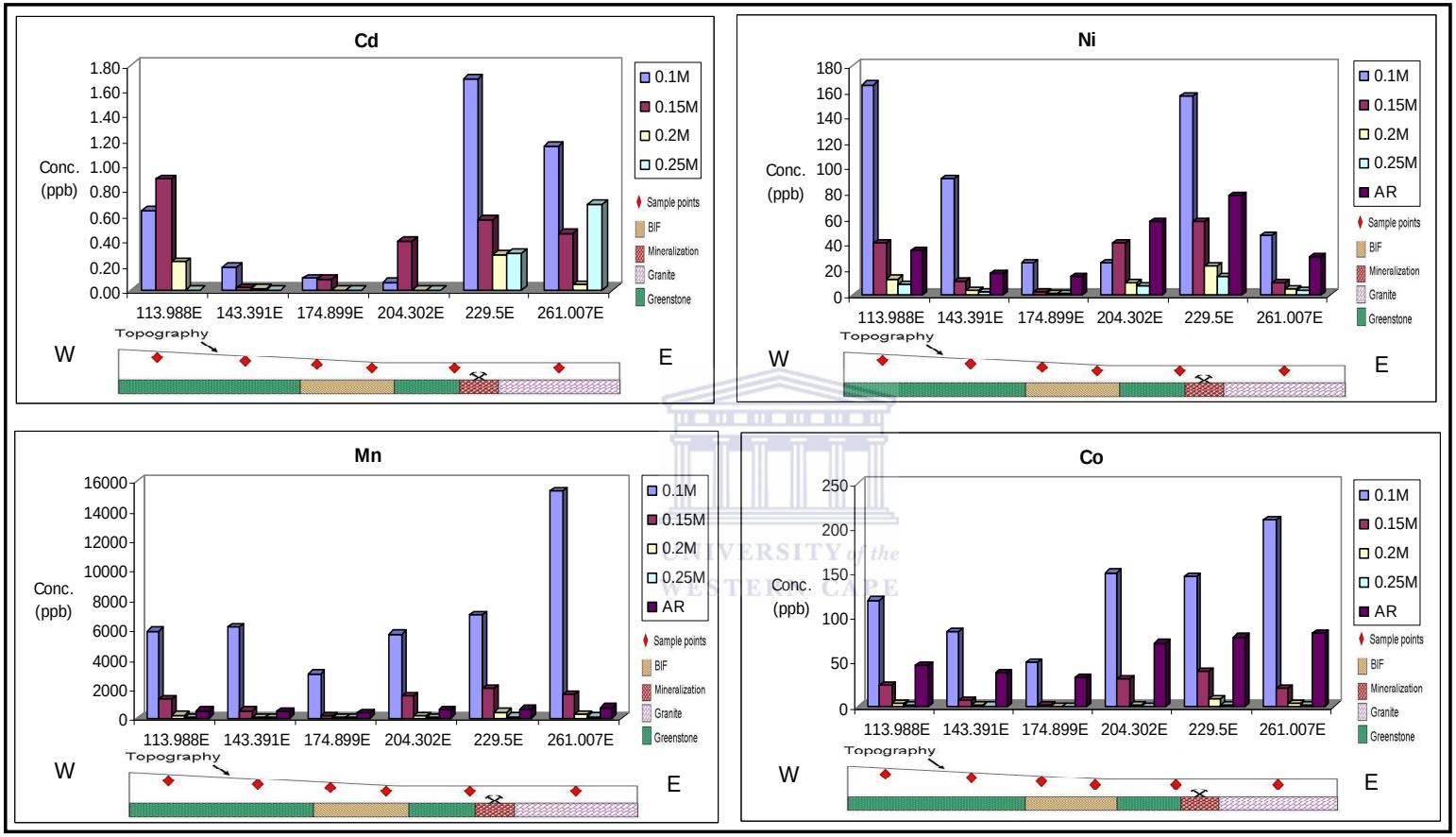

Figure 4.15 The plots of Cd, V, Ru and Ag distribution in regolith samples from Amalia Blue Dot Mine at different concentration of hot hydroxylamine hydrochloride leach.

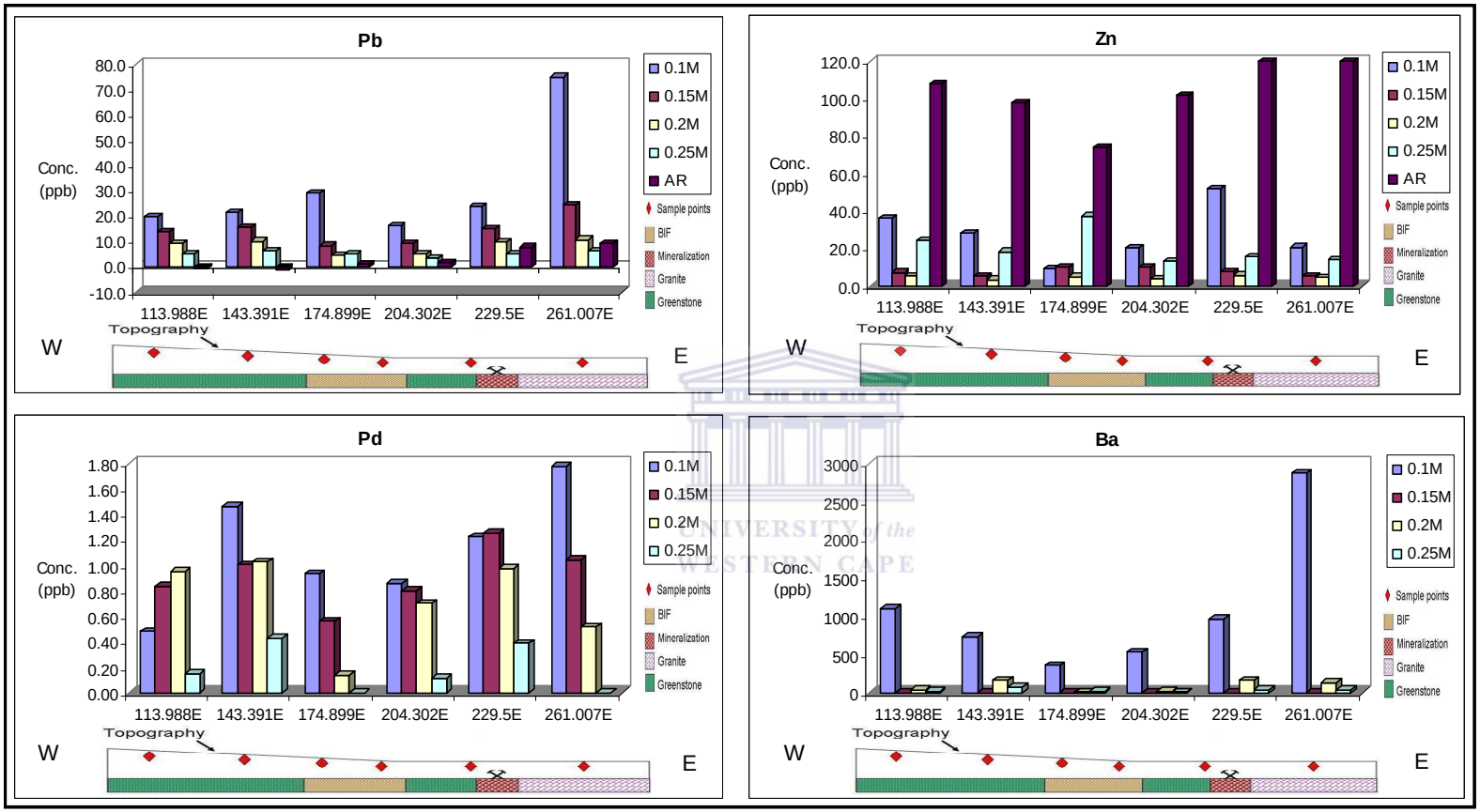

Figure 4.16 The plots of Pb, Zn, Pd and Ba distribution in regolith samples from Amalia Blue Dot Mine at different concentration of hot hydroxylamine hydrochloride leach.

- Narrow but apical anomalies with over x7 contrast to background values: that occurs over the mineralised area e.g. Pt, Au, Pb, and Ba.
- Anomalous element contents that appear to reflect both the bedrock type and mineralised area. These form broad anomalies with over x4 the background contents e.g. Ni and Co reflecting greenstone and mineralised area.
- Broad anomalous zones with over x3 the background values occur in Ag, Cu and Cd
- Anomalies with very weak contrast to background values e.g. Zn, Pd and Mn and other element are not presented.

4.1.4.2 Kabanga Main

Selected element distributions in soil traverses are plotted against the sample sites in Figures. 4.17-4.18. These plots comprise of results from hydroxylamine partial leaches (0.1-0.25M) and aqua regia leach and allow a comparative appraisal of both partial extraction techniques.

The soil traverse L9850N cuts across the Kabanga Main mineralization with a footwall host rocks comprising of quartzite and spotted schist and two ore zones, which are enclosed within the ultramafic rocks at a depth of over 150 metres.

Four major patterns of element distribution are recognizable across the profile:

- Elements whose anomalous contents of up to x7 the background concentration coincide with areas underlain by the ultramafic bodies i.e. at the flanks of the massive ore zone e.g. Cu, Co, Ba and Pb.
- Those elements with elevated content of up to x10 the background values that occur in soils down the slope, which is overlain by the ultramafic body e.g. Mn, Ni, Sr, Cr, Zn and Pd.
- Elevated contents of Pt and Ir occur only on the hill top coinciding with the ultramafic body or mineralization.
- The last group of elements generally do not show meaningful trends values or relevant patterns across the traverse e.g. As, Re, Rh, Ru, Cd, U, V, Rb, Ag

Ni, Cu with the exception of Co has maximum extractability in aqua regia partial leach (Figure 4.17). They also show good extractability in 0.25M hydroxylamine partial leach

but the anomalies are displaced. Pronounced apical anomalous to background contrast occur in the distribution patterns of Ni, Cu and Co by 0.25M hydroxylamine partial leach. This suggests the 0.25M hydroxylamine partial leach as more suitable for geochemical mapping of concealed around the Kabanga Ni-Cu deposit.

Important features of sections 4.1.4.1& 4.1.4.2

The overall assessment of the geochemical pattern of element distribution by hot hydroxylamine leach (HAL) suggests the followings;

- Occurrence of strong or presence of pronounced geochemical anomalies in aeolian regolith sands overlying the Amalia gold mineralization.
- The presence of very pronounced and a clear cut displaced geochemical anomalies in lateritic regolith overlying Ni-Cu mineralization in Kabanga Main. These observed geochemical anomalies were amplified by the westerly dipping slope of the landscape.
- The 0.1M hot hydroxylamine leach appears to give good reflection of bedrock and mineralization in both Amalia Blue Dot Mine and Kabanga study sites but the base metals are better reflected by 0.25M hot hydroxylamine leach at Kabanga Main (Ni-Cu ore deposit).

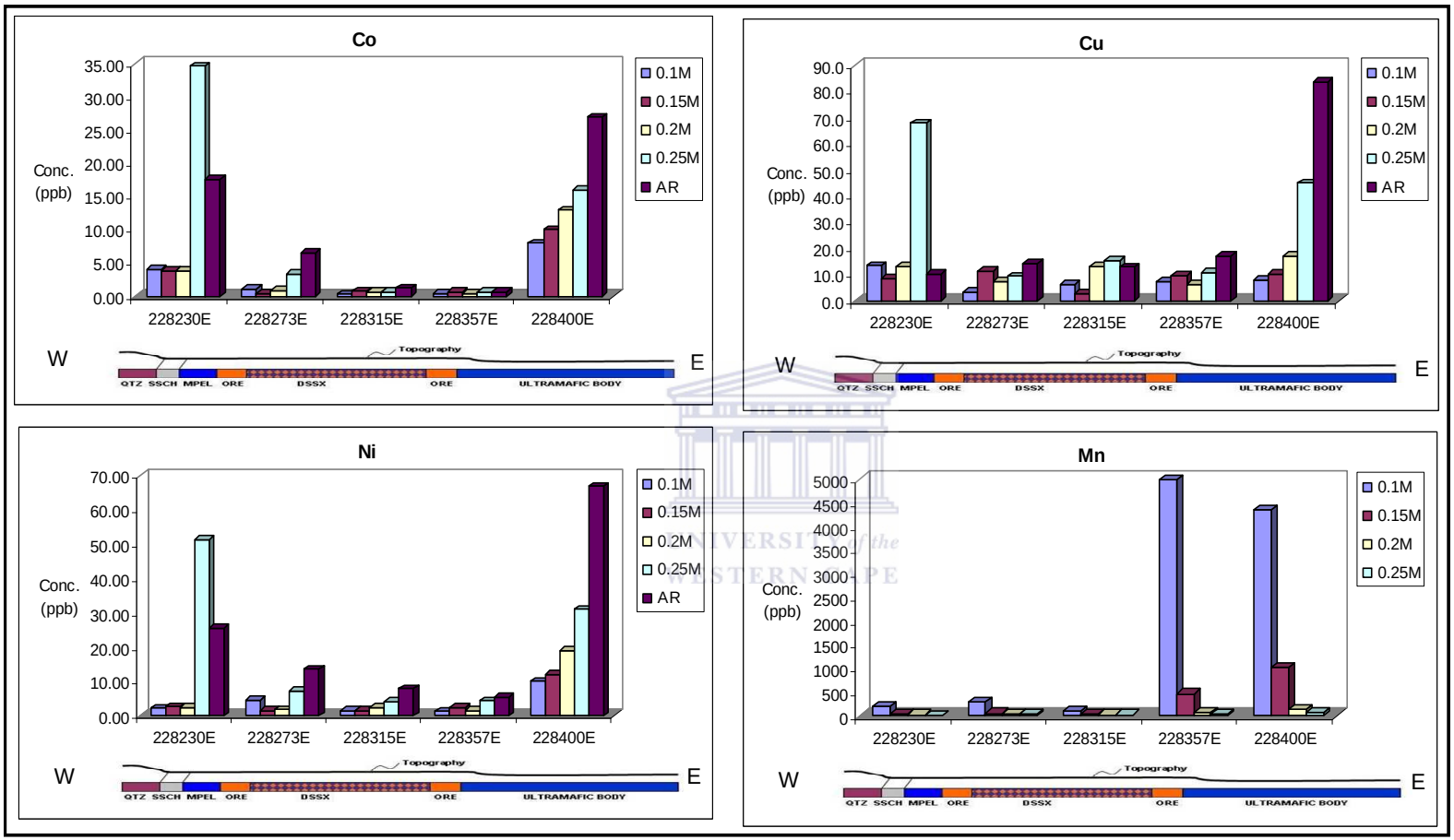

Figure 4.17 The plots of Co, Cu, Ni and Mn distribution in regolith samples from Kabanga Ni-Cu prospect at different concentration of hot hydroxylamine hydrochloride leach.

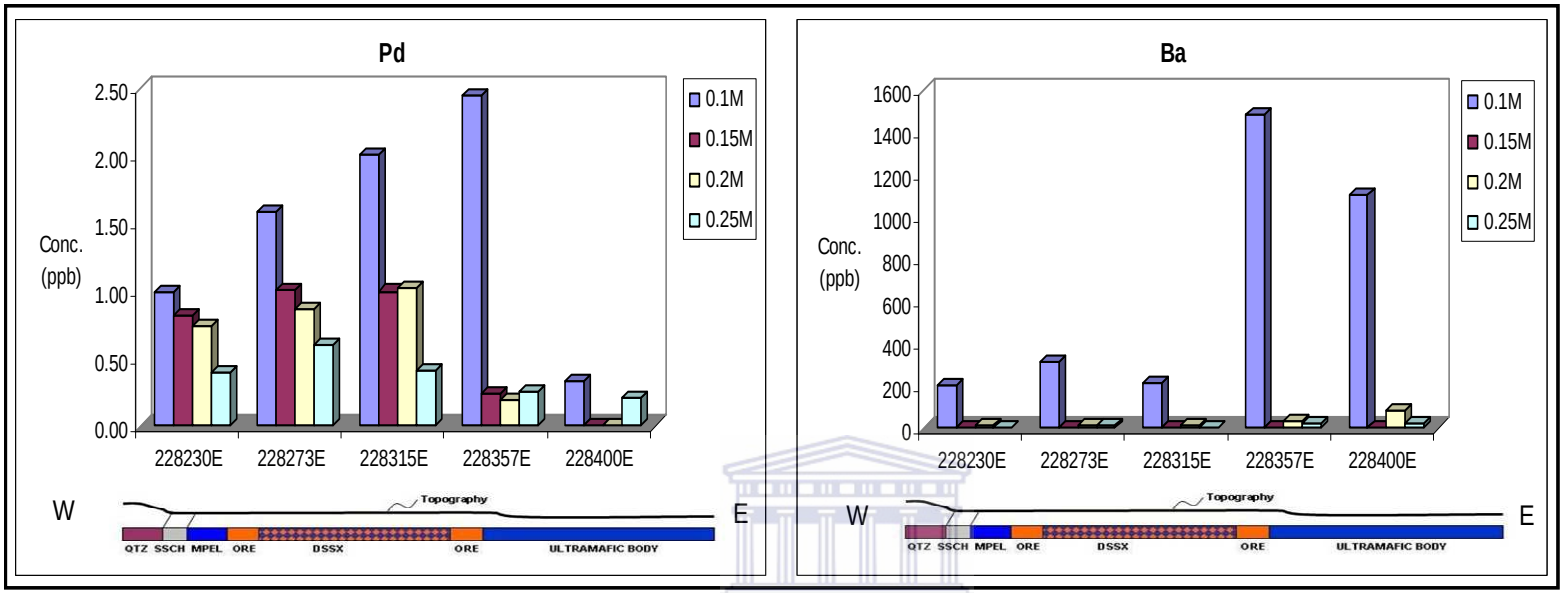

Figure 4.18 The plots of Pd and Ba distribution in regolith samples from Kabanga Ni-Cu prospect at different concentration of hot hydroxylamine hydrochloride leach.

4.2 Results of the Main study

The orientation survey revealed a varying degree and changing patterns of extractability of various elements into hydroxylamine hydrochloride. The chemistry of the underlying bedrock/concealed mineralization in aeolian regolith appears to be best reflected by partial extraction of aeolian regolith samples using 0.1 M hydroxylamine hydrochloride. The 0.25M hydroxylamine hydrochloride partial extraction appears to be most suitable in the geochemical mapping of concealed bedrock and mineralization in the lateritic regolith terrain. The objective of the main study is therefore to demonstrate the use of these optimum conditions of hydroxylamine partial extraction in geochemical mapping/mineral prospecting in two selected sites.

The result of the main study consists of the following;

Analytical data derived from 0.1M hydroxylamine hydrochloride partial extraction of samples from regolith overlying two mineralised area at Amalia.

The analytical data are presented in the Appendix D_2. The summary statistics and the box and whiskers plots are shown in Tables 4.7 & 4.8 and Figure 4.19 respectively. Geochemical maps of various elements were plotted and are presented in Figures 4.21- 4.28. Other geochemical maps are shown in the Appendix A_4-A_{11}.

Analytical data derived from 0.25M hydroxylamine hydrochloride partial extraction of samples from regolith overlying two mineralised area at Kabanga and the Luhuma prospect. The results of the multi-element analysis by ICP-MS are presented in appendix C_1 & C_2 while various graphical presentations of related data as well as a summary of analytical data are shown in Tables 4.9 & 4.10.

4.2.1 Geochemical mapping at Amalia using 0.1M hot hydroxylamine hydrochloride leaches

Analytical data for the geochemical mapping exercise are presented in Appendix D_2 and statistically summarized into Tables 4.7 and 4.8 for Amalia. A statistical summary of element contents obtained by 0.1M partial extraction for the upper and lower horizons shown in Table 4.7 These show a wide range of concentration for all elements except Cr, U, Rh, Pt, Ir, Re, Cd, Ag, which also have values of about 1ppb or less. Box and whiskers plots were used to further estimate the degree of variability and contrast of the elements in regolith overlying various bedrock and mineralization.

The data set for 0.1M hydroxylamine partial leach were treated with principal component analysis (PCA) to identify (i) groups of elements that have similar behaviour and (ii) determine changing patterns of element association in the 0.1M hydroxylamine leach. This may significantly contribute to understanding the patterns of element association in the upper and lower soil horizons. This in-turn throws light on the relationship of element association to the chemistry of underlying bedrock and mineralization.

The principal component plots for the analytical data from the lower and upper soil samples (Figure 4.20) shows two main groups of element association.

- Group I : that shows a close association with Fe and Mn. The close association suggest these elements to be linked with Fe-Mn oxides and may have been liberated in leachant by hydroxylamine (Ni, Co, Zn, Cd, Fe, Mn, Ba, Pb, U, Cu, Rb, Pd and V).

- Group II: elements in the group show diverse association with low concentration and therefore weak extractability into hydroxylamine. These may be elements that are weakly adsorbed to surfaces termed exchangeable (Rh, As, Ru, Pt, Re, Cr, Ag, Os, Au, Ir and Se).

Fig 4.20 also shows a changing pattern of elements in the two groups outline above. The Fe-Mn in group I for data from lower horizon contains a greater number of elements and differs

from the upper soils in V, Pb, Pd, Ag and Cu. On the contrary upper soils show an association of Zn and Cd with Fe-Mn (oxides). The changing pattern of the elements association in the lower soil versus the upper soils suggests or may reflect change in mineralogy of soils with increasing depth.

The exchangeable elements in group II for data from upper horizon contains a greater number of elements and differs from the lower soils in Pb, Au, Cu, Ag, Rb and Pd association.

The changing patterns of elements observed in the result of principal component plots may suggest the following;

- An occurrence of vertical zoning of the elements in the aeolian sand. The elemental zoning may occur as a result of pedogenesis (upward migrating fluid).This phenomenon thus enriched the lower horizon in Fe-Mn nodules and upper horizon in Fe-Mn solution (Okujeni et al., 2005).
- The extraction of elements adsorbed to Fe-Mn nodules in the lower horizon by hydroxylamine hydrochloride leach reflects the chemistry of the bedrock (Section 4.1. 4.3). This makes the lower horizon suitable for geochemical mapping using hydroxylamine hydrochloride leach.
- The clustering of elements associated with the exchangeable geochemical phase. This makes the choice of another partial leach for the exchangeable desirable.

Background, threshold and anomalous values were estimated using Sigma plot software® (S-plot). The estimated values are presented in Table 4.8 and used in the construction of the geochemical maps using Surfer and presented in Figures 4.21 - 4.28. The maps are shown in the order of the element associations, which were determined using the principal component analysis. Selection of geochemical maps was done to illustrate those elements that have (i) ability to reflect the bedrock chemistry and (ii) possibly reflects mineralization with the hydroxylamine partial leach.

The pattern of those elements in geochemical maps would be use to explain the ability of the hydroxylamine partial leach to reflects bedrock and mineralisation in the Amalia.

Table 4.7 Summary statistics of the hot hydroxylamine hydrochloride digestion of the samples taken in Amalia Blue Dot Mine.

Amalia samples		**(All data in ppb)**			**n = 69**			
0.1M								
Upper horizon					**Lower horizon**			
Element	Min.	Max.	Mean	Std.Dev.	Min.	Max.	Mean	Std.Dev.
Ni	0	93.77	52.26	36.28	4.82	162.61	84.4	66.75
Co	29.55	155.41	101.8	45.2	53.49	231.5	124.5	61.74
Cu	16.56	53.38	31.66	11.16	13.38	143.64	69.51	43.08
Zn	33.19	71.88	43.07	12.28	29.57	248.65	68.54	68.04
As	2.92	9.65	6.21	3.21	1.06	24.88	8.5	9.73
Se	1.46	15.21	7.84	4.3	0.5	14.15	6.83	5.28
Rb	8.38	15.33	11.8	2.47	4.42	19.71	12.49	4.22
Sr	44.35	292.6	107.4	81.51	75.28	524.77	207.7	149.6
Pd	0.51	2.12	1.09	0.48	0.28	2.73	1.47	0.75
Ag	0.06	0.31	0.16	0.08	0.07	0.84	0.31	0.29
Mn	2040	8071.5	5999.6	2047.1	3047	14380	7232.5	3159.86
V	28.43	83.19	51.13	17.8	42.32	147.3	93.69	29.63
Cd	0.05	0.46	0.29	0.15	0.03	0.38	0.21	0.11
Ba	308.4	1021.8	610.61	240.47	394.2	3063.6	1153.8	780.63
Re	0.01	0.06	0.03	0.02	0.01	0.03	0.02	0.01
Os	6.3	122.84	39.96	44.07	0.51	48.47	16.5	19.87
Ir	0.02	0.21	0.09	0.08	0.01	0.11	0.06	0.05
Cr	2.76	5.97	4.12	1.54	5.71	59.77	22.88	25.63
Au	0.19	6.3	1.72	2.13	0.21	1.85	0.88	0.65
Pb	17.69	37.69	26.72	8.25	1.37	79338	34.07	20.78
U	0.17	0.51	0.34	0.12	0.27	1.6	0.7	0.47
Ru	0.45	0.05	0.05	NA	0.23	0.23	0.23	NA
Rh	0.01	0.05	0.23	0.02	0.01	0.04	0.02	0.01
Pt	0.09	0.16	0.13	0.04	0.04	0.15	0.08	0.05
Fe	1254	5110.6	3490.4	1254.5	1201	6749.6	4123.3	1767.8

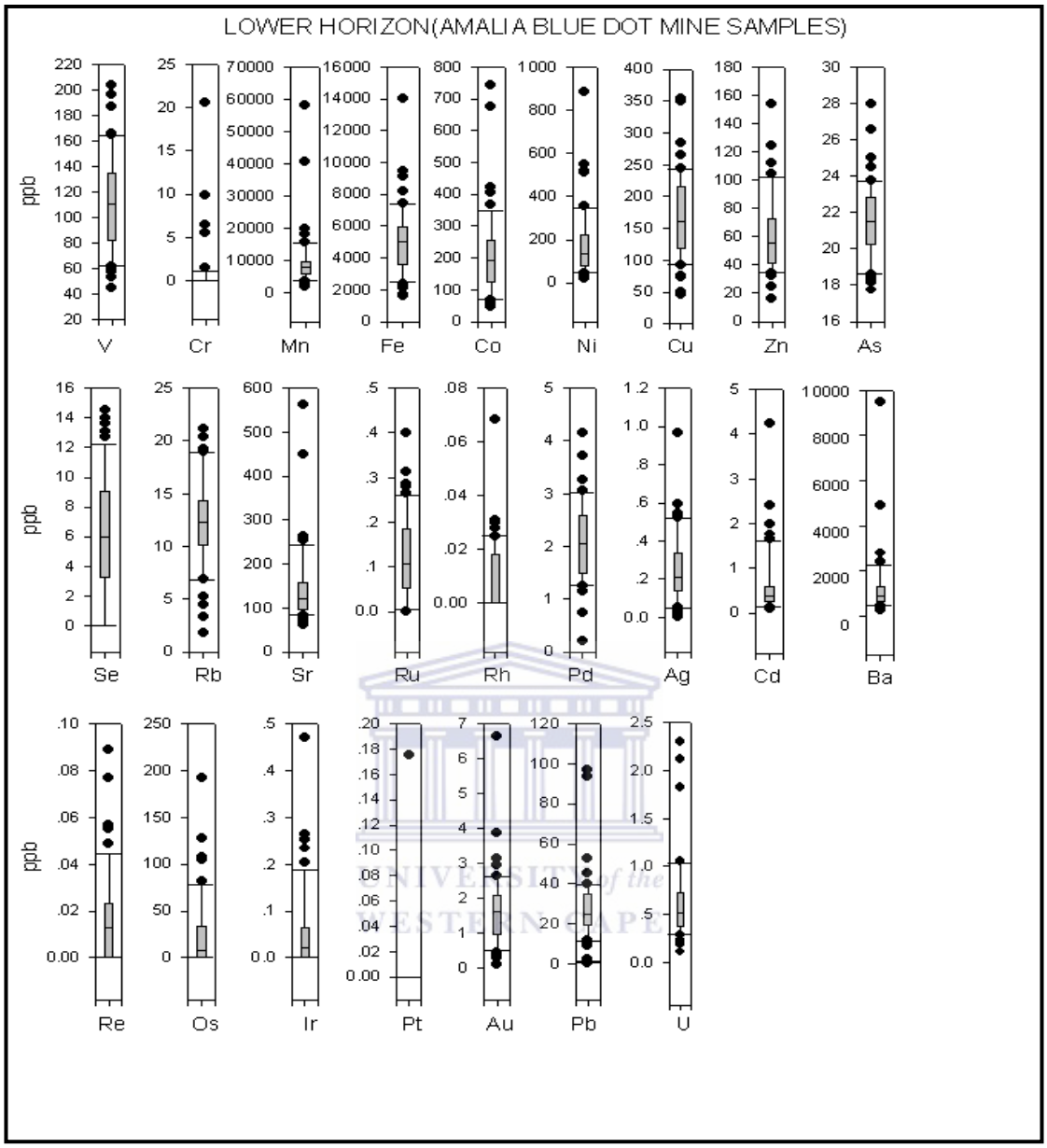

Figure 4.19 Box and whisker plots showing element contents in the upper (U) and lower (L) horizon in Amalia Blue Dot Mine. The middle line corresponds to the background value (median); lower and upper bounds of the box indicate 25th and 75th percentiles respectively. Values above the 75th percentile are considered. Element contents between the 50th and 75th percentiles are regarded as the threshold (Turkey, 1977).

Table 4.8 Estimated background-anomalous values of the various elements for Amalia samples.

Amalia samples (All data in ppb)			
0.1M			
Lower horizon			
Element	Background	Threshold	Anomaly
V	122.5	137.5	163.5
Cr	10	22	32
Mn	100	2300	4600
Fe	4800	8800	11929
Co	5	10.5	32.5
Ni	25	30	202.22
Cu	22	34	145.18
Zn	*n.d*	*n.d*	186.88
As	58	65	24.85
Se	5.6	14	15.55
Rb	17	23	20.25
Sr	150	475	480.8
Rh	0.03	0.041	0.04
Ru	0.048	0.075	NA
Pd	2.36	2.57	2.84
Ag	0.24	0.44	0.752
Cd	0.15	0.29	0.47
Ba	480	700	2727.16
Re	n.d	0.02	0.04
Os	16	36	47.79
Ir	0.05	0.1	0.14
Pt	0.052	0.135	0.17
Au	1.6	2.5	0.63
Pb	42	50	72.26
U	1.2	1.5	1.58

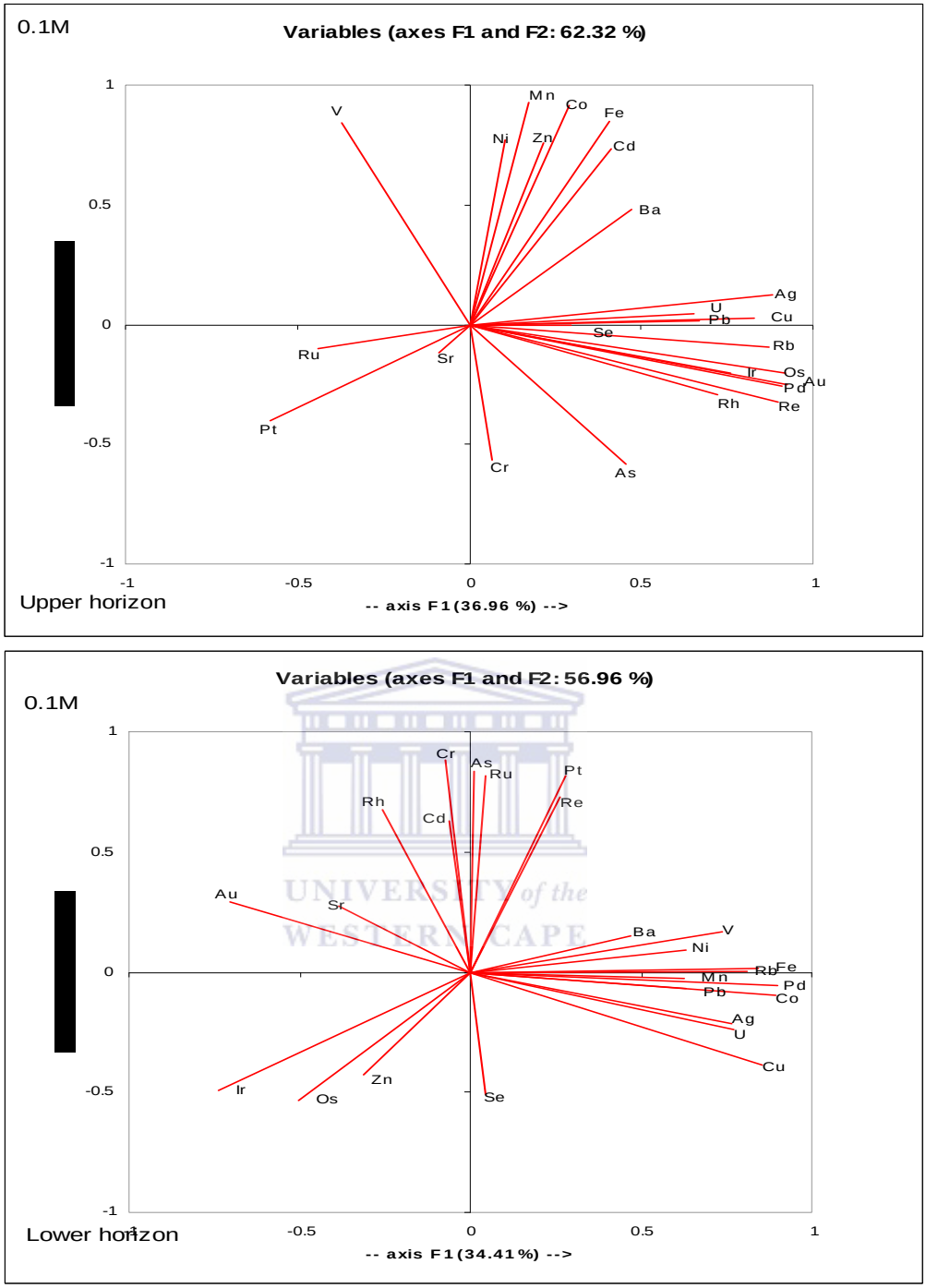

Figure 4.20 Principal component analysis plots for 0.1M concentration of hydroxylamine hydrochloride leach (lower and upper horizons) in Amalia Blue Dot Mine.

4.2.1.1 Geochemical maps

Gold mineralisation at Amalia occurs in three areas as follows; the Goudplaats area (B), the Bothmasrust area(C), the Abelskop area (D) and the prospect at area (A).

Area A (Prospect area) is underlain by the poorly exposed granitic body which cut across the inferred greenstone succession. Goudplaats mineralised area (B) is flanked by granitic body which trends north-easterly direction towards Bothmasrust (Kiefer, 2004). The BIF succession in Goudplaats area has undergone more deformation compared to Abelskop (Kiefer, 2004). The BIF is rich in carbonate especially in the mineralised zone. The Abelskop area (D) is underlain by a largest continuous BIF succession. BIF consist of two lithologic units, the central BIF which is more cherty with thinner bands of hematite-magnetite and the reddish brown ferruginous distal BIF (Kiefer, 2004).

Bothmasrust area(C) is underlain by discontinuous lithologies such as oxide facies BIF, metamorphosed mafic lavas, quartz rich schists, brecciated horizons and outcrop accretionary lapilli. This mineralised zone is characterised by extremely intense deformation (Kiefer, 2004).

Gold (Au)

Gold contents are generally high in ultramafic rocks and especially elevated in greenstone. In weathering solution Au occurs in complexes of cyanide, chloride, thoiurea, thiocyanate and thiosulfate ions by the formation of stable complex (Marsden and House, 2006). Au in soils is found in mobile complexes such as Au Br_4^-, AuI_2^-, Au $(N)_2^{2-}$ and is transported as organometallic complexes(Alloway, 1995).

In regolith Au is concentrated in the lower part of the bauxite zone, the middle of the clay saprolite and the lower saprolite (LeGleuher et al., 2005). In aeolian sand Au concentration in lower part mostly in Fe-nodules (Okujeni et al., 2005).

The principal component plots shows diametric relationship with element in Fe-Mn group suggesting a possible occurrence of free gold or a disseminated occurrence in Fe-Mn nodules (Figure 4.20). Fig. 4.21 for example in the Goudplaats area (area B) anomalous zone occurs detached from the site of mineralisation possible following the drainage pattern. The anomaly to the west (area A) coincides with zones of weak mineralisation (Kiefer, 2004). Pronounced Au anomalies occur around the Abelskop mineralisation (area D). At the Bothmasrust (area C), the anomalies occur at the foot of mineralisation. These elevated values coincided with areas of high aeromagnetic anomaly (Ackon, 2001).

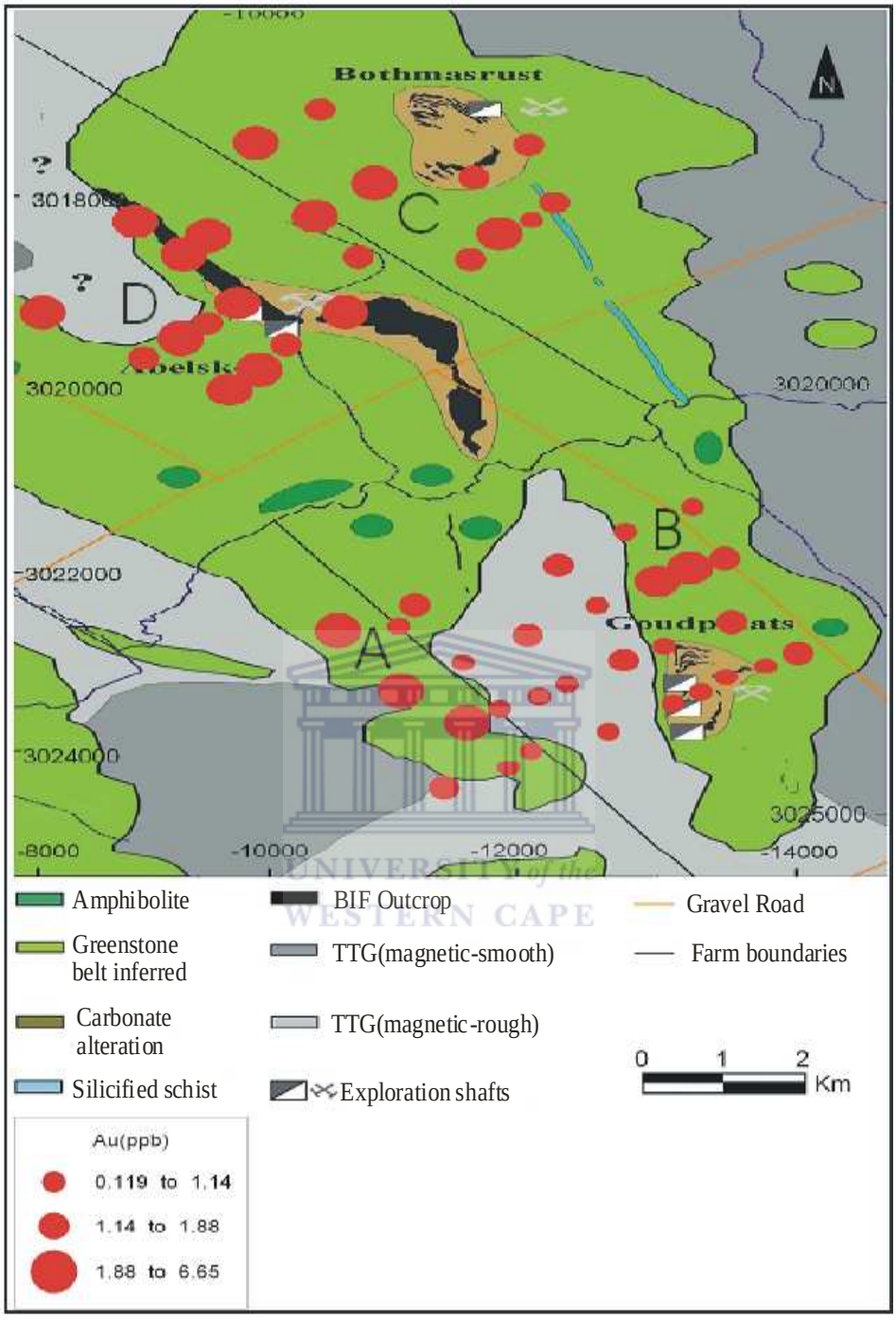

Fig 4.21 Geochemical map of Au in regolith samples by 0.1M hydroxylamine partial leach

A cluster of anomalies gold values with contrast of about 3 times background concentration occur in the area labelled A, B, C and D (Fig 4.21 & Table 4.8). Most of these are concentrated around the greenstone areas but some anomalies concentrates around the BIF. The distribution pattern of Au in lower soil and anomaly contrast obtained with hydroxylamine hydrochloride leach are similar to the previous selective extraction by Ammonium citrate (Ackon, 2001).

Silver (Ag)

Silver primarily occurs in minerals such are tetrahedrite (Cu, Fe, Zn, $Ag_{12}Sb_4S_{13}$), freibergite (tetrahedrite with up to 30% Ag), pyragyrite (Ag_3SbS_3), argentite (Ag_2S), proustite (Ag_3AsS_3) and ceragyrite (AgCl). Silver also occur in gold ores occurs as a minor amounts often as a natural gold-silver alloy called electrum. The element is easily released during weathering and then precipitates under alkaline reducing conditions from sulfur enriched solutions forming a variety of anions and cations (Greger, 2004). Ag contents in soils would typically reflect the sulphide mineralization. Fe-Mn oxyhydroxides are notorious scavenger of silver in weathering environment. The principal component plots shows strong association of Ag in Fe-Mn group suggesting a possible occurrence of silver in Fe-Mn oxides (Figure 4.20).

The geochemical map shows 4 areas of occurrence of Ag anomalies (Fig 4.22).

In area B, clusters of Ag content occur detached from the site of mineralisation possibly following the drainage pattern.

The anomaly to the west (area A) coincides with zones of weak Au mineralisation (Kiefer, 2004). Pronounced Ag anomalies occur around the Abelskop mineralisation (area D). At the Bothmasrust (area C), the anomalies occur at the foot of mineralisation.

The anomaly contrasts of about 5 times background concentration occur in the highlighted areas A, B, C and D (Fig. 4.22&Table 4.8). Similar to Au distribution pattern, the Ag anomalies are concentrated mostly in greenstone areas and around the BIF. The clusters of Ag anomalies are wider than those of Au in the Goudplaats area. Ag anomaly contrasts in lower soil obtained with hydroxylamine hydrochloride leach but are more pronounced than those obtained by partial extraction in TAL (Ackon, 2001).

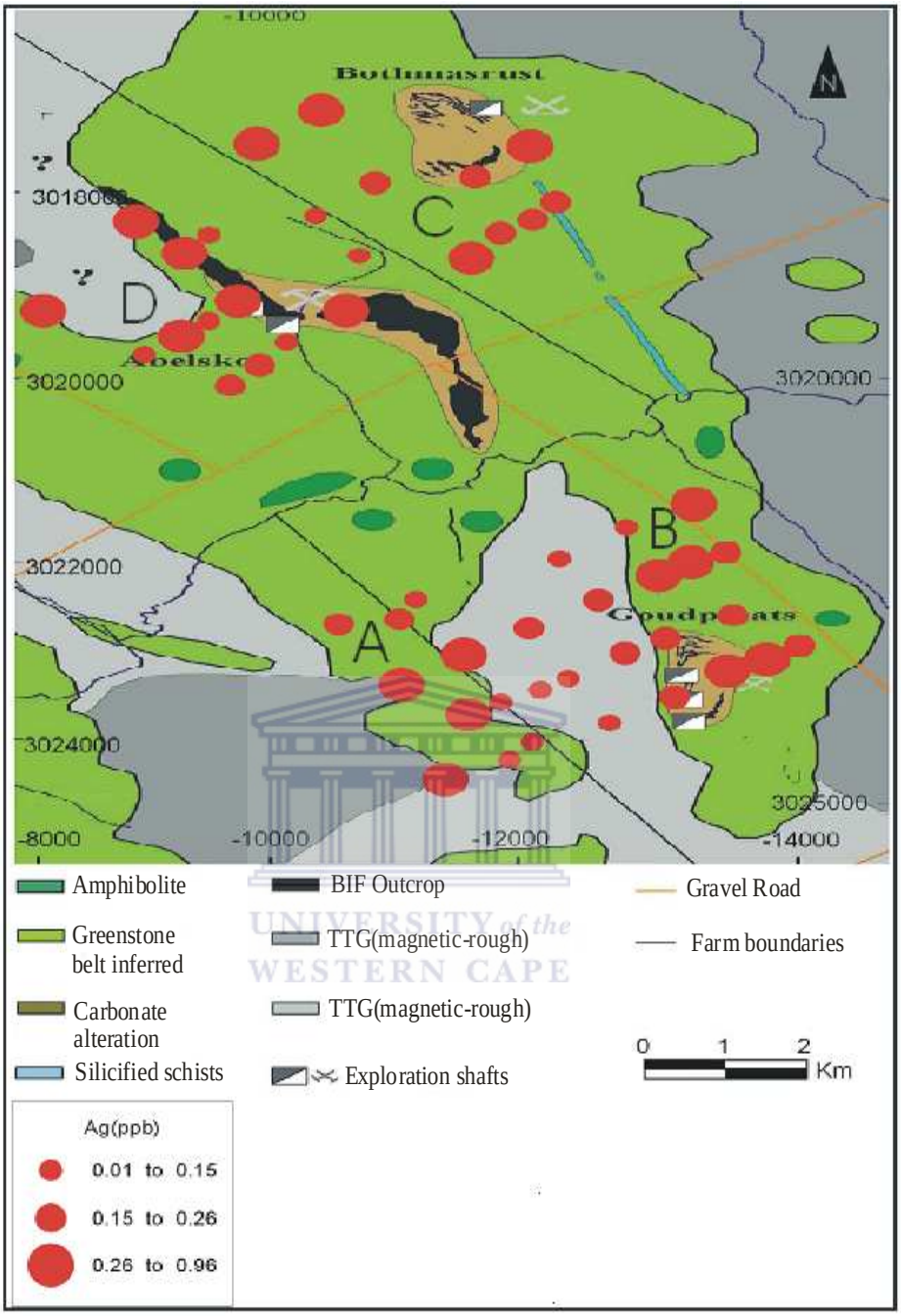

Fig 4.22 Geochemical map of Ag in regolith samples by 0.1M hydroxylamine partial leach.

Nickel (Ni)

Nickel is easily adsorbed by Fe-Mn oxyhydroxides in the weathering environment. Amorphous Fe-Mn oxhydroxides are abundant in aeolian sand regolith. Four areas of Ni anomalies occur in the geochemical map (Fig 4.23).

Principal component plots shows association of Ni in Fe-Mn group which implies its occurrence in Fe-Mn nodules (Fig 4.20).

Ni anomalies occur in 4 areas in the geochemical map (Fig 4.23).

In the Goudplaats area (area B), a cluster of Ni anomalies occur detached from the site of mineralisation possible following also the drainage pattern. Another cluster of anomalies in the area A coincides with the zones of weak Au mineralisation (Kiefer, 2004). Further cluster of anomalies further occur around the Abelskop mineralisation (area D). At Bothmasrust (area C), the Ni anomalies occur at the foot of mineralisation.

Anomaly/background contrast of about 8 times background concentration occurs in the highlighted areas A, B, C and D (Figure 4.23 & Table 4.8). Ni anomaly contrasts in lower soil obtained with hydroxylamine hydrochloride leach but are more pronounced than those obtained by previous partial extraction in TAL (Ackon, 2001).

Cobalt (Co)

Cobalt occurs naturally as the arsenide $Co(As_2)$, known as smaltite or speiss cobalt; as cobalt sulfarsenide (CoAsS), known as cobaltite or cobalt glance; and as hydrated arsenate ($Co(AsO_4)_2.8H_2O$), known as erythrite or cobalt bloom. It is easily adsorbed by the amorphous Fe-Mn oxhydroxides in the weathering environment. Co is dominantly hosted by secondary Fe oxides in the regolith and may be locally enriched by co-precipitation with Mn oxides (Brand, 2001).

The principal component plot shows strong association of Co in Fe-Mn group suggesting a possible occurrence in Fe-Mn oxyhydroxides/oxides (Figure 4.20).

The geochemical map shows 4 areas of occurrence of Co anomalies (Figure 4.24). For example in the area B anomalous Co content occur detached from the site of mineralisation possible following the drainage pattern. The anomaly to the west (area A) coincides with the zones of weak Au mineralisation (Kiefer, 2004). Cobalt anomalies concentrated mostly in greenstone areas and around the BIF. The pronounced apical anomalies occur around the Abelskop mineralisation (area D).

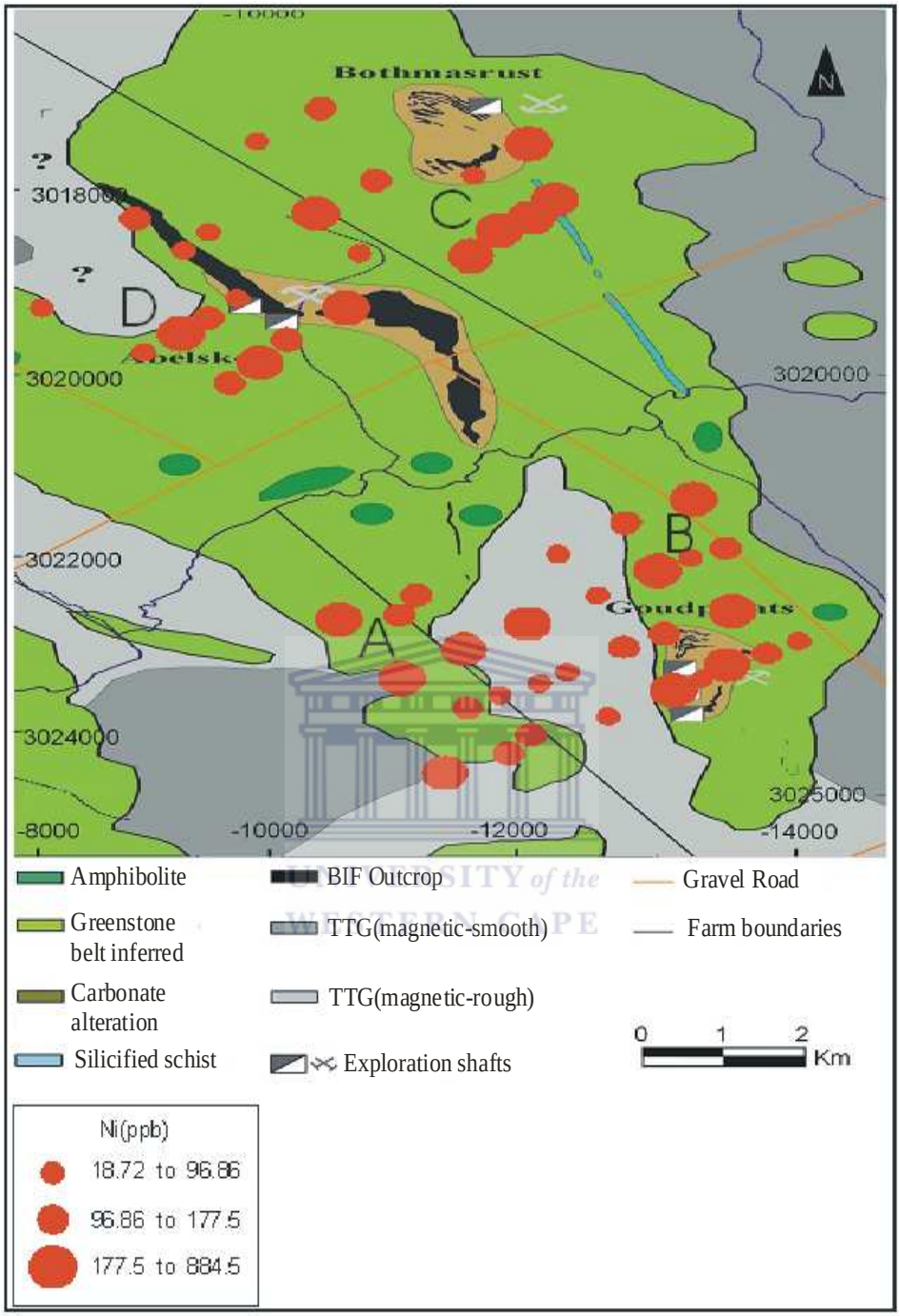

Fig 4.23 Geochemical map of Ni in regolith samples by 0.1M hydroxylamine partial leach.

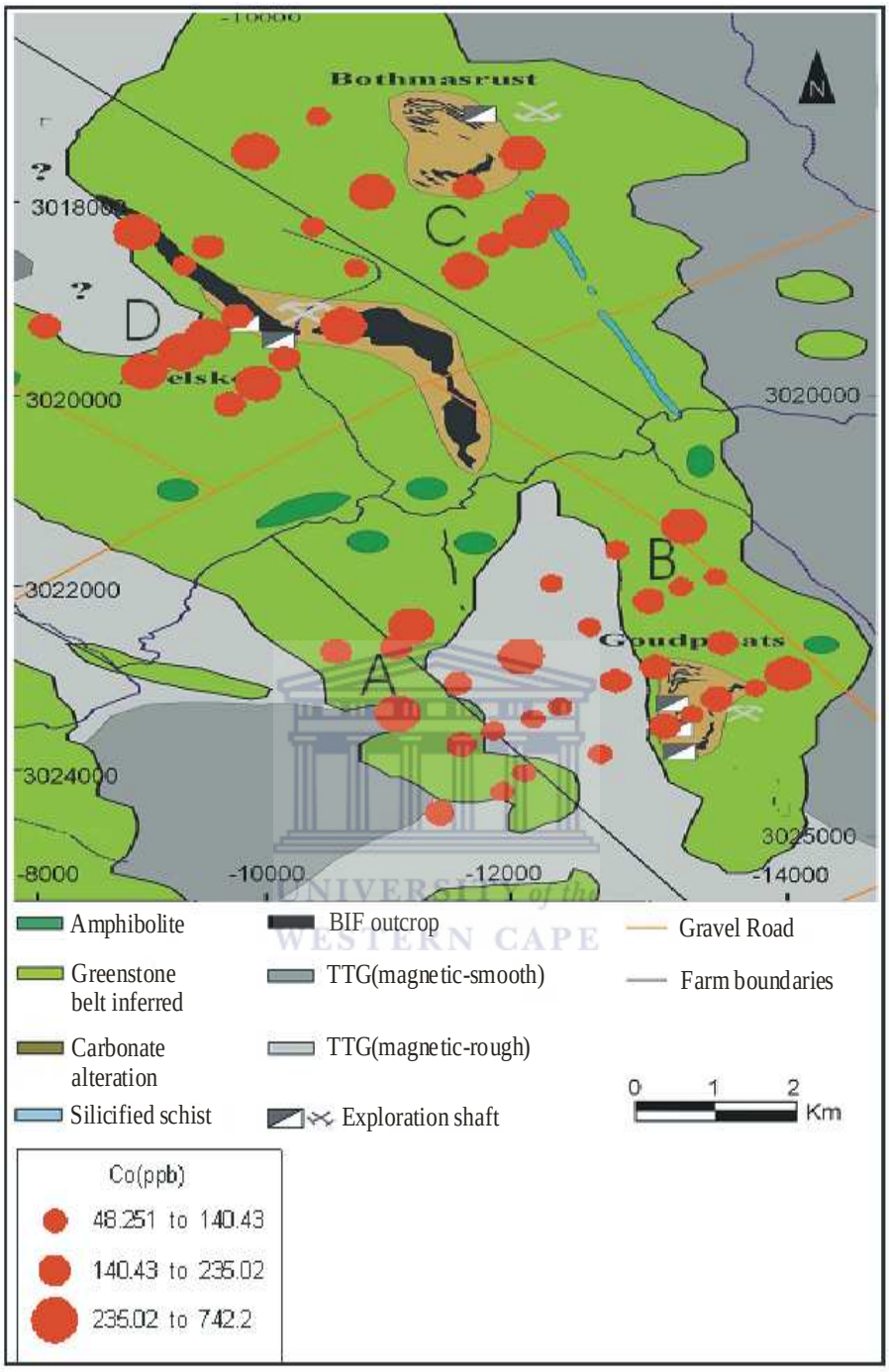

Fig 4.24 Geochemical map of Co in regolith samples by 0.1M hydroxylamine partial leach

At the Bothmasrust (area C), the anomalies occur at the foot of mineralisation. Co anomaly contrasts in lower soil obtained

with hydroxylamine hydrochloride leach are more pronounced than those obtained by previous partial extraction in TAL (Ackon, 2001).

Copper (Cu)

Anomalous Cu contents in soils will often reflect the occurrences of sulphide mineralisation such as chalcopyrite (Kabata-Pendias and Pendias, 1984). Cu in regolith commonly adsorbed or scavenged by Fe-Mn oxhydroxides/oxides.

The principal component plot shows association of Cu in Fe-Mn group suggesting a possible occurrence in Fe-Mn oxyhydroxides/oxides (Figure 4.20). The geochemical map shows 4 areas with occurrences of Cu anomalies (Fig 4.26). A cluster of Cu anomalies coincides with the site of mineralisation possibly following the drainage pattern at Goudplaats (area B).

The asymmetrical anomaly train to the west (area A) coincides with the zones of weak Au mineralisation. Pronounced apical Cu anomalies occur around BIF in the Abelskop section (area D). At the Bothmasrust (area C), the anomalies occur at the foot of mineralisation. Copper anomaly/background contrast of about 2 times background concentration occurs in the areas A, B, C and D (Figure 4.26 & Table 4.8). Cluster of elevated Cu values generally trending from north-westerly to north south direction which coincides with high aeromagnetic anomalies (Ackon, 2001). The Cu anomalies occur mostly in greenstone and around BIF. Cu anomaly contrasts in lower soil obtained with hydroxylamine hydrochloride leach are more pronounced than those obtained by partial extraction using TAL (Ackon, 2001).

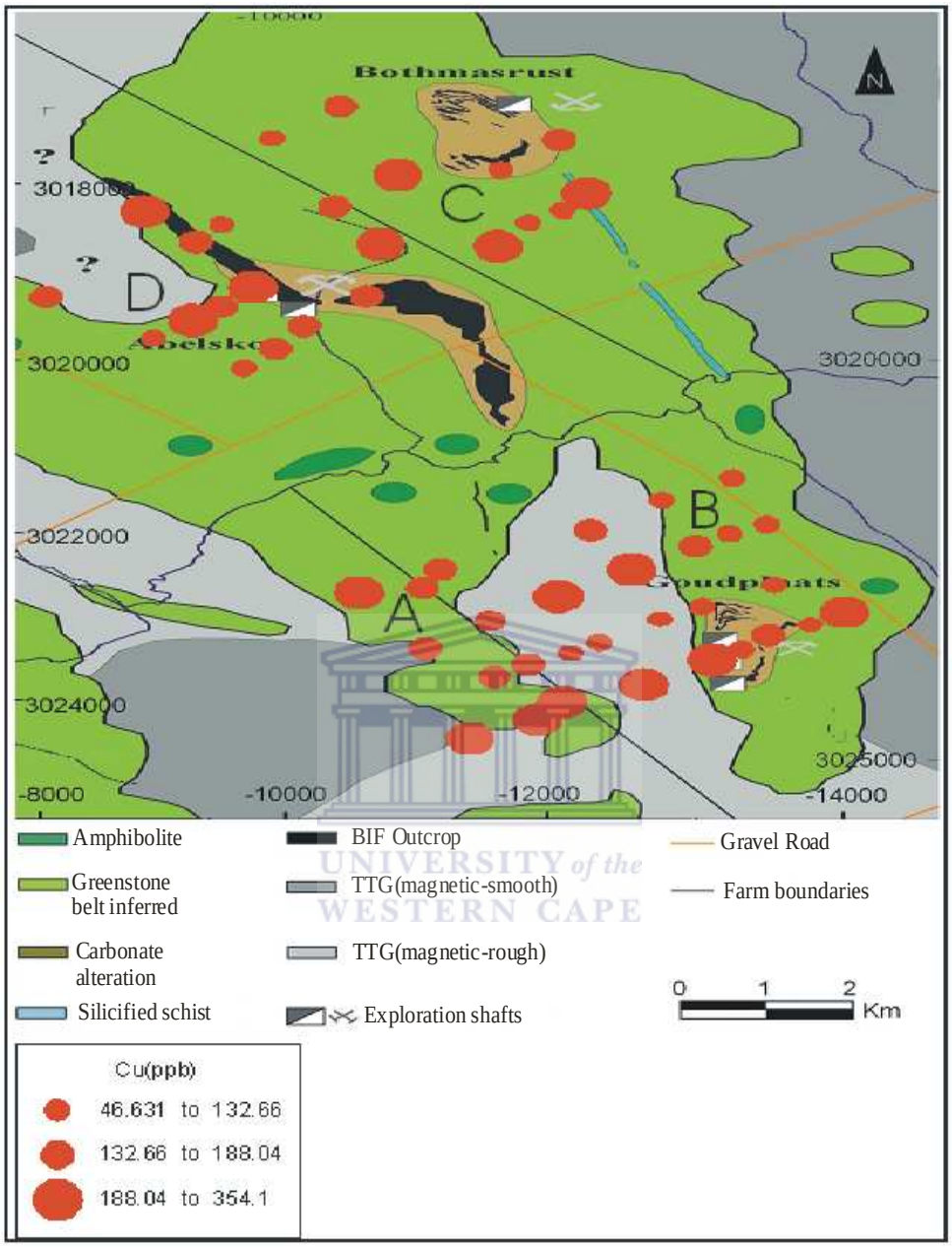

Fig 4.26 Geochemical map of Cu in regolith samples by 0.1M hydroxylamine partial leach.

Vanadium (V)

The principal ores of vanadium includes carnotite, patronite and vanadinite. Vanadium is easily adsorbed by the amorphous Fe-Mn oxyhydroxides in soils.

The principal component plots show V in strong relationship with Fe-Mn group suggesting association of vanadium with Fe-Mn nodules (Figure 4.20).

Four areas of V anomalies were occurring in the geochemical map (Figure 4.25).

In the Goudplaats area (area B) the anomalous occur detached from the site of mineralisation. The anomalies in the area B are aligned with the drainage pattern. The cluster of V anomalies to the west of Goudplaats coincides with the zones of weak Au mineralisation as reported in Kiefer (2004). The cluster of elevated vanadium contents occurs around the BIF outcrops at Abelskop mineralization (area D). At the Bothmasrust (area C), the anomalies occur at the foot of mineralisation and around the fault zone.

The anomaly/background contrast of about 5 times background concentration occurs in 4 areas in the geochemical map (Figure 4.25 & Table 4.8).

Zinc (Zn)

Zinc occurs widely in both igneous and sedimentary rocks. Its never occurs in native state in nature. Some of its most important ores are smithsonite, or zinc spar or zinc carbonate ($ZnCO_3$); sphalerite, or zinc blende or zinc sulfide (ZnS); zincite, or zinc oxide (ZnO); willemite, or zinc silicate ($ZnSiO_3$); and franklinite [(Zn, Mn, Fe)O (Fe, Mn_2)O_3]. Zinc is co-precipitate and adsorbed by the Fe-Mn oxyhydroxides/oxides in the secondary environment. The sorbed forms of zinc in soils are normally more stable than most Zn minerals except franklinite (Alloway, 1995).

The principal component plot shows Zn in diametric relationship with the exchangeable group suggesting a possible occurrence in exchangeable geochemical phase (Figure 4.20).

The zinc anomalies occur detached from the site of mineralisation in the Goudplaats area (area B). The cluster of anomalies to the west of Goudplaats section (area A) coincides with the zones of weak Au mineralisation. Clusters of Zn anomalies occur around the BIF in the Abelskop mineralisation (area D). The cluster of zinc anomalies also occur at the foot of mineralisation and around the fault zone in Bothmasrust (area C).

An anomaly/background contrast of about 5 times background concentration occurs in the 4 areas shown in the geochemical map (Figure 4.19&Table 4.8).

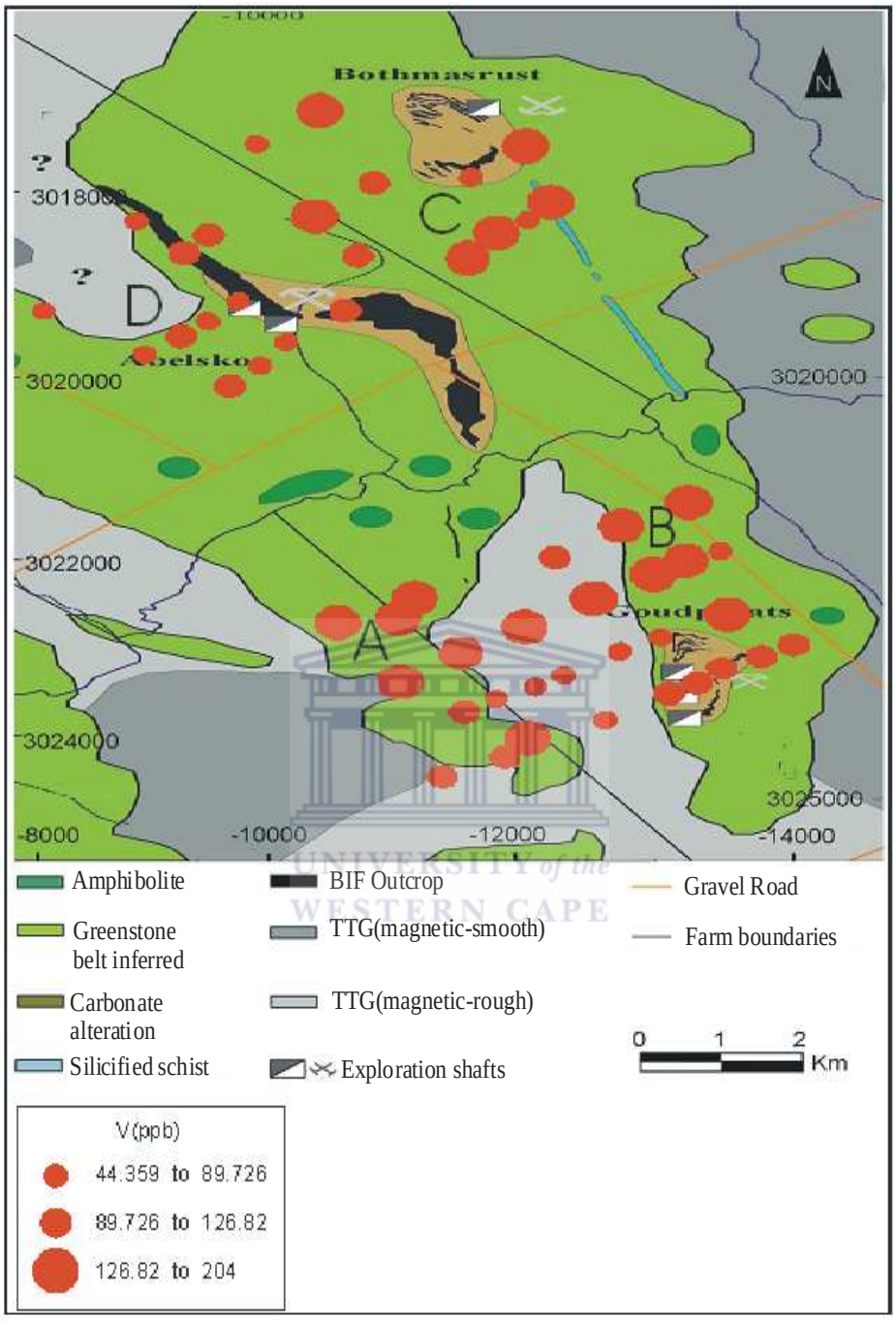

Fig 4.25 Geochemical map of V in regolith samples by 0.1M hydroxylamine partial leach.

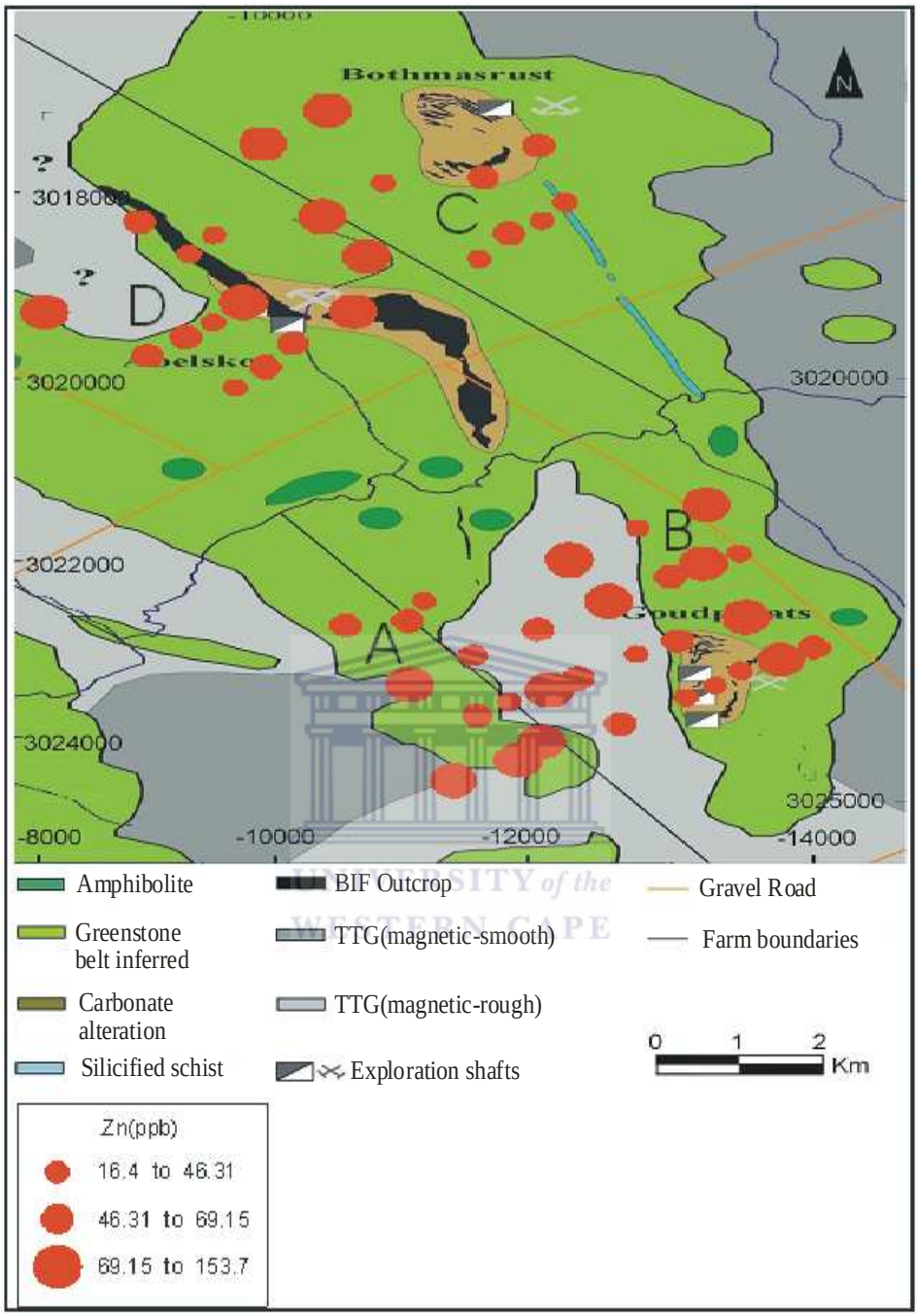

Fig 4.27 Geochemical map of Zn in regolith samples by 0.1M hydroxylamine partial leach.

Zn anomaly contrasts in lower soils obtained with hydroxylamine leach are more pronounced than those obtained by previous partial extraction by TAL (Ackon, 2001).

Cadmium (Cd)

Low contents of cadmium occur generally in volcanic rocks, sedimentary rocks (limestone and sandstones) and clays. In sedimentary rocks, clay has most abundant of cadmium containing up to 0.3mg/kg. Cadmium forms its own minerals: greenockite (CdS), otavite CdCO3), monteponite (CdO); however, these minerals occur as accessories in assorted ore. In the weathering environment, cadmium is most sorbed by the clay materials. The principal component plot shows strong relationship with element in the exchangeable group suggesting a possible occurrence of cadmium in clays (Figure 4.20). Anomaly/background contrast of about 10 times background concentration occurs in four areas in the geochemical map (Figure 4.19&Table 4.8). For example at Goudplaats (area B) anomalous Cd contents occur detached from the site of mineralization possibly following the drainage pattern. The anomaly to the west (area A) coincides with the zones of weak Au mineralization (Kiefer, 2004). Pronounced Au anomalies occur around the Abelskop mineralization (area D). The cluster of anomalies at the Bothmasrust (area C), occur at the foot of mineralization and around the fault zone.

Important features of section 4.2.1 are as follows;

- The establishment of four areas of anomalies for the occurrence for Au, Ni, Ag, Cu, Co, V, Zn and Cd in the Amalia Blue Dot Mine study area.
- Hydroxylamine hydrochloride leaches show more pronounced anomaly contrast in Ni, Ag, Cu, Co and Zn than those obtained by triple acid leach.
- Elements in hydroxylamine leach are associated with low background values, this make hydroxylamine leach more suitable for geochemical mapping.

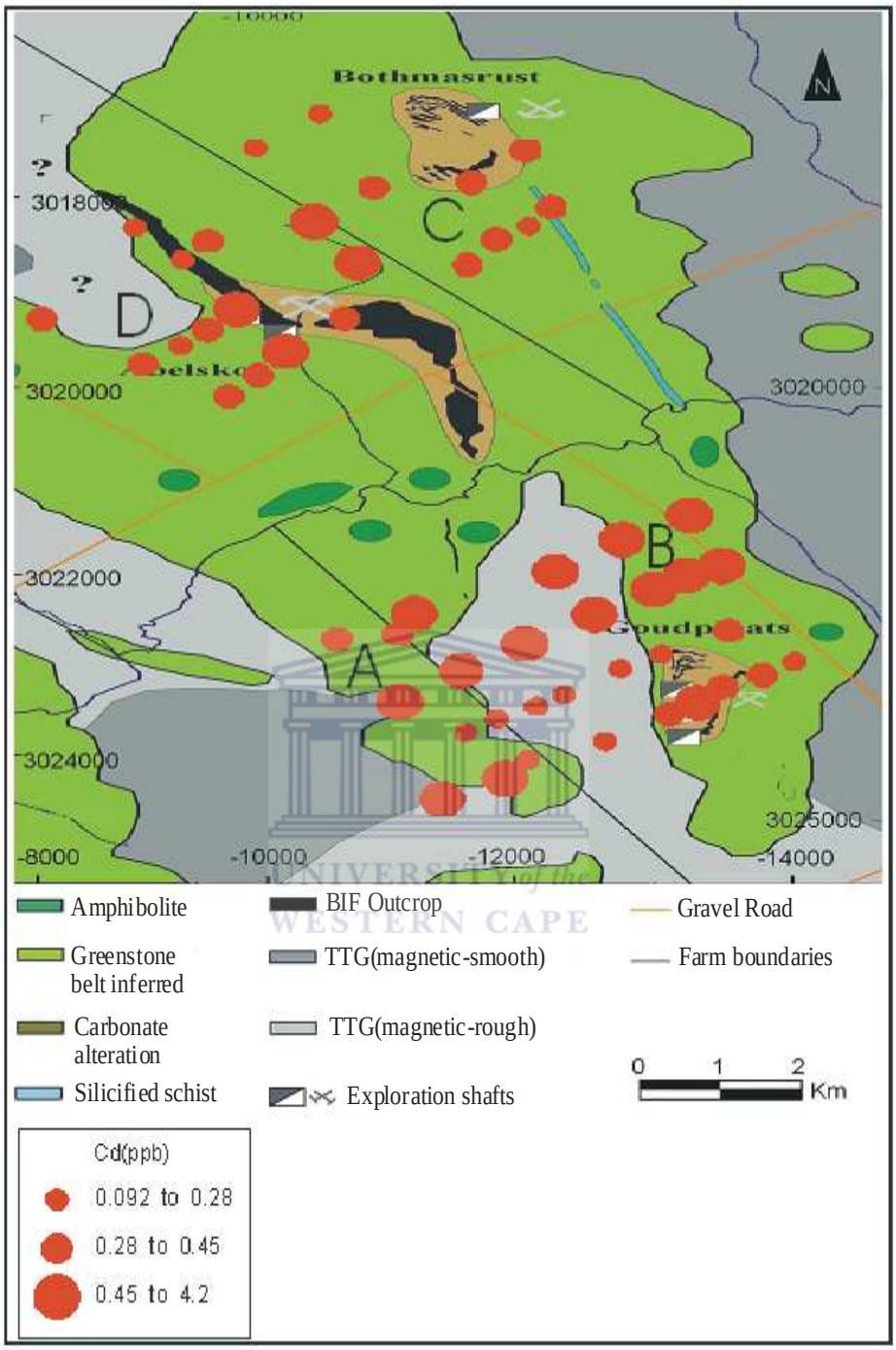

Fig 4.28 Geochemical map of Cd in regolith samples by 0.1M hydroxylamine partial leach.

4.2.2 Geochemical mapping at Kabanga using 0.25M hot hydroxylamine hydrochloride leaches.

The results of the orientation work suggests the use of 0.25M hydroxylamine hydrochloride extraction as most suitable for mapping bedrock or concealed mineralization in the lateritic regolith samples. Analytical data set for the study are presented in Appendix D_3 and statistically summarized into Tables 4.10 and 4.11 for Kabanga (Main & North).

A statistical summary of element contents obtained by 0.25M partial extraction shown in Table 4.10 shows a wide range of concentration for all elements except Cr, U, Rh, Pt, Ir, Re, Cd, Ag, which also have values of about 1ppb or less.

Table 4.9 Eigen values for the principal component analysis (PCA) for the analytical data from 0.25M hydroxylamine hydrochloride leach (Kabanga samples).

Value	Eigen value	% Variance	Cumulative %
F1	8.326	33.305	33.305
F2	5.000	19.999	53.304
F3	3.681	14.722	68.026
F4	1.807	7.227	75.253
F5	1.521	6.085	81.338
F6	1.331	5.325	86.663
F7	1.202	4.809	91.472
F8	1.012	4.047	95.519

Principal component plots generated with XLSTAT showing patterns of element association in soil overlying Ni-Co deposits in Kabanga is presented in Figures 4.11 and the Eigen values, percentage variance and cumulative percentage are in the Table 4.9. The total data variability in the principal components I, II & III used for the plot is well above 65 percent (Table 4.9). The Principal component plots for the analytical data from the Kabanga (Main & North) (Figure 4.30) show three main groups of element association.

- Group I: that shows a close association with Fe and Mn. The close association suggest these elements to be linked with Fe-Mn oxides and may have been liberated into leachant by hydroxylamine (Ni, Co, Cu, Ag, Sr, Ba, Pt, Rh and Cd).

Table 4.10 Summary statistics of the hot hydroxylamine hydrochloride digestion of the samples taken in Kabanga and Luhuma.

Kabanga main samples					**Kabanga north samples**				**Luhuma samples**			
0.25M			**(All data in ppb)**				**n = 42**					
Element	Min.	Max.	Mean	Std.Dev.	Min.	Max.	Mean	Std.Dev.	Min	Max	Mean	Std.Dev.
Ni	1.21	41.19	23.13	11.28	8.58	65.46	23.02	19.37	2.76	41.75	8.45	9.77
Co	2.09	32.19	8.73	8.39	1.67	10.73	3.94	3.02	1.91	45.08	16.87	11.82
Cu	15.35	72.97	28.19	16.07	15.47	52.48	23.24	11.11	22.39	79.76	43.56	15.36
Zn	13.01	179.03	36.77	41.78	22.3	46.79	29.04	7.55	7.33	70.33	33.62	15.56
As	32.28	78.19	57.88	12.3	36.54	90.81	58.82	16.56	43.51	68.67	52.88	6.69
Se	0.57	20.07	8.57	6.83	4.93	38.73	16.26	1219	2.21	30.97	14.45	8.03
Rb	6.32	39.93	18.97	9.29	8.39	21.52	12.96	4.51	7.27	39.13	16.66	7.22
Sr	32.93	887.64	288.48	307.44	9.98	304.01	96.26	108.1	4.97	303.09	98614	82.08
Pd	0.66	3.73	1.86	0.98	0.57	1.78	1.15	0.01	3.79	19.66	10.92	4.88
Ag	0.18	0.71	0.3	0.18	0.15	0.46	0.26	0.09	0.18	1.67	0.8	0.36
Mn	129.4	4623.64	1375.8	1642.6	34.04	1394.02	433.49	558.88	52.49	6284.71	1106.6	1308.3
V	73.58	9681572	2766238	4538709	96.14	145.36	12366	1845	66.98	117.57	86.48	12.63
Cd	0.02	0.43	0.2	0.14	0.71	0.17	0.11	0.09	0.02	0.25	0.09	0.06
Ba	210.19	1470.18	605.97	415.82	193.52	734.74	378.5	172.9	0.06	1394.98	681.97	358.81
Re	0.02	0.03	0.03	0.06	0.03	0.03	0.03	NA	0.01	0.11	0.04	0.03
Os	8.99	93.33	38.85	29.77	0.23	5.45	2.66	215	0.23	126.18	2254	32.6
Ir	0.03	0.17	0.08	0.04	0.01	0.04	0.02	0.01	0.015	0.61	0.16	0.17
Cr	1.56	31.43	13.27	8.43	11.36	31.01	20.09	5.99	0.89	34.38	11.96	7.31
Au	0.12	5.41	1.73	1.38	0.4	1.81	1.08	0.44	0.29	7.02	1.27	1.43
Pb	25.23	64.39	41.79	12.4	29.02	52.85	39.88	6.96	32.52	106.06	72.12	20.51
U	0.2	2.36	1.1	0.7	0.59	1.74	39.88	6.96	0.99	6.57	2.98	1.49
Ru	0.01	0.15	0.07	0.05	0.08	0.19	0.14	0.05	0.02	0.15	0.06	0.03
Rh	0.01	0.07	0.03	0.02	0.02	0.04	0.02	0.01	0.01	0.09	0.03	0.02
Pt	0.03	0.19	0.09	0.05	0.02	0.13	0.07	0.09	0.01	0.08	0.04	0.02
Fe	1944.49	11929.3	660.49	3475.54	3942.6	7745.56	6417.6	1299.4	3616.21	14473.2	7807.26	2600.9

Group II: elements in the group show a diametric relationship with Fe and Mn group. These may be elements that are weakly adsorbed to surfaces and therefore termed as exchangeable (Pb, Pd, Re and U).

- Group III: elements in the group lie between the groups I & II. These may be elements that are either absorbed with Fe-Mn or weakly adsorbed to surfaces termed exchangeable (Au, Ir, Os, Rb, Zn, Se, Cr, As, Ru and V).

Box and whiskers plots were made to further estimate the degree of variability and contrast of the elements in regolith overlying various bedrock and mineralization. Background, threshold and anomalous values were estimated using box plots. The estimated values are presented in Figure 4.29 and Table 4.11. The Kabanga Main estimated background, threshold and anomalous values would be used in this work to evaluate data from the Kabanga North and Luhuma area.

The plots of element along sample traverse are presented in Figures 4.31-4.34 while others are shown in the Appendix A_{12}-A_{16}. These plots are shown in the order of the element associations, which were determined using the principal component analysis (PCA).

The geochemical data were plotted along sample traverse (Fig 4.31-Fig 4.34) that cut across both the Kabanga Main and the Kabanga North mineralization. The Ni-Cu mineralization occurs within the metapelites in both areas and these are flanked by disseminated schist, spotted schist and ultramafic bodies in both Kabanga (Main & North) sections.

Figure 4.31 shows Ni, Co, Zn and Cu distribution patterns in profile L9893N and L9850N, which cuts across the Kabanga Main mineralization with a footwall host rocks comprising of quartzite, spotted schist and two orezones, which are enclosed within the ultramafic rocks at a depth of over 300m.

Ni, Co and Cu show variable ability in reflecting mineralization in traverses L9893N and L9850N. Anomalous values of Ni, Co and Cu lie outside the mineralised area in traverse

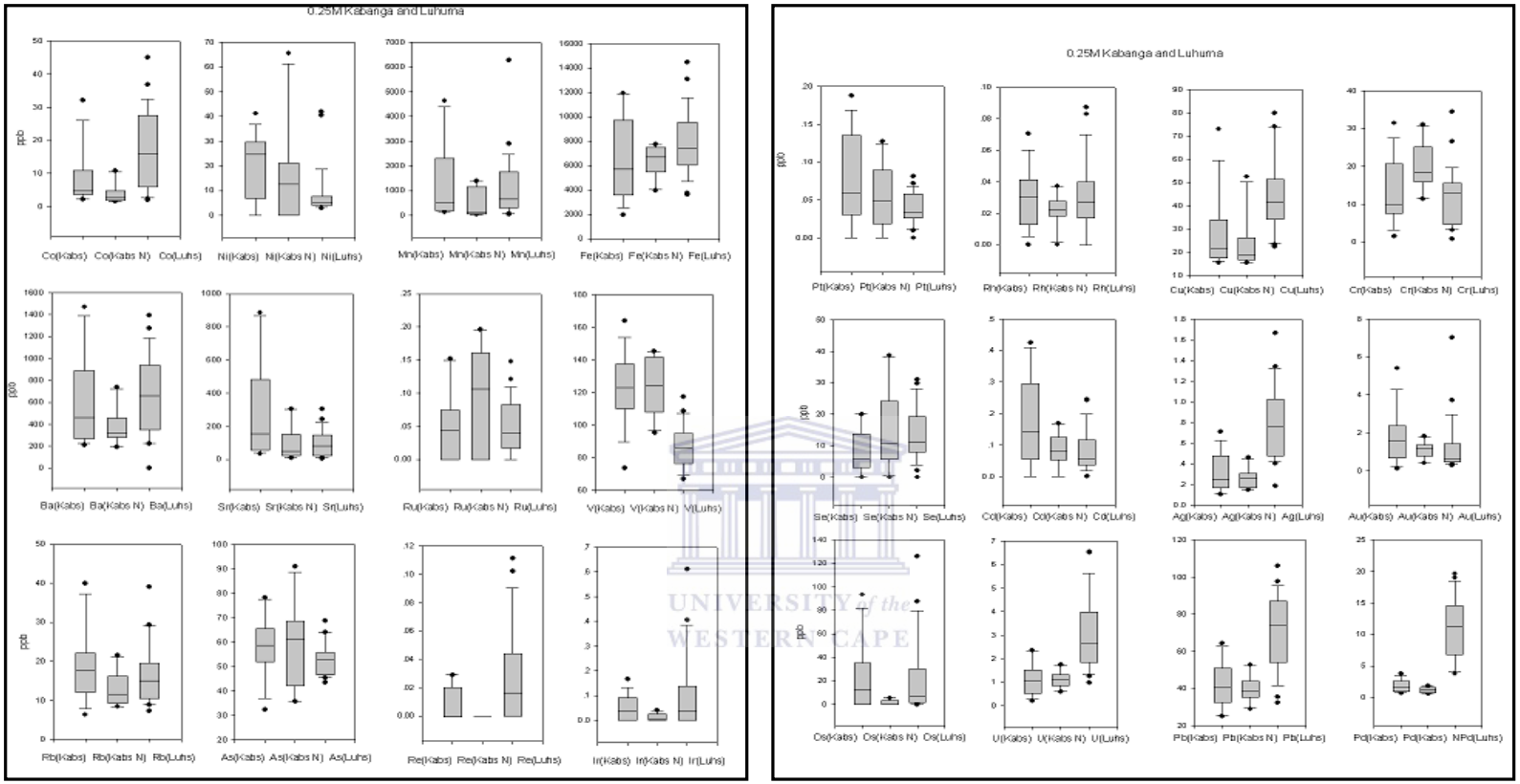

Figure 4.29 Box and whisker plot for suite of element in samples taken for regolith overlying the Kabanga Main (ore deposit), Kabanga North and Luhuma (Ni-Cu prospect). The middle line corresponds to the background value (median); lower and upper bounds of the box indicate 25th and 75th percentiles respectively. Values above the 75th percentile are considered. Element contents between the 50th and 75th percentiles are regarded as the threshold (Turkey, 1977).

Table 4.11 Estimated background-anomalous values of the various elements in Kabanga and Luhuma.

Kabanga main samples				**Kabanga north samples**			**Luhuma samples**		
0.25M		**(All data in ppb)**			**n = 42**				
Element	Background	Threshold	Anomaly	Background	Threshold	Anomaly	Background	Threshold	Anomaly
V	122.5	137.5	163.5	122.5	141.5	142	85	95	105
Cr	10	22	32	18	25	31	13	15	26
Mn	500	2300	4600	100	1100	1300	700	800	2800
Fe	4800	8800	11929	6800	7600	7100	6300	6800	8000
Co	5	10.5	32.5	2.5	5	10.5	16.5	27.5	35.6
Ni	25	30	40.5	12	32	65	6	9.5	40
Cu	22	34	74	19	28	50	42	52	74
Zn	*n.d*	*n.d*	*n.d*	*n.d*	*n.d*	*n.d*	*n.d*	*n.d*	*n.d*
As	58	65	78	80.5	68	88	52	54	64
Se	5.6	14	20	10.5	25	37	12	19	30
Rb	17	23	37	11	15	20	15	19.7	30
Sr	150	475	887.6	50	150	300	70	150	260
Rh	0.03	0.041	0.07	0.024	0.028	0.03	0.028	0.04	0.08
Ru	0.048	0.075	0.15	0.12	0.17	0.19	0.038	0.8	0.13
Pd	2.36	2.57	3.6	2.2	n.d	1.5	11.25	14.97	18.5
Ag	0.24	0.44	0.74	0.23	0.26	0.44	0.59	1.2	1.38
Cd	0.15	0.29	0.4	0.08	0.18	0.15	0.05	0.12	0.25
Ba	480	700	1440	320	440	540	640	920	1320
Re	*n.d*	0.02	0.03	*n.d*	*n.d*	*n.d*	0.016	0.045	0.1
Os	16	36	90	*n.d*	2	5	4	29	90
Ir	0.05	0.1	0.18	0.02	0.04	0.03	0.05	0.14	0.4
Pt	0.052	0.135	0.186	0.05	0.08	0.13	0.0375	0.055	0.07
Au	1.6	2.5	5.5	1.2	1.4	1.6	0.8	1.4	3.6
Pb	42	50	63	39	44	50	74	90	98
U	1.2	1.5	2.5	1.2	1.4	1.6	2.6	4	6.5

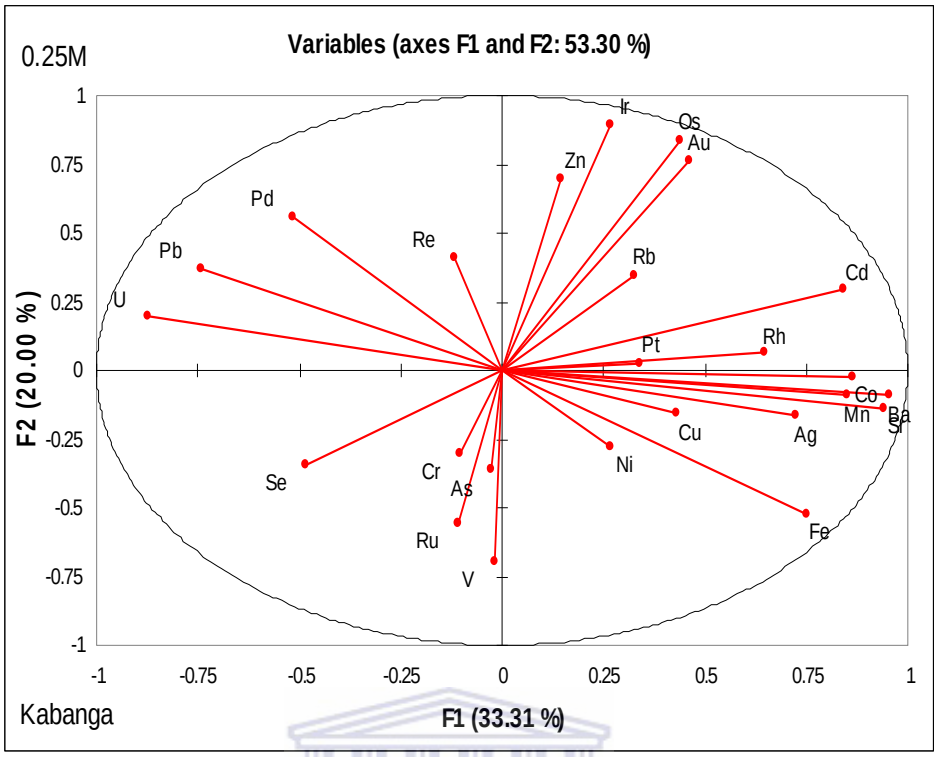

Figure 4.30 Principal component analysis plots for 0.25M concentration of hydroxylamine hydrochloride leach (Kabanga Main & North study sites).

L9850N. In Fig 4.31 the asymmetrical dispersion apron of Ni, Co and Cu reflects the underlying mineralization in profile L9893N. The variable reflection ability of Ni, Co and Cu along the two traverses is due to depth. An elevated content of Ni, Co and Cu is between 2 and 3 times the background concentration in soils overlying the ultramafic body and accompanying mineralization (Fig 4.31 & Table 4.11).

The general slope of the landscape appears to have influenced the pattern of element dispersion and a down slope displacement of the geochemical anomalies in soils along the sampling traverses.

Distribution pattern of Ag does not show meaningful patterns along both L9850N and L9893N sampling traverses. The apical anomalous values of Pd outline the mineralisation in L9893N sampling traverse however; the contrast of the anomalies is weak.

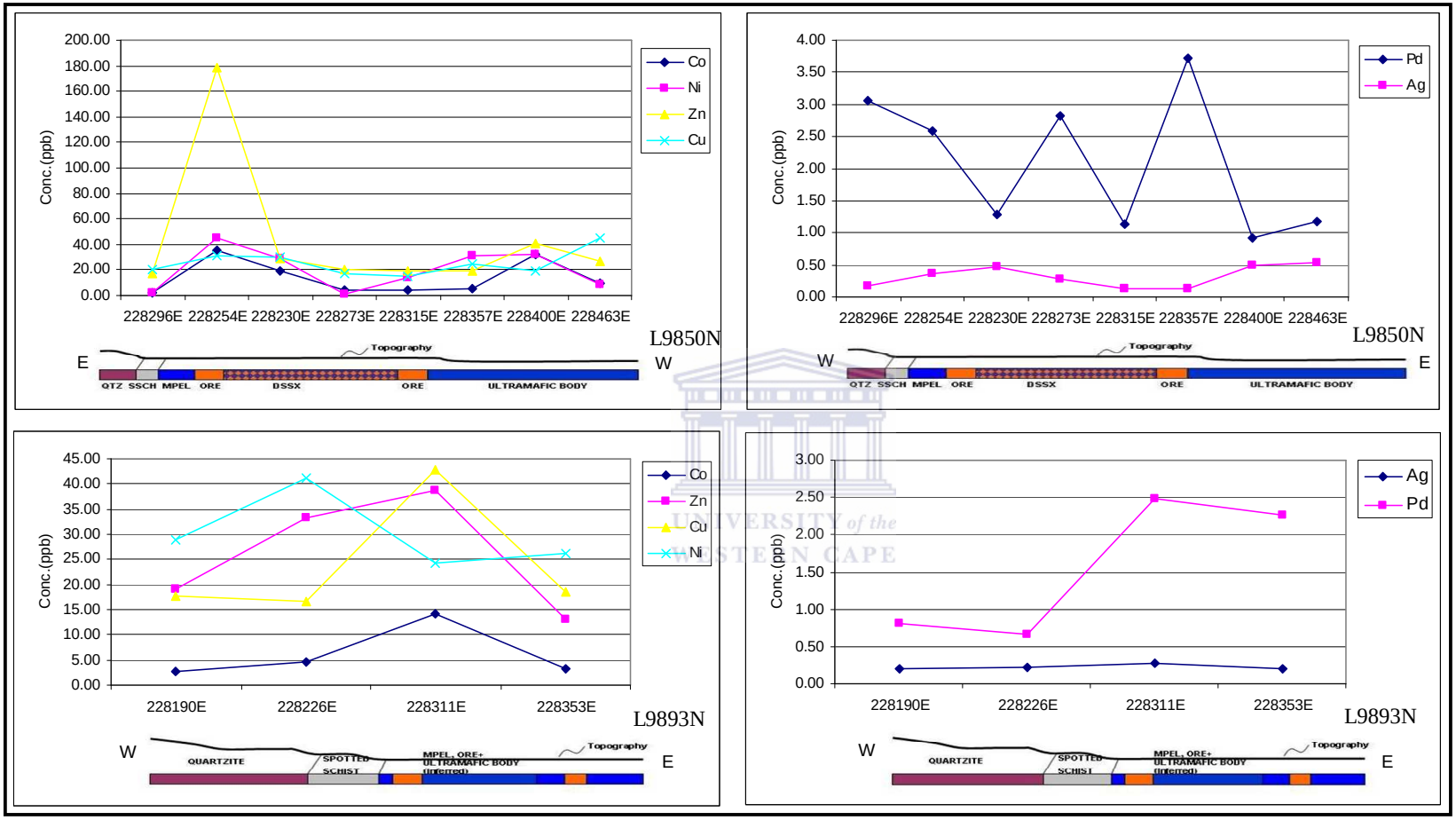

Figure 4.31 Element distribution pattern in traverses L9850N and L9893N across the Kabanga Main (Ni-Cu deposit).

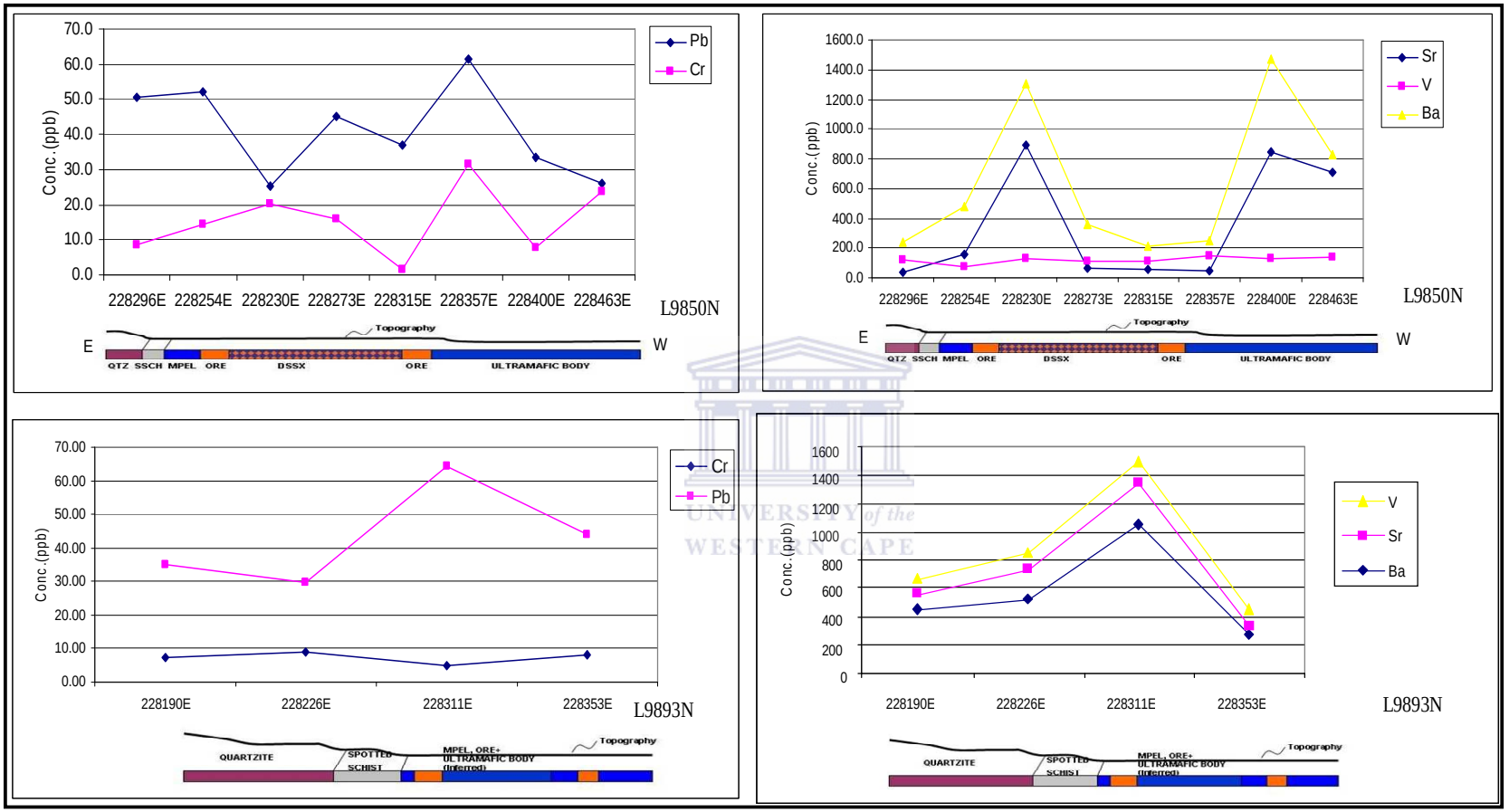

Figure 4.32 Element distribution pattern in traverses L9850N and L9893N across the Kabanga Main (Ni-Cu deposit).

Fig 4.32 shows V, Sr and Ba with variable distribution pattern along both L9850N and L9893N sampling traverses. Elevated contents of V, Sr and Ba outline bedrock and mineralisation in traverse L9893N and to the west of L9850N sampling traverse. The contrast of Ba anomalies is between 2-3 times background concentrations in both L9850N and L9893N. Vanadium does not show meaningful distribution pattern in L9850N though it appears to reflect the bedrock and mineralisation in L9893N with anomalous contents up to about 9 times the background concentration in soils overlying Kabanga Main area.

The distribution of Ag and Cu show contrasting pattern of distribution along traverses which cuts across the Kabanga Main mineralization. Anomalous contents of Cu are up to 3 times the background values in soils overlying the ultramafic body and accompanying mineralization. This enrichment pattern of Cu may be influenced by the general slope of the landscape.

Both sample traverses L11670N and L11528N have similar subsurface geology. Patterns of distribution of Ni, Co, Cu, and Zn are somewhat consistent and similar in each of the sampled traverses in Kabanga North (Ni-Cu deposit). Fig 4.33 shows Ni, Co, Cu and Zn with elevated values reflect mineralisation to the east of the L11670N sampled traverse. Enrichment pattern of these elements may be influenced by the general slope of the landscape.

Elevated contents of Ni, Co, Cu and Zn reflect mineralisation to the east of the L11528N sampling traverse. Anomalous contents of Co and Cu with a contrast between 2 and 4 the times background concentration occur in soils overlying Kabanga North (Ni-Cu deposit). These element show preferred enrichment over the mineralised zones and ultramafic body.

V, Ba and Sr show similar distribution patterns in traverse L11670N and L11528N, which cut across the Kabanga north mineralization with footwall host rocks comprising of spotted schist, metapelites and ore zones enclosed within the ultramafic bedrocks (Figure 4.33).

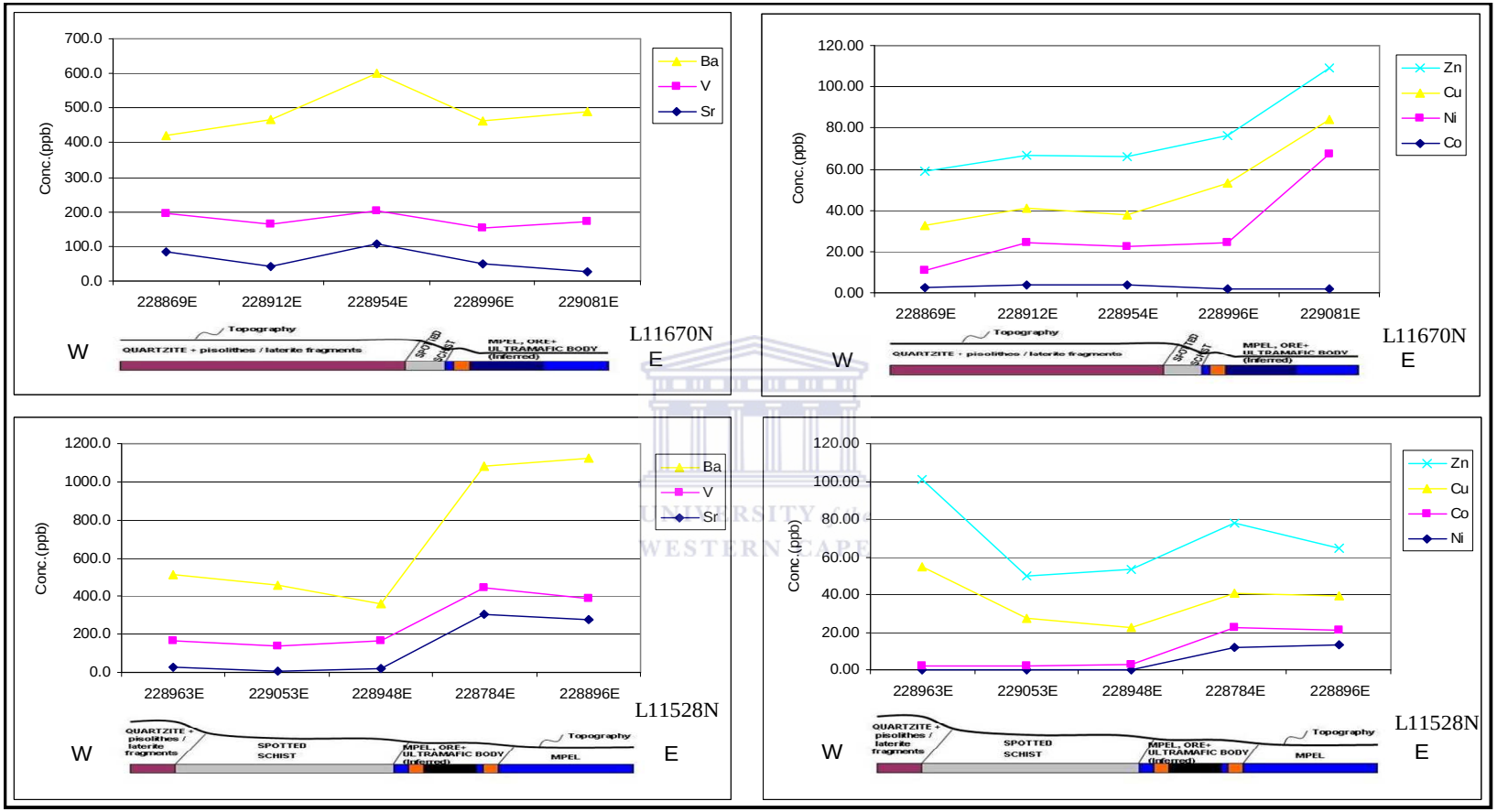

Figure 4.33 Element distribution pattern in traverses L11670N and L11528N across the Kabanga North (Ni-Cu deposit).

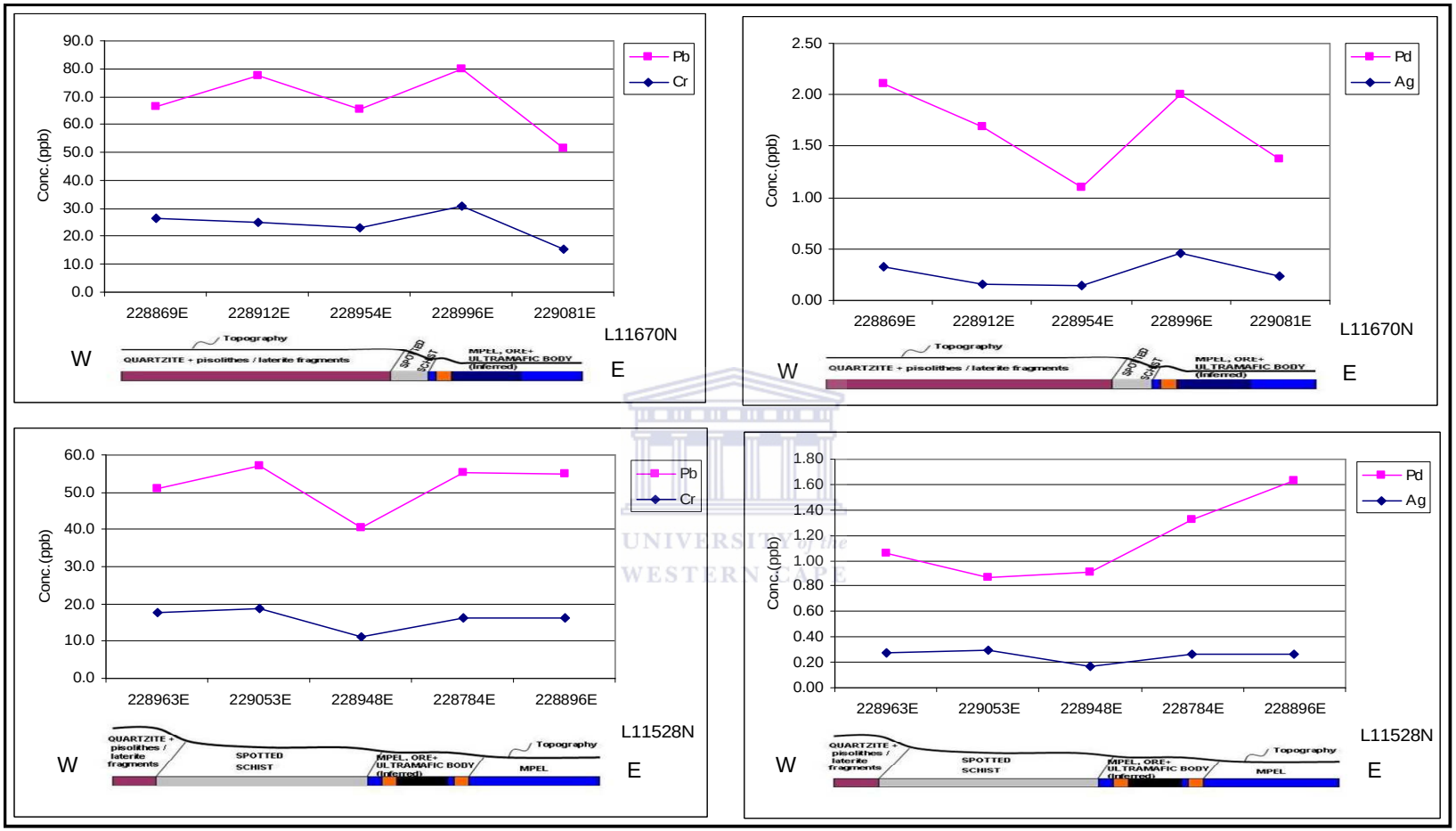

Figure 4.34 Element distribution pattern in traverses L11670N and L11528N across the Kabanga North (Ni-Cu deposit).

Elevated contents of Ba, Sr and V are between 2 and 3 times the background concentration in soils overlying the ultramafic bedrocks and accompany mineralization in L11528N. Elevated values of Ba, Sr and V in L11670N sampling traverse do not reflect the mineralisation.

Fig 4.34 show variable pattern of Ag and Pd around the mineralisation in both L11670N and L11528N sampling traverses. Both elements reflect mineralisation in L11670N but have a weak anomalous/ background contrast. Ag and Pd distribution pattern in L11528N traverse do not show meaningful geochemical trends.

Pb and Cr have variable geochemical trends in L11670N and they both reflect mineralisation. A slightly elevated value of Pb and Cr coincides with the pisolites and lateritic fragment. The elevated contents of Pb and Cr are between 2 and 3 times background concentration in soils overlying Kabanga North (Ni-Cu deposit).

Important features of the section 4.2.2 are as follows;

- The plots of aqua regia data along L9850N, L9893N, L11528N and L11670N geotraverses in section 4.1.2 show that Ni, Cu, Co, Zn and Pb has similar pattern with those obtained from 0.25M hydroxylamine leach in section 4.2.2. However, the 0.25M hydroxylamine show more pronounced contrast to background contents than data obtained by aqua regia leach.

- The 0.25M hydroxylamine leach show an element occurrence pattern though such elements have displaced geochemical anomalies associated with pisolites overlying Ni-Cu ore in Kabanga Main. Similarly, pronounced geochemical anomalies are also associated with the mineralization in Kabanga North.

4.2.3 Geochemical mapping at Luhuma using 0.25M hot hydroxylamine hydrochloride leaches

Analytical data of soils samples from the Luhuma area are presented in Appendix D_4 and statistically summarized into Tables 4.5 and 4.6. These data that were obtained by 0.25M partial extraction shown(Table 4.6) show a wide range of concentration for Ni, Co, Cu, Zn, As, Se, Rb, Sr, Pd, Mn, V, Ba, Os, Au, Pb and Fe with exception of Cr, U, Rh, Pt, Ir, Re, Cd, Ag that show contents of about 1ppb or less.

The plots of principal component I & II (Figure 4.35) show two main groups of element association.

- Group I: that shows an association with Fe and Mn and thus linked with Fe-Mn oxides e.g. Ni, Cu, Co, Cd, Fe, Mn, Ba, As, Sr, Rb and V.

- Group II: elements in the group show may have been liberated by high concentration of hydroxylamine hydrochloride. It contains a less number of elements and consists of such elements that have values of about 1ppb or less. The nature of association is unclear but this may relate to Fe and Mn group or are weakly adsorbed to exchangeable phases e.g., Pt, Re, Ir, Au, Zn, Se, Pd and U.

The Kabanga Main estimated background, threshold and anomalous values (Table 4.8) would be used as geochemical norm in this work to evaluate data from the Luhuma area.
Geochemical maps of elements that associate with Fe-Mn oxyhydroxides group are presented in Figures 4.36 - 4.41. The selected elements appear to reflect the bedrock and possible mineralization.

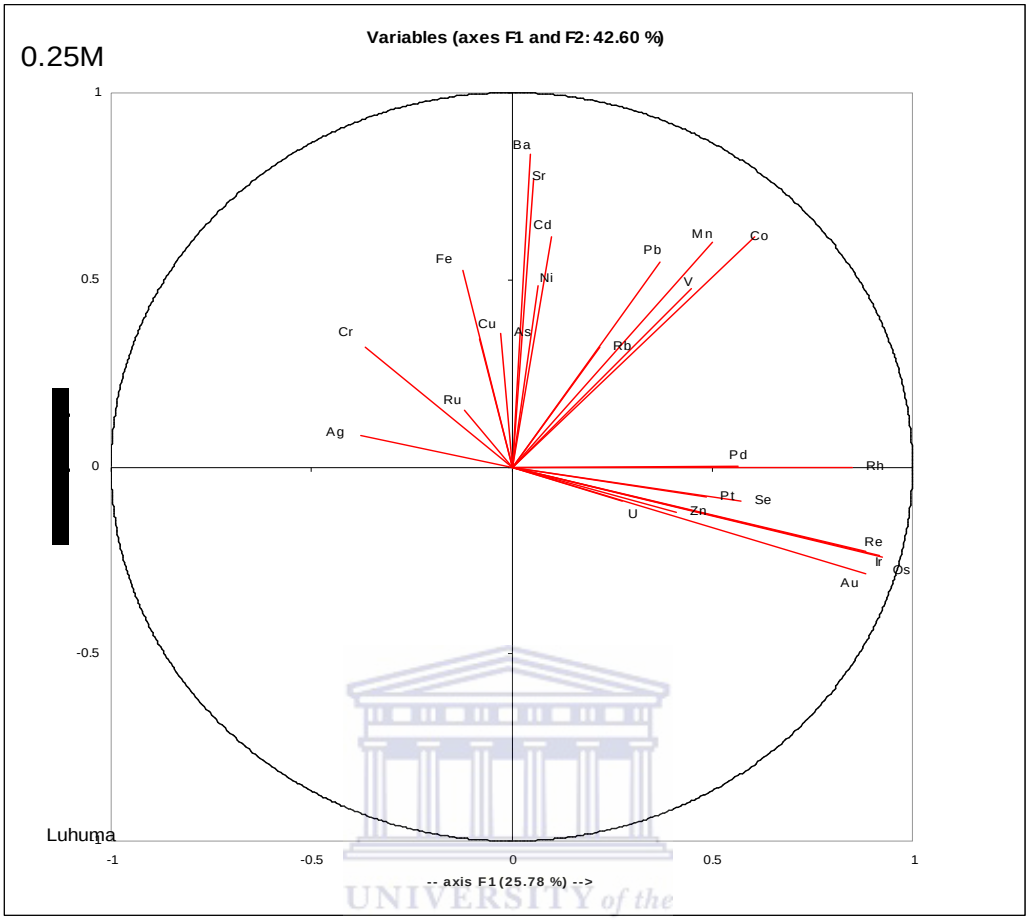

Figure 4.35 Principal component analysis plots for 0.25M concentration of hydroxylamine hydrochloride leach (Luhuma study sites).

4.2.3.1 Geochemical maps

The Luhuma study area is characterize by the occurrence of metasedimentary rocks that comprises of metapelites (MPEL) that have been intruded by mafic-ultramafic rocks. The intrusive bodies appear to be structurally controlled (Simon, 2003). The information from drilled hole suggests close similarity between Luhuma and Kabanga. The metapelites are found occurring as a small unit at the centre of the studied area very close to the mafic-ultramafic bodies. Large parts of Luhuma area is covered with the undifferentiated spotted schist while graphitic schist occupies the eastern parts. Quartzite rubbles were found outcropping in the area. In the southern part of the Luhuma study area; there is an occurrence of fault gouge.

Figure 4.36 show nickel distribution pattern in three areas of occurrence. For example in the northern part of the ultramafic complex (area A); the anomaly coincides with the

position of the ultramafic body. Pronounced Ni anomalies also occur in south of the ultramafic complex (area B). Beyond the ultramafic body in the south; there are also occurrences of Ni anomalies (area C). Anomaly contrast of about 2 times background concentration occurs in the areas A and B (Figure 4.19 & Table 4.8). The distribution and anomaly contrast of Ni in Luhuma soil with hydroxylamine hydrochloride leach is more pronounced than results obtained by aqua regia leach (Simon, 2003). The Ni anomalies contrasts in Luhuma are similar to those occurring in Kabanga area.

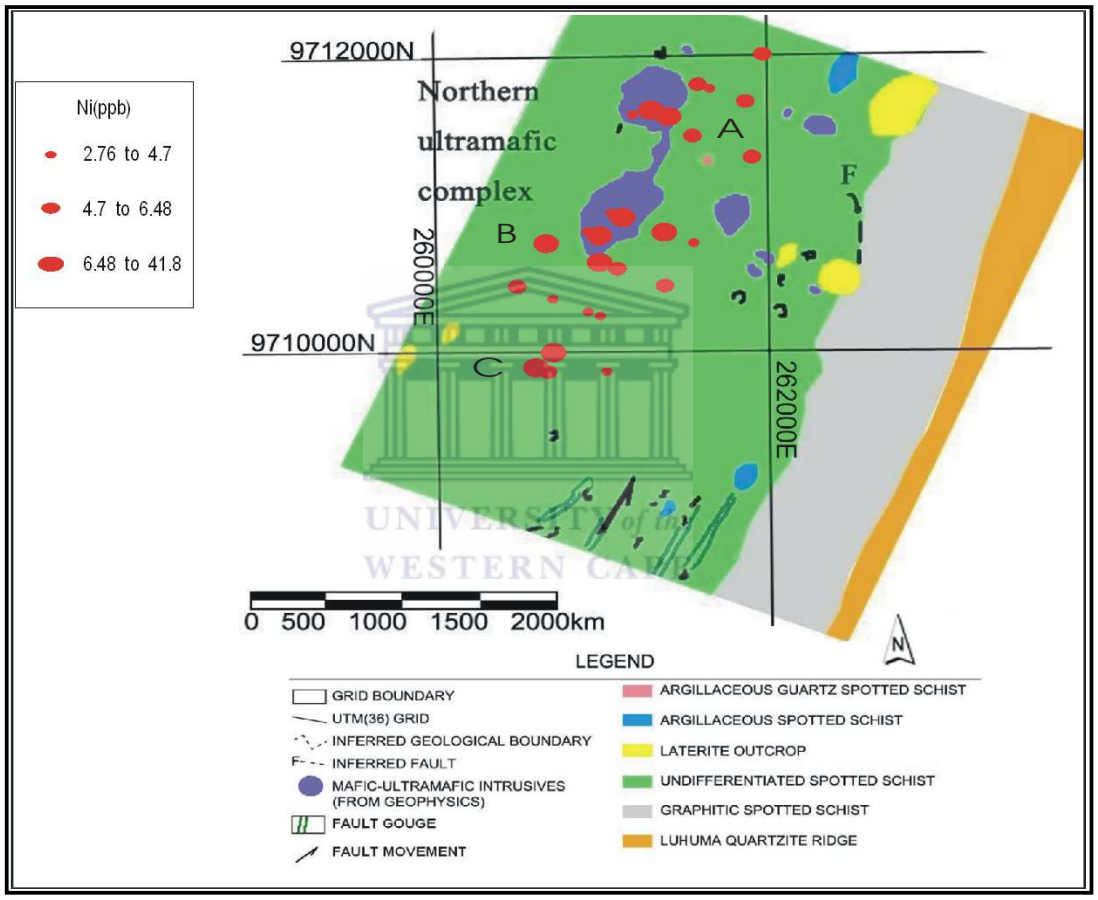

Figure 4.36 The plots of 0.25M hydroxylamine leach for Ni (ppb) in lateritic regolith samples taken from Luhuma.

In figure 4.37, the geochemical map of Cu shows 2 areas of occurrence. In the northern part of the ultramafic complex (area A) the Cu anomalous occurs detached from the ultramafic body. Pronounced Cu anomalies lie within and around the southern portion of ultramafic complex (area B). Anomaly contrast of about 4 times background concentration occurs in the areas A and B (Figure 4.19 & Table 4.8). The anomaly contrasts of Cu obtained by hydroxylamine hydrochloride leach are more pronounced than results obtained by aqua regia leach (Simon, 2003). Cu shows higher anomaly contrasts in Luhuma than those obtained from Kabanga area.

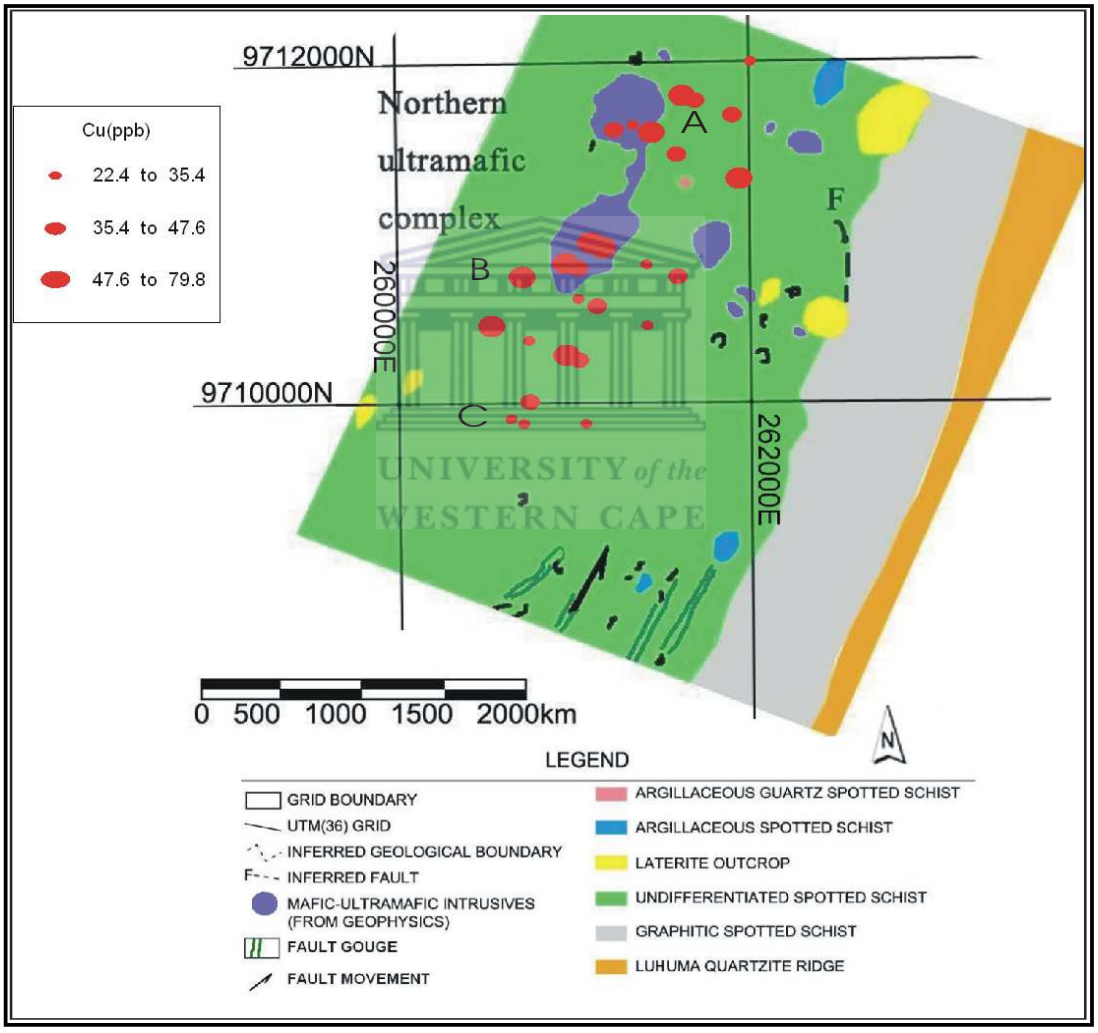

Figure 4.37 The plots of 0.25M hydroxylamine leach for Cu (ppb) in lateritic regolith samples taken from Luhuma.

Figure 4.38 show distribution pattern of Ag in the 2 areas of anomalies occurrences. For example in the area A the anomalous of Ag occur detached from the northern ultramafic body. Silver anomalies also lie within and around the southern portion of ultramafic complex (area B). The anomaly contrast of about 7 times background concentration occurs in the areas A and B (Figure 4.19 & Table 4.8). Ag shows higher anomaly contrasts in Luhuma than Kabanga area.

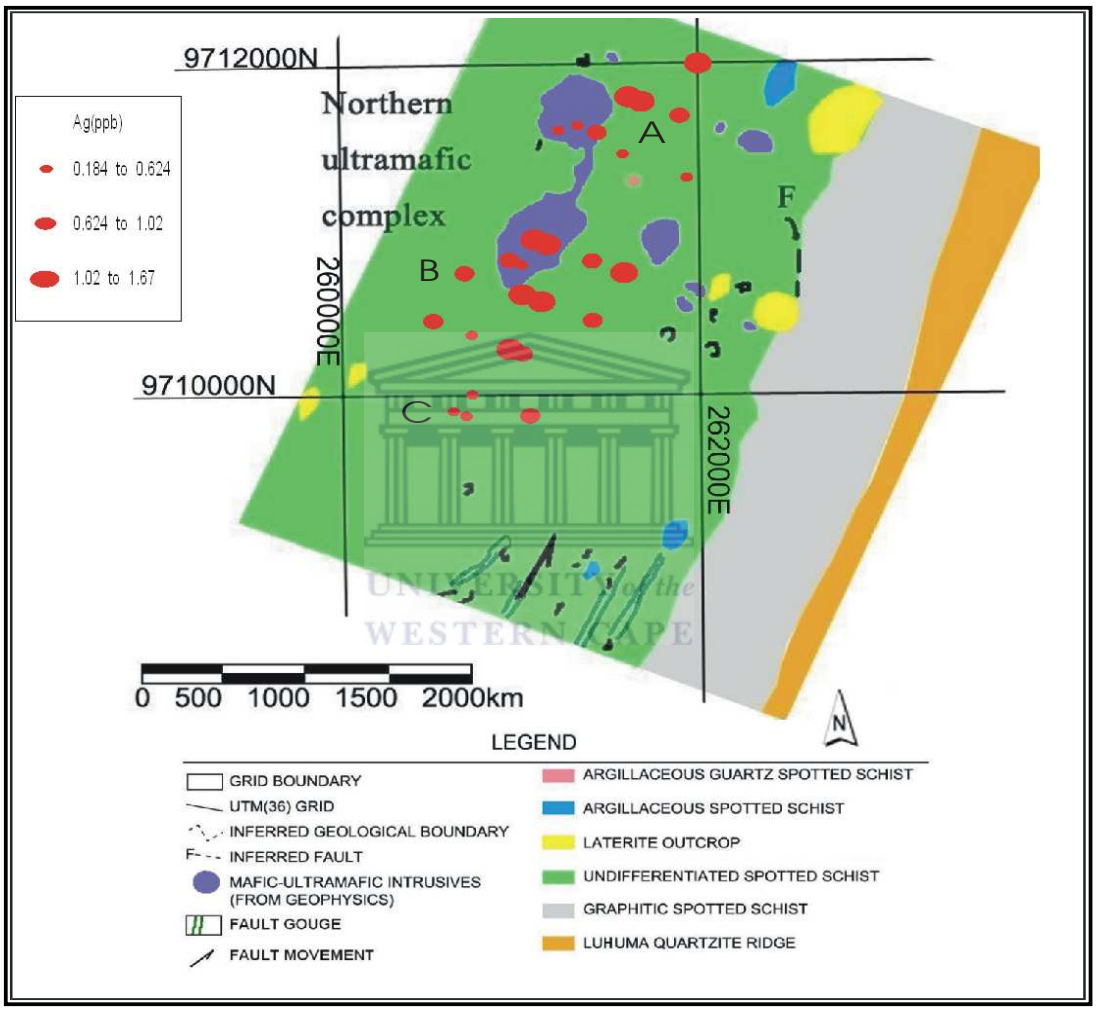

Figure 4.38 The plots of 0.25M hydroxylamine leach for Ag (ppb) in lateritic regolith samples taken from Luhuma.

The Geochemical map in Figure 4.40 shows 2 areas of occurrence of Au anomalies. For example in the area A the anomalous contents of Au occur detached from the northern ultramafic body. Cluster of Au anomalies occur detached and around the southern portion of ultramafic complex (area B). A cluster of Au anomalies also occurs in the area C. The anomaly contrast of about 4 times background concentration occurs in the areas A, B and C (Figure 4.19 & Table 4.8). Gold has more pronounced anomaly contrast in soils overlying Luhuma than those obtained from Kabanga area.

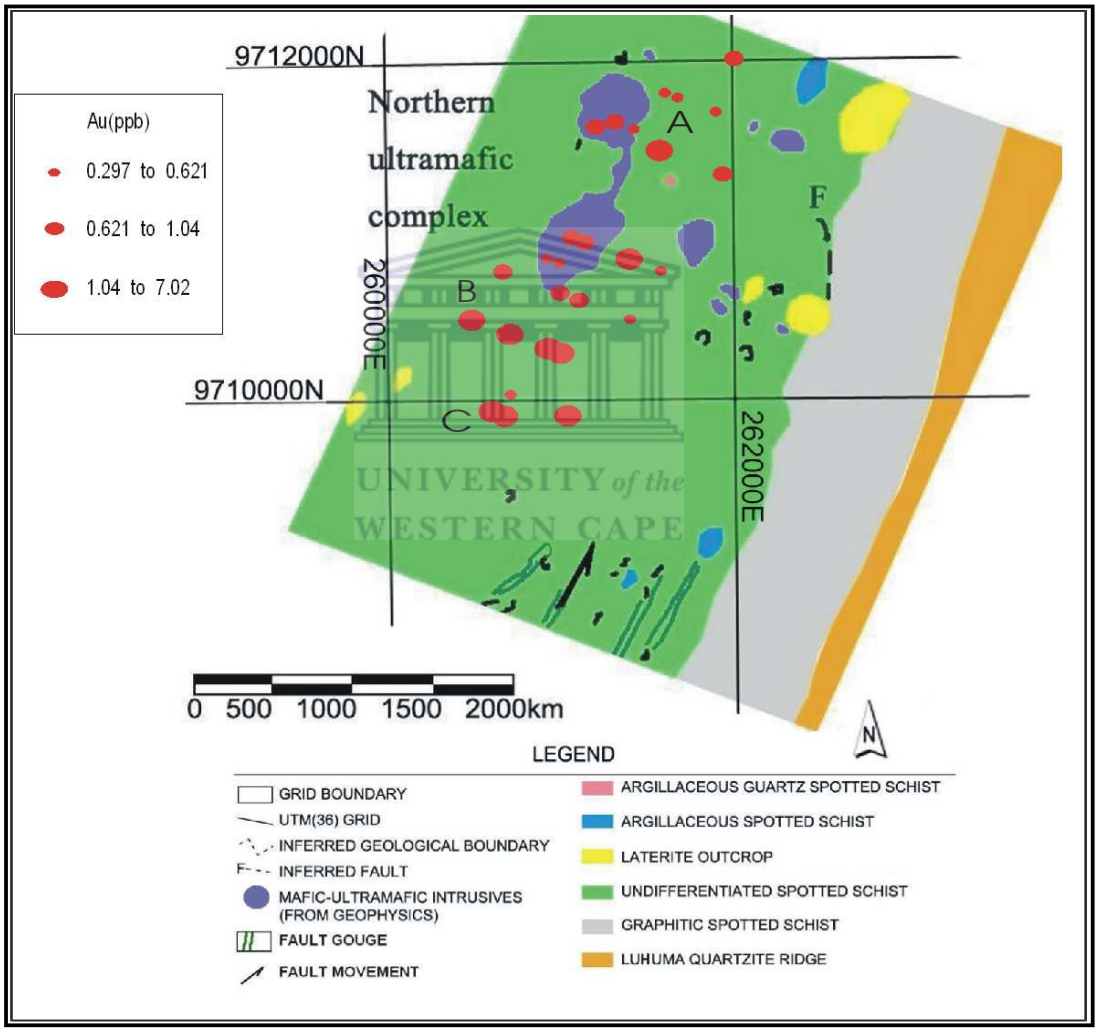

Figure 4.40 The plots of 0.25M hydroxylamine leach for Au (ppb) in lateritic regolith samples taken from Luhuma.

Geochemical map of Co in Figure 4.41 shows 2 areas of occurrence of Co anomalies. In the area A the anomalous of Co contents coincide with the position and around the northern ultramafic body. Cobalt anomalies also lie within and around the southern portion of ultramafic complex (area B). Anomaly contrast of about 9 times background concentration occurs in the areas A, B and C (Figure 4.19 & Table 4.8). Anomaly contrast of Co contents by hydroxylamine leach is more pronounced than results obtained by aqua regia extraction in soils overlying Luhuma prospect (Simon, 2003). Cobalt shows higher anomaly contrasts in Luhuma than those obtained from Kabanga soils.

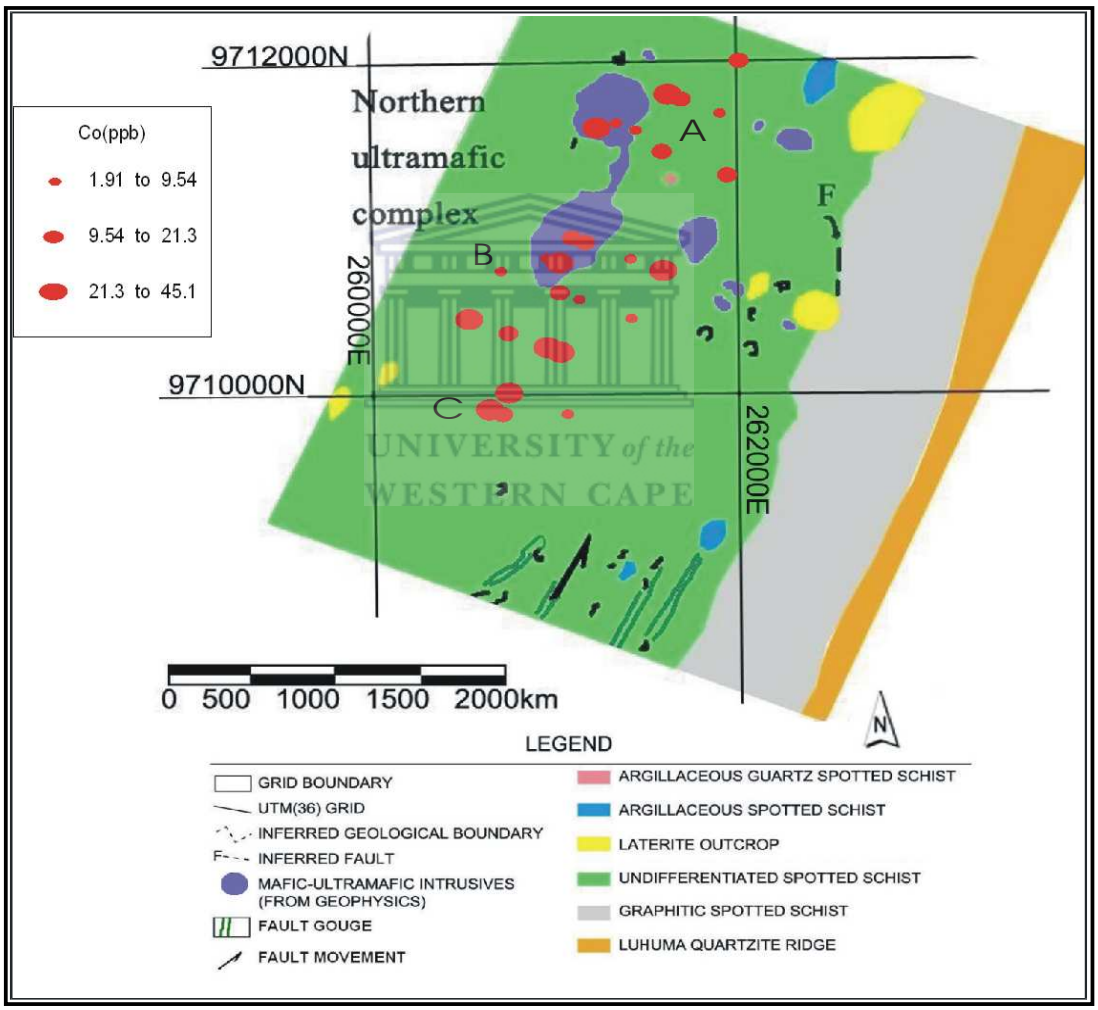

Figure 4.41 The plots of 0.25M hydroxylamine leach for Co (ppb) in lateritic regolith samples taken from Luhuma.

In Figure 4.41 the geochemical map shows 2 areas of occurrence of Ba anomalies. In the area A the anomalous of Ba occur detached and around the northern ultramafic body. Barium anomalies also lie within and around the southern portion of ultramafic complex (area B). Another cluster of anomaly occurs in the area C. Anomaly contrast of about 3 times background concentration occurs in the areas A, B and C (Figure 4.19 & Table 4.8). Barium anomalies/background contrasts in Luhuma are same with those occurring in Kabanga area.

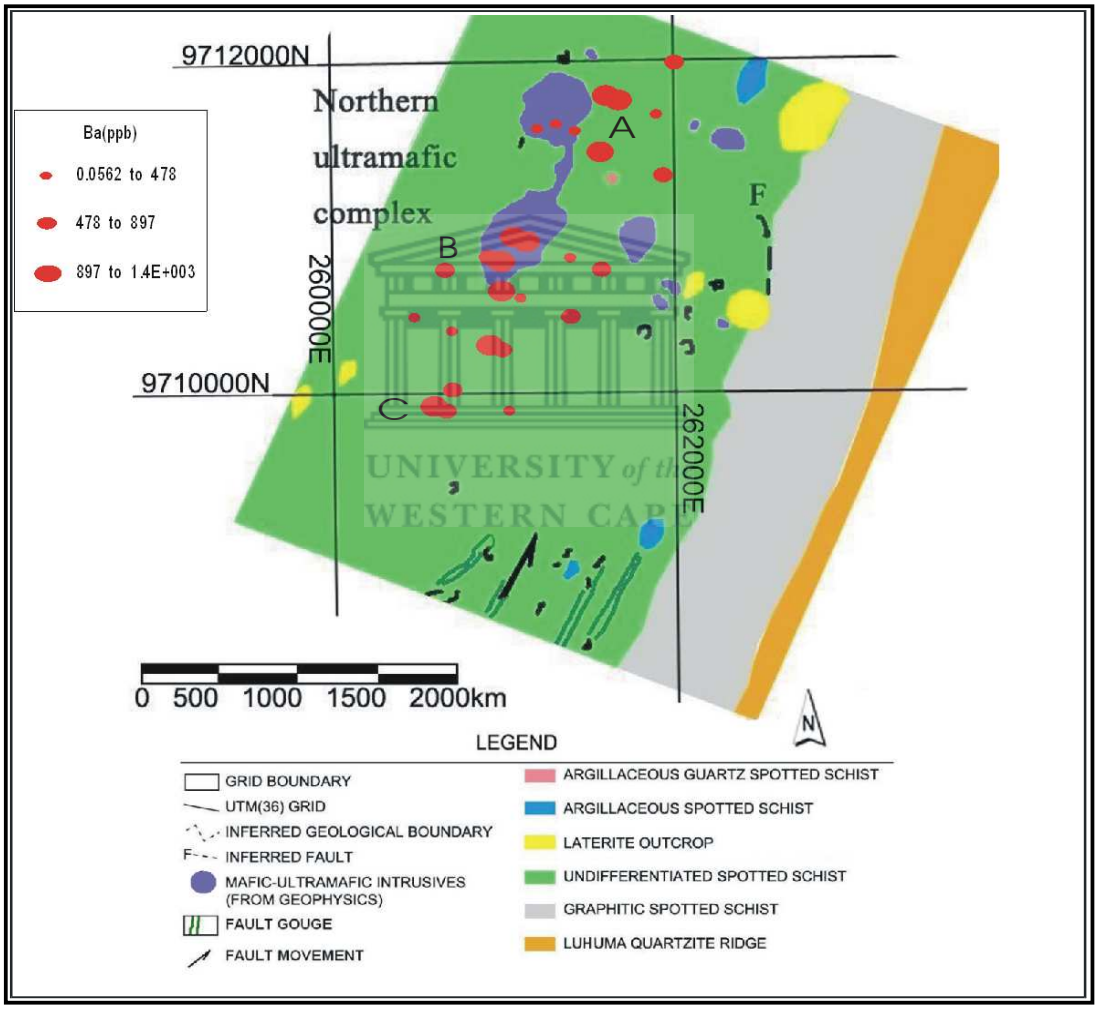

Figure 4.41 The plots of 0.25M hydroxylamine leach for Ba (ppb) in lateritic regolith samples taken from Luhuma.

Important features of section 4.2.3 are as follows;

- Three areas of anomalous occurrence of Au, Ni, Ag, Cu, Co and Ba in the Luhuma prospect.
- Variable anomalous contrasts were obtained in Luhuma when compare with Kabanga area. Ni and Ba have the same anomaly contrast in both study areas. Elements like Au, Ag, Cu and Co show higher anomalies contrast in Luhuma area.
- Ni Cu and Co show more pronounced anomaly contrast in hydroxylamine leach than those obtained by aqua regia leach.
- The linear trends of the anomalies further confirm the earlier assertion that the mineralised intrusive ultramafic body are structurally controlled.

CHAPTER FIVE

5.1 Discussion and conclusion

5.1.1 Discussion

This study is focussed on optimizing hydroxylamine hydrochloride leach for geochemical mapping purposes. The outcome of various approaches used for the optimization has been presented as follows; i) A re-evaluation of analytical data of soil samples from Amalia and Kabanga to create a baseline for this study ii) Optimization of hydroxylamine hydrochloride leaches and comparison of these results with those of aqua regia leach(base line study). iii) Geochemical mapping using hydroxylamine hydrochloride leach and its appraisal of its ability to reflect bedrock and concealed mineralisation.

A re-evaluation of predictive strength of geochemical anomalies associated with triple acid leach corroborates results outlined by Ackon (2001). Generally the geochemical signatures are weak with anomaly/background ratios of less than 3 which are typical of most strong acid leaches (Hall et al., 1996; Kelley et al., 2003). The element dispersion aprons on the surface are generally narrow, except along slopes.

Aqua regia leach results show Cu, Ni, Co, Zn and Pb contents with a variable anomalous patterns along traverses studied at Kabanga. The geochemical anomaly contrast is weak due to high background values and depth of concealment of mineralization at over 400metres (Simon, 2003). The above is in consonance with similar studies around the gold deposits in Ecuadorian Andes, where observed high geochemical noise was also linked to the use of aqua regia leach (Williams, 2002). Weak anomaly contrast associated with triple acid leach and aqua regia leach is similarly due to dissolution of matrix composition.

Aqua regia and triple acid leach which have high ionic solution strength and a low pH (acid) may attack all of these mineral species in samples to some extent (Chao, 1984). The degree of dissolution may depend to large extent on the intensity of weathering a sample has undergone and resultant matrix species in the sample (ALS Chemex, 2002).

The hydroxylamine hydrochloride leaches selectively extract metals from a specific mineral phase thus its degree of dissolution does not depend on resultant matrix mineral species (Hall et al., 1996; Chao and Sanzolone, 1992). Hydroxylamine hydrochloride leach is formulated to attack or extract elements absorbed to the Mn-oxides or amorphous Fe-oxides (Tessier et al., 1979; McAlister and Smith 1999).

Hydroxylamine hydrochloride partial leaches are dependent on several experimental conditions such as;

- Concentration of the reagents; the use of 0.1M hydroxylamine hydrochloride in 0.01M HNO_3 at pH 2, the action of hydroxylamine under the above condition is specific to manganese oxides (Chao, 1972).
- Leach duration (Fonseca and da Silva, 1998)
- Other experimental conditions like temperature, effective sample weight and sample size was investigated by Yang (2006) and Xu (2006).

Temperature and hydroxylamine hydrochloride concentration were experimental conditions resolved in this work with the use of cold and hot hydroxylamine. Other experimental conditions used in this work such as; 75µm sample size, 1gram sample weight, use of 90ml of hydroxylamine hydrochloride solution and one hour shaking time was adopted from previous investigations or studies(Yang, 2006; Xu, 2006).

The result of temperature variation during hydroxylamine leaches showed an increase in the overall degree of element extractability up to 6 times higher in hot than cold hydroxylamine partial extraction. The use of hot hydroxylamine allows temperature as a fixed parameter and thus allowed monitoring of the influence of hydroxylamine concentration on element extractability. Copper and to some extent cobalt generally show poor extractability in hot hydroxylamine leach especially at low hydroxylamine concentration. This could indicate a variable pattern of element extractability which may depend on a multiple factors outline above (Kelley et al., 2003).

Hydroxylamine concentration does shows a variable influence on the level of element extractability that ranges from low level of extraction of refractory elements e.g. Ir, Pt, Rh,

Ru, Ag, Cd and Rh to intense dissolution of V, Co, Ni, Cu and Zn. These observed element patterns corroborate the work done by Darymple et al., (2005).

Two main groups of element association were identified in the principal component plots for the analytical data from lower and upper soils in Amalia, Kabanga and Luhuma; first group consists of elements that were linked with Fe-Mn oxides and second group appear to be weakly adsorbed to particle surfaces that are therefore termed exchangeable. These observation corroborate similar results presented by Yang (2006) and Xu (2006); Mc Alister et al., (1999), Kelley et al., (2003). Element with strong association to Mn oxides may be best extractable using 0.1M hydroxylamine and those linked to amorphous Fe-oxides are best extracted by 0.25M hydroxylamine. The optimization of hydroxylamine leach suggests that there could be a dominance of Mn-oxides in aeolian regolith and amorphous Fe-oxides in lateritic regolith.

The geochemical maps consistently show 4 areas of occurrence of anomalies at Amalia for the following elements; Au, Ag, Ni, Co, V, Cu, Zn and Cd. These elements are adsorbed to Mn oxides and amorphous Fe oxides group. Darymple et al., 2005 described Ni, Co, Zn and Cd as rapid reaction group. The distribution and pattern of the anomalies for Au, Ag, Ni, Co and Cu show variable pattern in the Goudplaats area (area B), the Abelskop mineralization (area D), the Bothmasrust area (area C) and the prospect area (area A). Gold and silver were termed as hydroxylamine stabilised group (Darymple et al., 2005).

The plot of analytical data 0.25M hydroxylamine leach along traverses L11528N, L11670N, L9850N and L9893N at Kabanga show similar distribution pattern with those obtained of aqua regia leach. However, the geochemical contrast obtained from 0.25M hydroxylamine leach is more pronounced compared to aqua regia leach. The use of hydroxylamine hydrochloride leach has therefore help to reduce the effect of the matrix composition.

At Luhuma the geochemical map shows 2 areas of occurrence of Ni, Co, Au and Ba anomalies Cu and Ag have 3 areas of anomalous occurrence. The anomaly contrast of Ni, Cu and Co distribution at Luhuma using hydroxylamine leach is more pronounced than those obtained by the aqua regia leach. The linearity of the anomalies may confirm an earlier assertion that the ultramafic body in Luhuma prospect has a linear configuration (Simon, 2003).

This study therefore shows that the use of hydroxylamine hydrochloride leach for geochemical mapping has several advantages as follows; i) In eliminating background geochemical noise ii) In selection of element suite that are adsorbed to Mn-oxides and amorphous Fe-oxides and those capable of reflecting the chemistry of the concealed bedrock. iii) Delineating anomalous zones of considerable width, area and contrast.

There is however limitation in delineating concealed bedrock and mineralisation as observed at Kabanga. Hydroxylamine hydrochloride partial extraction appears to produce inconsistent results where the mineralisation lies at depth over 400 metres and this may also have been compounded by surface occurrence of lateritic pisolites over mineralisation. The latter could be relate to occurrences of false anomaly.
Successful geochemical exploration work has been undertaken in transported regolith terrain where mineralisation was buried at similar depth e.g. in northern Chile (Kelley et al., 2003) and aeolian sand in South Africa (Yang, 2006 and Xu, 2006). It appears that the loosely packed nature of transported regolith allows the upward migration of labile metals and the element content can easily be reflecting concealed mineralisation.

This study further suggests that delineation of geochemical anomalies may be most feasible using multi-element analysis. Hydroxylamine hydrochloride partial extraction further provides an approach to selecting of element suite linked to Fe-Mn oxides. These appear most suitable for mapping of concealed bedrock/mineralisation. The second group of element termed exchangeable is another suite that can be used in unravelling the deeply buried mineralisation and bedrock at both study sites (Mc Alister et al., 1999). This study therefore proposes the use of more suitable reagent e.g. Ammonium acetate that is capable of targeting the suite of this element.

In conclusion, the use of hydroxylamine leach shows advantages than triple acid and aqua regia leaches in geochemical mapping as follows;

- Hydroxylamine leach is associated with low geochemical background therefore pronounced geochemical anomaly contrast.
- eliminates the matrix composition effects which affect the aqua regia and triple acid leaches

- The contrast of the anomaly in hydroxylamine leach is more pronounced compared triple acid leach and aqua regia leach.
- Hydroxylamine leach is effective in reflecting deeply buried mineralisation and bedrock in transported overburden (Kelley et al., 2003).

REFERENCES

Ackon, P. 2001. Selective leach techniques as a tool for prospecting Gold deposits concealed by Aeolian regolith: A case study at Blue Dot mine, Amalia, Northwest province, South Africa, M.Sc. Thesis. Univ. of the Western Cape. Bellville, 127pp.

Agrawal, S., Moehmer, A., Hemp, A., vanAalst, M., Hitz, S., Smith, J., Meena, H., Mwakifwamba, S.M., Hyera, T. and Mwaipopo, O.U. 2003. Development and climate change in Tanzania: focus on Mount Kilimanjaro. COM/ENV/EPOC/DCD/DAC FINAL REPORT 5. 72pp.

Alloway, B.J. 1995. Heavy metals in soils-second edition, Kluwer academic publishing 384pp.

ALS Chemex. 2002. The regolith, backgrounds, anomalies and partial leaches. News bulletin, issue 1, 6pp.

Anand, R.R. 2001. Evolution, classification and use of ferruginous regolith materials in gold exploration, Yilgarn Craton, Western Australia. Geochemistry: Exploration, Environment, Analysis, Vol. 1 pp. 221-236.

Anand, R.R. and Butt, C.R.M. 1998. Approaches to Geochemical Exploration in lateritic and Related Terrains: a comparison of Australian and African terrains. Africa: Geology and Mineral Exploration, AIG Bulletin, Vol. 25 pp. 17-34.

Anand, R.R. and Smith, R.E. 1993. Regolith distribution, stratigraphy and evolution of the Yilgarn Craton. In Williams P.R. & Haldane J.A. (comp.), An international Conference on Crustal Evolution, Metallogeny and Exploration of the Eastern Gold-fields. Kalgoorlie '93. Australian Geological Survey Organisation, Record 54, pp.187-193.

Anand, R.R., Smith, R.E., Phang, C., Wildman, J.E., Robertson, I.D.M and Munday, T.J. 1993. Geochemical exploration in complex lateritic environments of the Yilgarn Craton, Western Australia. CSIRO Division of Exploration Geoscience, Perth, Restricted Report Number 442R, Volumes 1, 2 & 3, 569pp.(Reissued as open File Report 58, CRC LEME, Perth, 1998).

Anhaeusser, C.R. and Walvaren, F. 1999. Episodic granitoid emplacement in the Western Kaapval Craton: evidence from the Archean Kraaipan granite-greenstone terrane, South Africa. Journal of African Earth Sciences, Vol. 28, No.2, pp.289-309.

Anhaeusser, C.R., Jones, I.M., Marshall, T.R., Robb, L.J. and Zimmermann, O.T. 1991. The Archaean Kraaipan group volcano-sedimentary rocks and associated granites and gneisses of the South-western Transvaal, North-western Cape province and Bophuthatswana. Excursion guidebook for summer field school organised by the Department of Geology, University of Witwatersrand, Johannesburg and the Geological survey of South Africa. 44pp.

Brand, N.W. 1999. Element ratios in nickel sulphide exploration, vectoring towards ore environments. Journal of Geochemical exploration, Vol. 67, pp.145-165.

Butt, C.R.M., Lintern, M.J. and Anand, R.R. 2000. Evolution of regoliths and landscapes in deeply weathered terrain-implications for geochemical exploration. Ore geology reviews, Vol. 16, pp.167-183.

Cahen, L., Snelling, N.J., Delhal, J., Vail, J.R., Bonhomme, M. and Ledent, D. 1984. The Geochronology and Evolution of Africa. Clarendon press, Oxford.512 pp.

Chao, T.T.1972. Selective dissolution of manganese oxides from soils and sediments with acidified hydroxylamine hydrochloride. Soil Sci. Soc. Am. Proc.36, pp.764-768.

Chao, T.T.1984. Use of partial dissolution techniques in geochemical exploration, Journal of Geochemical Exploration, Vol.20, pp.101-135.

Chao, T.T. and Sanzolone R.F. 1992. Decomposition Techniques. Journal of Geochemical Exploration, Vol. 44 (13), pp.65-106.

Clark, J. R. 1993. Enzyme-induced leaching of B-horizon soils for mineral exploration in areas of glacial overburden. Trans. Inst. Min. Metall. Sect.B: Applied Earth Science, Vol.102, B19-B29.

Dalrymple, I. J., Cohen, D.R. and Gatehouse, S.G. 2005. Optimisation of partial extraction chemistry for buffered acetate and hydroxylamine leaches. Geochemistry: Exploration, Environment, Analysis, Vol. 5, pp.279-285.

Danielson, V. 1997. Sutton Resources Ltd press release, Northern Miner, 83 (22), 11.

Drever, J. I. 1988. The Geochemistry of Natural waters-second edition, Prentice hall publishing, 345pp.

Duchesne, J.C., Liegeois, J.P., Deblond, A. and Tack, L. 2004. Petrogenesis of the Kabanga-Musongati layered mafic-ultramafic intrusions in Burundi (Kibaran Belt): geochemical, Sr-Nd isotopic constraints and Cr-Ni behaviour. Journal of African Earth Sciences, Vol. 39, pp. 133-145.

Du toit, A.L.1906. Geological survey of portiond of the divisions of Vryburg and Mafikeng. Annual Report Geology Conference, Cape of Good Hope(1905).pp205-258.

Evans, D. M., Byemelwa, L. and Gilligan, J. 1999. Variability of magmatic sulphide compositions at the Kabanga nickel prospect, Tanzania. Journal African Earth Sciences, Vol. 29, pp. 329-351.

Evans, D.M., Boadi, I., Byemelwa, L., Gilligan, J., Kabete, J. and Marcet, P. 2000. Kabanga magmatic nickel sulphide deposits, Tanzania: morphology and geochemistry of associated intrusions. Journal of African Earth Sciences, Vol. 30, No. 3 pp. 651-674.

Fonseca E.C. and da Silva E.F.1998.Application of selective extraction techniques in metal-bearing phases identification: a South European case study. Journal of Geochemical Exploration, Vol. 61 pp.203-212.

Gray, D.J., Wildman, J.E. and Longman, G.D. 1999. Selective and partial analyses of transported overburden for gold exploration in the Yilgarn Craton, Western Australia. Journal of Geochemical Exploration, Vol.67, pp. 51-66.

Greger M. 2004. Uptake of nuclides by plants. Technical Report.TR-04-14.70pp.

Grey, I. M. 1967. Geological Map of Ngara with Explanation. Mineral Resources Division, Dodoma, Tanzania. Quarter Degree Sheet 29 and 29W, scale 1: 125000.

Hall, G.E. M., MacLaurin, A. I. and Vaive, J.E. 1995. Readsorption of gold during the selective extraction of the "soluble organic" phase of humus, soil and sediment samples. Journal of Geochemical Exploration, Vol. 54, (1): pp. 27-38.

Hall G.E.M., Vaive, J.E., Beer, R. and Hoashi, M., 1996. Selective leaches revisited, with emphasis on the amorphous Fe-oxyhydroxide phase extraction. Journal of Geochemical Exploration Vol. 56: pp.59-78.

Harris, J. F. 1961. Summary of the Geology of Tanganyika.-Mem. Min. Res. Div. Geol. Surv. Tanganyika 1, part IV Economic Geology, pp.1–141; Dar es Salaam.

.

Ikingura, J.R., Reynolds, P.H., Watkinson, D.H. and Bell, K. 1992. 40Ar/39 Ar dating of granites of NE Kibaran Belt (Karagwe-Ankolean), NW Tanzania. Journal of African Earth Sciences, Vol. 15, (3/4): pp. 501-511.

Jones, I. M. and Anhaeusser, C.R. 1991. The Kraaipan Group-Amalia greenstone belt, south-western Transvaal. In: C.R. Anhaeusser (Editor), The Archean Kraaipan Group volcano-sedimentary rocks and associated granites and gneisses of the South-western Transvaal, North-Western Cape Province and Bophuthatswana excursion guide book, Information circular, Economic Geology Research unit , University of Witwatersrand, Johannesburg, Vol. 244: pp.13-25.

Jones, I.M. and Anhaeusser, C.R. 1993. Accrectionary lapilli associated with Archean banded iron formations of the Kraaipan Group, Amalia Greenstone Belt, South Africa, Precambrian Research, Vol. 61, pp. 117-136.

Kabata-Pendias A. and Pendias H. 1984. Trace element in soils and plants CRC Press, Inc. 315pp.

Kelley, D.L., Cameron, E.M. and Southam, G. 2004. Secondary geochemical dispersion through transported overburden. Paper presented at Applied Geochemist conference. Pp.1-4. www.appliedgeochemists.org/tmp/seg_abst/kelley.pdf

Kelley, D.L., Hall, G. E. M., Closs, L.G., Hamilton, I. and Mcwen, R.M. 2003. The use of partial extraction geochemistry for copper exploration in northern Chile. Geochemistry Exploration, Environment, Analysis, Vol. 3, pp 85-104.

Kiefer, R.D. 2004. Regional geology, tectonic evolution and controls of gold mineralization in the Archean Amalia Greenstone Belt, Kraaipan Terrane, South Africa. Ph.D. Thesis. Univ. the Witwatersrand, Johannesburg, 500pp.

LeGleuher, M., Anand R., Eggleton R. A. and Radford N. 2005. Mineral hosts for gold and trace metals in regolith: A LA-ICP-MS STUDY. Regolith, pp. 183 -186.

Lintern, M.J., Sheard, M.J. and Gray, D.J. 1999. Exploration on the Stuart Shelf using regolith geochemistry- an example from the Mount Gunson copper deposits. MESA Journal, Vol. 13.pp.16-21.

Mardsen, J.O and House C.I. 2006. The chemistry of gold extraction (second edition).ISBN-13.680pp.

Mann, A.W., Birrell, R.D., Mann, A.T., Humphreys, D.B. and Pedrix, J.L. 1998. Application of the mobile metal ion technique to routine geochemical exploration, Journal of Geochemical Exploration, Vol. 61, pp.87-102.

Mann, A.W., Gay, L.M., Birrell, R.D., Webster, J.G., Brown, K.L., Mann, A.T., Humphreys, D.B. and Perdrix, J.L. 1995b. Mechanism of formation of mobile metal ion anomalies. Minerals and Energy Research Institute of Western Australia. Report No. 153, 407pp.

McAlister, J.J. and Smith, B.J. 1999. Selectivity of Ammonium Acetate, Hydroxylamine Hydrochloride, and Oxalate/Ascorbic Acid Solutions for the Speciation of Fe, Mn, Zn, Cu, Ni, and Al in Early Tertiary Paleosols. Microchemical Journal, Vol. 63, pp. 415-426.

McBride, M.B. 1994. Environmental Chemistry of Soils. Oxford University Press.395pp.

MMI Workshop, 1999. Organised by Geological Society of South Africa (Unpublished).95pp.

Muhongo, S. 1994. Field excursion quide in the Mozambique Belt of East Africa UNESCO/IUGS/IGCP 348.1pp

Nolan, A.L., Baltpurvins, K., Hamilton, I. C. and Lawrance, G.A. 2003. Chemostat-controlled selective leaches of model soil phases- the hydrous manganese and iron oxides. Part 1.Geochemistry: Exploration, Environment, Analysis, Vol. 3 2003, pp. 157-168.

O'Connor, P.J. and Reimann, C., 1993. Multielement regional geochemical reconnaissance as an aid to target selection in Irish Caledonian terrains. Journal of Geochemical Exploration, Vol. 47, pp. 63–89.

Okujeni, C. D. 1999. Conceptual and methodological model for geochemical prospecting in areas overlain by Kalahari sand in Southern Africa, volume abstract, Geological society of South Africa conference proceedings, Journal of Geochemical, Vol. 67, pp.67-82.

Okujeni, C.D., Ackon, P., Baugaard, W. and Langa, N. 2005. Controls of element dispersion in aeolian sand and calcrete-dominated regolith associated with gold

mineralization in the Kraaipan greenstone belt, South Africa. Geochemistry: Exploration, Environment, Analysis, Vol. 5, pp.1-9.

Panda, D., Subramanian, V. and Panigraphy, R.C. 1995. Geochemical fractionation of heavy metals in Chilka Lake (east coast of India) - A Tropical coastal lagoon. Environ. Geol., Vol. 26: pp.199-210.

Pina, P. 1999. The Proterozoic framework of Southern Africa. Journal of Africa, Vol. 28 (4A): 63.

Poujol, M., Anhaeusser, R.A. and Armstrong, R.A. 2002. Episodic granitoid emplacement in the Archean Amalia-Kraaipan terrane, South Africa: confirmation from single zircon U-Pb geochronology. Journal of African Earth Sciences, Vol. 35, pp.147 - 161.

Rumuvegeri, B.T. 1991.Tectonic significance of Kibaran structures in Central and Eastern Africa. Journal African Earth Science, Vol. 13, (2): pp.267-276.

Simon, A. 2003. Litho geochemical vectors associated with the Kabanga Ni-Cu sulphide deposits north-western Tanzania. M.Sc. Thesis, Univ. of the Western Cape, Bellville. 126 pp.

Smith, B.J. and McAlister, J.J. 1995. Mineralogy, Chemistry and palaeoenvironmental significance of an Early Tertiary Terra Rossa from Northern Ireland: A preliminary review. Journal of Geomorphology Vol. 12, pp. 63 -73.

Smith, R.E., 1996. Regolith research in support of mineral exploration in Australia. Journal of Geochemical Exploration, Vol. 57, (1-3), pp.159-173.

Tack, L., Liegeois, J.P., Deblond, A. and Duchesne, J.C. 1994. Kibaran A-type granitoids and mafic rocks generated by two mantle sources in a late Orogenic setting (Burundi). Precambrian Research, Vol. 68, pp.323-356.

Tessier, A., Campbell, P.G.C. and Bisson, M. 1979. Sequential extraction procedure for the speciation of particulate trace metals. Analytical chemistry, Vol. 51, No 7.pp. 844-851

Turkey, J.W. 1977. ”Box and whisker plots” ¤2C in Exploratory Data Analysis Reading, M A: Addison-Wesley, pp.39-43.

Van Straaten, H. P. 1984. Contributions to the geology of the Kibaran belt in northwest Tanzania. UNESCO Geology for Development, Newsletters, Vol. 3, pp.59-68.

Viljoen, M.J. and Kiefer, R. 1999. Application of MMI techniques in regolith around Amalia (gold mine).Presentation at the MMI workshop, University of Witwatersrand.

Wamtech Proprietary Limited.1997. Operations manual for mobile metal ion geochemical soil surveys. 69pp.

Wilkinson, L., Harris, J.R., and Grunsky, E.C. 1999. Building a Litho geochemical Database for GIS Analysis: Methodology, problems and solutions. Geological Survey of Canada open file 3788.

Williams T.M., Gunn A.G. 2002. Applications of enzyme leach soil analysis for epithermal gold exploration in the Andes of Ecuador. Applied Geochemistry Vol. 17, issue 4 pp.367-385.

Xu, J. 2006. Exploration Geochemical Mapping of the Northwestern section Morokweng Impact Crater, South Africa. M.Sc. Thesis. Univ. of the Western Cape. Bellville, 77pp.

Yang, J. 2006. Exploration Geochemical Mapping of the Northeastern section Morokweng Impact Crater, South Africa. M.Sc. Thesis. Univ. of the Western Cape. Bellville, 76pp.

Yeager, J.R., Clark, R.J., Mitchell, W. and Renshaw, R. 1998. Enzyme leach anomalies associated with deep Mississippi valley-type Zinc Ore bodies at the Elmwood Mine, Tennesse. Journal of Geochemical Exploration, Vol. 55, pp. 49-53.

Zimmermann, O.T. 1994. Aspects of the geology of the Kraaipan Group in the Northern Cape Province and the Republic of Bophuthatswana. M.Sc. Thesis, Univ. of the Witwatersrand, Johannesburg, 145pp.

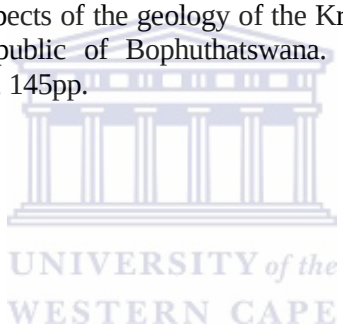

APPENDIX

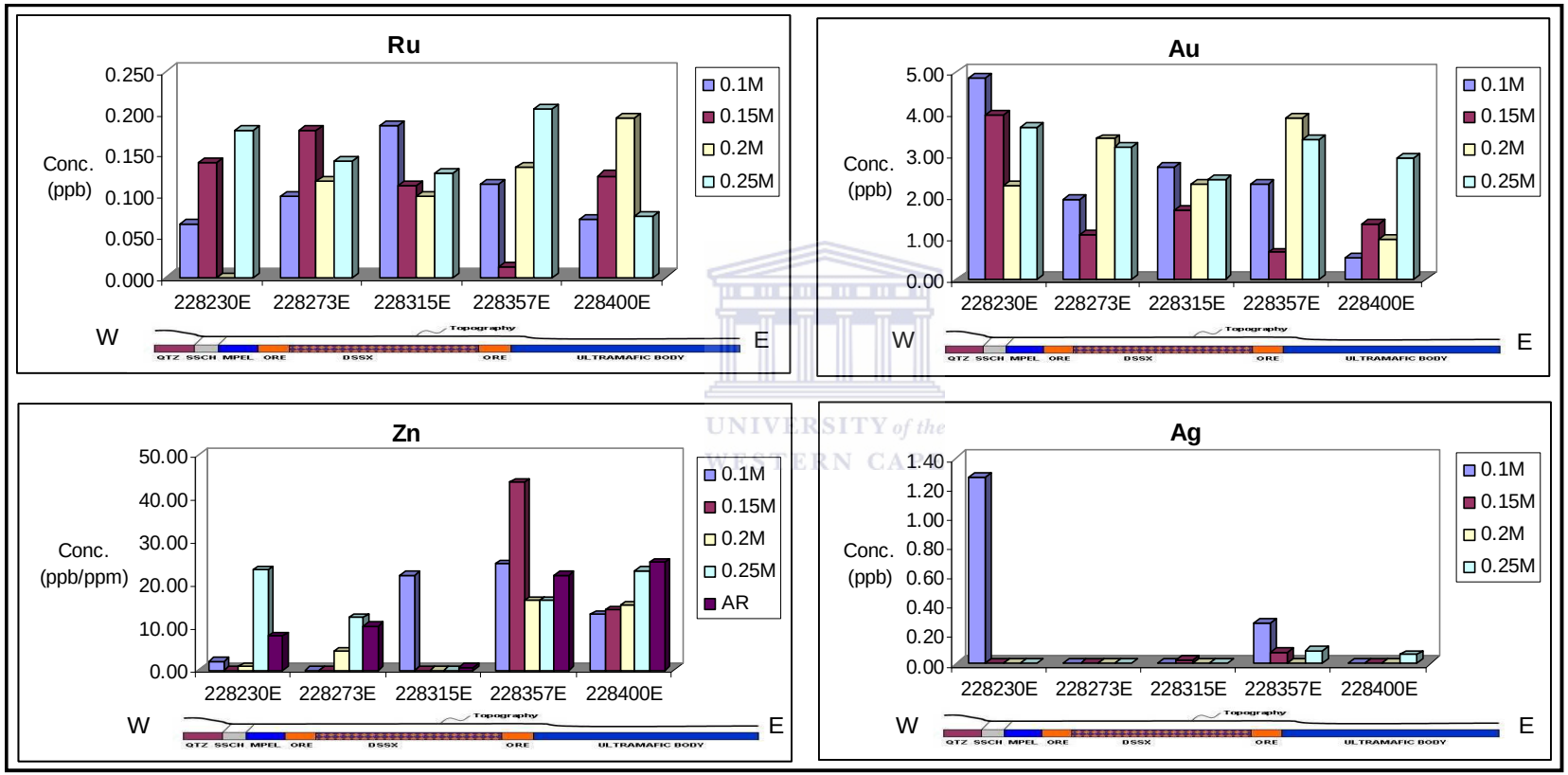

Appendix A1: The plots of Ru, Au, Zn and Ag distribution in regolith samples from Kabanga Ni-Cu prospect at different concentration of hot hydroxylamine hydrochloride leach.

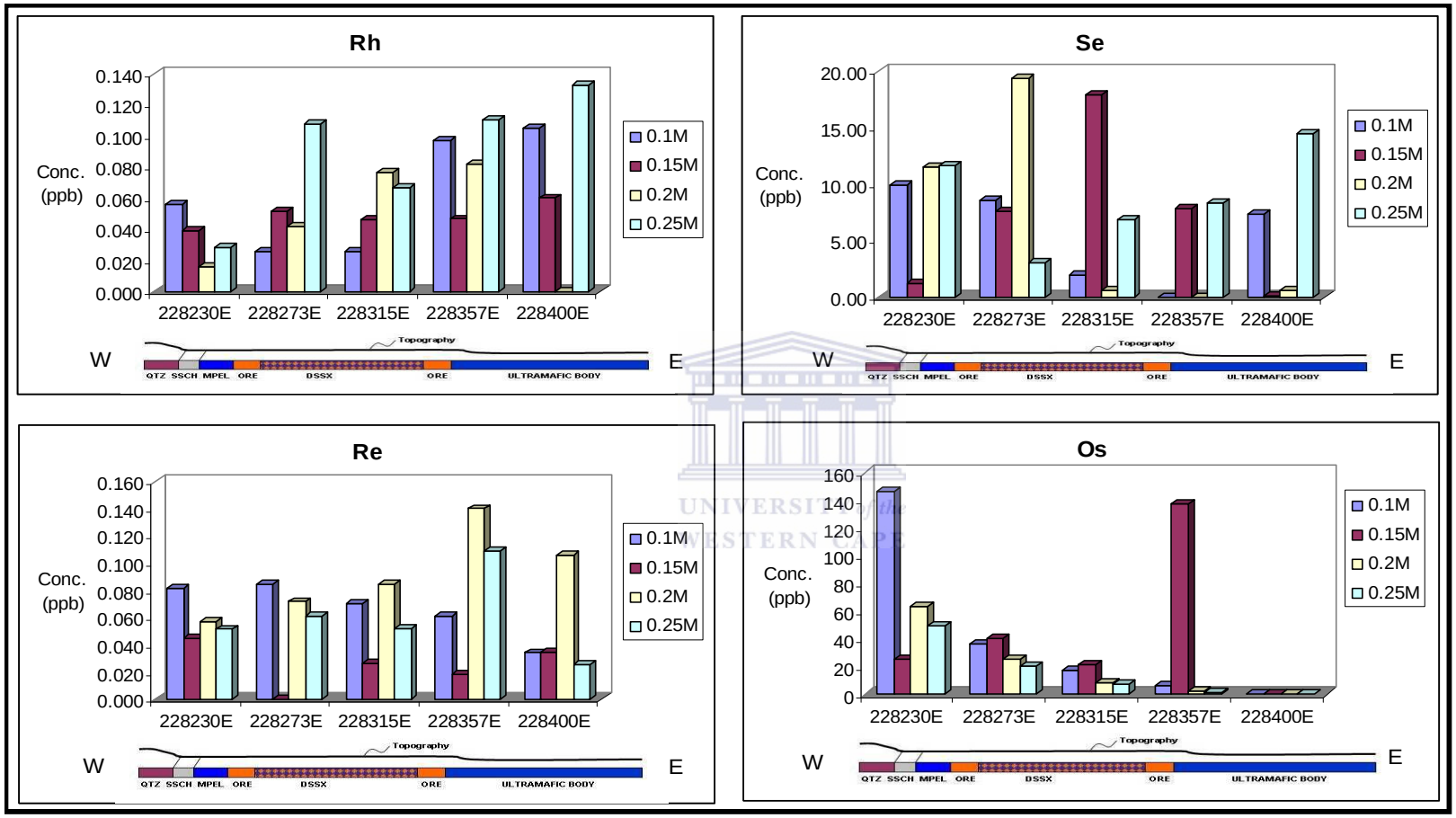

Appendix A2: The plots of Se, Rh, Re and Os distribution in regolith samples from Kabanga Ni-Cu prospect at different concentration of hot hydroxylamine hydrochloride leach.

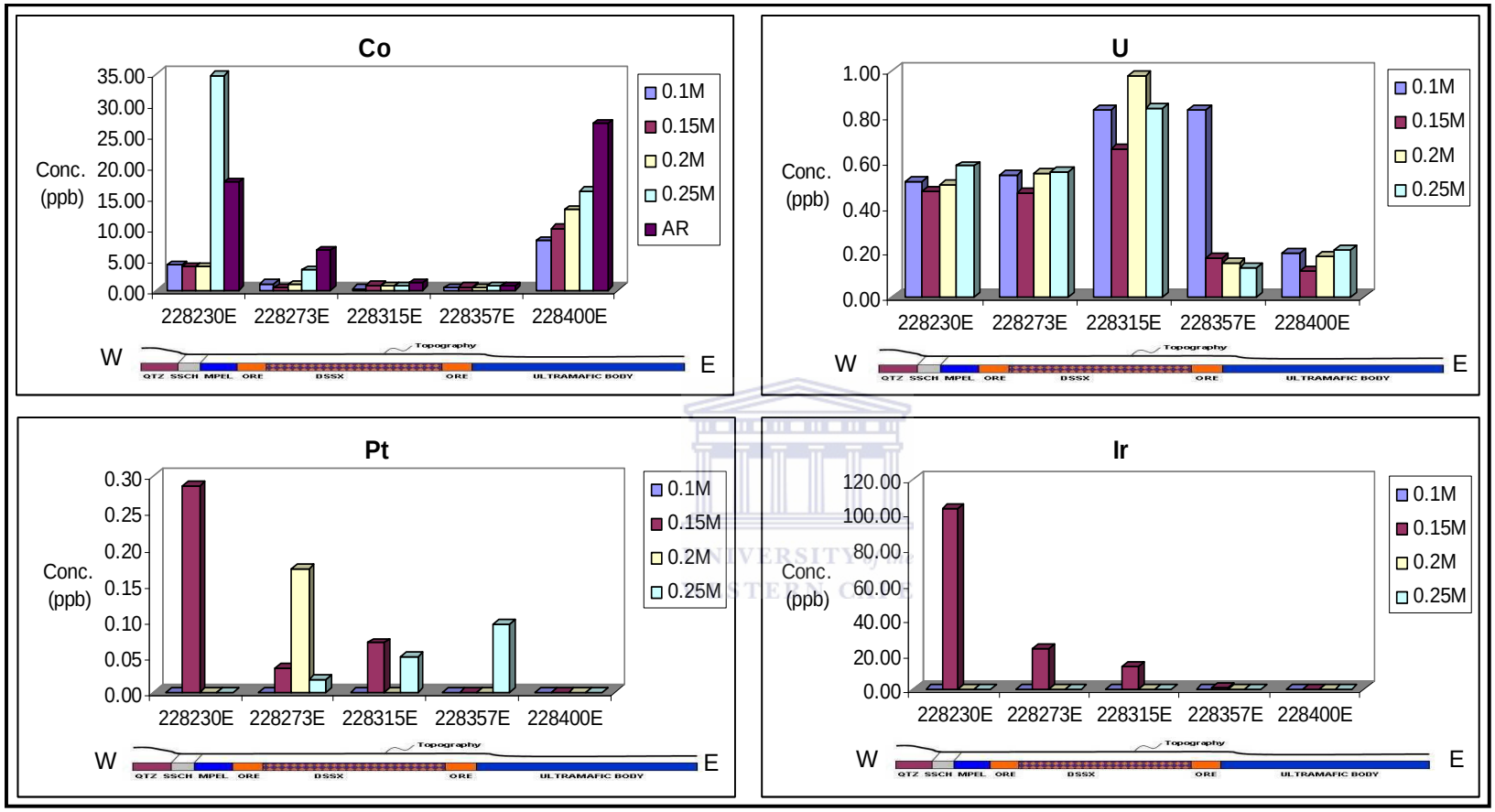

Appendix A3: The plots of Co, U, Pt and Ir distribution in regolith samples from Kabanga Ni-Cu prospect at different concentration of hot hydroxylamine hydrochloride leach.

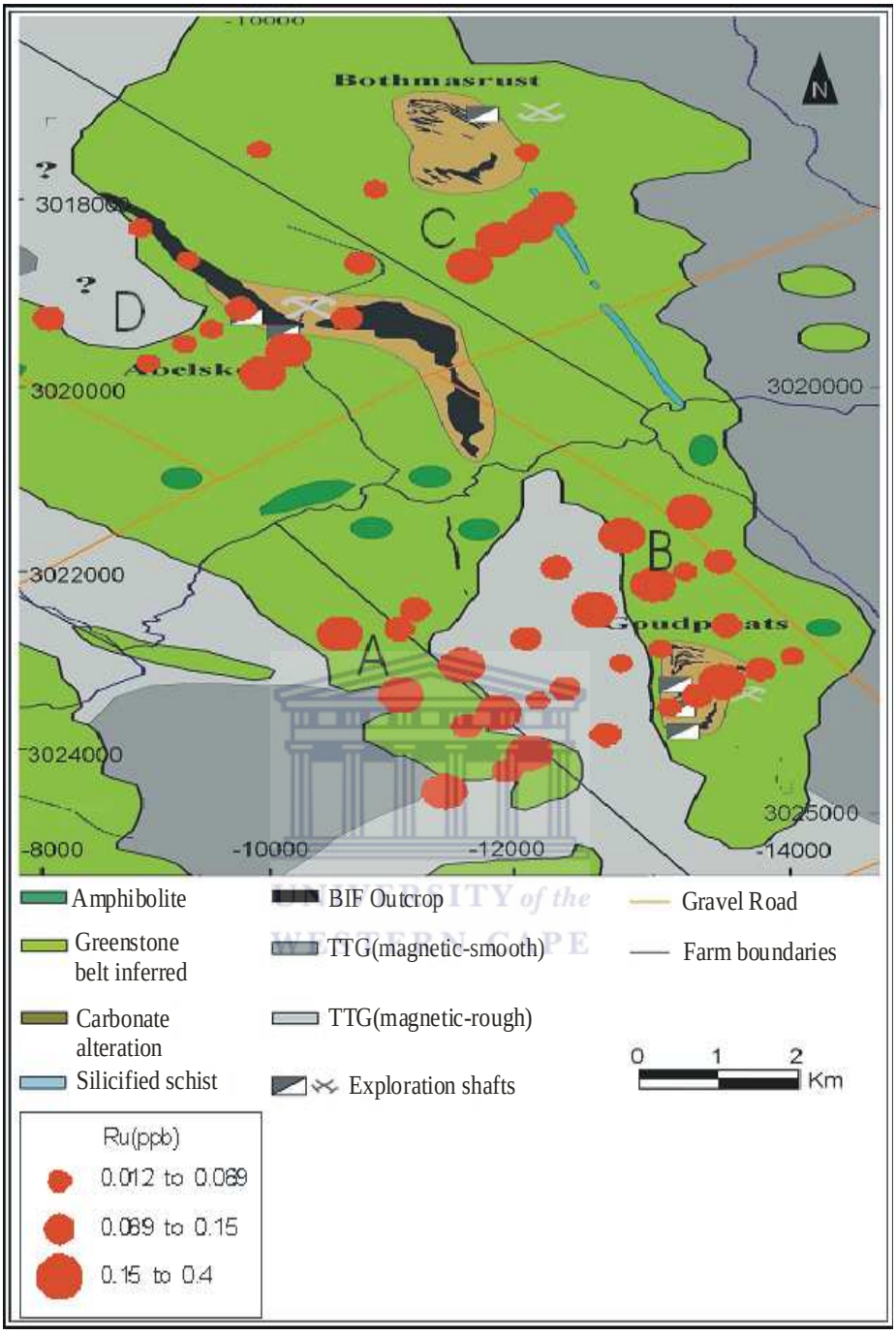

Appendix A4: Geochemical map of Ru (ppb) in regolith samples by 0.1M hydroxylamine partial leach (Amalia Blue Dot Mine).

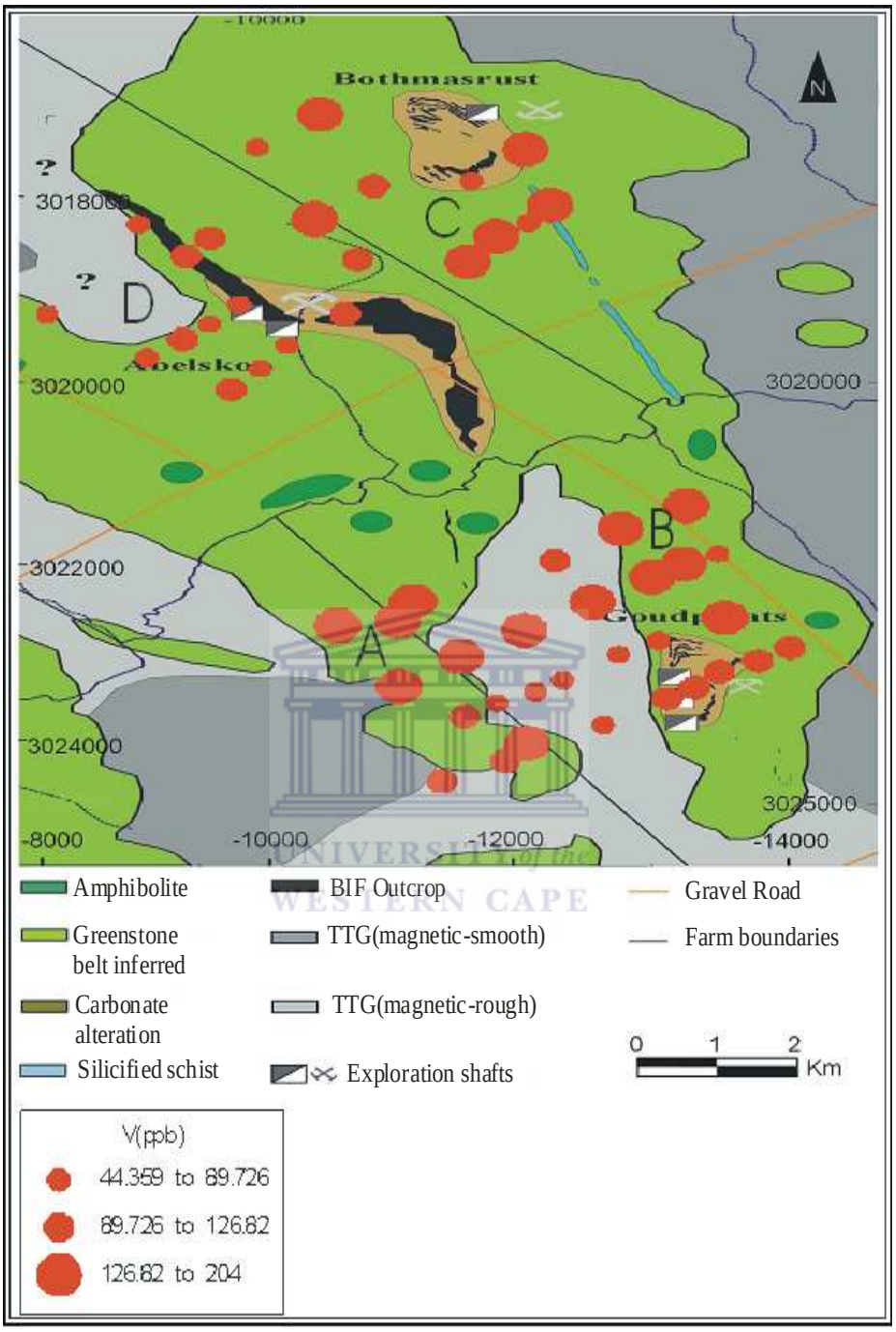

Appendix A5: Geochemical map of V (ppb) in regolith samples by 0.1M hydroxylamine partial leach (Amalia Blue Dot Mine).

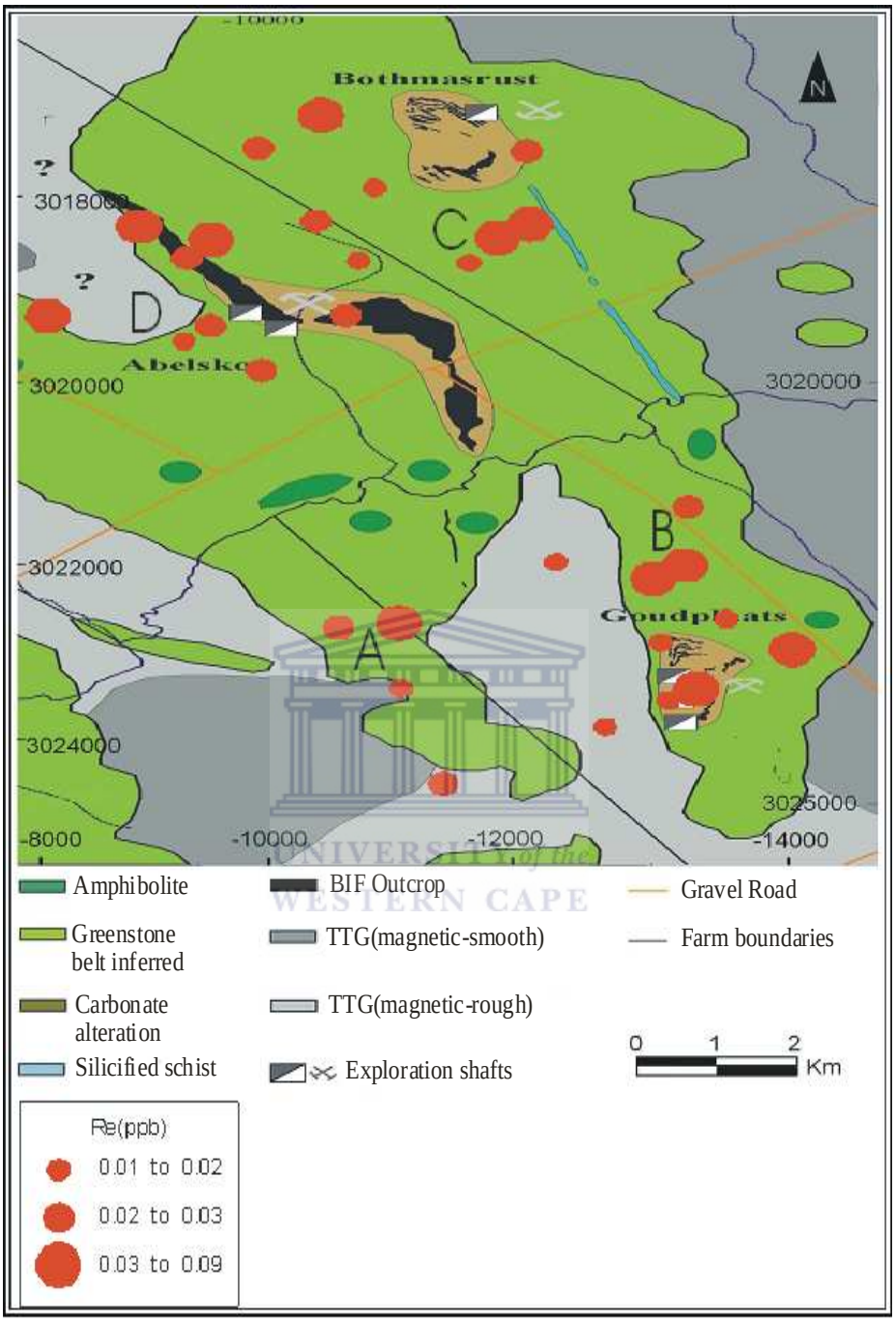

Appendix A6: Geochemical map of Re (ppb) in regolith samples by 0.1M hydroxylamine partial leach (Amalia Blue Dot Mine).

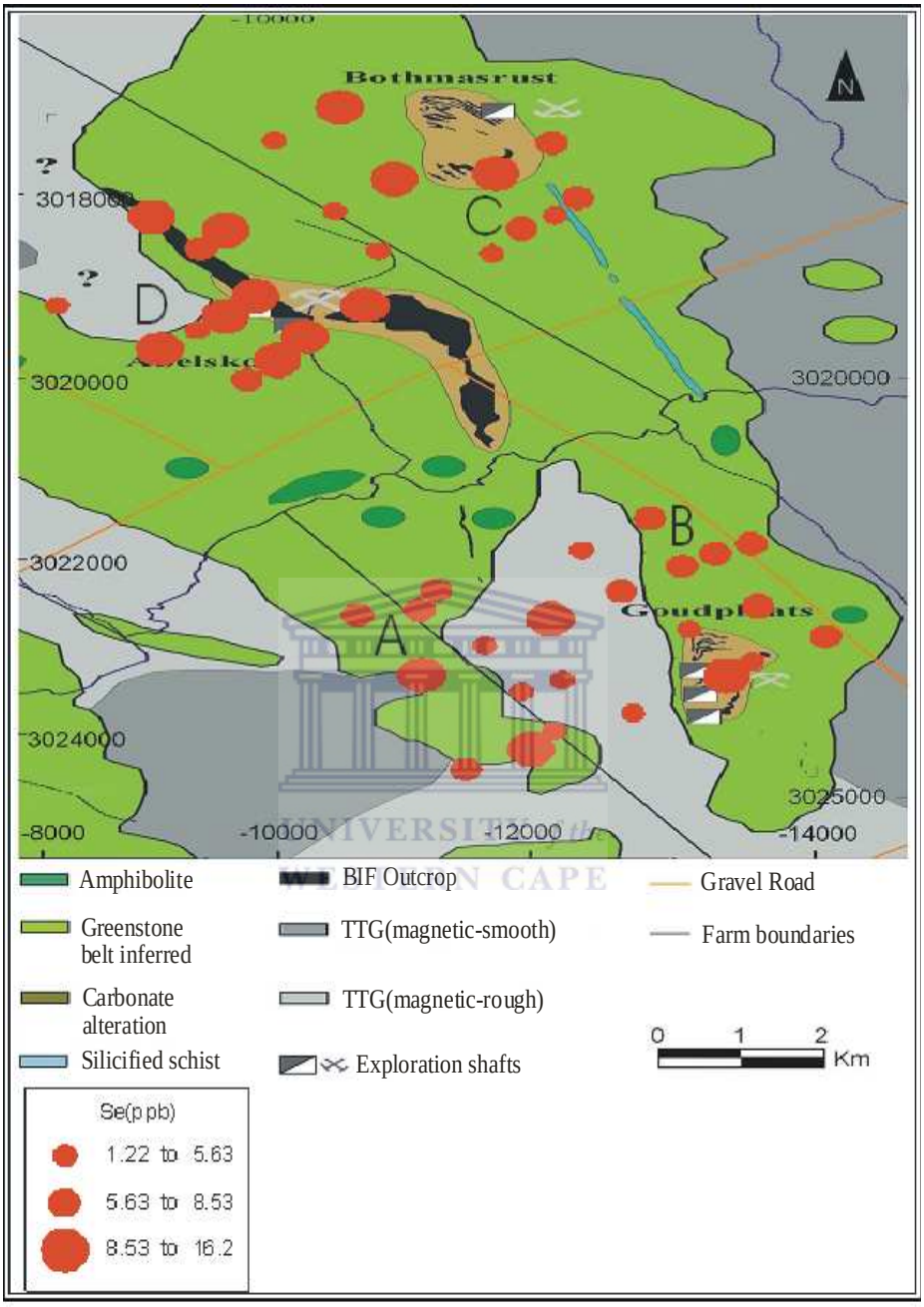

Appendix A7: Geochemical map of Pd (ppb) in regolith samples by 0.1M hydroxylamine partial leach (Amalia Blue Dot Mine).

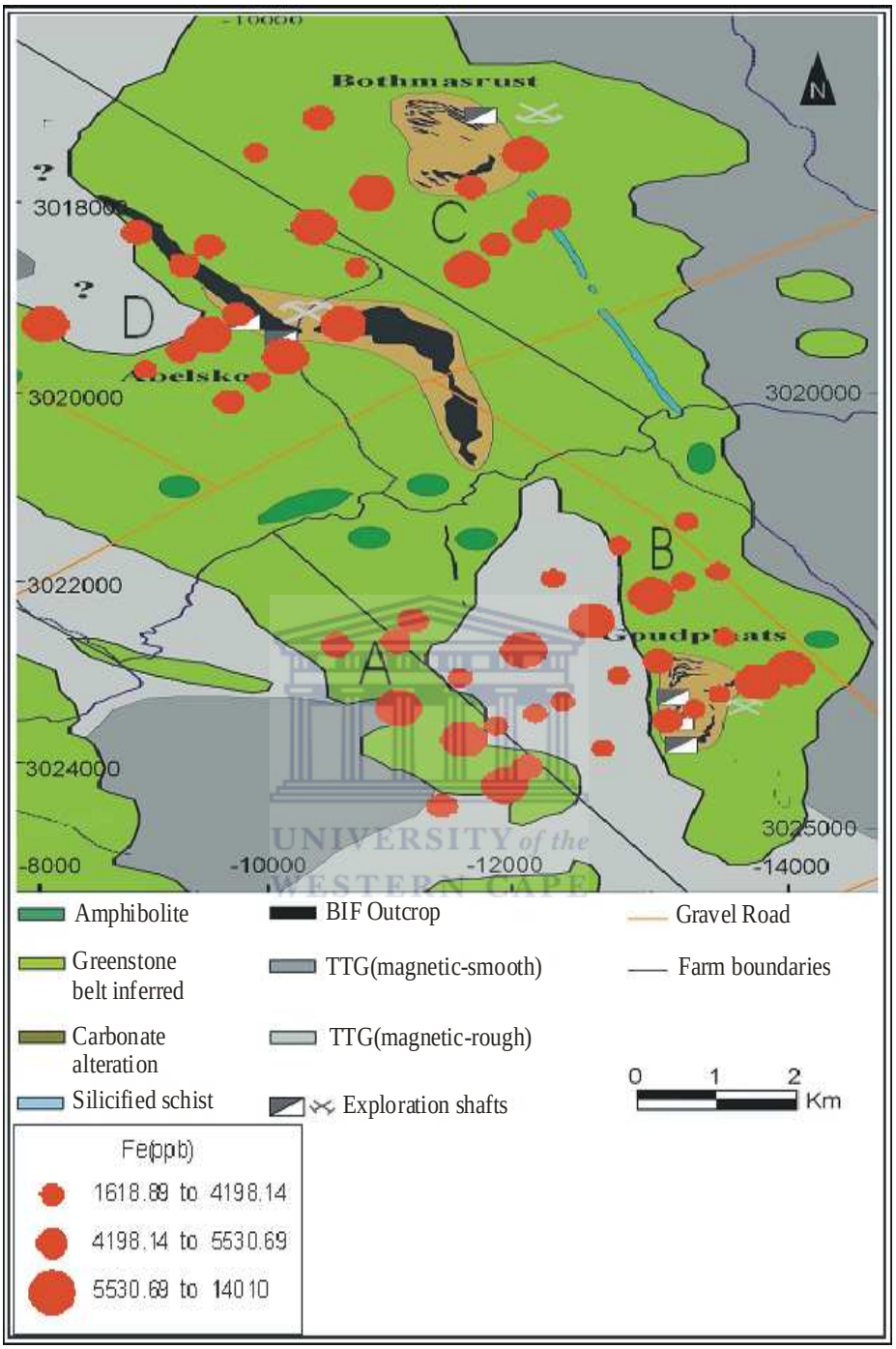

Appendix A8: Geochemical map of Fe(ppb) in regolith samples by 0.1M hydroxylamine partial leach (Amalia Blue Dot Mine).

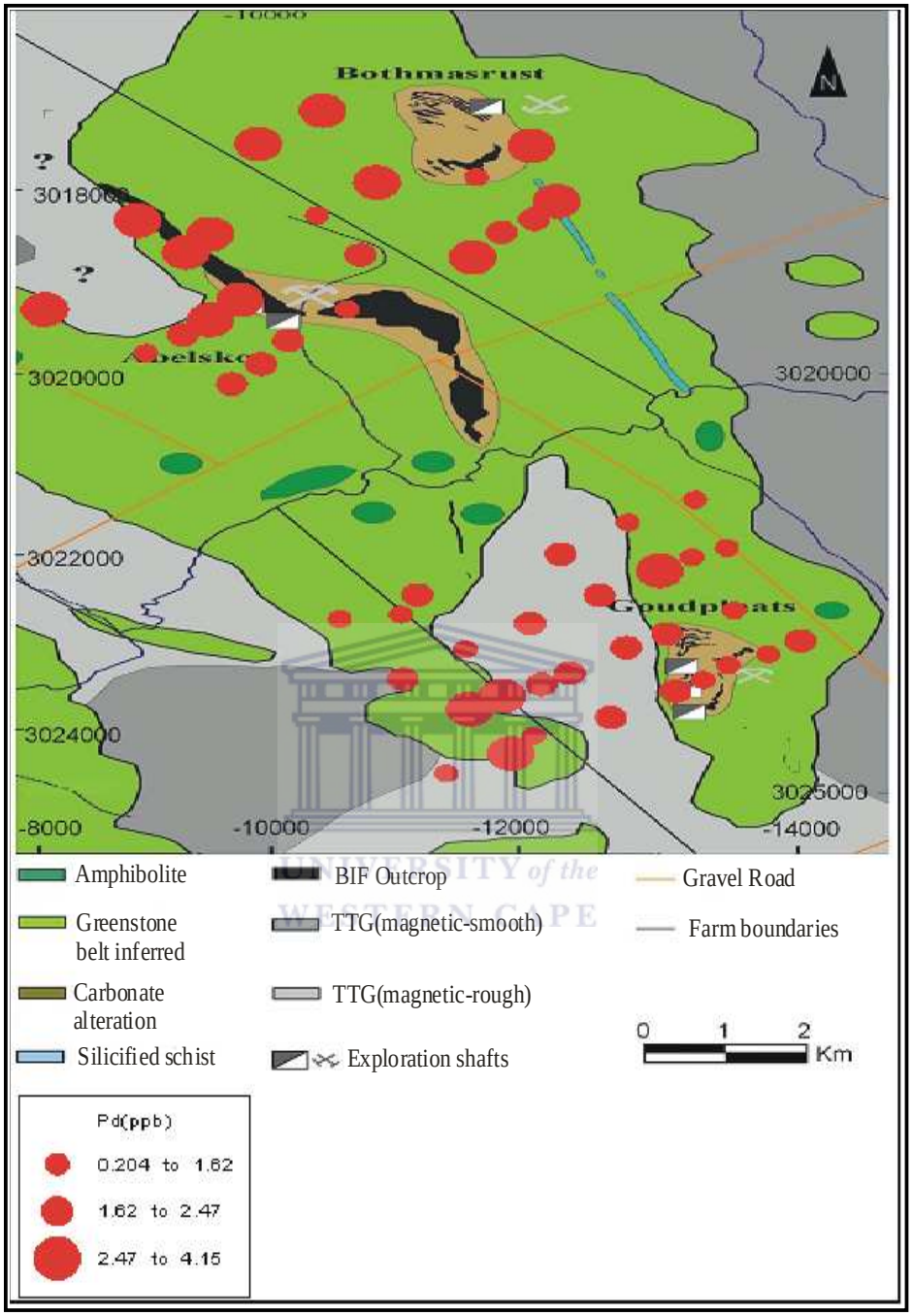

Appendix A9: Geochemical map of Sr (ppb) in regolith samples by 0.1M hydroxylamine partial leach (Amalia Blue Dot Mine).

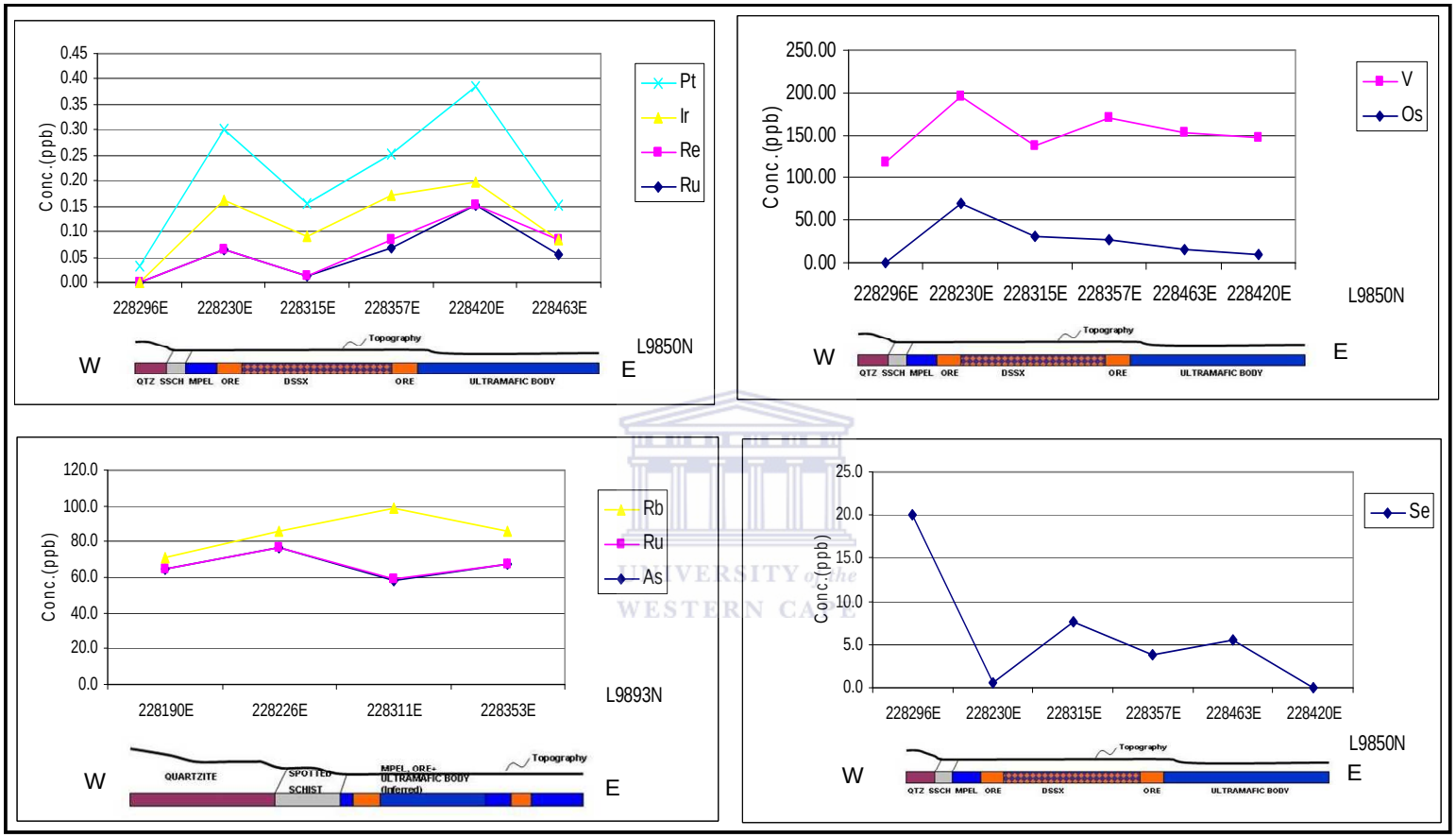

Appendix A10: Plot of correlated element (Rb, Ru, As, V, Sr, Se, Os, Ir, Re and Pt) in lateritic samples taken at both profile 1 and 2 in Kabanga main (Ni-Cu deposit).

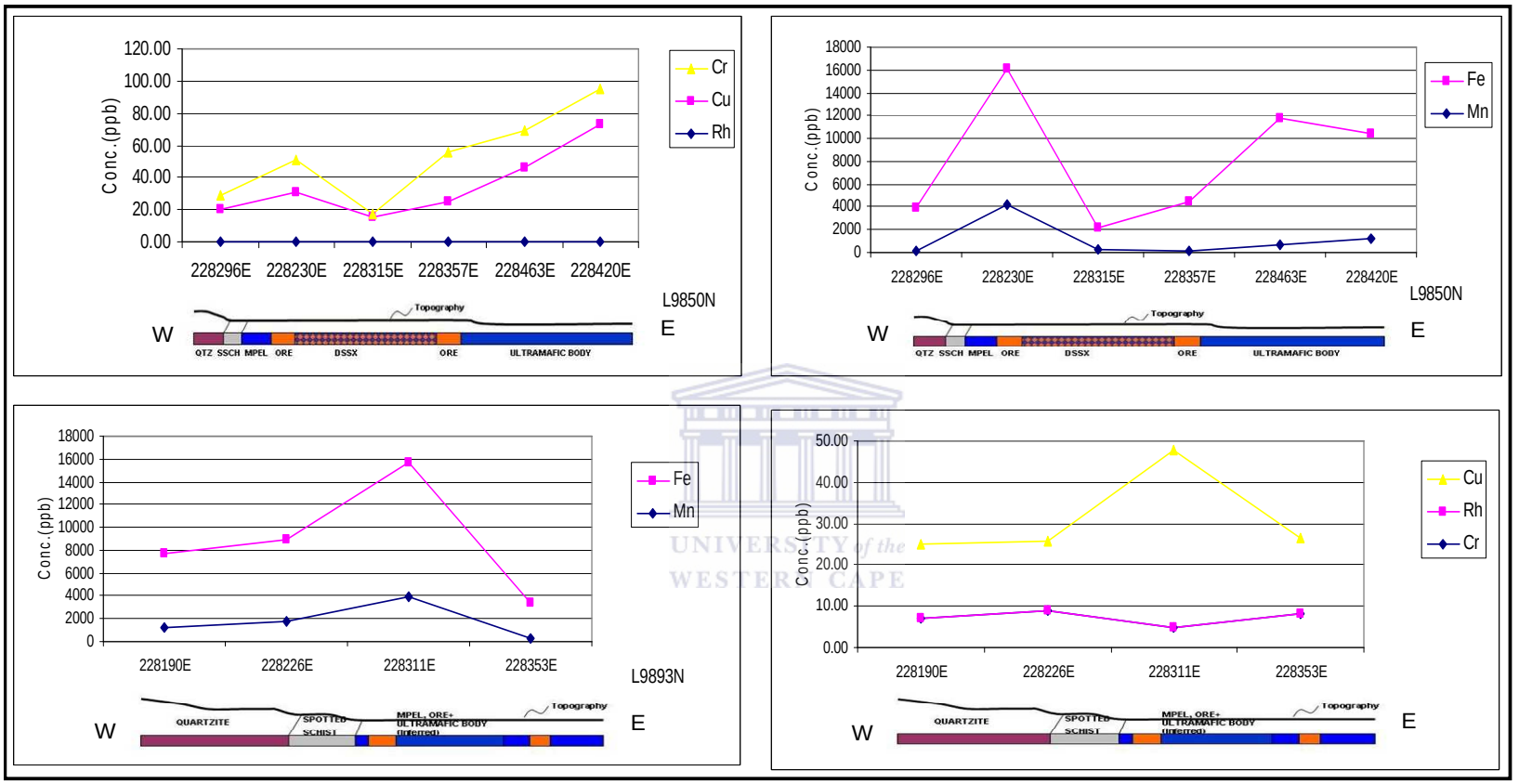

Appendix A11: Plot of correlated element (Fe, Mn, Cu, Rh and Cr) in lateritic samples taken at both profile 1 and 2 in Kabanga Main (Ni-Cu deposit).

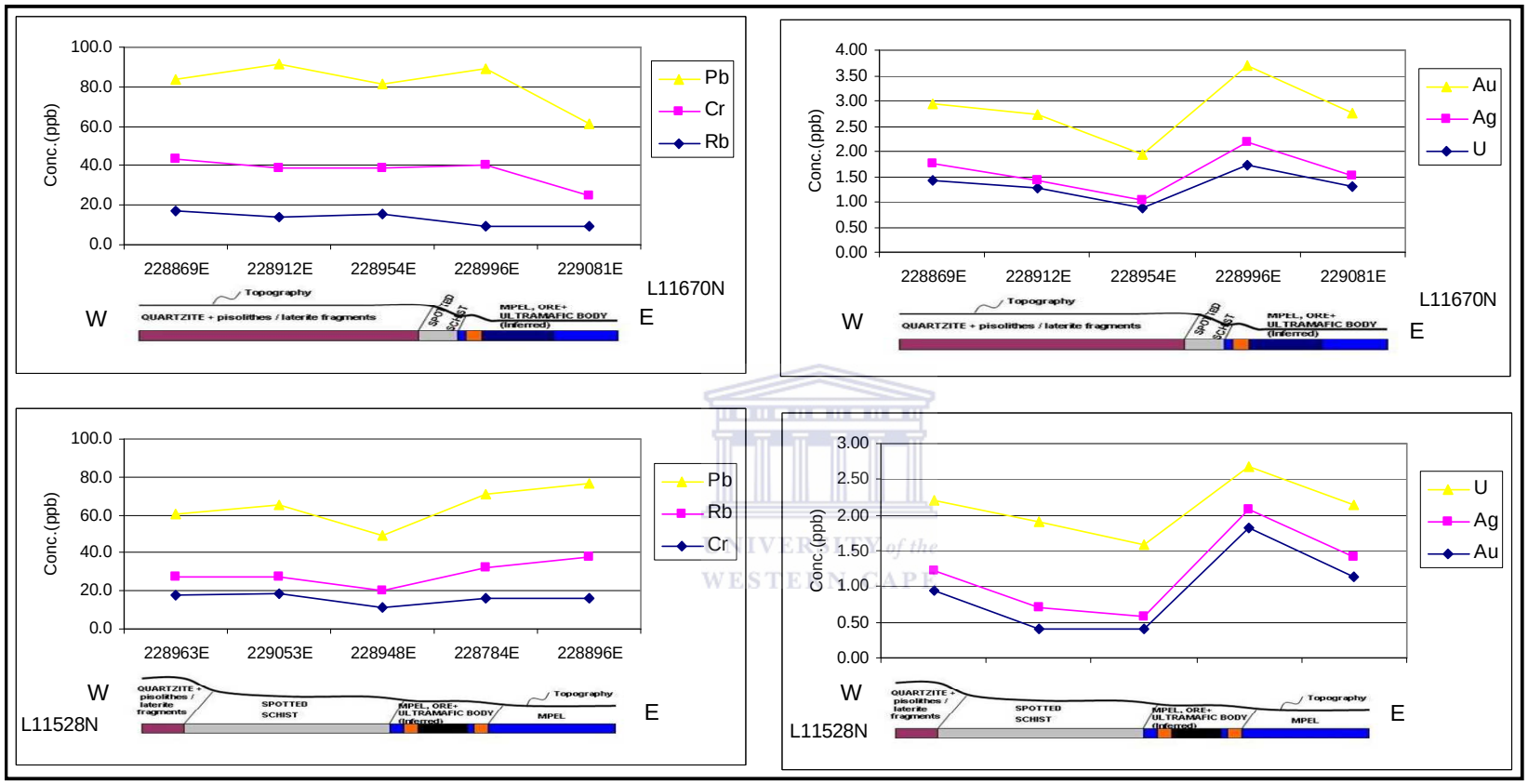

Appendix A12: Plot of correlated element (Pb, Rb, Cr, U, Ag and Au) in samples taken along profile 1&2 in samples taken along profiles in Kabanga north (Ni -Cu deposit).

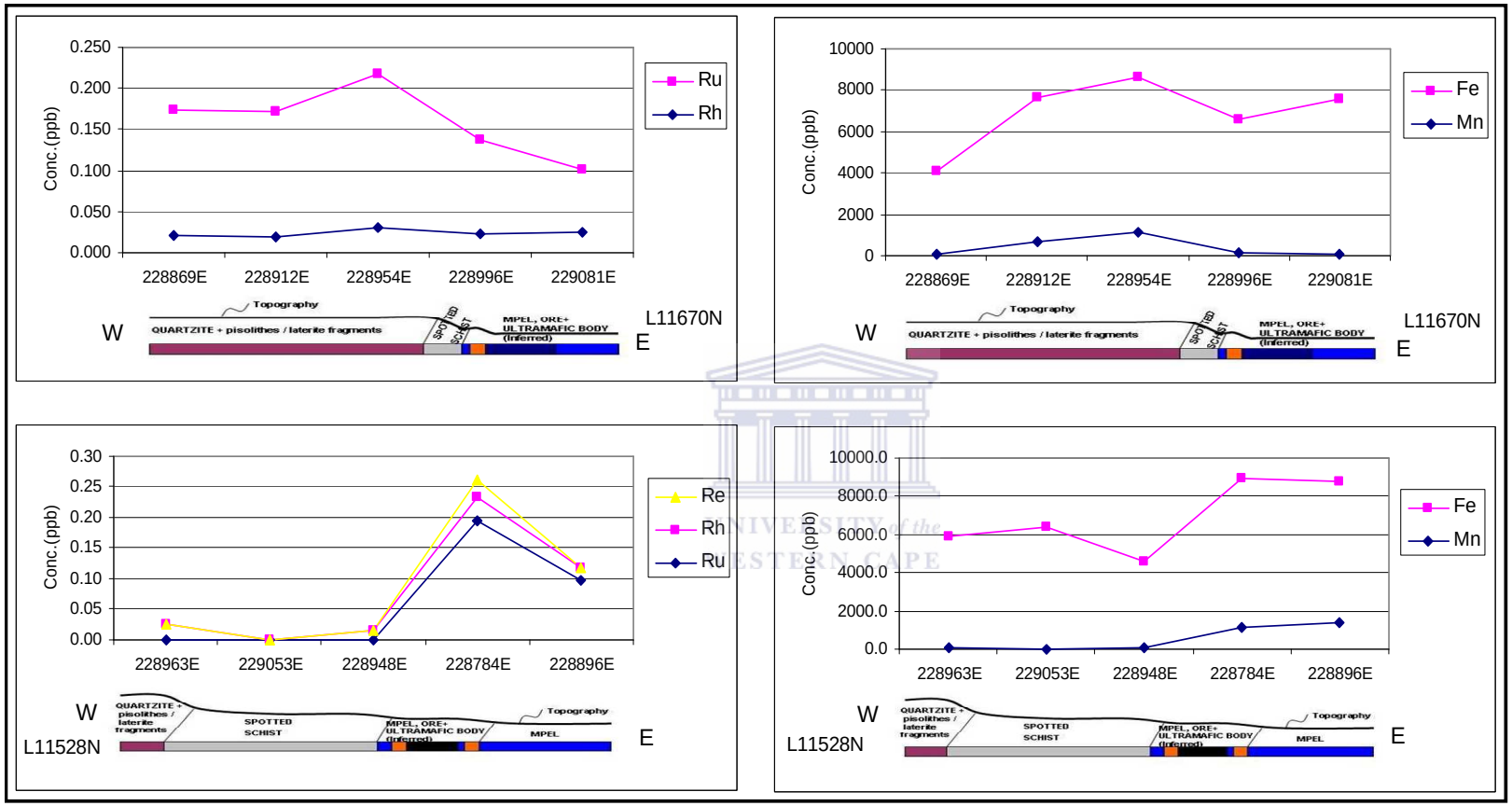

Appendix A13: The plot of correlated element (Ru, Rh, Re, Fe and Mn) along a profile 1 & 2 in samples taken along a profiles in Kabanga north Nickel -Copper prospect.

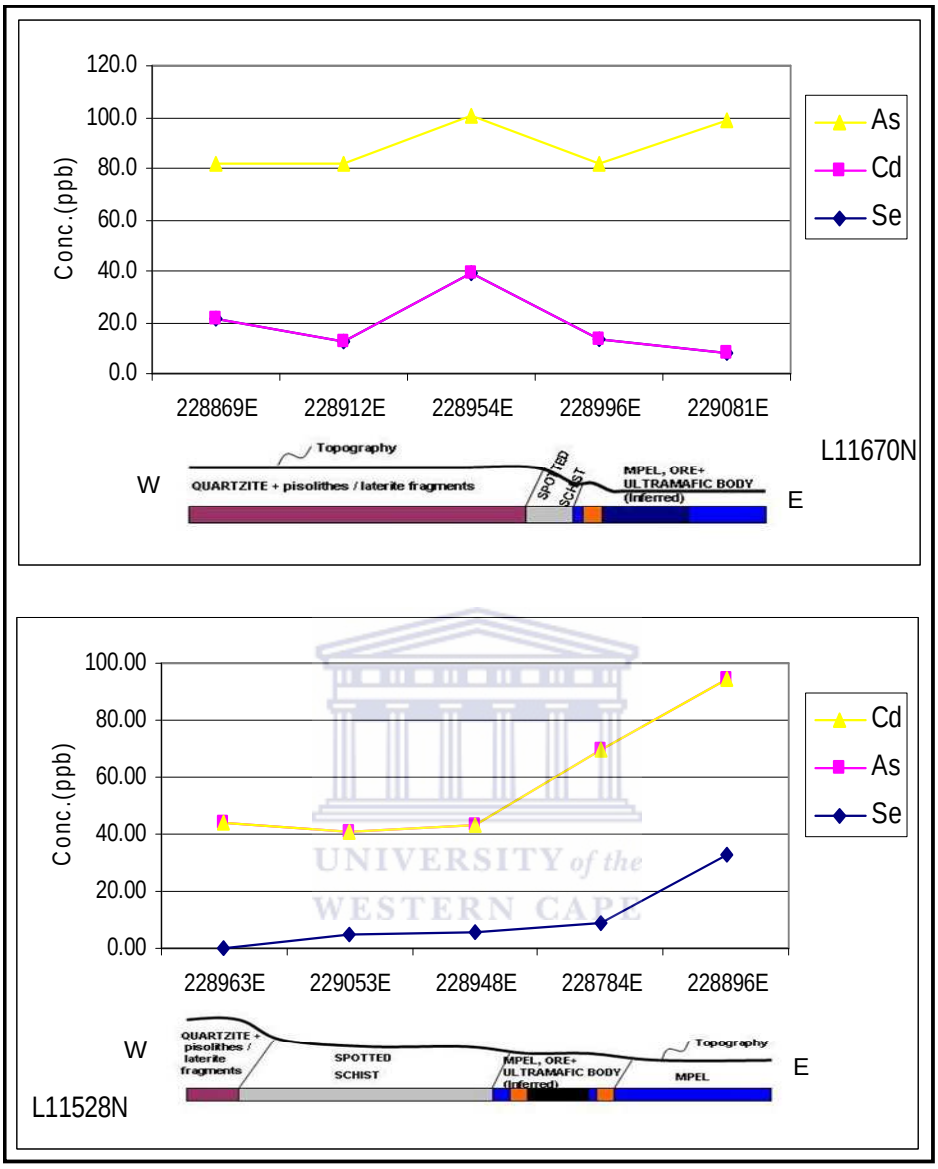

Appendix A14: The plot of element (Cd, As and Se) in sample taken along a profile1&2 in Kabanga north Nickel - Copper prospect.

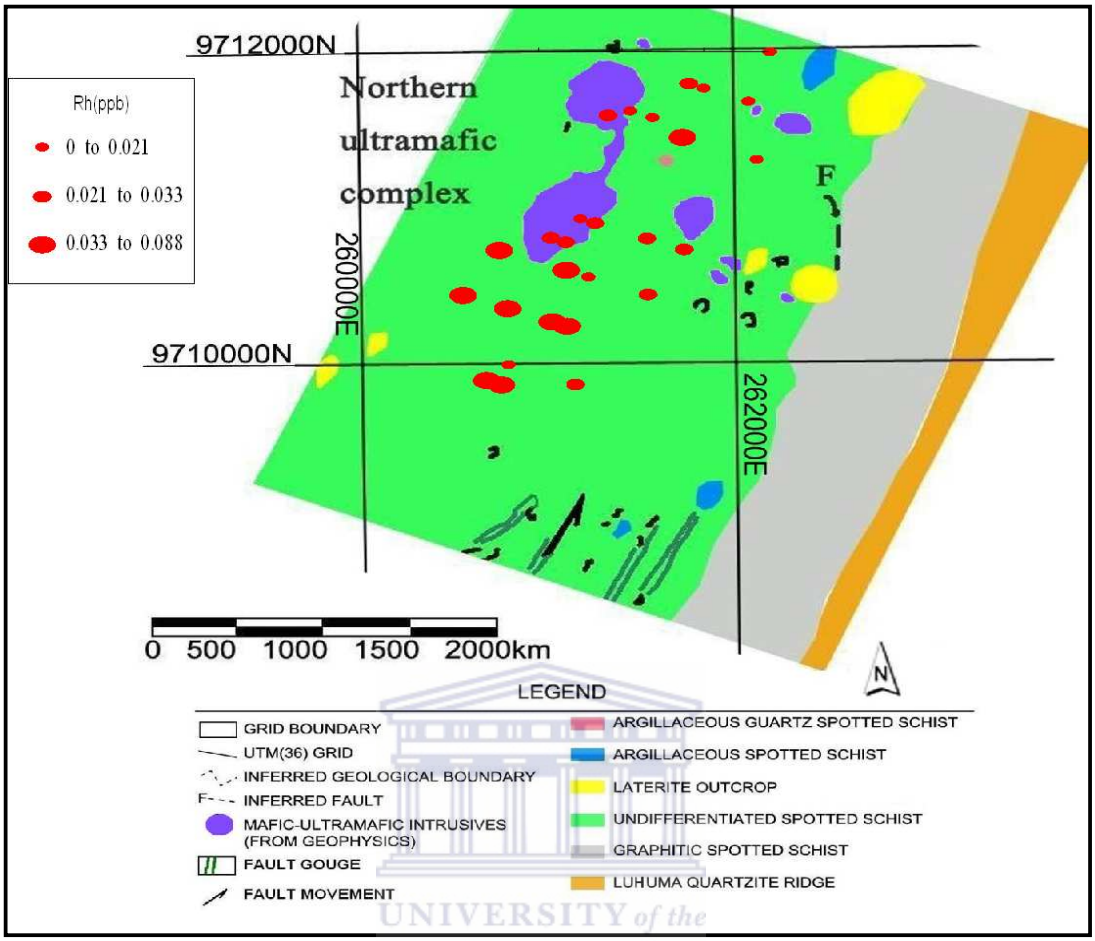

Appendix A15: Geochemical map of Rh (ppb) in lateritic regolith samples by 0.25M hydroxylamine partial leach (Luhuma Ni-Cu prospect).

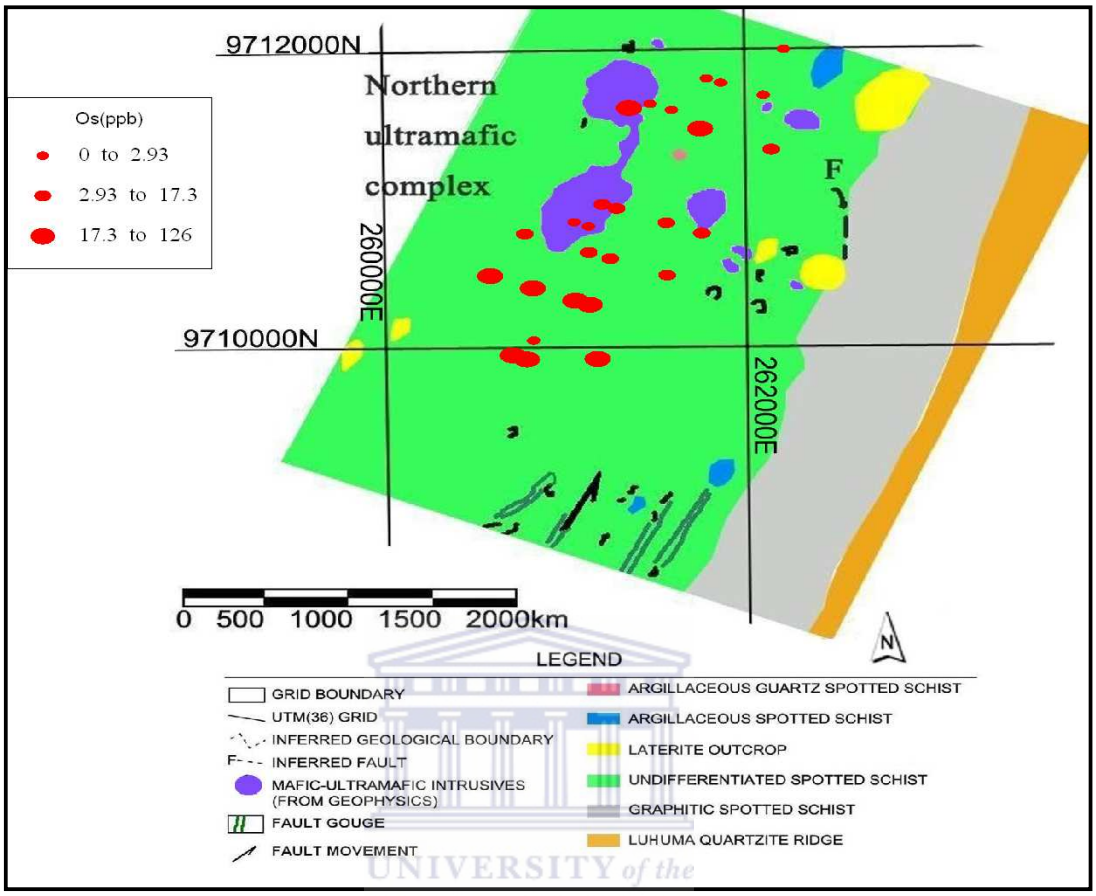

Appendix A16: Geochemical map of Os (ppb) in lateritic regolith samples by 0.25M hydroxylamine partial leach (Luhuma Ni-Cu prospect).

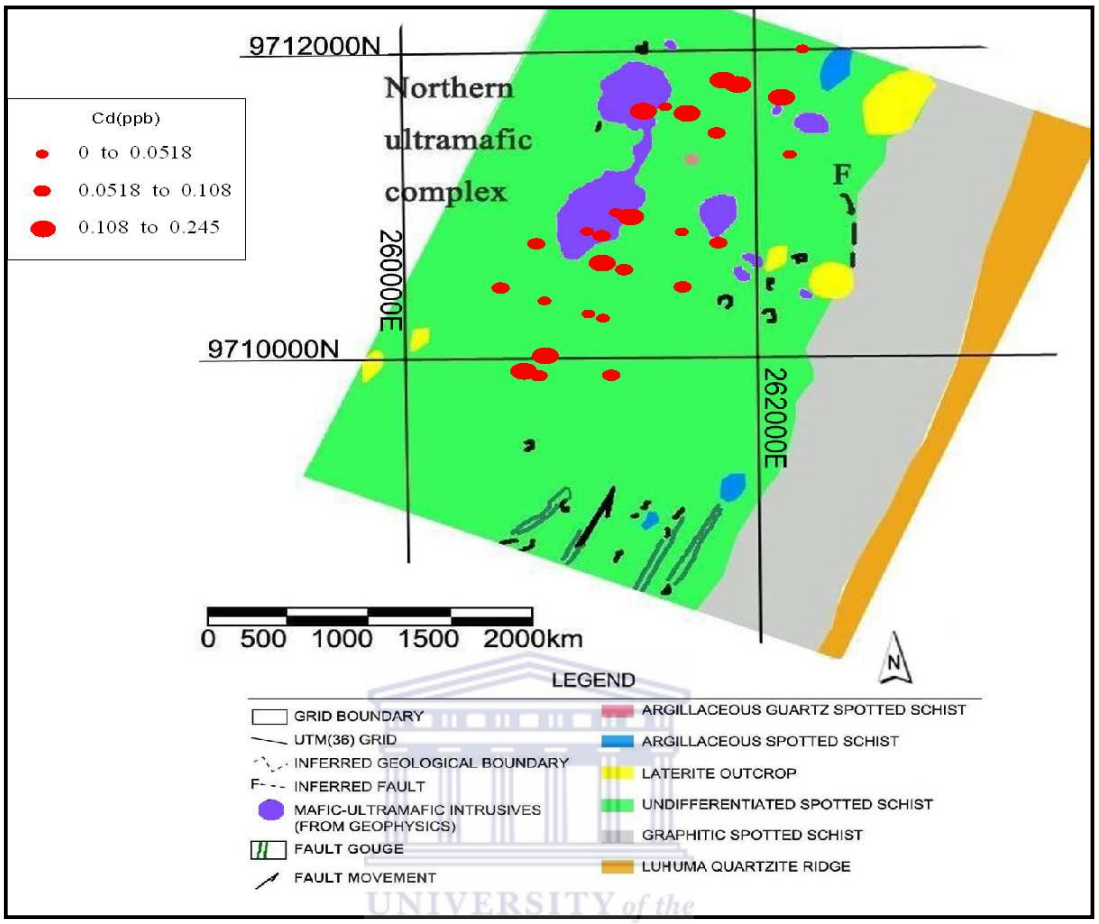

Appendix A17: Geochemical map of Re (ppb) in lateritic regolith samples by 0.25M hydroxylamine partial leach (Luhuma Ni-Cu prospect).

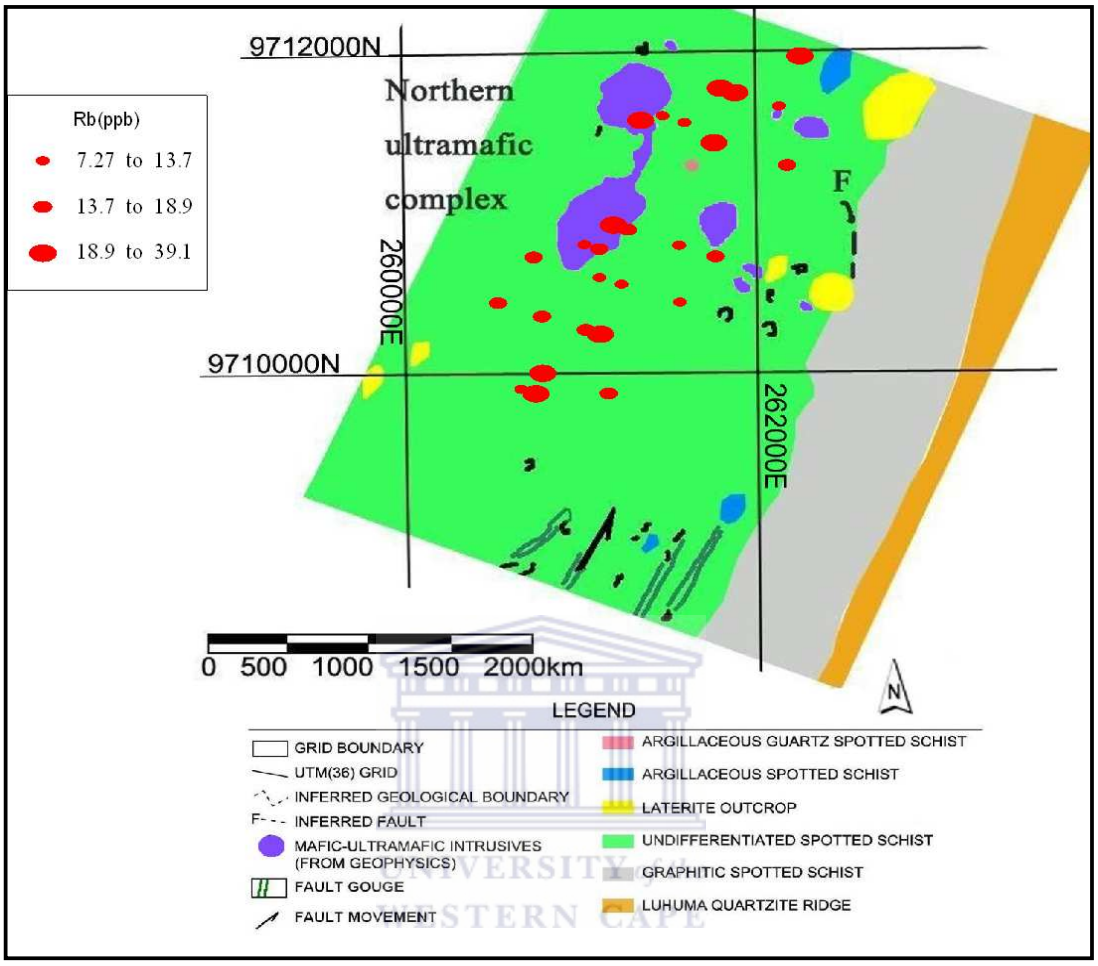

Appendix A18: Geochemical map of Se (ppb) in lateritic regolith samples by 0.25M hydroxylamine partial leach (Luhuma Ni-Cu prospect).

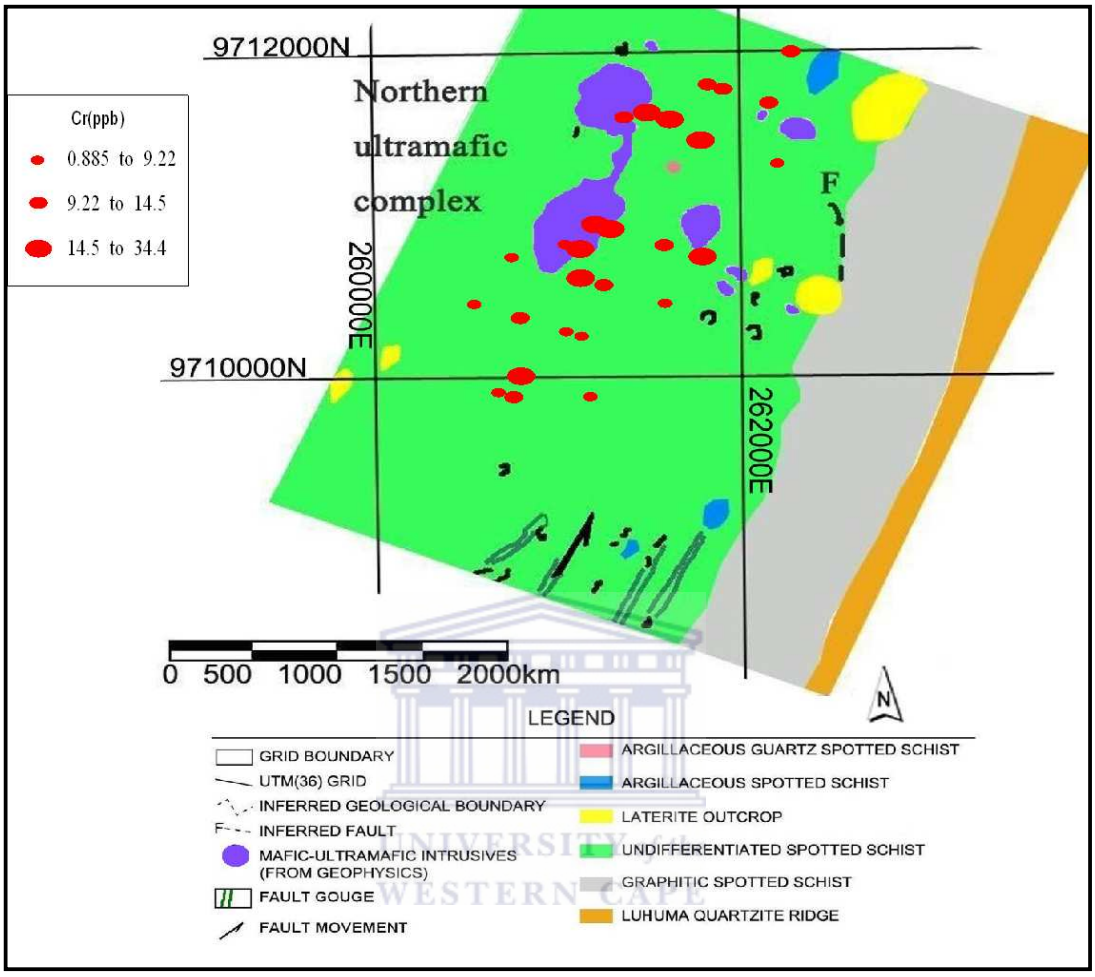

Appendix A19: Geochemical map of Cr (ppb) in lateritic regolith samples by 0.25M hydroxylamine partial leach (Luhuma Ni-Cu prospect).

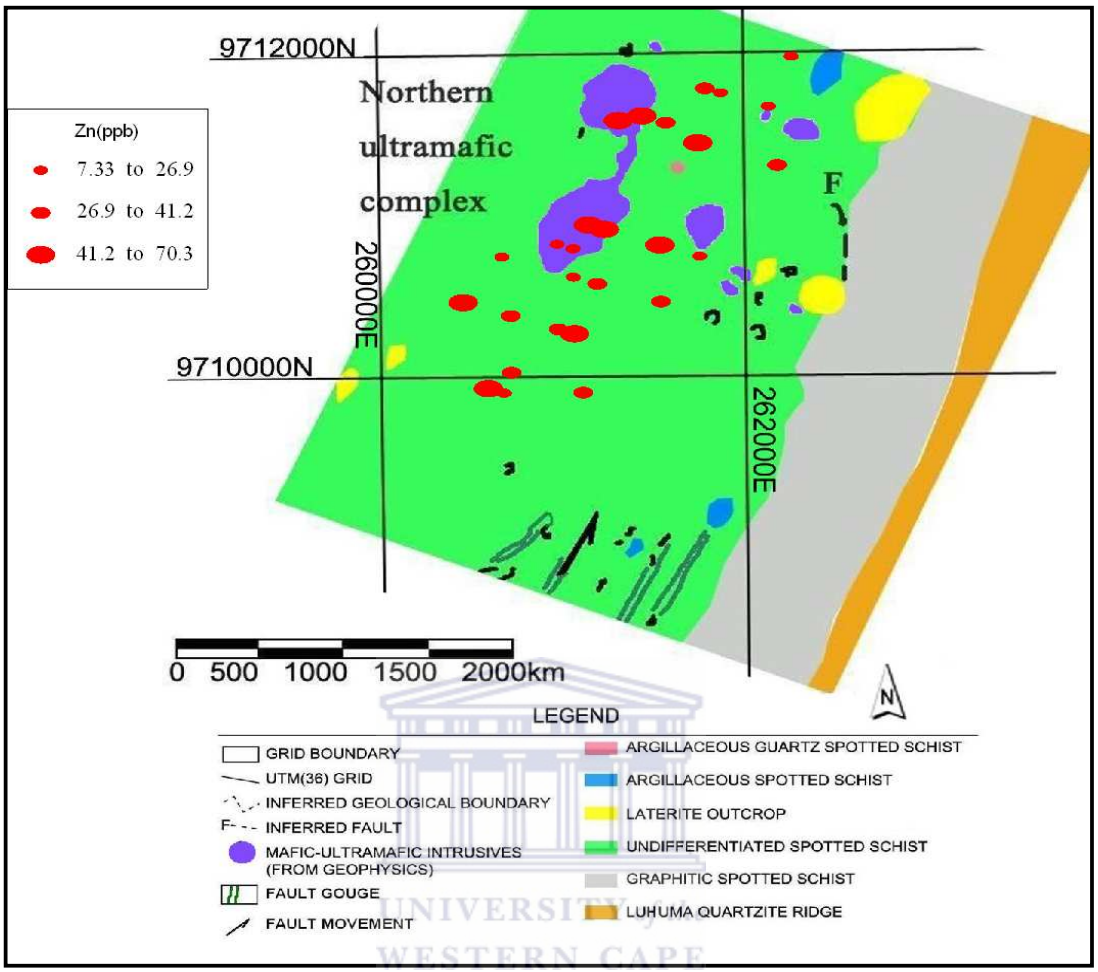

Appendix A20: Geochemical map of Zn (ppb) in lateritic regolith samples by 0.25M hydroxylamine partial leach (Luhuma Ni-Cu prospect).

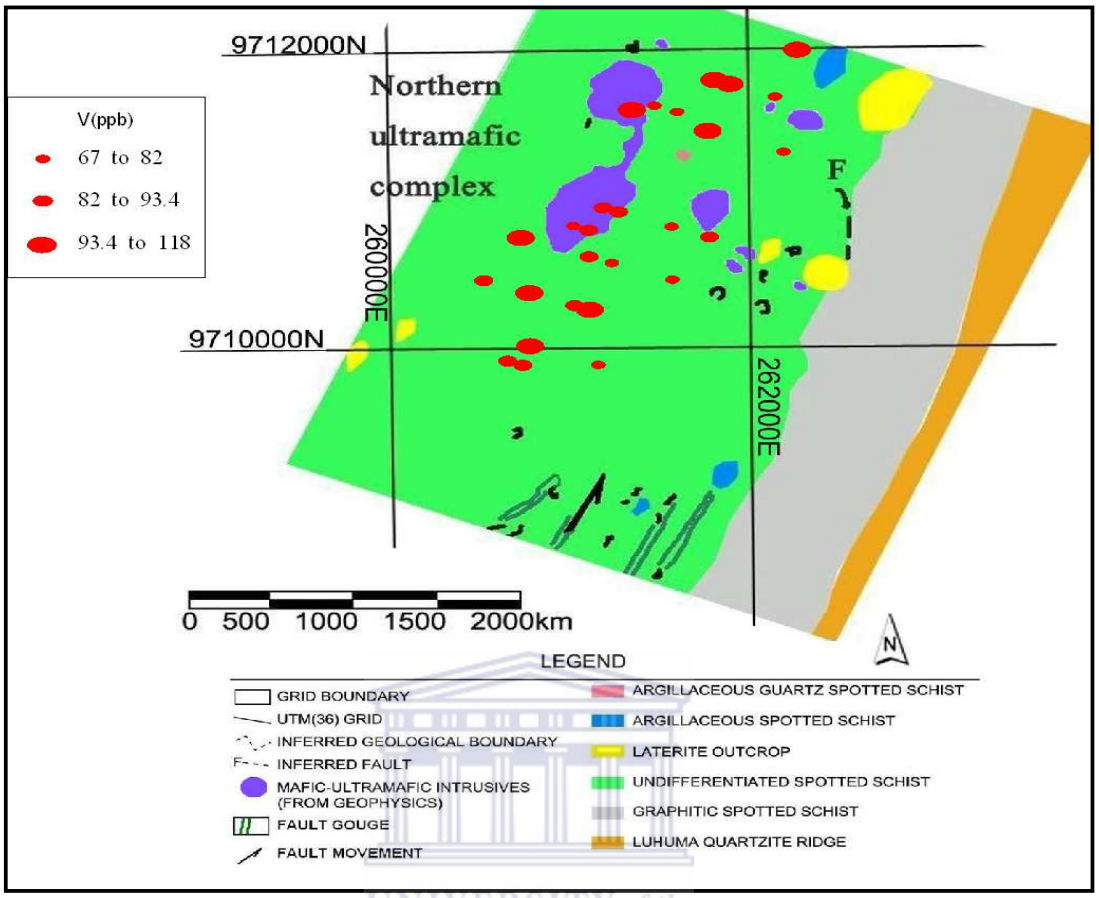

Appendix A21: Geochemical map of V (ppb) in lateritic regolith samples by 0.25M hydroxylamine partial leach (Luhuma Ni-Cu prospect).

APPENDIX II

APPENDIX A1: Triple acid leach (TAL) data for both upper and lower horizons along a profile in Amalia Blue Dot Mine.

AMALIA BLUE DOT MINE			(All data in ppm)															
			UPPER HORIZON								LOWER HORIZON							
SAMPLE ID	Y	X	Co	Zn	Cu	Pb	Ni	Mn	Ca	Mg	Co	Zn	Cu	Pb	Ni	Mn	Ca	Mg
13.1	188	113.988E	48.51	108.33	90.06	5.45	39.48	576.11	892.78	122.88	46.27	107.93	93.23	bdl	34.644	518.29	764.32	21.54
13.1i	188	130.814E	32.81	87.08	68.68	bdl	17.25	478.05	1133	123.14	44.03	106.75	78.98	bdl	22.083	486.83	365.58	74.81
13.2	192.2	143.391E	44.03	73.7	50.48	3.93	7.59	554.89	2998.3	126.52	37.29	98.09	55.22	bdl	16.285	439.99	118.6	69.48
13.3	185.89	174.899E	28.32	93.77	51.25	6.98	11.45	389.5	1686.9	130.81	32.81	74.49	45.71	0.87	14.353	339.74	26.9	bdl
13.4	185.89	204.302E	68.71	104.39	108.28	7.74	47.2	639.04	1862.1	140.03	70.96	102.03	121.75	1.64	57.834	582.69	499.05	121.45
13.4i	185.89	216.879E	55.25	111.48	93.23	1.64	35.61	591.47	794.35	118.85	46.27	146.89	113.28	13.85	47.203	609.77	3328.6	142.63
13.5	188	229.5E	70.96	128.39	109.08	6.22	47.2	617.09	627.51	128.59	77.69	119.74	127.29	7.74	78.125	611.23	268.81	25.43
13.5i	185.89	246.283E	61.99	148.46	109.08	7.74	43.34	673.43	1164.7	8.02	66.47	141.78	100.36	9.27	51.07	662.46	997.89	128.99
13.6	185.89	261.007E	46.27	113.84	72.64	6.22	24.02	551.23	667.55	16.46	82.18	109.12	78.19	9.27	29.813	710.75	11.89	bdl

APPENDIX A2: Aqua regia leach (ARL) for samples taken from Luhuma and Kabanga (Main & North).

All data in ppm																			
Luhuma Samples							**Kabanga Main Samples**							**Kabanga North Samples**					
Y	X	Ni	Co	Cu	Pb	Zn	Y	X	Ni	Co	Cu	Pb	Zn	Y	X	Ni	Co	Cu	Pb	Zn
9707763	259080E	24	12	30	28	35	9681422	228338E	20	12	17	21	16	9682846	228963E	10	12	14	23	13
9707763	259619E	20	10	14	27	24	9681422	228296E	14	11	12	22	15	9682902	229053E	12	13	12	28	12
9707237	260158E	29	14	18	29	28	9681475	228254E	13	10	10	19	16	9683027	228948E	16	10	8	17	13
9707150	260338E	30	14	20	30	29	9681437	228230E	10	8	8	16	13	9683296	228784E	18	14	11	17	19
9705988	260439E	14	7	9	20	14	9681411	228273E	12	10	10	19	14	9683286	228896E	12	8	11	17	17
9707763	260833E	23	11	20	28	24	9681384	228315E	19	13	17	23	15	228869	9683243E	17	10	10	18	16
9707763	261732E	18	9	16	30	20	9681358	228357E	31	16	45	28	23	228912	9683217E	14	8	9	16	15
9701482	262631E	11	7	11	21	17	9681331	228400E	67	27	84	33	25	228954	9683190E	16	9	8	17	17
9709298	260496E	18	8	18	21	22	9681351	228463E	114	45	92	42	32	228996	9683164E	14	8	10	16	17
9709210	260676E	13	7	15	18	19	9681378	228420E	146	37	145	31	27	229081	9683111E	8	8	7	13	11
9708903	261305E	7	5	10	14	17	9681572	228190E	10	5	6	12	13							
9707763	261754E	21	8	14	18	22	9681550	228226E	10	6	8	12	15							
9707785	261316E	18	8	12	20	22	9681497	228311E	18	10	16	21	25							
9708136	260597E	24	9	12	20	34	9681470	228353E	15	9	11	20	16							
9708268	260327E	18	9	11	15	25														
9708662	259518E	15	6	16	21	22														
9712630	262789E	33	5	21	27	34														
9711644	262530E	22	11	16	21	20														
9711907	261991E	27	6	19	27	28														
9711994	261811E	25	6	23	28	31														
9711319	261370E	51	7	44	27	28														
9711451	261101E	18	18	17	13	23														
9708827	260322E	31	8	23	27	27														
9708914	260142E	15	12	22	23	22														
9706382	259630E	27	13	20	27	18														
9706067	259365E	15	10	14	19	19														
9705979	259545E	23	11	16	22	22														

APPENDIX B1: The result obtained from cold and hot hydroxylamine leach for randomly selected samples from Kabanga.

Kabanga Samples									**(All data in ppm)**												
Cold HAM																					
0.1M							**0.15M**					**0.2M**					**0.25M**				
Y	X	Ni	Co	Cu	Mn	Fe	Ni	Co	Cu	Mn	Fe	Ni	Co	Cu	Mn	Fe	Ni	Co	Cu	Mn	Fe
9682902	229053	5.4	6.3	34.2	0.9	130.5	12.6	14.4	33.3	1.8	36	18	16.2	33.3	35.1	2.7	21.6	20.7	34.2	3.6	16.2
9681422	228338	6.3	8.1	33.3	5.4	25.2	14.4	7.2	33.3	10.8	23.4	17.1	16.2	33.3	13.5	2.7	26.1	23.4	34.2	4.5	7.2
9681411	228273	9	8.1	33.3	12.6	79.2	16.2	15.3	34.2	5.4	27	20.7	18	34.2	18.9	5.4	27.9	20.7	34.2	6.3	25.2
9681384	228315	13.5	9	34.2	4.5	32.4	17.1	15.3	35.1	3.6	20.7	22.5	18.9	34.2	6.3	4.5	28.8	24.3	36	5.4	9.9
9681351	228463	15.3	9.9	34.2	72.9	64.8	18.9	16.2	33.3	14.4	94.5	20.7	21.6	34.2	41.4	9	28.8	24.3	34.2	8.1	69.3
Hot HAM																					
0.1M							**0.15M**					**0.2M**					**0.25M**				
Y	X	Ni	Co	Cu	Mn	Fe	Ni	Co	Cu	Mn	Fe	Ni	Co	Cu	Mn	Fe	Ni	Co	Cu	Mn	Fe
9682902	229053	38.7	53.1	11.7	10.8	162.9	38.7	48.6	10.8	9.9	123	45.9	144	9.9	9.9	163	49.5	113	9.9	11.7	102
9681422	228338	39.6	13.5	11.7	18.9	259.2	41.4	97.2	11.7	9.9	51.3	45.9	191	11.7	9	124	47.7	88.2	9	12.6	60.3
9681411	228273	36.9	39.6	11.7	31.5	48.6	42.3	36.9	10.8	9.9	20.7	45.9	63.9	10.8	9	86.4	55.8	83.7	10.8	9.9	88.2
9681384	228315	42.3	67.5	10.8	16.2	508.5	41.4	126	10.8	9.9	526	45	72	10.8	9.9	74.7	48.6	115	11.7	10.8	111
9681351	228463	43.2	9	11.7	72	239.4	45	40.5	11.7	13.5	20.7	46.8	123	12.6	9.9	441	49.5	112	9.9	11.7	117

APPENDIX B2: The result obtained from cold and hot hydroxylamine leach for randomly selected samples from Luhuma.

Luhuma Samples									**(All data in ppm)**												
Cold HAM																					
0.1M							**0.15M**					**0.2M**					**0.25M**				
Y	X	Ni	Co	Cu	Mn	Fe	Ni	Co	Cu	Mn	Fe	Ni	Co	Cu	Mn	Fe	Ni	Co	Cu	Mn	Fe
9707763	259080	8.1	55.8	2.7	85.5	62.1	9	76.5	9	65.7	129	15.3	82.8	0.9	32.4	119	18	1.25	1.8	65.7	215
9707500	259619	8.1	57.8	1.8	56.7	64.8	11.7	70.2	11.7	35.1	95.4	14.4	84.6	*n.d*	40.5	91.8	16	1.39	1.8	67.5	145
9711359	260833	4.5	55.8	1.8	108.9	57.6	7.2	63	7.2	71.1	107	16.2	90	1.8	55.8	107	11.5	1.28	1.8	139	229
9710920	261732	8.1	53.1	0.9	87.3	85.5	10.8	67.5	10.8	58.5	97.2	12.6	87.3	2.7	62.1	140	20	1.23	1.8	47.7	197
9708684	261754	9.9	57.6	1.8	76.5	81	9.9	72	9.9	43.2	98.1	11.7	92.7	0.9	52.2	103	18	1.12	0.9	57.6	194
Hot HAM																					
0.1M							**0.15M**					**0.2M**					**0.25M**				
Y	X	Ni	Co	Cu	Mn	Fe	Ni	Co	Cu	Mn	Fe	Ni	Co	Cu	Mn	Fe	Ni	Co	Cu	Mn	Fe
9707763	259080	36.9	121.5	12.6	82.8	270.9	41.4	63.9	11.7	13.5	104	43.2	83.7	13.5	9.9	307	47.7	134	10.8	10.8	201
9707500	259619	36.9	44.1	12.6	38.7	104.4	39.6	82.8	10.8	10.8	269	57.6	99.9	12.6	9	221	47.7	83.7	9.9	14.4	178
9711359	260833	38.7	21.6	11.7	54.9	267.3	41.4	57.6	11.7	19.8	264	45	97.2	11.7	11.7	369	47.7	80.1	10.8	9	101
9710920	261732	36.9	6.3	11.7	125.1	307.8	39.6	76.5	11.7	12.6	504	45.9	76.5	11.7	10.8	369	48.6	128	9.9	9	49.5
9708684	261754	39.6	49.5	10.8	54.9	350.1	41.4	54.9	11.7	11.7	234	45.9	137	11.7	9.9	239	51.3	108	9.9	13.5	108

APPENDIX C1: Multi element analysis data for hot hydroxylamine leach of samples taken at basal horizon along a profile in Amalia Blue Dot Mine.

Amalia Blue Dot Mine																								
Lower horizon (Hot HAM)																								
0.1M						**(All data in ppb)**																		
	V	Cr	Mn	Co	Ni	Cu	Zn	As	Se	Rb	Sr	Ru	Rh	Pd	Ag	Cd	Ba	Re	Os	Ir	Pt	Au	Pb	U
L13.1D	54.3	*n.d.*	5874	119	165	41.1	36.2	17.6	*n.d.*	10.8	107	*n.d.*	*n.d.*	0.48	0.64	0.20	1110	*n.d.*	*n.d.*	*n.d.*	*n.d.*	*n.d.*	19.9	0.29
L13.2D	58.7	*n.d.*	6142	83.6	91.5	61.4	28.4	16.8	22.1	10.9	171	*n.d.*	*n.d.*	1.46	0.19	0.23	742	*n.d.*	141	0.33	*n.d.*	3.03	21.6	0.26
L13.3D	36.1	*n.d.*	2994	48.9	24.7	38.6	9.56	20.0	10.2	10.3	68.2	*n.d.*	*n.d.*	0.94	0.092	*n.d.*	361	*n.d.*	31.8	0.032	*n.d.*	0.47	29.2	0.55
L13.4D	33.0	*n.d.*	5669	150	24.7	51.9	20.4	14.5	18.3	8.53	70.5	*n.d.*	*n.d.*	0.86	0.066	0.19	534	*n.d.*	9.33	*n.d.*	*n.d.*	*n.d.*	16.1	0.35
L13.5D	80.7	*n.d.*	6949	146	156	63.9	51.9	29.1	11.9	19.5	91.8	0.17	0.31	1.22	1.69	0.65	970	0.30	34.0	0.41	1.26	14.2	24.0	0.30
L13.6D	45.2	*n.d.*	15334	210	47.0	64.5	20.8	17.5	37.5	15.6	172	*n.d.*	*n.d.*	1.78	1.15	*n.d.*	2874	*n.d.*	*n.d.*	*n.d.*	*n.d.*	*n.d.*	75.1	0.79
0.15M																								
	V	Cr	Mn	Co	Ni	Cu	Zn	As	Se	Rb	Sr	Ru	Rh	Pd	Ag	Cd	Ba	Re	Os	Ir	Pt	Au	Pb	U
L13.1D	59.9	*n.d.*	1282	23.2	40.4	22.6	7.39	28.6	*n.d.*	5.46	21.1	*n.d.*	*n.d.*	0.84	0.89	*n.d.*	*n.d.*	*n.d.*	256	*n.d.*	*n.d.*	*n.d.*	13.9	0.29
L13.2D	40.7	*n.d.*	517	6.68	10.6	30.9	5.66	29.0	20.6	5.71	25.6	*n.d.*	*n.d.*	1.01	0.022	*n.d.*	*n.d.*	*n.d.*	323	97.3	0.22	2.19	15.8	0.28
L13.3D	26.9	*n.d.*	125	1.39	2.46	33.6	10.1	27.0	38.2	4.22	4.06	*n.d.*	*n.d.*	0.57	0.089	*n.d.*	*n.d.*	*n.d.*	37.9	22.1	0.037	0.78	8.28	0.41
L13.4D	34.5	*n.d.*	1458	30.0	40.5	30.4	10.2	24.8	19.3	5.41	16.2	*n.d.*	*n.d.*	0.80	0.39	*n.d.*	*n.d.*	*n.d.*	137	5.63	*n.d.*	*n.d.*	9.12	0.30
L13.5D	53.2	*n.d.*	2016	38.5	57.8	43.3	8.15	24.6	25.9	8.56	27.6	*n.d.*	*n.d.*	1.25	0.57	*n.d.*	*n.d.*	*n.d.*	418	0.80	*n.d.*	*n.d.*	15.0	0.34
L13.6D	29.2	*n.d.*	1606	20.7	9.55	28.8	5.63	24.7	25.8	6.63	22.1	*n.d.*	*n.d.*	1.04	0.45	*n.d.*	*n.d.*	*n.d.*	540	*n.d.*	*n.d.*	*n.d.*	24.4	0.34
0.2M																								
	V	Cr	Mn	Co	Ni	Cu	Zn	As	Se	Rb	Sr	Ru	Rh	Pd	Ag	Cd	Ba	Re	Os	Ir	Pt	Au	Pb	U
L13.1D	77.2	*n.d.*	195	3.06	12.4	33.5	5.49	45.7	5.09	3.94	3.77	*n.d.*	*n.d.*	0.95	0.23	*n.d.*	48.5	*n.d.*	*n.d.*	*n.d.*	*n.d.*	*n.d.*	9.30	0.38
L13.2D	47.3	*n.d.*	83.4	0.81	3.17	24.4	3.53	40.1	25.6	4.43	8.50	*n.d.*	*n.d.*	1.03	0.014	*n.d.*	169	*n.d.*	60.5	0.13	*n.d.*	0.25	10.1	0.25
L13.3D	26.9	*n.d.*	29.7	*n.d.*	1.27	12.3	5.16	35.7	7.52	2.68	1.32	*n.d.*	*n.d.*	0.14	*n.d.*	*n.d.*	12.1	*n.d.*	16.6	*n.d.*	*n.d.*	*n.d.*	4.46	0.39
L13.4D	47.2	*n.d.*	118	1.76	8.86	36.5	3.82	37.7	24.5	4.34	2.29	*n.d.*	*n.d.*	0.70	*n.d.*	*n.d.*	22.0	*n.d.*	5.12	*n.d.*	*n.d.*	*n.d.*	5.28	0.37
L13.5D	57.6	*n.d.*	401	8.43	22.4	33.7	5.84	36.2	19.1	5.93	7.27	*n.d.*	*n.d.*	0.97	0.28	*n.d.*	166	*n.d.*	*n.d.*	*n.d.*	*n.d.*	*n.d.*	9.96	0.38
L13.6D	52.1	*n.d.*	215	2.92	4.29	47.9	4.42	40.7	14.1	4.99	4.84	*n.d.*	*n.d.*	0.52	0.046	*n.d.*	137	*n.d.*	*n.d.*	*n.d.*	0.017	*n.d.*	10.6	0.49
0.25M																								
	V	Cr	Mn	Co	Ni	Cu	Zn	As	Se	Rb	Sr	Ru	Rh	Pd	Ag	Cd	Ba	Re	Os	Ir	Pt	Au	Pb	U
L13.1D	83.7	*n.d.*	54.0	0.70	8.09	33.0	24.6	58.9	*n.d.*	2.58	1.64	*n.d.*	*n.d.*	0.15	*n.d.*	*n.d.*	19.9	*n.d.*	*n.d.*	*n.d.*	*n.d.*	*n.d.*	5.27	0.32
L13.2D	63.4	*n.d.*	50.8	0.34	2.27	18.9	18.5	54.1	8.60	2.96	4.18	*n.d.*	*n.d.*	0.43	*n.d.*	0.072	76.9	*n.d.*	45.1	0.12	*n.d.*	1.23	6.07	0.23
L13.3D	36.0	*n.d.*	16.7	*n.d.*	1.22	21.1	37.6	44.4	14.7	1.36	1.61	*n.d.*	*n.d.*	*n.d.*	*n.d.*	*n.d.*	17.3	*n.d.*	11.7	*n.d.*	*n.d.*	*n.d.*	4.93	0.31
L13.4D	58.7	*n.d.*	38.4	*n.d.*	7.30	20.8	13.1	47.3	10.4	3.31	1.40	*n.d.*	*n.d.*	0.11	*n.d.*	*n.d.*	10.2	*n.d.*	2.08	*n.d.*	*n.d.*	*n.d.*	3.11	0.35
L13.5D	65.9	*n.d.*	97.7	1.95	14.0	100	16.0	48.2	4.24	3.88	2.38	*n.d.*	*n.d.*	0.39	0.30	*n.d.*	46.1	*n.d.*	*n.d.*	*n.d.*	*n.d.*	*n.d.*	5.18	0.33
L13.6D	66.3	*n.d.*	93.6	1.10	3.41	24.4	14.1	54.4	38.5	3.21	2.39	*n.d.*	*n.d.*	*n.d.*	0.69	*n.d.*	39.6	*n.d.*	*n.d.*	*n.d.*	*n.d.*	*n.d.*	6.19	0.44

APPENDIX C2: Multi element analysis data for hot hydroxylamine leach of samples taken along a profile in Kabanga main.

Kabanga Main																								
Hot HAM																								
0.1M	**(All data in ppb)**																							
	V	Cr	Mn	Co	Ni	Cu	Zn	As	Se	Rb	Sr	Ru	Rh	Pd	Ag	Cd	Ba	Re	Os	Ir	Pt	Au	Pb	U
KAB 50017	9.76	*n.d.*	192	4.03	2.20	13.3	2.08	21.0	9.90	16.8	47.6	0.064	0.056	0.99	1.27	0.10	204	0.081	147	0.36	*n.d.*	4.84	20.7	0.51
KAB 50018	28.8	*n.d.*	296	3.80	2.58	8.31	*n.d.*	24.7	8.63	14.3	57.2	0.098	0.026	1.58	*n.d.*	0.24	318	0.085	36.7	0.10	*n.d.*	1.95	25.3	0.54
KAB 50019	43.5	7.20	110	3.80	2.38	13.1	0.88	26.5	1.99	13.7	40.5	0.18	0.026	2.01	*n.d.*	0.12	211	0.070	16.9	0.057	*n.d.*	2.70	34.3	0.83
KAB 50020	72.2	15.9	4994	34.7	51.3	68.1	23.1	27.7	*n.d.*	38.9	885	0.11	0.097	2.45	0.27	0.40	1490	0.061	5.86	0.046	*n.d.*	2.30	43.9	0.83
KAB 50021	27.6	*n.d.*	4353	17.6	25.6	10.1	7.95	22.9	7.36	15.9	889	0.070	0.11	0.33	*n.d.*	0.23	1106	0.034	*n.d.*	*n.d.*	*n.d.*	0.53	6.33	0.19
0.15M																								
	V	Cr	Mn	Co	Ni	Cu	Zn	As	Se	Rb	Sr	Ru	Rh	Pd	Ag	Cd	Ba	Re	Os	Ir	Pt	Au	Pb	U
KAB 50017	26.3	*n.d.*	43.9	1.08	4.66	3.14	*n.d.*	32.0	1.21	5.77	5.02	0.14	0.039	0.82	*n.d.*	*n.d.*	0.045	0.045	25.3	103	0.29	3.96	13.4	0.47
KAB 50018	35.2	*n.d.*	53.7	0.41	1.52	11.5	*n.d.*	34.0	7.60	4.58	5.27	0.18	0.051	1.01	*n.d.*	*n.d.*	*n.d.*	*n.d.*	40.4	23.4	0.034	1.09	17.0	0.46
KAB 50019	42.4	4.16	31.1	0.84	1.70	7.48	4.42	36.8	17.9	3.19	3.62	0.11	0.046	1.00	0.029	0.029	0.029	0.027	20.9	13.6	0.069	1.67	16.8	0.66
KAB 50020	41.6	*n.d.*	467	3.28	7.30	9.28	12.1	34.4	7.86	9.86	62.0	0.012	0.047	0.24	0.080	0.080	0.080	0.019	137	1.49	*n.d.*	0.66	13.2	0.17
KAB 50021	38.7	*n.d.*	1032	6.49	13.5	14.3	10.2	34.1	0.12	4.44	163	0.12	0.060	*n.d.*	*n.d.*	*n.d.*	*n.d.*	0.035	0.17	*n.d.*	*n.d.*	1.35	9.04	0.11
0.2M																								
	V	Cr	Mn	Co	Ni	Cu	Zn	As	Se	Rb	Sr	Ru	Rh	Pd	Ag	Cd	Ba	Re	Os	Ir	Pt	Au	Pb	U
KAB 50017	41.4	*n.d.*	20.4	0.29	1.52	6.19	22.0	42.6	11.5	2.87	1.38	*n.d.*	0.016	0.74	*n.d.*	0.062	8.77	0.06	63.2	0.15	*n.d.*	2.26	7.95	0.49
KAB 50018	63.5	2.64	27.3	0.74	1.43	2.67	*n.d.*	44.8	19.4	2.37	1.60	0.12	0.042	0.87	*n.d.*	0.18	10.9	0.072	25.7	0.041	0.17	3.38	10.7	0.55
KAB 50019	55.0	*n.d.*	20.4	0.64	2.27	13.1	*n.d.*	49.7	0.60	1.98	1.67	0.097	0.076	1.03	*n.d.*	0.19	14.1	0.084	8.18	0.032	*n.d.*	2.28	12.6	0.98
KAB 50020	60.2	7.69	64.1	0.69	4.24	15.3	*n.d.*	49.8	*n.d.*	6.87	5.00	0.13	0.082	0.19	*n.d.*	0.18	29.3	0.14	2.31	0.056	*n.d.*	3.89	15.8	0.15
KAB 50021	53.2	*n.d.*	130	1.19	7.78	12.8	0.65	42.9	0.65	1.91	13.9	0.19	*n.d.*	*n.d.*	*n.d.*	0.075	86.6	0.11	*n.d.*	*n.d.*	*n.d.*	0.97	14.9	0.18
0.25M																								
	V	Cr	Mn	Co	Ni	Cu	Zn	As	Se	Rb	Sr	Ru	Rh	Pd	Ag	Cd	Ba	Re	Os	Ir	Pt	Au	Pb	U
KAB 50017	74.1	*n.d.*	20.0	0.40	1.27	7.25	24.7	59.7	11.6	1.87	1.91	0.18	0.029	0.39	*n.d.*	0.16	7.26	0.052	49.2	0.13	*n.d.*	3.67	5.77	0.58
KAB 50018	82.3	3.78	23.8	0.55	2.27	9.68	43.4	59.9	3.09	1.74	1.86	0.14	0.11	0.61	*n.d.*	0.072	12.8	0.062	19.8	0.066	0.018	3.18	11.4	0.55
KAB 50019	80.5	10.7	21.0	0.35	1.55	6.22	16.1	59.2	6.91	1.24	1.74	0.13	0.067	0.42	*n.d.*	0.19	7.39	0.052	6.90	0.023	0.050	2.42	8.46	0.83
KAB 50020	77.3	12.0	36.4	0.67	4.29	10.7	16.1	60.7	8.36	4.33	2.70	0.20	0.11	0.25	0.084	0.17	23.5	0.11	1.26	*n.d.*	0.095	3.38	13.8	0.13
KAB 50021	84.3	11.5	64.4	0.62	5.52	17.0	22.0	64.3	14.5	1.63	3.19	0.074	0.13	0.20	0.061	0.20	21.9	0.026	*n.d.*	0.053	*n.d.*	2.91	19.5	0.21

APPENDIX D1: Multi element analysis data for 0.1M hot hydroxylamine leach of samples taken at both upper and lower horizons along a profile in Amalia Blue Dot Mine.

Amalia Blue Dot Mine																									
Upper horizon																									
0.1M		**(All data in ppb)**																							
	V	Cr	Mn	Fe	Co	Ni	Cu	Zn	As	Se	Rb	Sr	Ru	Rh	Pd	Ag	Cd	Ba	Re	Os	Ir	Pt	Au	Pb	U
L13.1U	54.7	*n.d.*	7929	5111	142	93.8	28.6	43.6	3.16	1.46	14.5	106	*n.d.*	0.013	1.28	0.22	0.36	1022	0.024	77.7	0.21	*n.d.*	3.51	28.6	0.34
L13.1iU	28.4	4.81	5356	3763	91.7	26.6	53.4	43.0	9.65	9.83	15.3	147	*n.d.*	0.047	2.12	0.31	0.39	764	0.062	123	0.19	*n.d.*	6.30	37.7	0.51
L13.2U	34.2	*n.d.*	4466	2813	62.7	*n.d.*	24.4	35.0	2.92	7.49	11.2	57.0	*n.d.*	*n.d.*	1.19	0.15	0.046	356	*n.d.*	32.5	0.061	*n.d.*	0.92	36.6	0.29
L13.3U	39.3	2.76	2040	1254	29.5	*n.d.*	29.9	33.2	8.04	4.45	11.8	70.3	*n.d.*	*n.d.*	0.85	0.062	0.11	308	0.010	6.30	0.063	0.095	0.72	17.9	0.33
L13.4U	46.3	2.94	6190	2690	123	0.0	31.6	39.5	9.53	15.2	12.2	44.3	*n.d.*	0.027	0.92	0.13	0.23	437	0.024	19.7	0.023	*n.d.*	1.19	21.9	0.30
L13.4iU	60.5	*n.d.*	7660	4130	140	88.2	27.6	42.3	3.95	8.50	8.56	63.7	*n.d.*	*n.d.*	0.51	0.20	0.46	592	*n.d.*	11.5	0.021	*n.d.*	0.23	17.7	0.17
L13.5U	83.2	*n.d.*	8072	4826	155	61.9	41.2	71.9	*n.d.*	7.97	12.5	78.9	*n.d.*	*n.d.*	1.08	0.12	0.42	637	*n.d.*	*n.d.*	*n.d.*	*n.d.*	0.19	32.7	0.52
L13.6U	62.3	5.97	6284	3336	69.7	43.0	16.6	36.1	*n.d.*	*n.d.*	8.38	293	0.045	0.018	0.79	0.085	0.25	769	*n.d.*	9.12	0.044	0.16	0.68	20.8	0.27
Lower horizon																									
0.1M			**(All data in ppb)**																						
	V	Cr	Mn	Fe	Co	Ni	Cu	Zn	As	Se	Rb	Sr	Ru	Rh	Pd	Ag	Cd	Ba	Re	Os	Ir	Pt	Au	Pb	U
L13.1D	107	5.71	6802	3540	136	163	59.0	48.3	9.33	0.50	11.7	118	*n.d.*	*n.d.*	1.34	0.17	0.38	1260	0.028	*n.d.*	*n.d.*	0.085	0.53	25.3	0.35
L13.1iD	104	59.8	6507	3948	113	84.3	49.0	40.6	24.9	4.03	14.2	224	0.23	0.044	1.83	0.32	0.25	1166	0.023	*n.d.*	*n.d.*	0.15	1.45	38.5	0.72
L13.2D	81.4	*n.d.*	6380	2874	88.5	47.2	59.1	249	1.06	14.2	10.5	182	*n.d.*	0.016	1.04	0.17	0.13	800	*n.d.*	48.5	0.11	*n.d.*	1.85	24.9	0.27
L13.3D	42.3	*n.d.*	3047	1201	53.5	4.82	41.1	39.0	5.39	4.44	11.0	75.3	*n.d.*	*n.d.*	1.15	0.12	0.030	394	*n.d.*	22.8	0.077	*n.d.*	0.53	35.4	0.65
L13.4D	114	*n.d.*	7377	4763	186	154	144	52.0	*n.d.*	12.3	11.8	81.4	*n.d.*	*n.d.*	2.29	0.84	0.10	598	*n.d.*	0.51	*n.d.*	0.042	*n.d.*	30.7	1.60
L13.4iD	72.7	20.3	4369	2744	54.4	8.64	13.4	29.6	*n.d.*	*n.d.*	4.42	366	*n.d.*	0.028	0.27	0.097	0.29	706	*n.d.*	2.69	0.034	*n.d.*	1.32	1.37	0.31
L13.5D	147	5.76	7951	6750	171	161	134	55.3	1.84	5.53	19.7	104	*n.d.*	0.016	2.73	0.77	0.13	1225	0.012	8.05	*n.d.*	*n.d.*	0.21	43.8	1.36
L13.5iD	96.9	*n.d.*	8281	5061	85.8	53.1	48.0	50.6	*n.d.*	*n.d.*	12.9	525	*n.d.*	0.010	0.92	0.065	0.30	1171	*n.d.*	*n.d.*	0.011	*n.d.*	0.28	27.4	0.41
L13.6D	77.0	*n.d.*	14380	6231	232	*n.d.*	77.9	52.8	*n.d.*	*n.d.*	16.3	193	*n.d.*	*n.d.*	1.61	0.20	0.24	3064	*n.d.*	*n.d.*	*n.d.*	0.050	*n.d.*	79.3	0.63

APPENDIX D2: Multi element analysis data for 0.1M hot hydroxylamine leach of samples taken at lower horizon in Amalia Blue Dot Mine.

LOWER HORIZON(AMALIA BLUE DOT MINE SAMPLES)																											
0.1M HAM							**(All data in ppb)**																				
	Y	X	V	Cr	Mn	Fe	Co	Ni	Cu	Zn	As	Se	Rb	Sr	Ru	Rh	Pd	Ag	Cd	Ba	Re	Os	Ir	Pt	Au	Pb	U
L101iD	3022692	-11020.03	142	*n.d*	8667	5190	217	147	172	60.9	21.3	5.81	6.83	130	0.12	0.012	1.38	0.21	0.3	734	0.057	6.79	0.014	*n.d*	0.87	11.4	0.28
L10.2D	3022473	-11150	147	*n.d*	8090	4198	255	111	133	36.5	20.2	7.37	10.1	113	0.12	0.012	2.31	0.13	4.23	997	*n.d*	4.92	0.02	*n.d*	1.52	28.2	0.52
L10.4D	3022020	-12293.87	104	*n.d*	2677	2264	88.1	30.1	172	112	21.8	4.84	12	94.1	0.12	0.019	1.92	0.15	1.52	233	0.011	3.19	0.025	*n.d*	1.67	28.2	0.52
L10.5D	3021669	-12825.97	187	*n.d*	5124	2081	85.1	137	73.1	24.5	21.7	6.98	11.7	193	0.24	*n.d*	1.15	0.11	1.11	402	*n.d*	1.68	*n.d*	*n.d*	0.76	16.5	1.82
L10.6D	3021414	-13362.97	196	*n.d*	11596	3808	367	516	117	104	22.1	n.d	7.32	253	0.22	*n.d*	1.26	0.34	1.97	1271	0.02	0.72	*n.d*	*n.d*	0.66	22.7	0.52
L11.1D	3023413	-11037.96	165	*n.d*	40645	9426	676	884	152	69.1	23	10.3	14.5	126	0.18	*n.d*	2.1	0.49	1.65	4901	0.011	0.32	*n.d*	*n.d*	2.05	38.5	0.45
L11.2D	3023084	-11533.15	166	*n.d*	10125	3567	222	228	156	49.8	23.5	1.88	3.35	204	*0.2*	0.025	1.14	0.31	1.76	1268	*n.d*	*n.d*	*n.d*	*n.d*	0.94	14.5	0.43
L11.3D	3022791	-12049.24	204	*n.d*	57972	14003	742	252	245	49.2	22.7	10.5	21.2	137	0.13	0.019	2.24	0.18	1.51	9467	*n.d*	*n.d*	*n.d*	*n.d*	1.57	93.9	0.88
L11.4D	3022478	-12602.25	128	*n.d*	3277	6791	60.1	52.2	222	124	22.9	5.21	14.1	153	0.21	0.015	1.58	0.18	2.4	437	*n.d*	*n.d*	0.011	*n.d*	1	25.6	1.06
L11.4Db	3022478	-12602.25	95.6	*n.d*	3197	6604	54.9	42.2	254	101	22.4	7.71	14.4	146	0.063	0.016	1.62	0.062	0.54	417	*n.d*	*n.d*	*n.d*	*n.d*	0.7	27.5	1
L11.5D	3022206	-13081.41	130	*n.d*	8338	6023	214	223	186	64.1	18.2	7.87	9.66	125	0.15	0.025	2.75	0.54	1.49	726	0.055	128	*0.25*	*n.d*	3.88	32.9	0.76
L11.5iD	3022060	-13339.09	132	*n.d*	5010	3664	106	96.5	124	72.1	21.4	6.95	7.49	100	0.086	0.013	1.58	0.45	1.09	526	0.027	81.3	0.2	*n.d*	2.34	27.1	0.55
L11.6D	3021951	-13618.42	82.7	*n.d*	3947	2396	66.7	96.9	119	40.1	21.5	5.87	11.5	151	0.14	*n.d*	0.74	0.22	0.59	427	*n.d*	57.2	0.11	*n.d*	1.69	9.04	0.19
L12.1D	3023746	-11567.84	106	*n.d*	7807	5828	196	129	167	50.4	21.2	*n.d*	13.8	129	0.097	*n.d*	2.85	0.26	0.12	877	*n.d*	44.7	0.14	*n.d*	1.91	45	0.9
L12.2D	3023600	-11825.52	53.4	*n.d*	4764	3668	132	40.7	146	37.5	20.1	4.16	13.3	70.5	0.2	0.012	3.06	0.14	0.27	601	*n.d*	29.5	*0.064*	*n.d*	1.12	26.3	0.62
L12.2iD	3023470	-12141.02	70.2	*n.d*	3929	2629	108	47.6	93	93	22.3	4.9	14.3	134	0.026	*n.d*	2.08	0.056	0.092	643	*n.d*	*22.4*	*0.029*	*n.d*	1.1	30.2	0.7
L12.3D	3023344	-12362.53	60.5	*n.d*	1859	1619	48.3	18.7	130	49.3	21.5	*n.d*	14.3	83.5	0.1	*n.d*	1.83	0.014	0.15	386	*n.d*	17.9	*0.041*	*n.d*	0.76	30.9	0.8
L12.4D	3023061	-12814.45	63	*n.d*	7054	4134	149	132	119	33.7	23.5	*n.d*	13.9	81.2	0.072	*n.d*	1.99	0.15	0.25	578	*n.d*	*15.2*	*0.059*	*n.d*	1.33	31.9	0.73
L12.4iD	3022906	-13136.28	68	*n.d*	5679	4799	167	136	122	51.9	19.7	4.45	15.3	102	0.064	*n.d*	2.28	0.2	0.2	523	*0.015*	10.4	*0.016*	*n.d*	0.93	28.1	0.63
L12.5iD	3022650	-13673.29	142	9.8	8134	3362	148	244	96	82.7	23.6	7.74	15.7	225	0.12	*n.d*	1.46	0.25	0.43	1110	0.017	7.04	0.022	*n.d*	1.35	11.4	0.42
L13.1D	3024462	-11384.7	120	6.4	7201	5310	146	211	354	97.5	25	6.09	13	138	0.15	0.013	1.5	0.38	0.45	1321	*0.021*	6.1	0.026	*n.d*	1.72	22.9	0.43
L13.1iD	3024241	-11897.14	113	*n.d*	7074	5711	125	124	236	91.1	22.4	10.7	17.3	262	0.1	*n.d*	2.62	0.14	0.61	1304	*n.d*	2.53	*n.d*	*n.d*	0.67	52.6	1.06
L13.2D	3024042	-12076.06	124	*n.d*	7382	4003	105	121	160	55.6	21.5	1.22	12.1	207	0.09	*0.016*	1.44	0.01	0.17	728	*n.d*	7.63	*n.d*	*n.d*	0.72	24.5	0.38
L13.2Db	3024042	-12076.06	139	*n.d*	8422	4375	122	140	240	101	21.8	4.64	12.6	239	0.18	0.014	1.55	0.027	0.13	815	*n.d*	*1.22*	*n.d*	*n.d*	0.45	27.8	0.39
L13.3D	3023839	-12691.81	81.4	*n.d*	3663	2955	66.3	33.7	349	65.1	23.4	2.74	12	88.9	0.1	*n.d*	1.79	0.068	0.13	448	*0.01*	0.14	*n.d*	*n.d*	0.44	38.1	0.99
L13.4D	3023547	-13207.91	112	*n.d*	8037	5325	219	241	231	43	21.5	*n.d*	10.6	96.9	0.08	*n.d*	1.82	0.19	0.28	664	*0.011*	*n.d*	*n.d*	*n.d*	0.32	22.1	0.7
L13.4iD	3023422	-13428.66	92.5	0.18	5164	1715	61.6	88.3	49.2	16.4	23.5	9.3	5.28	450	0.11	*n.d*	0.2	*n.d*	0.57	765	*0.031*	*n.d*	0.02	*n.d*	0.45	*n.d*	0.34
L13.5D	3023259	-13629.24	118	*n.d*	8103	2758	175	185	170	41.2	21.7	4.58	18.9	109	0.18	*n.d*	1.47	0.37	0.4	898	*n.d*	*n.d*	*n.d*	*n.d*	0.12	21.9	0.48
L13.5iD	3023130	-13944.75	109	*n.d*	8638	7383	93.4	136	112	79.3	21.1	n.d	14.1	564	0.15	0.017	1.29	0.3	0.28	1217	*n.d*	*n.d*	*n.d*	*n.d*	0.3	25.6	0.44
L13.6D	3022983	-14203.17	108	5.56	15569	9118	306	76.6	216	58.5	23.8	5.63	19.2	201	0.084	*n.d*	2.19	0.15	0.1	2742	0.033	*n.d*	0.015	*n.d*	1.14	97	0.93

APPENDIX D3: Multi element analysis data for 0.25M hot hydroxylamine leach of samples taken along profiles in Kabanga (Main & North).

Kabanga North Samples																									
0.25M	**(All data in ppb)**																								
	V	Cr	Mn	Fe	Co	Ni	Cu	Zn	As	Se	Rb	Sr	Ru	Rh	Pd	Ag	Cd	Ba	Re	Os	Ir	Pt	Au	Pb	U
KAB 50001	140	17.9	65.9	5800	2.01	*n.d.*	52.5	46.8	44.0	*n.d.*	9.44	27.8	*n.d.*	0.027	0.77	0.28	0.16	343	*n.d.*	*n.d.*	*n.d.*	0.051	0.94	33.1	0.98
KAB 50003	127.3	18.74	34.0	6343	2.14	*n.d.*	25.1	22.3	35.5	4.93	8.39	9.98	*n.d.*	*n.d.*	0.57	0.30	*n.d.*	323	*n.d.*	*n.d.*	0.013	0.024	0.41	38.4	1.20
KAB 50009	144	11.4	41.8	4579	3.12	*n.d.*	19.1	30.8	37.2	5.91	8.77	21.5	*n.d.*	0.016	0.73	0.17	0.11	194	*n.d.*	*n.d.*	*n.d.*	*n.d.*	0.40	29.0	1.00
KAB 50038	107	16.3	1394	7355	7.98	13.3	18.0	25.2	61.2	32.9	21.5	281	0.098	0.019	1.36	0.27	0.11	735	*n.d.*	*n.d.*	*n.d.*	*n.d.*	1.14	38.7	0.74
KAB 50025	141	16.2	1180	7746	10.7	11.8	18.5	37.1	60.7	8.76	15.9	304	0.20	0.037	1.06	0.26	0.17	635	0.028	5.45	0.039	0.074	1.81	39.1	0.59
KAB 50027	111	26.3	112	3942	2.45	8.58	21.6	26.3	60.1	21.3	17.1	84.3	0.15	0.022	1.78	0.33	*n.d.*	226	*n.d.*	3.92	0.031	0.048	1.19	40.3	1.43
KAB 50028	121	24.8	676	6959	3.77	20.6	16.3	25.8	69.0	12.4	13.6	42.0	0.15	0.019	1.54	0.15	0.085	304	*n.d.*	2.80	0.022	0.033	1.30	52.8	1.28
KAB 50029	96.1	23.0	1148	7477	3.70	19.0	15.5	27.8	61.4	38.7	15.8	106	0.19	0.030	0.95	0.15	0.079	399	*n.d.*	0.87	0.014	0.099	0.90	42.4	0.88
KAB 50030	104	31.0	126	6442	1.82	22.4	29.0	23.1	68.4	13.4	9.56	50.9	0.11	0.023	1.55	0.46	0.075	309	*n.d.*	0.23	*n.d.*	0.086	1.49	48.8	1.74
KAB50032	145	15.3	57.6	7533	1.67	65.5	16.7	25.2	90.8	8.05	9.39	25.5	0.078	0.024	1.15	0.23	0.071	318	*n.d.*	*n.d.*	*n.d.*	0.13	1.22	36.2	1.30
Kabanga Main Samples																									
0.25M	**(All data in ppb)**																								
	V	Cr	Mn	Fe	Co	Ni	Cu	Zn	As	Se	Rb	Sr	Ru	Rh	Pd	Ag	Cd	Ba	Re	Os	Ir	Pt	Au	Pb	U
KABS 5001	164	11.2	172	4120	3.96	*n.d.*	22.6	23.7	41.6	5.83	24.9	157	*n.d.*	0.012	2.15	0.099	0.13	292	*n.d.*	*n.d.*	0.033	0.031	0.33	47.3	1.31
KABS 5001	117	8.59	132	3757	2.09	*n.d.*	20.6	17.7	32.3	20.1	14.7	32.9	*n.d.*	*n.d.*	3.05	0.18	0.065	240	*n.d.*	*n.d.*	*n.d.*	0.032	0.12	50.6	2.34
KABS 5001	73.6	14.5	431	3183	6.44	15.1	30.8	179	47.1	3.37	21.2	152	*n.d.*	0.023	2.58	0.36	0.40	478	0.029	93.3	0.17	0.13	5.41	52.1	1.16
KABS 5001	125	20.0	4168	11928	19.8	29.0	30.6	29.2	60.4	0.57	17.6	888	0.064	0.071	1.28	0.46	0.43	1310	*n.d.*	70.4	0.097	0.14	3.18	25.2	0.35
KABS 5001	111	15.8	328	4950	3.93	1.21	16.8	20.8	55.5	2.20	17.5	62.3	0.091	0.050	2.82	0.27	*n.d.*	361	0.029	48.4	0.098	*n.d.*	2.70	45.2	1.45
KABS 5001	106	1.56	212	1944	4.66	14.1	15.3	18.9	56.8	7.60	21.1	51.3	0.014	0.046	1.13	0.13	*n.d.*	210	*n.d.*	31.0	0.078	0.063	1.71	37.0	1.36
KABS 5002	143	31.4	129	4368	4.92	31.5	24.7	19.9	78.2	3.74	16.5	45.2	0.069	0.028	3.73	0.12	0.15	245	0.017	26.9	0.087	0.082	1.87	61.4	2.36
KABS 5002	129	7.73	4624	9256	32.2	32.4	19.1	40.5	53.6	3.80	34.7	850	0.031	0.032	0.91	0.49	0.38	1470	*n.d.*	15.4	0.039	*n.d.*	1.59	33.4	0.20
KABS 5002	138	23.6	1199	9157	9.93	8.65	45.7	26.7	58.5	5.54	10.8	712	0.055	0.032	1.18	0.53	0.27	832	*n.d.*	16.3	0.046	0.19	2.28	26.2	0.52
KABS 5002	138	22.5	633	11136	9.65	25.2	73.0	34.2	59.1	*n.d.*	12.3	408	0.15	0.040	1.02	0.71	0.21	748	0.028	8.99	*n.d.*	0.068	1.54	33.6	0.58
KABS 5004	108	7.24	1251	6472	2.66	28.8	17.6	19.2	64.7	17.8	6.31	106.1	0.055	0.013	0.81	0.20	0.09	447	*n.d.*	*n.d.*	*n.d.*	0.15	0.74	35.2	0.59
KABS 5004	121	8.92	1765	7229	4.52	41.2	16.6	33.4	76.6	8.44	9.39	214	0.15	0.034	0.66	0.23	0.13	521	*n.d.*	*n.d.*	*n.d.*	0.053	1.50	29.6	0.50
KABS 5004	137	4.73	3981	11772	14.2	24.2	42.8	38.6	58.6	20.1	39.9	302	0.033	0.019	2.48	0.27	0.15	1051	*n.d.*	*n.d.*	*n.d.*	0.030	0.68	64.4	0.93

APPENDIX D4: Multi element analysis data for 0.25M hot hydroxylamine leach of samples taken from Luhuma.

LUHUMA SAMPLES																									
0.25M	**(All data in ppb)**																								
	V	Cr	Mn	Fe	Co	Ni	Cu	Zn	As	Se	Rb	Sr	Ru	Rh	Pd	Ag	Cd	Ba	Re	Os	Ir	Pt	Au	Pb	U
LUH 10001	89.5	3.65	998	6025	23.3	4.71	60.0	70.3	53.4	31.0	14.5	8.79	0.027	0.088	16.6	0.63	0.078	323	0.11	126	0.61	0.061	7.02	78.2	4.37
LUH 10003	104	12.1	428	4929	14.2	2.82	29.3	35.7	55.9	21.9	14.7	4.96	0.050	0.059	18.4	0.44	*n.d.*	318	0.10	87.8	0.41	0.058	3.71	71.9	6.56
LUH10006	87.9	6.48	2272	8145	30.6	2.76	51.3	32.7	53.6	27.7	15.0	135	*n.d.*	0.040	13.5	1.02	0.035	897	0.060	57.8	0.27	0.034	2.57	86.6	2.29
LUH 10007	98.6	4.73	1931	9555	31.2	3.56	37.8	44.0	45.6	18.8	18.9	146.1	0.022	0.040	19.0	0.62	0.039	660	0.087	40.0	0.18	0.029	2.35	88.3	2.77
LUH 10010	72.3	4.68	110	3707	2.47	3.86	22.4	35.2	45.5	10.2	14.4	15.1	0.042	0.031	8.98	0.95	0.056	0.056	0.049	30.0	0.14	0.067	1.43	57.3	2.70
LUH 10019	94.7	11.1	2350	9195	31.4	3.66	36.6	49.6	46.6	21.1	39.1	58.5	0.022	0.023	19.7	0.42	0.19	225	0.042	23.0	0.11	0.031	1.00	83.8	2.65
LUH 10023	105	16.7	609	7430	17.3	4.84	41.6	44.8	45.5	2.21	29.2	219	0.021	0.044	13.0	0.46	0.056	926	0.022	17.3	0.10	0.081	1.19	86.2	3.99
LUH 10027	78.3	3.18	1407	5806	18.0	5.28	49.7	26.9	54.7	16.6	18.5	10.4	0.045	0.015	6.58	0.40	0.030	581	0.011	12.4	0.084	0.019	0.62	70.3	3.10
LUH 10039	83.7	15.5	488	13066	9.54	4.68	56.2	58.7	52.6	*n.d.*	21.7	133	*n.d.*	0.017	12.6	1.67	0.023	1100	0.022	11.6	0.064	0.026	0.95	87.2	2.20
LUH10040	86.0	34.4	394	14473	11.0	13.2	79.8	56.4	48.9	11.1	13.7	145	*n.d.*	0.027	5.29	1.27	0.25	1063	0.043	9.24	0.054	0.028	0.82	95.0	6.52
LUH 10043	67.0	14.2	75.5	8507	1.91	6.48	34.7	56.1	51.0	13.0	9.34	22.9	0.063	0.023	3.79	0.76	*n.d.*	382	*n.d.*	7.49	0.048	0.044	1.04	43.1	1.63
LUH 10044	82.0	16.0	672	5485	21.3	4.68	41.7	17.7	46.9	17.8	16.0	49.7	0.040	0.021	15.8	1.06	0.052	762	0.029	6.45	0.036	0.047	0.49	79.2	4.43
LUH 10045	69.8	4.15	103	8868	3.11	5.36	23.1	29.6	45.5	19.3	12.0	58.7	*n.d.*	0.031	9.89	0.71	0.052	478	0.013	3.92	0.017	0.028	0.48	54.0	2.65
LUH 10048	67.2	13.6	79.0	6216	3.93	4.70	36.4	28.5	43.5	7.50	8.77	11.9	0.017	*n.d.*	6.79	1.32	0.076	328	*n.d.*	4.23	0.018	0.049	0.63	35.6	2.65
LUH10049	85.1	14.5	1852	6520	18.0	40.6	24.1	22.7	48.3	10.8	9.64	303	0.092	0.034	4.25	1.02	0.14	1395	*n.d.*	3.66	*n.d.*	0.060	0.66	32.5	0.99
LUH 10052	118	8.32	386	7200	5.94	9.51	73.9	7.33	63.8	8.01	17.7	100	0.030	0.033	10.4	0.83	0.074	622	*n.d.*	2.93	0.018	0.030	0.72	67.3	4.53
LUH 10054	98.5	13.3	771	7431	16.1	5.13	35.2	14.3	45.6	8.95	19.4	35.4	0.061	*n.d.*	16.0	1.29	0.047	665	0.011	2.44	*n.d.*	0.010	0.62	95.1	5.42
LUH 10060	76.4	14.3	317	6174	8.21	6.44	35.4	16.5	52.1	6.53	13.7	10.1	0.083	0.017	11.3	0.78	0.11	229	*n.d.*	2.55	*n.d.*	0.012	0.36	46.4	2.46
LUH 10063	93.4	9.22	1174	9708	19.1	4.10	42.1	19.1	55.7	16.4	29.1	121	0.15	0.017	14.0	1.34	0.12	936	0.024	1.92	*n.d.*	0.039	0.48	97.7	2.56
LUH 10064	94.6	12.6	2892	10072	36.9	5.61	55.4	28.0	63.6	10.9	19.4	178	0.023	0.029	14.6	1.02	0.11	1160	*n.d.*	1.23	*n.d.*	0.023	0.47	106	2.53
LUH 40003	76.8	26.5	119	11185	5.23	12.6	73.9	35.3	57.9	4.92	10.4	58.4	0.12	*n.d.*	8.62	0.69	0.15	351	*n.d.*	0.22	0.015	0.034	0.57	74.4	1.84
LUH 40011	71.7	16.0	52.5	3616	2.73	7.64	34.2	42.8	58.1	7.98	7.27	37.1	0.11	0.015	4.01	0.58	0.036	471	0.011	0.49	*n.d.*	0.038	0.64	48.5	1.65
LUH 40013	91.0	16.2	1763	9487	27.6	6.88	46.6	18.0	64.0	24.0	18.8	100	0.016	0.022	11.9	0.48	0.053	1077	0.016	0.42	*n.d.*	0.020	0.39	94.1	3.20
LUH 40015	74.5	0.89	373	6030	8.76	4.17	47.6	23.5	55.6	4.29	9.38	187	*n.d.*	0.030	3.90	0.83	0.036	587	*n.d.*	1.03	*n.d.*	*n.d.*	0.30	43.3	1.25
LUH 40020	98.2	15.2	1070	6450	29.2	8.07	46.8	33.6	68.7	29.9	20.2	189	0.098	0.017	7.01	0.18	0.13	804	*n.d.*	*n.d.*	*n.d.*	0.045	0.51	82.3	2.25
LUH 40021	89.3	3.59	6285	5975	45.1	41.8	26.8	41.2	53.1	8.02	9.06	244	0.10	0.083	7.02	0.47	0.24	1278	0.053	77.3	0.38	0.072	2.75	70.9	1.37
LUH40023	82.6	11.7	908	9540	13.3	5.10	33.5	19.3	52.4	17.0	19.8	79.2	0.071	0.067	12.1	0.43	0.098	794	0.029	54.3	0.29	0.062	1.61	71.9	1.82

APPENDIX D5: Eigen values for the principal component analysis for analytical data from the three study sites.

Amalia(Upper horizon)				**Amalia(Lower horizon)**			**Kabanga Main**			**Kabanga North**			**Luhuma**		
0.1M							0.25M								
Value	Eigen value	% variance	Cumulative %	Eigen value	% variance	Cumulative %	Eigen value	% variance	Cumulative %	Eigen value	% variance	Cumulative %	Eigen value	% variance	Cumulative %
F1	9.24	36.59	36.95	36.96	20.92	20.92	8.102	32.41	32.41	8.26	33.02	33.02	6.45	25.78	25.78
F2	6.34	25.36	62.32	4.77	19.08	40.008	5.219	20.88	53.28	5.62	22.46	55.48	4.21	16.82	42.6
F3	4.24	16.97	79.28	2.7	10.8	50.809	3.324	13.29	66.58	3.26	13.04	68.51	3.78	15.101	57.7
F4	2.14	8.56	87.85	1.87	7.51	58.319	2.34	9.36	75.94	2.704	10.82	79.33	2.26	9.05	66.75
F5	1.77	7.09	94.95	1.41	5.64	63.959	1.75	7.005	82.94	1.89	7.54	86.87	1.63	6.54	73.29
F6	0.79	3.19	98.13	1.35	5.38	69.336	1.436	5.746	88.69	1.25	4.99	91.87	1.37	5.47	78.76
F7	0.47	1.87	100	1.14	4.55	73.88	1.241	4.963	93.65	0.97	3.898	95.76	1.15	4.61	83.36
F8	NA	NA	NA	1.03	4.13	78.017	0.578	2.312	95.96	0.72	2.897	98.66	0.86	3.42	86.78
F9	NA	NA	NA	0.94	3.76	81.778	0.427	1.707	97.67	0.34	1.34	100	0.712	2.85	89.63
F10	NA	NA	NA	0.78	3.12	84.898	0.309	1.238	98.91	NA	NA	NA	0.65	2.59	92.23
F11	NA	NA	NA	0.62	2.46	87.361	0.152	0.606	99.52	NA	NA	NA	0.42	1.68	93.9
F12	NA	NA	NA	0.55	2.21	89.571	0.078	0.312	99.83	NA	NA	NA	0.35	1.402	95.31
F13	NA	NA	NA	0.44	1.77	91.343	0.043	0.171	100	NA	NA	NA	0.31	1.24	96.54
F14	NA	NA	NA	0.42	1.67	93.008	NA	NA	NA	NA	NA	NA	NA	NA	NA
F15	NA	NA	NA	0.39	1.57	94.58	NA	NA	NA	NA	NA	NA	NA	NA	NA
F16	NA	NA	NA	0.31	1.25	95.83	NA	NA	NA	NA	NA	NA	NA	NA	NA
F17	NA	NA	NA	0.28	1.14	96.96	NA	NA	NA	NA	NA	NA	NA	NA	NA
F18	NA	NA	NA	0.24	0.96	97.92	NA	NA	NA	NA	NA	NA	NA	NA	NA
F19	NA	NA	NA	0.19	0.78	98.69	NA	NA	NA	NA	NA	NA	NA	NA	NA
F20	NA	NA	NA	0.13	0.52	99.22	NA	NA	NA	NA	NA	NA	NA	NA	NA
F21	NA	NA	NA	0.09	0.37	99.59	NA	NA	NA	NA	NA	NA	NA	NA	NA
F22	NA	NA	NA	0.06	0.24	99.83	NA	NA	NA	NA	NA	NA	NA	NA	NA
F23	NA	NA	NA	0.02	0.09	99.93	NA	NA	NA	NA	NA	NA	NA	NA	NA
F24	NA	NA	NA	0.01	0.04	99.97	NA	NA	NA	NA	NA	NA	NA	NA	NA
F25	NA	NA	NA	0.007	0.03	100	NA	NA	NA	NA	NA	NA	NA	NA	NA

APPENDIX E1: Duplicate samples analysis for the 0.1M hydroxylamine leach for samples taken at basal horizon along a profile in Amalia Blue Dot Mine.

Sample ID	X1 (Ni)	X2 (Ni)	Relative Range (%)	RPD (%)	X1 (Au)	X2 (Au)	Relative Range (%)	RPD (%)
L4.6D	122	121	0.92	0.82	2.54	1.88	65	29
L5.2iD	167	162	4.60	3.04	1.68	1.65	2.94	33
L5.3D	81.0	78.6	2.21	3.01	2.61	1.56	61.18	50
L11.4D	52.2	42.2	9.21	21.19	1.00	0.70	17.64	35
L13.2D	121	140	-17.49	-14.56	0.72	0.45	32.35	75

*X1= lab samples

*X2 = duplicate samples

APPENDIX E2: Duplicate samples analysis for the 0.25M hydroxylamine leach for samples taken along a profile in Kabanga Main.

Sample ID	X_1 (Au)	X_2 (Au)	Relative Range (%)	RPD (%)	X_1 (Cu)	X_2 (Cu)	Relative Range (%)	RPD (%)
KS50017	3.67	3.18	-22.17	14.31	7.25	30.6	229.6	123.4
KS50018	3.18	2.70	21.72	16.32	9.68	16.8	70	53.78
KS50019	2.42	1.71	-32.13	34.38	6.22	15.3	89	84.39
KS50020	3.38	1.87	125.84	57.52	10.7	24.7	137	79.09
KS50021	2.91	1.59	125.32	58.67	17.0	19.1	20.6	11.63

*X1= lab samples

*X2 = duplicate samples